ANALYSIS OF DATA FROM INSTRUMENTATION PROGRAM, OLD RIVER LOCK

Walter C. Sherman, Jr., et al

Army Engineer Waterways Experiment Station
Vicksburg, Mississippi

June 1972

TECHNICAL REPORT S-72-10

ANALYSIS OF DATA FROM INSTRUMENTATION PROGRAM, OLD RIVER LOCK

by

W. C. Sherman, Jr., C. C Trahan

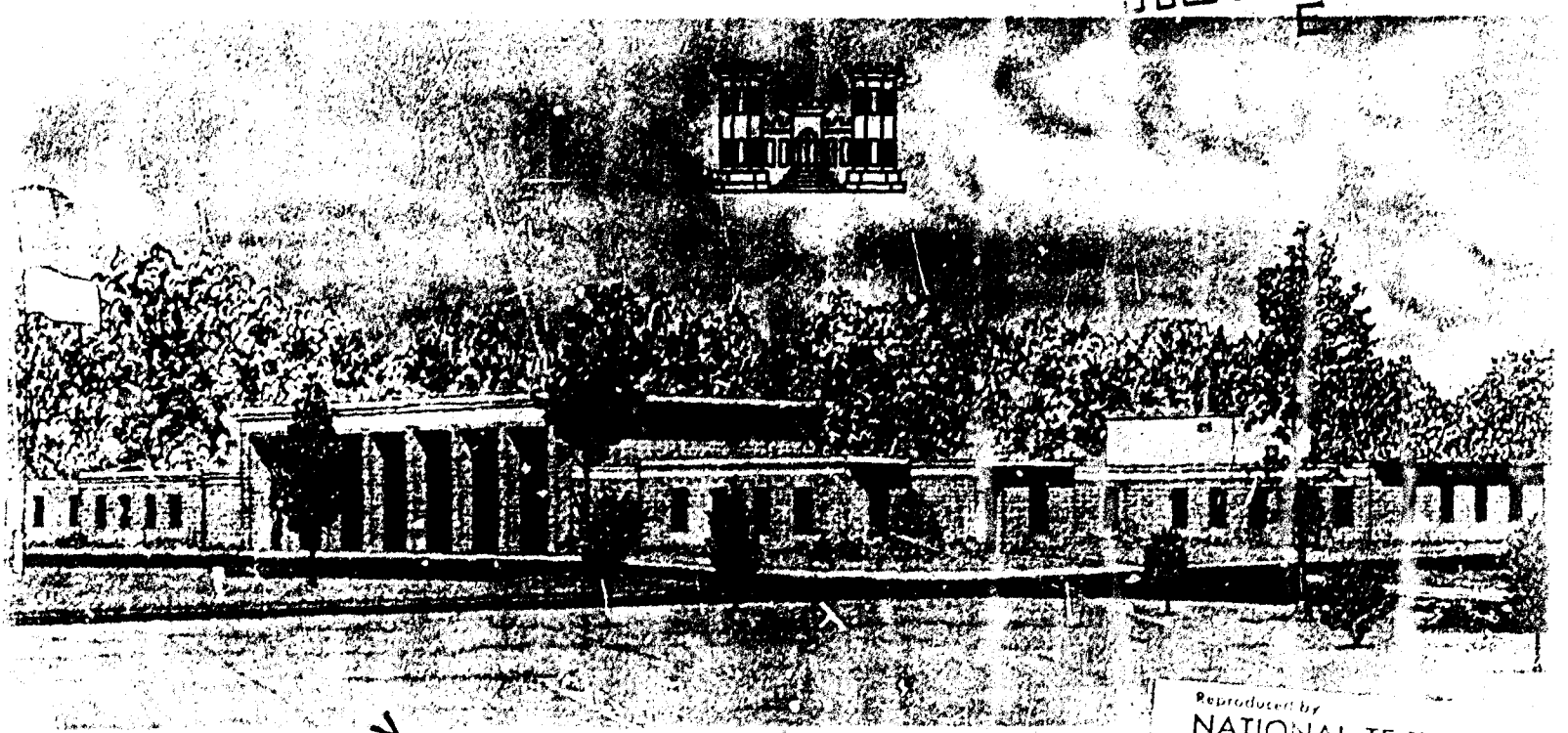

June 1972

Sponsored by Office, Chief of Engineers, U. S. Army

Conducted by U. S. Army Engineer Waterways Experiment Station
Soils and Pavements Laboratory
Vicksburg, Mississippi

Destroy this report when no longer needed. Do not return it to the originator.

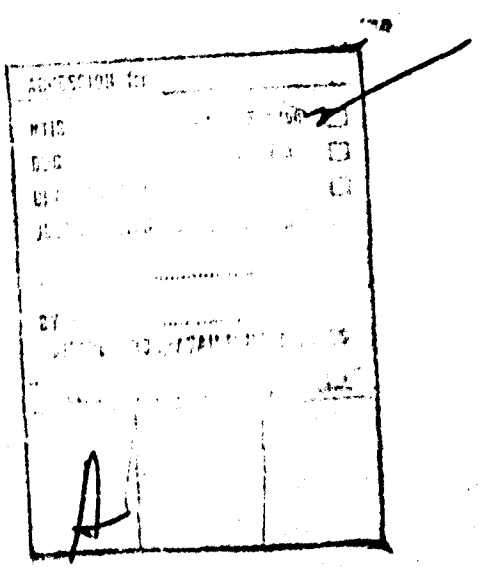

The findings in this report are not to be construed as an official Department of the Army position unless so designated by other authorized documents.

TECHNICAL REPORT S-72-10

ANALYSIS OF DATA FROM INSTRUMENTATION PROGRAM, OLD RIVER LOCK

by

W. C. Sherman, Jr., C. C Trahan

June 1972

Sponsored by Office, Chief of Engineers, U. S. Army

Conducted by U. S. Army Engineer Waterways Experiment Station
Soils and Pavements Laboratory
Vicksburg, Mississippi

ARMY-MRC VICKSBURG, MISS

Unclassified
Security Classification

DOCUMENT CONTROL DATA - R & D

(Security classification of title, body of abstract and indexing annotation must be entered when the overall report is classified)

1 ORIGINATING ACTIVITY (Corporate author)	2a. REPORT SECURITY CLASSIFICATION
U. S. Army Engineer Waterways Experiment Station Vicksburg, Mississippi	Unclassified
	2b. GROUP

3 REPORT TITLE

ANALYSIS OF DATA FROM INSTRUMENTATION PROGRAM, OLD RIVER LOCK

4 DESCRIPTIVE NOTES (Type of report and inclusive dates)

Final Report

5 AUTHOR(S) (First name, middle initial, last name)

Walter C. Sherman, Jr.
Charles C. Trahan

6 REPORT DATE	7a. TOTAL NO. OF PAGES	7b. NO. OF REFS
June 1972	224	18

8a. CONTRACT OR GRANT NO.	9a. ORIGINATOR'S REPORT NUMBER(S)
b. PROJECT NO.	Technical Report S-72-10
c.	9b. OTHER REPORT NO(S) (Any other numbers that may be assigned this report)
d.	

10 DISTRIBUTION STATEMENT

Approved for public release; distribution unlimited.

11. SUPPLEMENTARY NOTES	12. SPONSORING MILITARY ACTIVITY
Details of illustrations in this document may be better studied on microfiche.	Office, Chief of Engineers, U. S. Army Washington, D. C.

13 ABSTRACT

Old River Lock is a reinforced concrete U-frame structure located on the west bank of the Mississippi River about 300 miles above the Head of Passes. The structure was founded at a depth of 71 ft on alluvial sands, an abandoned channel deposit of the Mississippi River that extends in depth to 95 ft below the base of the structure. At the request of the MRC and with the approval of the OCE, Old River Lock was instrumented to obtain data for use in future analysis and design of similar structures and to determine the validity of certain assumptions and procedures used to design the lock. The program included the measurement of earth and hydrostatic pressures beneath the base slab and along the walls of the lock and the measurement of stresses and strains within the base slab and walls of the lock. Hydrostatic pressures were measured with piezometers. Soil pressures on the structure and stresses and strains within the structure were measured by electrical measuring devices. Settlement of the lock was determined from observations of settlement reference points, bolts, and plates at various locations in the lock. Deflections of the walls were determined by means of wall deflection pipes and a deflectometer. Engineering measuring devices were read at periodic intervals during and after construction. Observed rebounds were considerably greater than predicted; however, because the bench marks were damaged and, furthermore, may not have been set sufficiently deep, the validity of the measured rebounds is questionable. The magnitudes of observed settlements are also questionable for the same reason. In general, the lock settled at a uniform rate as construction loads were applied; after construction, the rate of settlement decreased sharply. Rebounds and settlements were recomputed using actual loading conditions, which differed somewhat from those assumed in design. The recomputed settlements at the sides of the lock were in good agreement with observed settlements, but recomputed settlements at the center of the lock were less than observed settlements. The observed settlements provided reasonable indications of the deflected shape of the lock. Observations of soil stress meters and piezometers beneath the lock chamber indicated that observed base pressures were greater than those based on the actual weight of the structure. The difference between the observed base pressures (reaction) and the total structure load is attributed mainly to frictional soil forces acting on the sides of the lock. The observed distribution of base pressure was similar to the base pressure distribution at Port Allen Lock except that pressures were greater beneath the culvert and smaller at the center line of the lock than pressures observed at Port Allen Lock. The coefficient of lateral earth pressure k varied along the height of the wall. For the construction condition, k varied from 0.3 along the culvert wall to 0.2 along the wall stem. The k values for the high water condition were similar to those for the construction condition except that they increased near the upper part of the wall stem. Moments computed from observed external loads were affected considerably by frictional forces acting at the outer sides of the lock. For the construction condition, assuming that the difference between observed and actual pressures was due to side friction, the computed moment in the base slab at the center of the lock was 2135 ft-kips, which is 22 percent higher than the design moment; assuming that the soil stress meters overregistered by 10 percent, the computed moment was 1705 ft-kips, or 38 percent less than the design moment; and assuming no side friction, the computed moment was negative.

DD FORM 1 NOV 68 1473 REPLACES DD FORM 1473, 1 JAN 64, WHICH IS OBSOLETE FOR ARMY USE.

Unclassified
Security Classification

14 KEY WORDS	LINK A		LINK B		LINK C	
	ROLE	WT	ROLE	WT	ROLE	WT
Engineering measuring devices						
Instruments and instrumentation						
Locks (waterways)						
Old River Lock						
Pressure measurement						
Soil stresses						

THE CONTENTS OF THIS REPORT ARE NOT TO BE USED FOR ADVERTISING, PUBLICATION, OR PROMOTIONAL PURPOSES. CITATION OF TRADE NAMES DOES NOT CONSTITUTE AN OFFICIAL ENDORSEMENT OR APPROVAL OF THE USE OF SUCH COMMERCIAL PRODUCTS.

FOREWORD

This report presents the results of instrumenting Old River Lock to obtain engineering data for use in the analysis and design of similar structures and to determine the validity of the assumptions and procedures used to design Old River Lock. The instrumentation of Old River Lock was conducted by the U. S. Army Engineer Waterways Experiment Station (WES), Vicksburg, Miss., at the request of the Office, Chief of Engineers (OCE), for the Mississippi River Commission (MRC), which has overall supervision of the comprehensive program for instrumentation of Old River Lock. Collection and analysis of data were made under CW 030, "Prototype Analysis, Structural Behavior of Concrete Structures." WES planned the instrumentation, provided technical supervision of installation of instruments and devices, analyzed all observational data, and prepared this report.

Old River Lock was designed for the U. S. Army Engineer District, New Orleans, La. (NOD), by the engineering firms of Bedell and Nelson Engineers, Inc., and A. W. Thompson and Associates and was built under the supervision of the NOD. Geological studies and soils investigation were made by WES. The plan of excavation, dewatering system, and slope designs were performed by NOD. The plan for the instrumentation was developed by WES, and the devices were installed by NOD, except for electrical measuring devices, which were installed by WES.

Calibration tests on electrical instruments and installation of the electrical measuring devices were supervised by Mr. L. M. Duke, Instrumentation Branch, WES; the field installation was supervised by Mr. A. Hedegaard, Project Engineer. Messrs. H. A. Hueseman, R. V. Bankston, C. J. Nettles, and J. A. Ducote, NOD, were also actively

engaged in the supervision of installation of instruments. Laboratory tests on concrete were conducted by the Concrete Laboratory, WES, under the direction of Mr. E. E. McCoy. Overall supervisor of the instrumentation program was Mr. R. I. Kaufman, MRC. Engineers at WES who were actively engaged in the investigation included Messrs. W. C. Sherman, Jr., and C. C. Trahan of WES and Messrs. J. D. Perrine and C. G. Hadjidakis, formerly of WES.

Messrs. Sherman and Trahan analyzed the data and prepared this report under the general supervision of Messrs. W. J. Turnbull, J. P. Sale, and J. R. Compton, Soils and Pavements Laboratory, WES. The report was reviewed by the NOD and reviewed and approved by the MRC and OCE prior to publication.

Directors of WES during the investigation and the preparation of this report were COL Edmund H. Lang, CE; COL Alex G. Sutton, Jr., CE; COL John R. Oswalt, Jr., CE; COL Levi A. Brown, CE; and COL Ernest D. Peixotto, CE. Technical Directors were Messrs. J. B. Tiffany and F. R. Brown.

CONTENTS

CONTENTS

CONVERSION FACTORS, BRITISH TO METRIC UNITS OF MEASUREMENT

British units of measurement used in this report can be converted to metric units as follows:

Multiply	By	To Obtain
inches	2.54	centimeters
feet	0.3048	meters
miles (U. S. statute)	1.609344	kilometers
square inches	6.4516	square centimeters
cubic yards	0.764555	cubic meters
gallons (U. S. liquid)	3.785412	cubic decimeters
pounds (mass)	0.45359237	kilograms
kips (mass)	453.59237	kilograms
pounds (force)	4.448222	newtons
pounds (force) per foot	14.59390	newtons per meter
pounds (force) per square inch	0.6894757	newtons per square centimeter
pounds (force) per square foot	47.88026	newtons per square meter
tons (force) per square foot	88.76052	kilonewtons per square meter
pounds (mass) per cubic foot	16.0185	kilograms per cubic meter
gallons per minute	3.785412	cubic decimeters per minute
foot-kips	1.3558	meter-kilonewtons
Fahrenheit degrees	5/9	Celsius or Kelvin degrees*

* To obtain Celsius (C) temperature readings from Fahrenheit (F) readings, use the following formula: $C = (5/9)(F - 32)$. To obtain Kelvin (K) readings, use: $K = (5/9)(F - 32) + 273.15$.

SUMMARY

Old River Lock is a reinforced concrete U-frame structure located on the west bank of the Mississippi River about 300 miles above the Head of Passes. The structure was founded at a depth of 71 ft on alluvial sands, an abandoned channel deposit of the Mississippi River that extends in depth to 95 ft below the base of the structure.

At the request of the Mississippi River Commission and with the approval of the Office, Chief of Engineers, Old River Lock was instrumented to obtain data for use in future analysis and design of similar structures and to determine the validity of certain assumptions and procedures used to design the lock. The program included the measurement of earth and hydrostatic pressures beneath the base slab and along the walls of the lock and the measurement of stresses and strains within the base slab and walls of the lock. Hydrostatic pressures were measured with piezometers. Soil pressures on the structure and stresses and strains within the structure were measured by electrical measuring devices. Settlement of the lock was determined from observations of settlement reference points, bolts, and plates at various locations in the lock. Deflections of the walls were determined by means of wall deflection pipes and a deflectometer.

Engineering measuring devices were read at periodic intervals during and after construction. Observed rebounds were considerably greater than predicted; however, because the bench marks were damaged and, furthermore, may not have been set sufficiently deep, the validity of the measured rebounds is questionable. The magnitudes of observed settlements are also questionable for the same reason. In general, the lock settled at a uniform rate as construction loads were applied; after construction, the rate of settlement decreased sharply. Rebounds and settlements were recomputed using actual loading conditions, which differed somewhat from those assumed in design. The recomputed settlements at the sides of the lock were in good agreement with observed settlements, but recomputed settlements at the center of the lock were less than observed settlements. The observed settlements provided reasonable indications of the deflected shape of the lock.

Observations of soil stress meters and piezometers beneath the lock chamber indicated that observed base pressures were greater than those based on the actual weight of the structure. The difference between the observed base pressures (reaction) and the total structure load is attributed mainly to frictional soil forces acting on the sides

of the lock. The observed distribution of base pressure was similar to the base pressure distribution at Port Allen Lock except that pressures were greater beneath the culvert and smaller at the center line of the lock than pressures observed at Port Allen Lock.

The coefficient of lateral earth pressure k varied along the height of the wall. For the construction condition, k varied from 0.3 along the culvert wall to 0.2 along the wall stem. The k values for the high water condition were similar to those for the construction condition except that they increased near the upper part of the wall stem.

Moments computed from observed external loads were affected considerably by frictional forces acting at the outer sides of the lock. For the construction condition, assuming that the difference between observed and actual pressures was due to side friction, the computed moment in the base slab at the center of the lock was 2135 ft-kips, which is 22 percent higher than the design moment; assuming that the soil stress meters overregistered by 10 percent, the computed moment was 1705 ft-kips, or 38 percent less than the design moment; and assuming no side friction, the computed moment was negative.

ANALYSIS OF DATA FROM INSTRUMENTATION PROGRAM
OLD RIVER LOCK

PART I: INTRODUCTION

Purpose of Instrumentation Program

1. At the request of the Mississippi River Commission (MRC) and with the approval of the Office, Chief of Engineers (OCE), a comprehensive plan was developed for the instrumentation of Old River Lock. The purpose of the instrumentation was to obtain data on external soil loading and settlement and internal structural stresses and strains for use in the analysis and design of similar structures and to determine the validity of certain assumptions and procedures used to design Old River Lock. At the time the program for instrumenting Old River Lock was initiated, work was under way on a similar instrumentation program for Port Allen Lock, which is founded on a moderately compressible silt foundation. As Old River Lock was to be founded on a sand foundation, it was considered that data obtained from Old River and Port Allen Locks would be of significant value to those Districts of the Corps of Engineers engaged in the design of future similar-type locks on earth foundations of moderate to low compressibility.

Scope of Report

2. This report presents a summary of soil and foundation studies made in connection with the design of the structure, a description of the engineering measuring devices used in the instrumentation program, analyses and evaluations of observations made during and after construction, conclusions regarding the design of Old River Lock, and recommendations pertaining to the design of similar structures. Appendix A describes the electrical measuring devices and pertinent features of installation of the devices. Appendix B presents the results of field and laboratory tests on concrete, reinforcing steel, and sand backfill.

Details of the design of the structure not included in this report are presented in reference 1. The plan of instrumentation is presented in reference 2. Detailed instructions for installing and observing the instruments are presented in reference 3. Reference 4 is an interim report on the instrumentation program. Information presented in the interim report is also reported herein.

Description of Structure

3. Old River Lock (see fig. 1) is located on the west bank of the Mississippi River about 300 miles* above the Head of Passes. The lock is located in Pointe Coupee Parish, La., about 900 ft south of and parallel to Old River and approximately 1 mile west of the confluence of Old River and the Mississippi River. A general plan of the area is shown in plate 1. The lock is a reinforced concrete U-frame lock structure having a usable chamber 75 ft wide by 1200 ft long with walls 78 ft high and a base slab 12 ft thick. A plan and profile of the structure are shown in plate 2; typical sections are shown in plate 3. A U-frame structure without piles was selected, as cost estimates indicated that this type structure was more economical than other types considered. A compacted sand backfill was provided behind the lock walls to provide lateral support when the walls are subjected to loadings producing outward deflections. Collector drains behind the walls discharge at the canal end of the lock. Gates for the lock are of the horizontal frame-miter type designed for a maximum lift of 37 ft. Filling and emptying of the chamber are accomplished by means of 13-ft-6-in. by 13-ft-6-in. longitudinal wall culverts with side ports in the upper approach monolith and lock chamber and a bottom lateral discharge system in the lower approach monolith. Flow is controlled by means of individually operated segmental valves of the reversed tainter type.

---

* A table of factors for converting British units of measurement to metric units is presented on page ix.

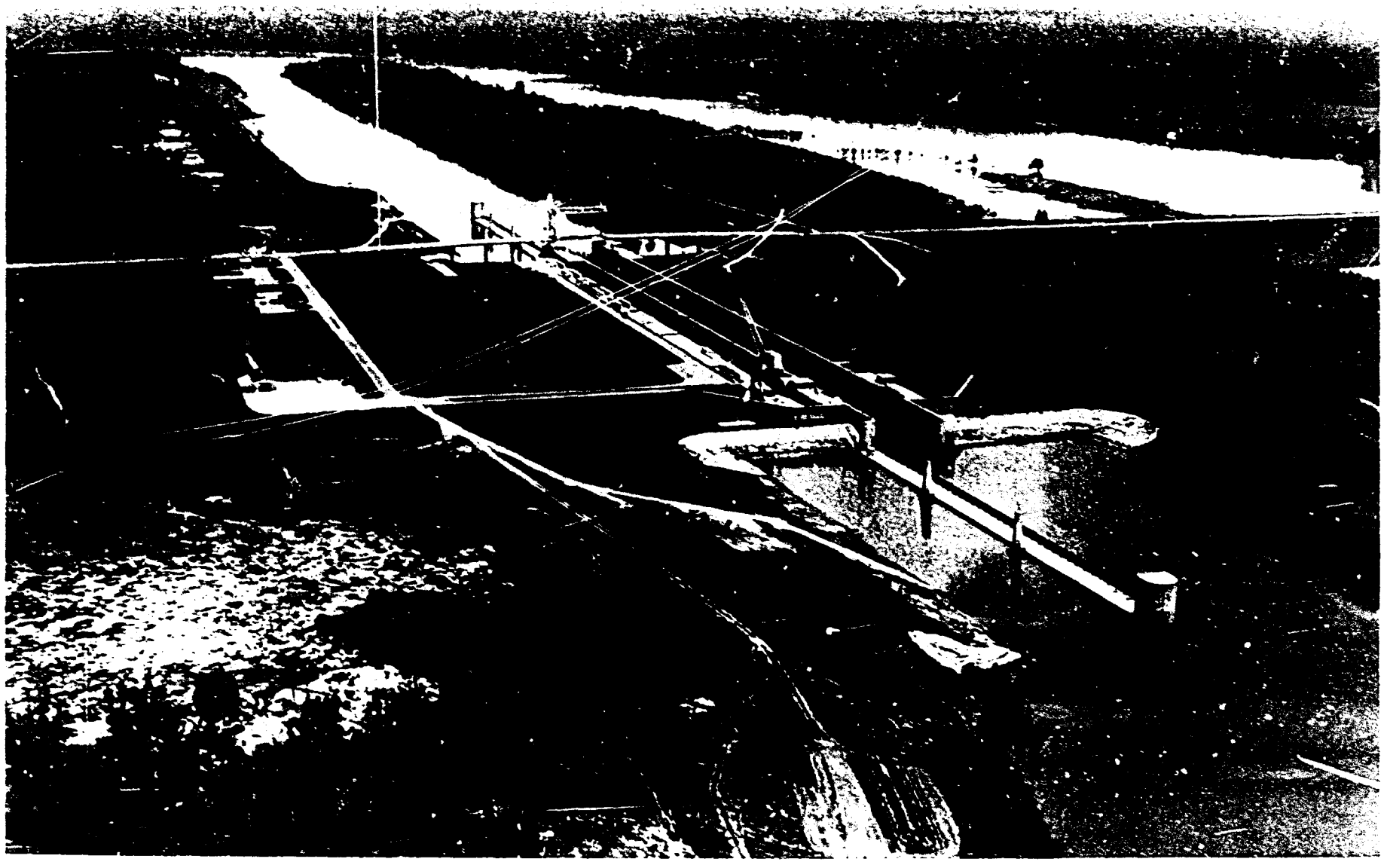

Fig. 1. Aerial view of lock

Construction

General

4. Old River Lock was constructed under the supervision of the U. S. Army Engineer District, New Orleans (NOD). Excavation was initiated in September 1958, and the lock was essentially completed in September 1962 when water was first introduced in the lock. The downstream channel connecting the lock to Old River was completed in December 1962; the upstream channel from the lock to the Mississippi River was completed in February 1963. The lock was placed in operation on 15 March 1963.

Excavation and dewatering

5. The construction of the lock required an excavation 1700 ft long and 71 ft deep, with a bottom width varying from 120 to 140 ft and side slopes averaging 1V on 4H. Natural ground surface at the site averaged el 47* and the bottom of the excavation was at el -24 in the lock chamber area. Plate 4 is a plan of the excavated area. The three-phase excavation is summarized as follows:

Phase	Excavation els	Excavation Began	Excavation Ended	Method of Excavation
1	47 to 27	Sep 58	Feb 59	Hauling equipment
2	27 to -18	Feb 59	May 59	Hydraulic dredge
3	-18 to -24	Jan 60	Mar 60	Hauling equipment

6. Use of hauling equipment for phase 3 excavation was made possible by dewatering the area after completion of phase 2. Dewatering was done by means of 37 deep wells surrounding the excavation and penetrating the sand aquifer. The wells consisted of 12-in.-ID wood-stave screens 85 ft long, with 1/8-in.-slots and surrounded by 9-in.-thick gravel filters. Each well was pumped with a 10-in., 3-stage well turbine having a maximum capacity of 1000 gpm. Details of the design of

---

* All elevations (el) cited herein are in feet referred to mean sea level (msl) unless otherwise noted.

the well system are given in reference 1. This system with minor modifications was used for dewatering during the entire construction period. Design computation indicated that the well system discharge would be 330 gpm per ft of drawdown. During the high-water periods in the springs of 1961 and 1962, the discharge per foot of drawdown was about 33 percent greater than the design value.

7. Upon completion of excavation, the stabilization slab of unreinforced concrete was placed at el -24 to provide a working platform. The slab was 6 in. thick at monolith 12 and 4 in. thick at all other areas. Fig. 2 is an aerial view of the excavation with the base slab partially in place.

8. Sand drains. The design of the dewatering system included 12-in.-diam vertical sand drains on 10-ft centers along the excavation slopes at el +16, penetrating 3 ft into foundation sands. The drains were designed to reduce excess hydrostatic pressures in the stratum of silt approximately between els 5 and 10. Two sections of sand drains were initially installed, one on the north excavation slope from sta 89+10 to 102+40 and the other on the south excavation slope from sta 87+0 to 95+10. Piezometer readings and field observations indicated that the sand drains were of little benefit in stabilizing the excavation slopes; therefore, no additional sand drains were installed.

9. Surface water disposal. Surface runoff was collected into sumps from three main collection ditches: one near natural ground level along the perimeter of the excavation, one along the excavation slope at el +16, and one near the bottom of the excavation. Water collected in the sumps was pumped over the cofferdam.

Concrete placement

10. Placement of concrete in the base slab of the lock was begun in April 1960 and was completed in October 1960. The lock walls were constructed from October 1960 to March 1962. Placement of concrete lifts in the wall monoliths was controlled by specifications to ensure as uniform a loading of the foundation as possible. The lifts of concrete in the walls were so scheduled and placed that at no time was the elevation of the top of concrete in the wall of one monolith more than

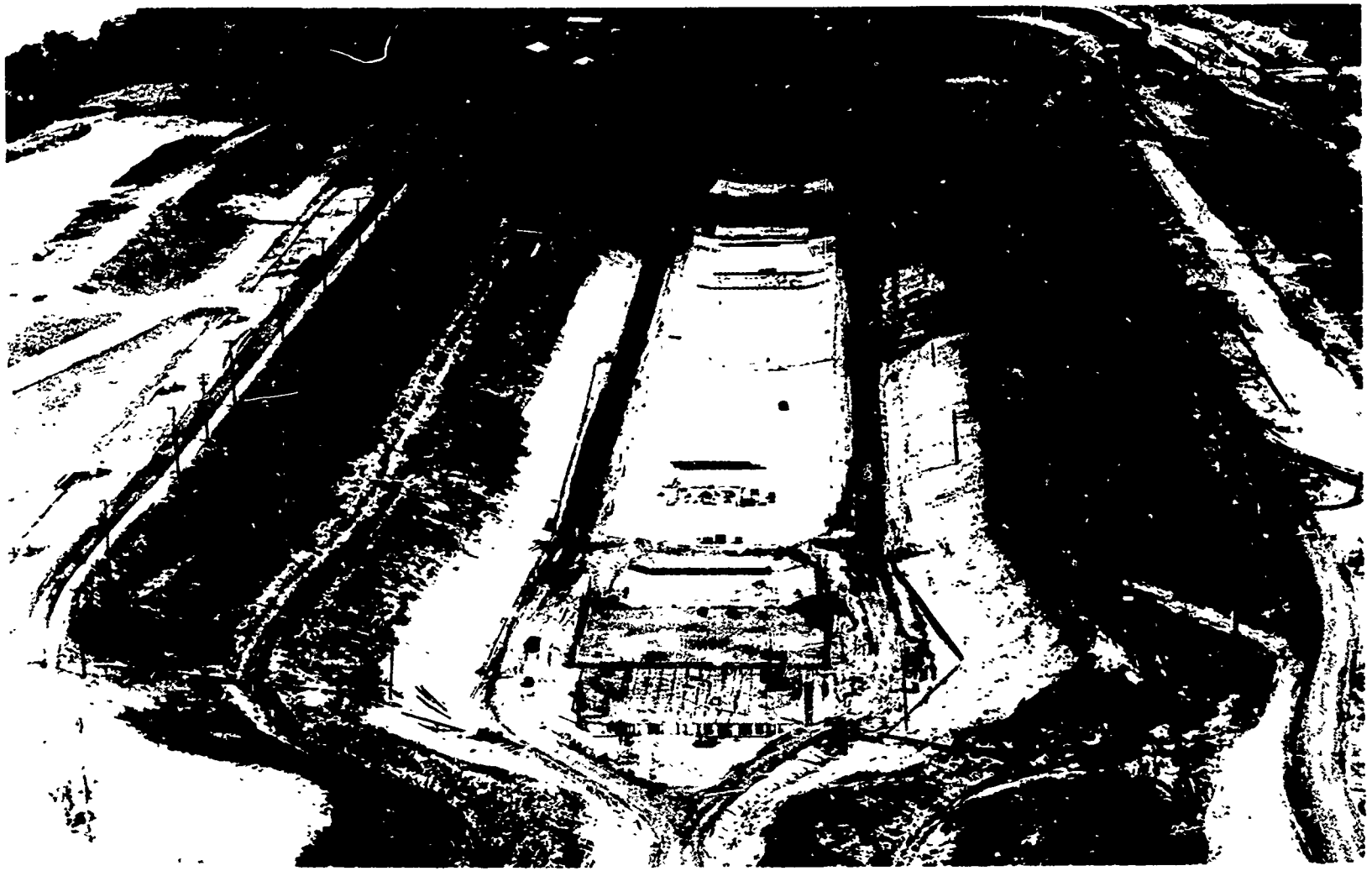

Fig. 2. Aerial view of lock during construction

one lift higher than the elevation of concrete in the opposite wall. Also, at no time was the elevation of the top of concrete in one wall of a monolith higher than one lift above the elevation of the top of concrete in adjacent walls, except in the vicinity of monolith 12. From February 1961, the tops of the walls in monolith 12 were two lifts higher than the tops of the walls in adjacent monoliths 11 and 13, which in turn were two lifts higher than the walls in adjacent monoliths 10 and 14.

Backfill

11. The design of Old River Lock provided for a wedge-shaped section of sand backfill and random backfill, as shown in plate 3. Sand dredged from a sandbar in Old River was used in the random fill area. Backfill behind the walls also included a 5-ft-thick layer of clay on the bottom of the excavation between the outer edge of the lock and upper impervious foundation strata and a 3-ft-thick clay blanket on top of the sand backfill.

12. Details of placement and compaction of the backfill are presented in Appendix B. Backfilling operations were conducted concurrently with wall construction. Specifications required that backfill not be placed until the concrete had cured at least 14 days, except in the case of the culvert walls where no backfill was placed until the roof of the culvert was placed. Backfill was placed simultaneously on opposite sides of the lock, and the elevation of the top of the backfill was kept as nearly uniform as possible throughout the entire length of the structure. The 5-ft-thick clay layer on the bottom of the excavation was placed in April 1961, sand backfill was placed from April 1961 to May 1962, and the 3-ft-thick clay blanket was placed from June to August 1962. The elevations of the top of the backfill and the top of concrete in the structure at monolith 12, together with piezometric levels in the backfill, are shown in plate 5.

PART II: FOUNDATION DESIGN

Foundation Conditions

Site conditions

13. Old River Lock was constructed in an area formerly occupied by an abandoned channel of a meander loop, which was separated from the main channel of the Mississippi River in 1831. The lock is founded directly on clean sand. Generalized soil profiles are shown in plate 6.

Field exploration

14. The locations of all pertinent borings made in the investigation of foundation conditions at the lock are shown in plate 1. Logs of borings along the center line are shown in plate 7. Borings were of the undisturbed and general sample types. Undisturbed samples were taken with 5-in.- and 3-in.-ID thin-wall Shelby tube samplers of the piston type. Generally, 5-in.-diam samples were taken in cohesive materials, and 3-in.-diam samples were taken in the underlying sands. Undisturbed samples of sand were obtained by methods similar to those described in reference 5.

15. In 1953, six piezometers (P-1, -4, -7, -9, -10, and -11) were installed in the sand stratum to determine the relationship between river stages and hydrostatic pressures in the sands. At the same time, five piezometers (P-2, -3, -5, -6, and -8) were installed in the upper silt stratum to determine hydrostatic pressures and groundwater levels in that stratum. Locations of the piezometers are shown in plate 6. Data from piezometers located in the sand stratum and the stages of Old River are shown in plate 8. These observations indicated that the hydrostatic pressures in the sands reflected the stage of Old River. Data for piezometers installed in the silty strata of the overburden and the stages of Old River are plotted in plate 9. Piezometers P-3 and P-5, located in a lean clay and silty sand, respectively, approximately at el 30 reflected a natural groundwater level that tended to rise with high river stages but normally remained relatively constant between els 30 and 32 during low river stages. Piezometers P-2, -6, and -8 were

installed in a silty stratum approximately between els 5 and 10 that was separated from the pervious substratum sands by a nearly continuous stratum of clay. The hydrostatic head in this silt stratum reflected a pressure intermediate between the groundwater level (as indicated by the upper piezometers) and the pressure in the underlying deep sands.

Soil conditions

16. The foundation soils at the lock proper consisted of a cohesive overburden approximately 45 ft thick underlain by a stratum of clean sand approximately 110 ft thick (see plate 6). Immediately below ground surface (el ±46), the overburden consisted of 8 to 15 ft of silty natural levee deposits. The remaining overburden consisted primarily of lean clays with pockets of fat clay and relatively continuous strata of silts and silty sands, and constituted filling in the old channel of the Mississippi River. The top of the clean sand underlying the overburden was fairly constant at about el 0 along the center line of the lock structure and sloped downward at a slope of about 1V on 40H toward Old River in a direction perpendicular to the center line of the lock. Soil conditions northwest and southeast of the lock site along the projected center line indicated the same general sloping top of sand surface with an increasing thickness of cohesive overburden toward the river. The sand stratum extends to el -118, at which depth Tertiary clays are encountered. A 3- to 8-ft-thick clay stratum was found approximately at el -75 beneath the lock site. The bottom of Old River adjacent to the structure extends down to el -43.

17. The water content of the natural levee deposits at the ground surface varied from about 12 to 45 percent and averaged about 25 percent. The underlying clays had water contents ranging from about 28 to 47 percent. The silty strata within the channel filling had water contents ranging from about 26 to 36 percent.

18. Split-spoon resistances of the foundation soils as indicated by boring L-30 were as follows: the natural levee deposits had a split-spoon resistance of 4 to 12 blows per ft; the resistance of the underlying clays ranged from 3 to 15 blows per ft, generally increasing with

depth; the split-spoon resistance of the underlying sands varied between 83 and over 100 blows per ft.

Laboratory tests

19. Classification data. Classification data, consisting of all mechanical analyses and Atterberg limit tests made on samples of the clay and silt overburden, and a summary of the grain-size curves for the foundation sands are shown in plate 10. The uniformity of the foundation sands between el 0 and -72 is depicted by their narrow range in gradation. The grain-size curves for samples from the lower portion of the sand (below el -80) indicate that these sands are considerably coarser and contain more gravel than those from the upper portion.

20. Density of sands. Natural density determinations were made on samples from continuous undisturbed borings in the sand stratum. The natural dry density for the upper portion of foundation sands (el 0 to -72) varied between 90 and 103 lb/cu ft, with an average value of about 99 lb/cu ft. The natural dry density below el -80 varied approximately between 102 and 108 lb/cu ft, with an average of about 104 lb/cu ft. The frequency distribution diagram shown in plate 10 indicates a modal natural dry density of about 101 lb/cu ft for 128 samples; the mean dry density was about 99 lb/cu ft.

21. Maximum and minimum dry density determinations were performed on several samples from about el -72 on which the natural dry densities had been obtained. The results of the density determinations are plotted versus D_{50} size in plate 10. Both maximum and minimum dry densities increased with increasing grain size, as did the natural dry density. The relative density was found to be practically constant for the range of grain sizes encountered in the upper sands at the lock site; the average relative density ranged from 61 to 67 percent, indicating that the foundation sands above el -72 are in a medium-dense condition.

22. Consolidation tests. Consolidation tests were performed on remolded and undisturbed samples of the foundation sands below el -24 to permit an estimate of settlement beneath the lock structure. A consolidation test also was performed on a sample of the deep clay stratum in

the sand foundation. The pressure-void ratio curves for the soils tested are shown in plate 11; pertinent data for each sample are summarized in the table on the same plate.

23. Four consolidation tests were performed on undisturbed samples of sand that had been kept frozen from the time the samples were removed from the ground until they were tested. These samples were loaded to the overburden pressure, unloaded to the estimated stress after excavation, then reloaded to obtain a recompression curve (see plate 11). Consolidation tests on remolded samples of sand were run at three different void ratios as shown in plate 11. These tests were performed to determine the effect of densification on the settlement characteristics of the sand and also to serve as a check on the results obtained from the undisturbed samples. The pressure-void ratio curves for the remolded samples at natural density are in fair agreement with pressure-void ratio curves for undisturbed samples of similar material. Some of the sands contained lignite; however, comparative tests indicated that the lignite did not significantly affect their consolidation characteristics.

U-Frame Design

Design procedures for U-frame locks

24. Old River Lock was designed as a reinforced concrete U-frame structure. The primary forces acting on such a structure are shown in fig. 3. The base pressures oppose the downward load of a lock, which consists of the weight of concrete in the lock W_C, the weight of the water inside the lock W_W, the weight of the backfill above the culverts W_B, and the vertical component of the lateral earth pressures E_V. The downward thrust W is resisted by the uplift forces μ and effective foundation base pressures p. The magnitude of the uplift pressures depends on the upstream and downstream water elevations, the character of the foundation strata, and the nature and effectiveness of measures installed to control uplift pressures. Uplift pressures generally vary significantly along the length of a lock. The distribution of

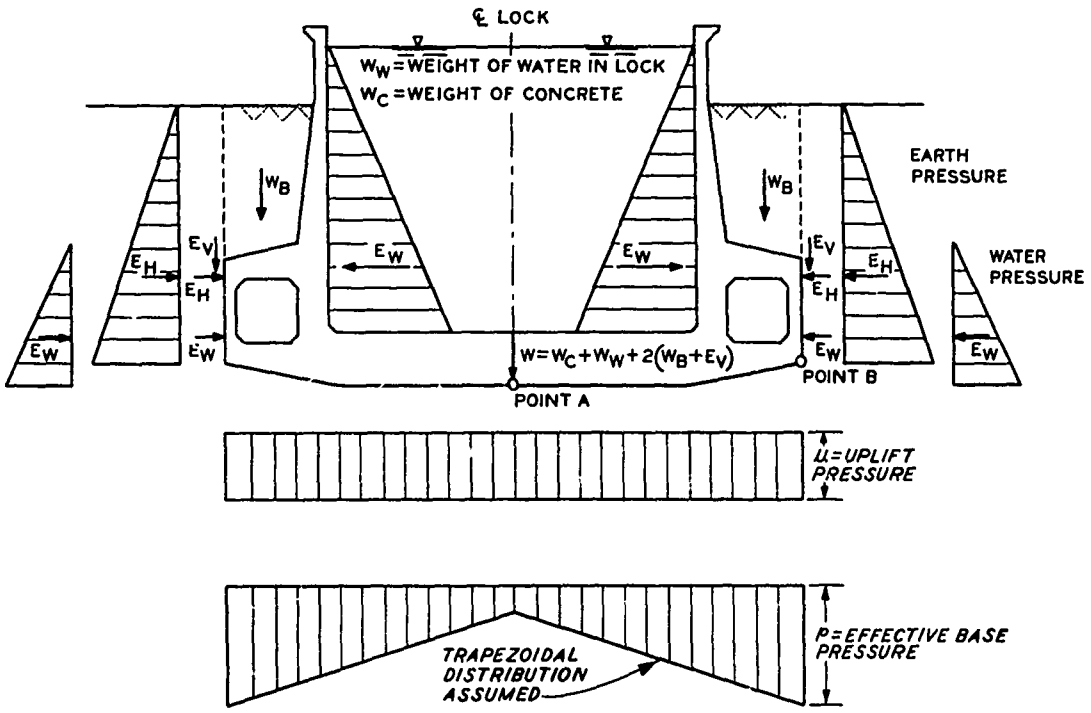

Fig. 3. Force system on lock and assumed base pressure distribution

effective base pressures is dependent upon complex interactions between soil and structural elements of a lock and is the major unknown factor in design. The lateral pressures exerted on lock walls include the water pressure in the backfill and in the lock E_W and the effective horizontal earth pressures E_H, which are dependent on the type and in-place characteristics of backfill material and are also functions of the wall movement. Consequently, the principal elements of design for a U-frame section consist of ensuring the safety of the chamber sections against flotation, determining the stresses occurring at the center of the base slab and at its juncture with the chamber walls, analyzing the culvert frame, if used, and analyzing the stability of the sidewalls. The design is always based on two principal load conditions: (a) lock empty and (b) lock full. Other load conditions (i.e., lock complete with no backfill placed and lock partially filled), oftentimes as critical, may develop during and after construction. These must also be considered in design.

Design of base slab

25. In determining the effective foundation base pressures, a trial procedure similar to that employed at Port Allen Lock was used. In this method, the rebound of the foundation due to excavation and the load imposed by the lock and backfill are taken into consideration, together with the attendant differential settlement between the lock walls and the center of the lock chamber. The distribution of the pressure was assumed to be defined by equating the deformations of the structural base slab and those of the foundation soils. A distribution of the foundation pressure that satisfies the normal equation of equilibrium is assumed. The corresponding deformations of the soil are then computed on the basis of the consolidation characteristics of the foundation soils. The arbitrary assumption of a base pressure distribution will generally indicate deformations of the slab that differ from the corresponding deformations of the soil. Consequently, new base pressure distributions are chosen and analyzed until the desired degree of agreement between structure and soil deformations is obtained. A trapezoidal distribution was assumed (see fig. 4) that has the advantage that the

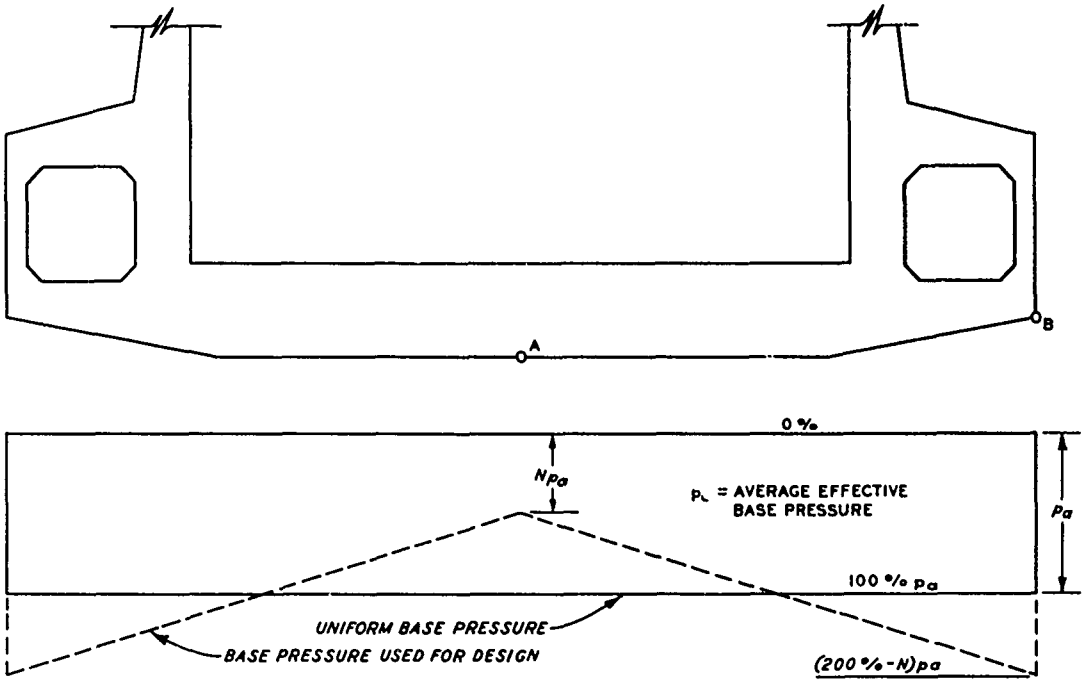

Fig. 4. Assumed base pressure distribution for design

distribution can be presented in terms of a single factor N for a wide variety of loadings. N is equal to the percentage of uniform base pressure acting beneath the center of the lock. The trapezoidal distribution also greatly facilitates the determination of vertical stresses within the foundation soils for purposes of estimating settlements. The assumption of a trapezoidal base pressure distribution was used for the design of Port Allen Lock[7] and the gate bays at Bayou Boeuf Lock.[8] In regard to Old River Lock, preliminary assumptions were made with respect to lateral earth pressures against the walls and distribution of the foundation base pressure as expressed by different values of N. Moments and deflections of the base slab were then computed and compared with the deformation of the foundation obtained from a settlement analysis using the assumed base pressure distribution. In computing deflections, base slabs were treated as unreinforced concrete sections, and the elastic deflections were computed assuming that E = 3,000,000 psi. Elastic deflections thus determined were then increased 100 percent to allow for the effect of plastic flow. Results of the rebound and settlement analyses that were made to determine the foundation base pressures for design loading conditions are described below. Analyses were made for each of the gate bays and the center monolith of the lock chamber; only the analysis made for the lock chamber is described.

Rebound and settlement analyses

26. Rebound analysis. It was assumed that the foundation was an isotropic material to which elastic theory could be applied. Vertical stresses in the foundation were computed using charts and tables based on Boussinesq's equations. In computing the changes in stress due to excavation, it was assumed that the surface of the foundation was located at the level of the bottom of the excavation, assumed to be at el -23.5, and that the weight of the excavated material was applied as a negative stress at this level. At any depth, the negative stress resuling from excavation added algebraically to the original overburden pressure gave the excavation pressure. The overburden and excavation pressures were computed for the midpoints of each of the design strata below points A and B (see fig. 5) under the lock chamber. Analyses were made

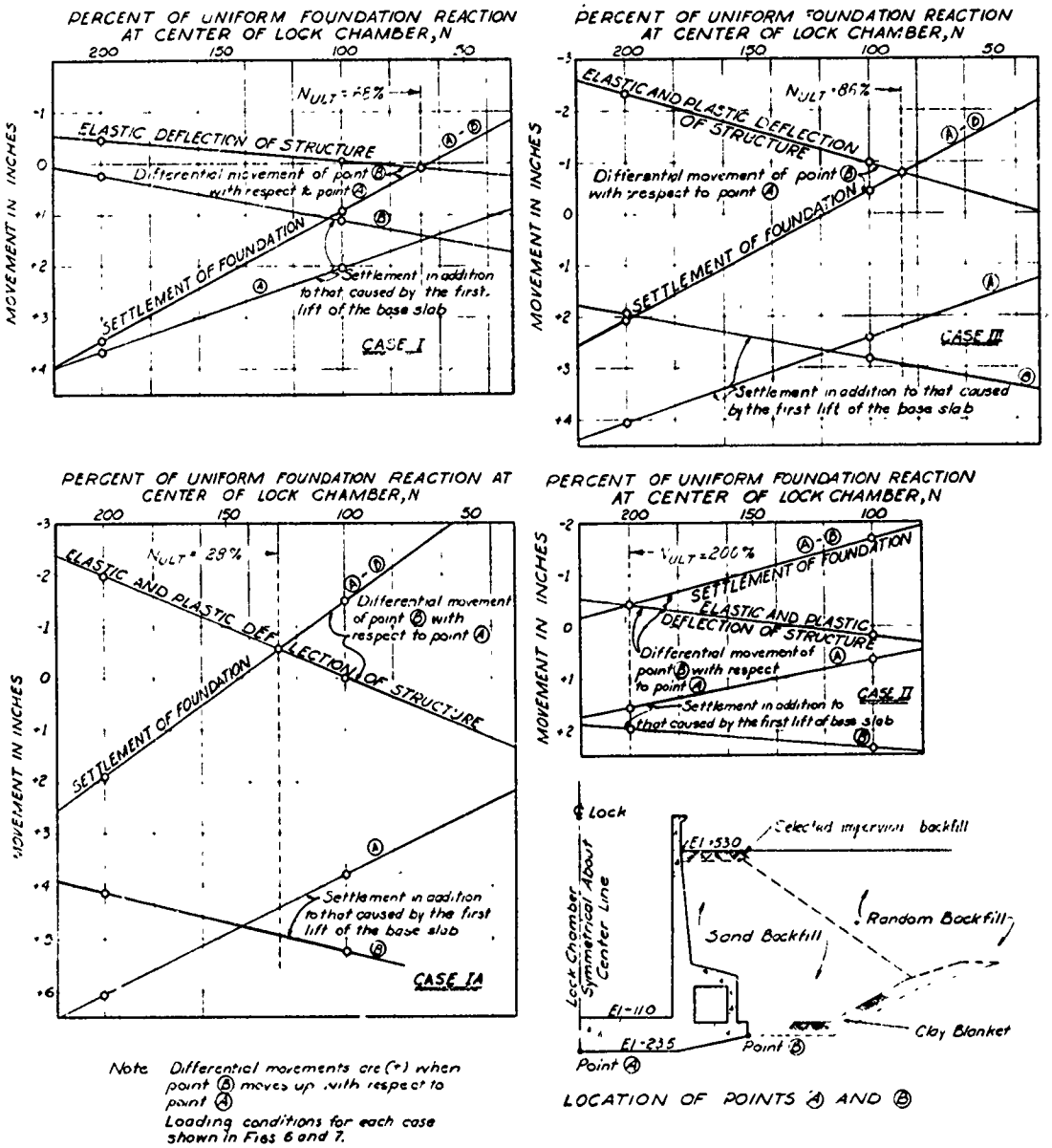

Fig. 5. Determination of base pressure distribution and settlement for design

for conditions at boring LS-2, which were considered typical of soil conditions beneath the lock (see plate 7 for boring log).

27. The piezometric data shown in plates 8 and 9 were used in estimating the original overburden pressure. For design purposes, it was assumed that excavation would be performed during low-water season. Therefore, in computing the original overburden pressure, the water table was assumed to be at el 10. It was assumed that the water table would be 5 ft below the bottom of the excavation (el -28.5) when excavation was completed

28. The foundation rebounds were computed using the rebound loops of the laboratory pressure-void ratio curves. The laboratory curves were adjusted, when necessary, to the computed overburden and excavation pressure for both points. The computed rebound was 0.29 and 0.21 ft at points A and B, respectively.

29. Settlement analysis and determination of N. For design of the lock, settlement and effective base pressure beneath the lock chamber were computed assuming that all foundation rebound would occur before construction of the base slab was initiated. The assumption was considered reasonable, as the laboratory consolidation tests indicated that the major portion of the rebound would occur instantaneously. Ultimate settlements were computed for the following four cases:

a. Case I. Structure complete with no backfill in place. Hydrostatic pressures in foundation sands assumed lowered to 5 ft below bottom of excavation (el -28.5).

b. Case IA. Structure complete with backfill in place, but no water in the lock. Uplift pressure beneath the base slab assumed equal to 10.5 ft (el -13).

c. Case II. Structure dewatered. Uplift pressure beneath base slab assumed equal to 61.5 ft (el +38).

d. Case III. Structure in operation with water level in the lock at el 65. Uplift pressures beneath base slab assumed equal to 76.5 ft (el 53).

30. At each point selected for analysis, ultimate settlements caused by the weight of the first lift of concrete for the base slab were computed assuming this portion of the slab to act as a heavy fluid. All successive differential movements in the structure and foundation

were referred to the elevations of the points after the first lift of concrete had set.

31. The ultimate settlement and foundation reaction for each case listed were computed for assumed values of N (percentage of uniform base pressure at center of lock) of 100 and 200 percent. The settlements at points A and B for each value of N , after the settlement caused by the first lift of the base slab had been deducted, were plotted as shown in fig. 5. On the same plots, the differential settlement between points A and B and the differential movement between points A and B resulting from elastic and plastic movement of the structure under load are also shown as functions of N . The intersection of the line of differential movement of points A and B due to foundation settlement and the line of differential movement of points A and B due to deflection of the structure gave the foundation base pressures in terms of N for each case. A summary of settlements and N values for each case is shown in fig. 5.

32. Design base pressures. Values of N = 68 percent and N = 128 percent were computed for the foundation base pressure distributions for Cases I and IA, respectively, and those values were used to compute moments in the base slab for the two cases. A value of N = 200 percent was computed for Case II. However, it was found that a slight variation in N would cause a relatively large change in moments in the base slab. Therefore, the value of N = 150 percent was arbitrarily selected for Case II and was found to be more critical. For Case III, the lock chamber was designed for N = 104 percent. Summaries of the foundation base pressures used for design are shown in figs. 6 and 7.

Design of lock chamber walls

33. As shown in figs. 6 and 7, the lock chamber walls were designed assuming an at-rest earth pressure for Case IA and Case II and a combination of passive earth pressure and at-rest pressure for Case III. A coefficient of at-rest earth pressure equal to 0.5 was assumed. It was considered that maximum wall movements toward the backfill during Case III loading would not be sufficient to develop a full passive earth

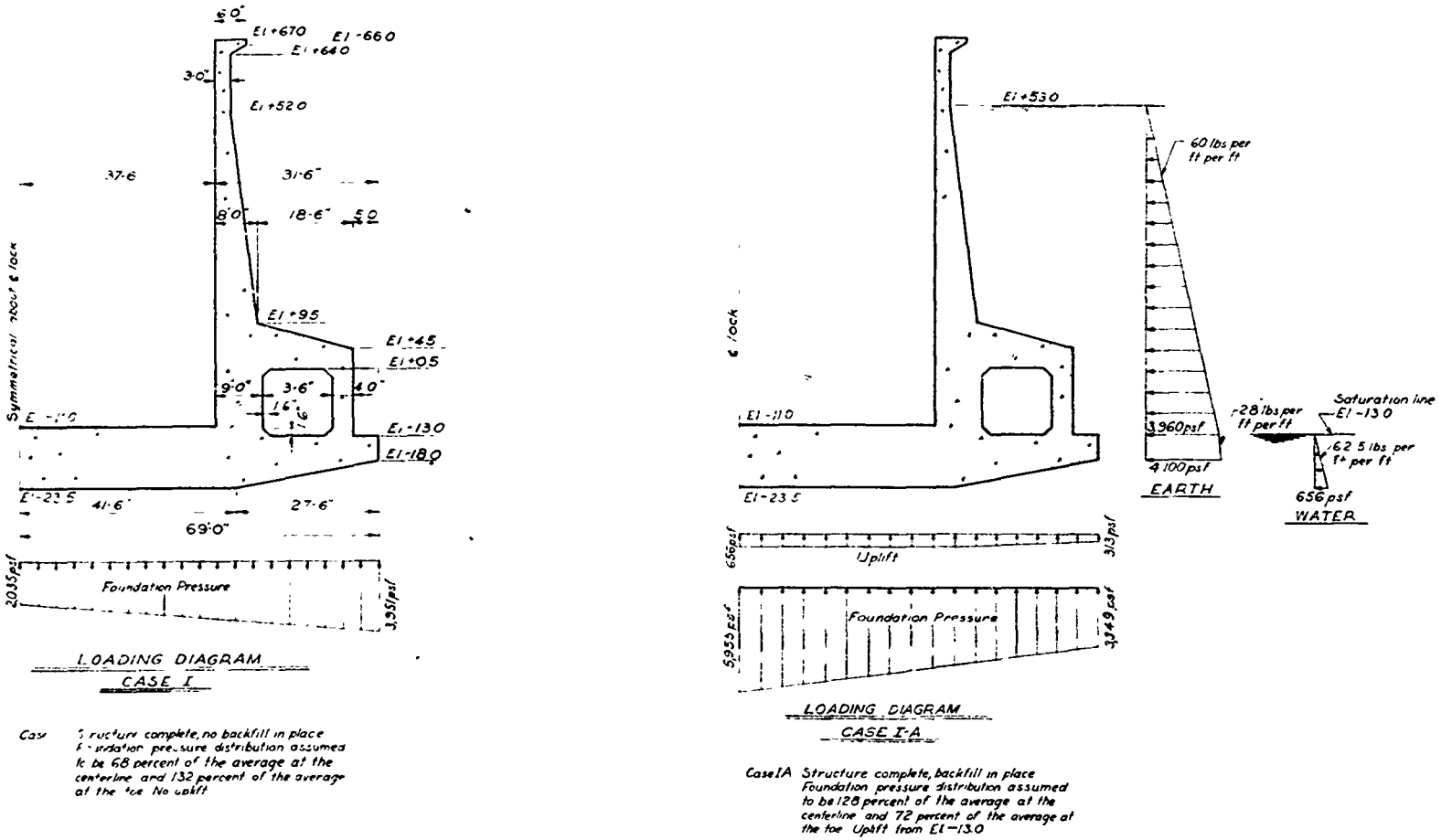

Case I Structure complete, no backfill in place Foundation pressure distribution assumed to be 68 percent of the average at the centerline and 132 percent of the average at the toe No uplift

Case IA Structure complete, backfill in place Foundation pressure distribution assumed to be 128 percent of the average at the centerline and 72 percent of the average at the toe Uplift from El −130

Fig. 6. Summary of base pressures used for design, Cases I and IA

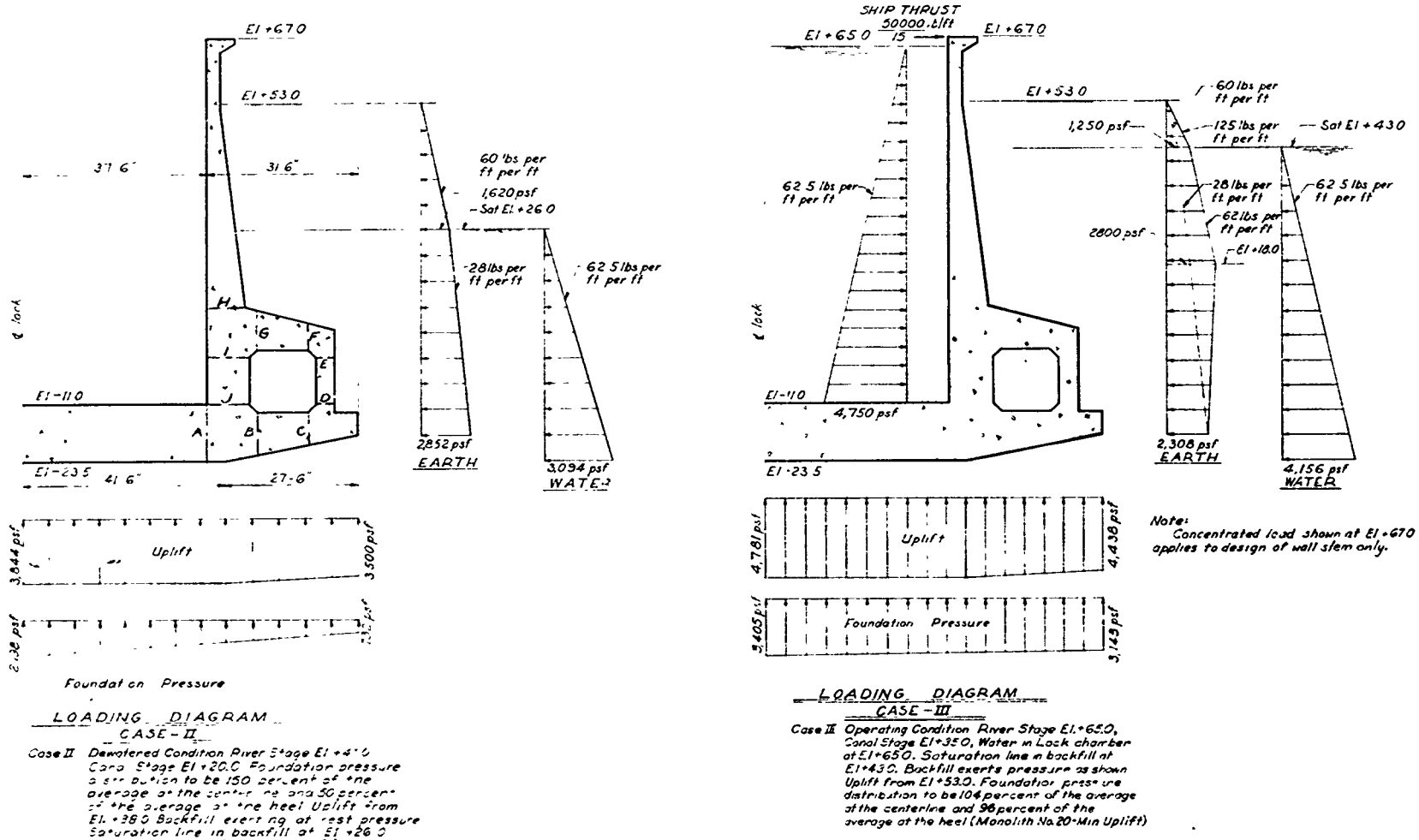

Fig. 7. Summary of base pressures used for design, Cases II and III

pressure. On the basis of relationships between wall movement and lateral earth pressure given by Terzaghi,[9] it was assumed that the mobilization of partial passive pressures could be presented by a coefficient of lateral earth pressure equal to 1. For Case III, a coefficient of lateral earth pressure equal to 1 was assumed from the top of backfill to the middepth of fill (el 18), with the earth pressure decreasing linearly below el 18 to at-rest pressure at the base of the structure.

Design of joints

34. To allow for expansion and contraction and to provide for settlement, the lock was constructed in monoliths ranging from 60 to 100 ft in length as shown in plate 2. Monolith joints were treated as expansion joints in the walls and as crack-control joints in the base slab. Details of the joints between the chamber monoliths are shown in fig. 8. The joints in the base slab contained a 1/2-in.-thick expanding filler for a distance of about 1-1/2 ft from the top and bottom of the slab. Between these two joints, the concrete was placed in contact with adjacent slabs. Three-bulb waterstops were installed near the top and bottom of the slabs. Steel dowels extended through the joints in the base slab and were wrapped about 2 ft on each side of the joint to prevent bonding with the concrete if contraction should occur and cause the joint to open slightly. These dowels consist of smooth bars and are designed to tie the monoliths together but still allow opening of the joint due to contraction of the concrete. The dowels are also designed to prevent differential settlement between adjacent monoliths at the joint.

35. The thickness of the joint filler in wall joints was determined to allow for structure expansion and movement due to differential settlement of adjacent monoliths. Between lock chamber monoliths, where differential settlement would be minor, the thickness of joint material varies in steps from 1 in. at the top of the wall to 1/2 in. at the bottom. At the gate-bay monoliths, where greater movement was anticipated, the thickness of the joint material at the top of the walls was increased, the maximum being 2 in. between the river approach bay and the river gate bay and between the canal approach bay and canal gate bay.

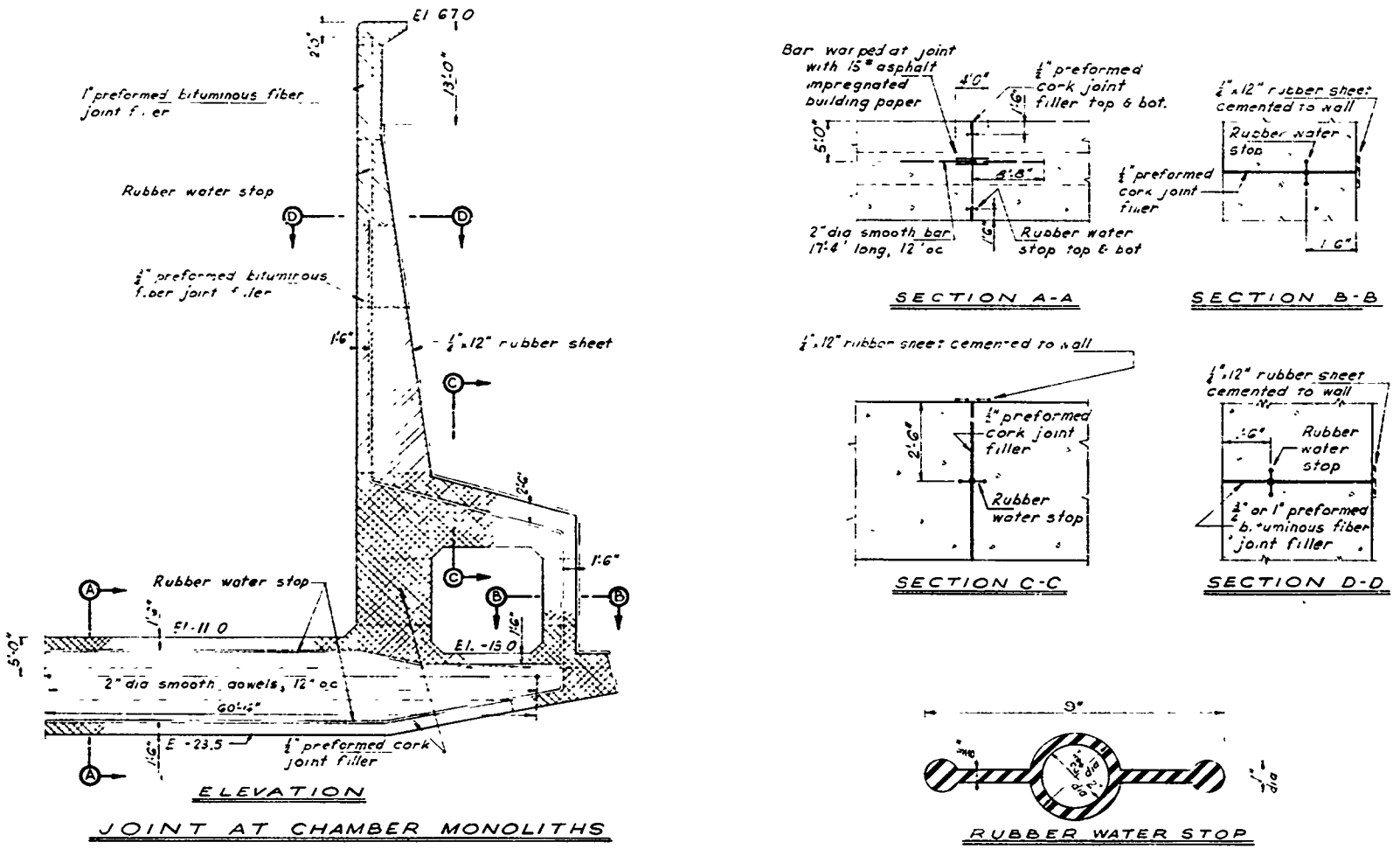

Fig. 8. Details of chamber monolith joints

Each joint was provided with a three-bulb waterstop and covered with a rubber strip to prevent backfill from infiltrating into the joint. To minimize differential settlement of the monoliths, it was specified that backfill be brought up concurrently on each side of the lock as soon as possible and at as uniform a depth as possible.

PART III: INSTRUMENTATION

General Plan

36. The plan of instrumentation of Old River Lock included installation of the following engineering measuring devices:

a. Two permanent bench marks.

b. Heave plugs to measure foundation rebound during excavation.

c. Settlement reference points, bolts, and plates to determine settlement at selected points in the lock during and after construction.

d. Sounding wells to determine the elevation of the water at various points in the lock chamber and gate bays.

e. Piezometers to measure hydrostatic pressures beneath the structure and in the backfill behind the walls of the lock.

f. Earth pressure cells to determine the magnitude and distribution of foundation and wall pressures.

g. Strain meters and stress meters and a pore pressure cell installed in concrete to measure stresses, strains, and pore pressures within the structure.

h. Resistance thermometers in concrete to determine the temperature near the top of the lock walls.

i. Wall deflection pipes to determine the deflections of the walls by means of a deflectometer.

37. The locations of engineering measuring devices are shown in plates 12 and 13. The primary installation of measuring devices, including all electrical measuring devices, was located near the center of the lock at monolith 12. Measuring devices, except for electrical instruments, were also installed in both of the gate bays.

Bench Marks and Level Observations

38. Two bench marks were initially installed at the site at the following locations:

Bench Mark	Lock Station	Offset from ℄ in ft	Elevation in ft msl Bottom	Top
PBM-1	105+50	400 N	-92.8	+41.870
PBM-2	118+00	800 N	-93.0	+53.309

The bench marks were founded in deep sands with the riser pipes protected by sleeves to eliminate the effects of drag resulting from movements of the overburden soil. Details are shown in fig. 9. During the early part of construction, PBM-1 was damaged and PBM-2 destroyed by heavy construction equipment. PBM-1 was subsequently repaired and its elevation reestablished. In general, all level observations were referred directly to the permanent bench mark by means of precise leveling techniques.

Heave and Settlement Reference Points

Heave points

39. To determine the rebound of the foundation during and after excavation, nine heave points were installed in the foundation prior to construction. The heave points, each consisting of a 5-in.-diam, 2-ft-long steel pipe with a vented cap, were driven below the bottoms of auger holes to elevations corresponding to about 2 ft below final excavation, and the exact elevation of the top of each heave point was determined at the time of installation. The locations and initial elevations of the heave points are given in table 1. As soon as the excavation was brought to grade, the soil above the top of the heave point was excavated carefully by hand and the top of the heave point was uncovered enough that its elevation could be determined. The elevations were corrected for the lateral offsets of the heave points from the points of installation at ground surface. The lateral offsets are shown in table 1 with the corresponding corrections used to determine the exact elevations of the heave points. Two of the heave points, H-2 and H-9, were inadvertently destroyed during excavation, and no rebound measurement could be made of those two points.

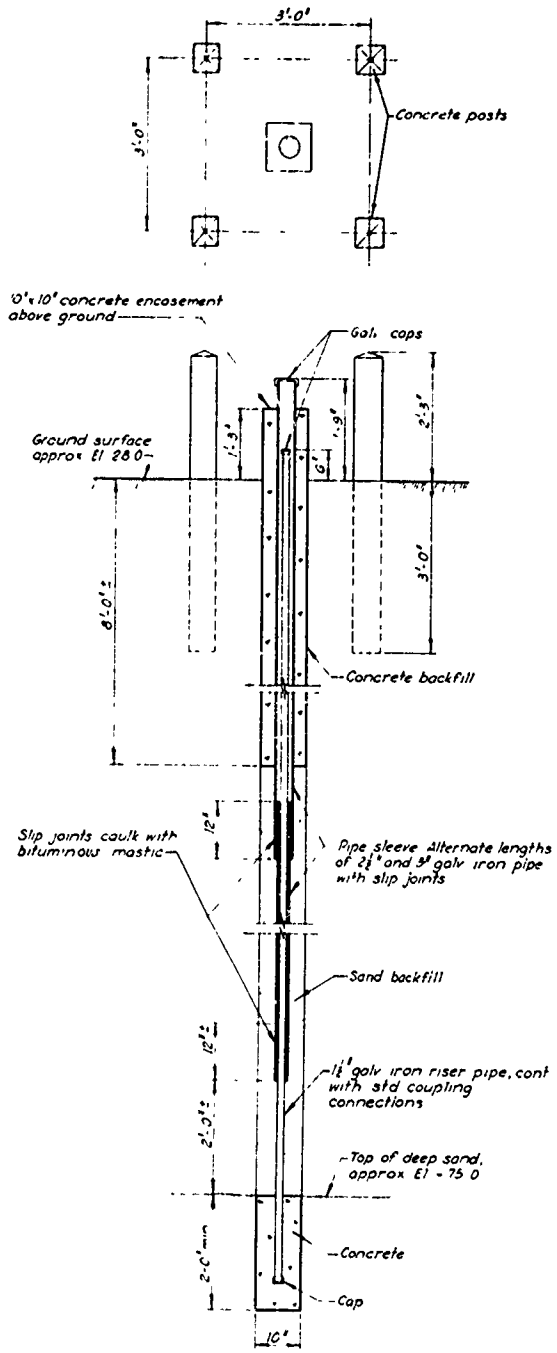

Fig. 9. Details of bench mark

40. The observed rebounds and subsequent settlements are shown in plates 14-17. Maximum observed rebound varied from 0.48 ft at monolith 2 to 0.42 ft at monolith 1. However, as the bench mark was damaged and subsequently repaired between the initial observation and the observation made after recovery, there is some question as to the accuracy of the measured rebounds. Analysis of the observed rebound and settlements is presented in Part IV.

Temporary settlement reference points

41. Temporary settlement reference points were installed to determine settlement of the foundation during construction until permanent reference points were installed. Three of the points were installed in the canal-end gate bay (monolith 2), four were installed in the river-side gate bay (monolith 22), and five in monolith 12. Details of the reference points are shown in fig. 10. The reference points, which consisted of 1-1/4-in.-diam steel pipe, were driven about 3-1/2 ft into the foundation at the bottom of the final excavation just prior to placement of the stabilization slab. A reference cap was fastened to the top of the pipe to permit accurate determinations of elevations. The temporary reference points were observed until the elevations were transferred to permanent reference points on the floor of the lock and on top of the culvert. The observed movements of the temporary reference points are shown in plates 14-16.

Type A reference points

42. Two type A reference points were installed in the foundation beneath the north edge of monolith 12 to obtain a comparison between the observed and estimated settlement of the foundation. One of the points was installed in the deep sands at el -100; the other was installed just above the clay layer at el -66. Two additional type A reference points were installed in the deep sands at el -100 at the river-side and land-side gate bays. Details of the type A reference points and locations of the points are shown in fig. 11 and in plates 13 and 14. Each point consisted of a 10-in.-diam by 2-ft-long concrete plug with an embedded riser pipe that extended to ground surface. Additional sections of riser pipe were added as backfill was placed above the reference points.

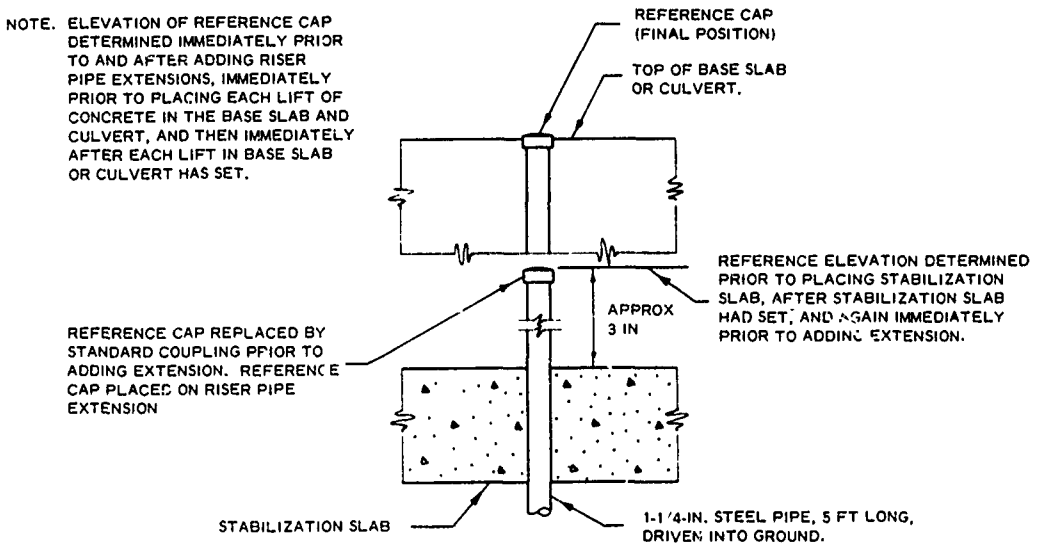

TEMPORARY SETTLEMENT REFERENCE POINT

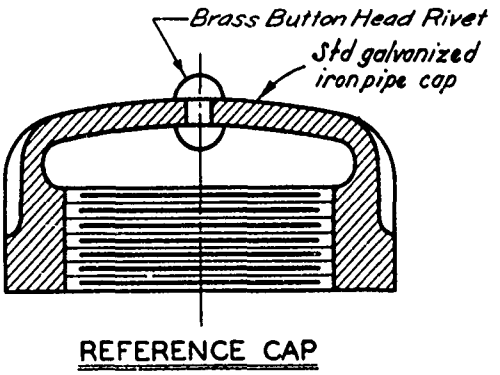

REFERENCE CAP

LOCATION OF TEMPORARY SETTLEMENT REFERENCE POINTS

POINT NO.	MONOLITH NO	LOCK STATION	OFFSET FROM ℄ LOCK, FT	DATE INSTALLED
T-1	22	90+71	37 N	22 MARCH 1960
T-2	22	90+71	℄	22 MARCH 1960
T-3	22	90+71	37 S	22 MARCH 1960
T-4	22	90+71	67 S	22 MARCH 1960
T-5	12	96+95	66 N	2 APRIL 1960
T-6	12	96+95	37 N	2 APRIL 1960
T-7	12	96+95	3 N	2 APRIL 1960
T-8	12	96+95	37 S	2 APRIL 1960
T-9	12	96+95	66 S	2 APRIL 1960
T-10	2	103+17	37 S	22 MARCH 1960
T-11	2	103+17	℄	22 MARCH 1960
T-12	2	103+17	37 N	22 MARCH 1960

Fig. 10. Temporary settlement reference points

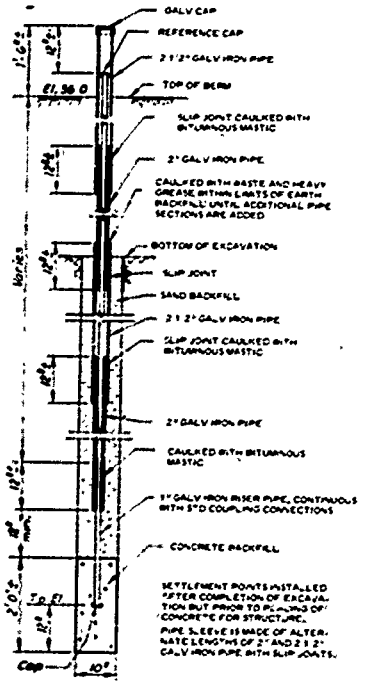

SETTLEMENT REFERENCE POINT TYPE "A"

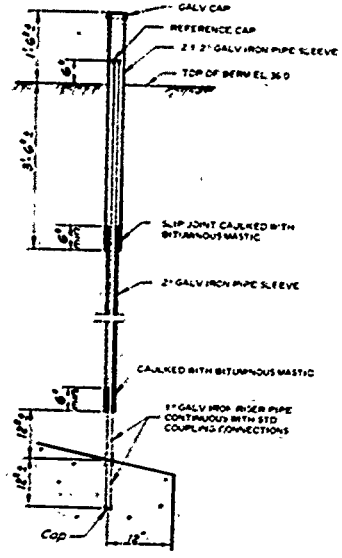

SETTLEMENT REFERENCE POINT TYPE "B"

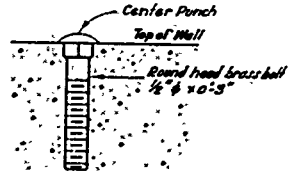

SETTLEMENT REFERENCE BOLT

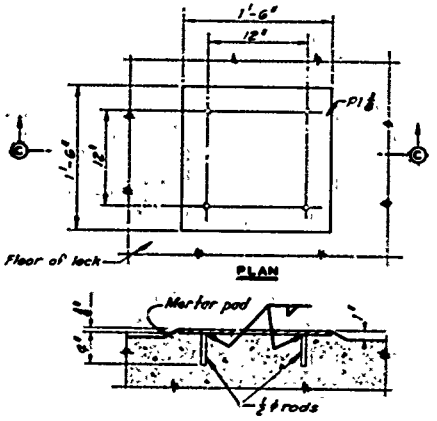

STEEL REFERENCE PLATE

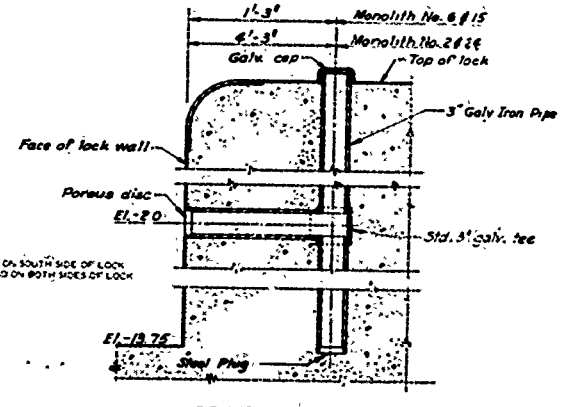

SOUNDING WELL

LOCATION OF SETTLEMENT REFERENCE POINTS, TYPE A

POINT NO	MONOLITH NO	LOCK STATION	OFFSET FROM ℄ LOCK, FT	TIP EL.	DATE INSTALLED
SR 1	22	90+77	77 N	+100	2 MAR. 1960
SR 2	12	97+03	77 N	+66	2 MAR. 1960
SR 3	12	97+06	77 N	+100	2 MAR. 1960
SR 4	2	103+00	76 N	+100	1 MAR. 1960

LOCATION OF SETTLEMENT REFERENCE POINTS, TYPE B

POINT NO	MONOLITH NO	LOCK STATION	OFFSET FROM ℄ LOCK, FT	DATE INSTALLED
SR 5	22	90+77	67.5 N	3 DEC. 1960
SR 6	22	90+77	67.5 S	4 JAN. 1961
SR 7	12	97+01	69 N	12 JAN. 1961
SR 8	12	97+01	69 S	12 JAN. 1961
SR 9	2	103+22	70 N	4 JAN. 1961
SR 10	2	103+23	70 S	7 DEC. 1960

NOTE: SOUNDING WELLS INSTALLED ON SOUTH SIDE OF LOCK AT STA 90+81 AND 103+23 AND ON BOTH SIDES OF LOCK AT STA 98+01.

Fig. 11. Settlement reference points and plates and sounding wells

The observed movements of the type A reference points are shown in plate 18.

Type B reference points

43. The elevations of the tops of the culverts at monoliths 2, 12, and 22 were determined from type B settlement reference points. Details and locations of these points are shown in fig. 11. Each point is a riser pipe that has its lower end embedded in the concrete structure and its upper portion surrounded by an outer sleeve. The observed data are shown in plates 14-16.

Settlement reference plates

44. Seven stainless-steel-clad settlement reference plates, 18-in. square, were installed near the center of each gate bay and in monolith 12 to permit measurements of the deflection and settlement of the base slab during construction and after the lock was placed in operation. Details and locations of the settlement reference plates are shown in fig. 11.

45. Initial elevations of the plates were determined using both the precise leveling method and a water-level measuring device described below. After the lock was flooded, the elevations of the plates were determined using either the water-level device shown in fig. 12 or a deepwater sounding device, shown in fig. 13. Detailed descriptions of the devices are given in reference 7. The water-level device required the use of a boat and was generally used when the water level in the lock was less than 25 ft. Observations of the settlement plates are shown in plates 14-16. Deflections of the base slab computed from the settlement observations are shown in plates 19-21.

Reference bolts on tops of walls

46. Reference bolts (see fig. 11) for determining the settlement and movement of the walls of the lock were installed in the concrete at the tops of the walls immediately after their completion at the locations shown in plate 12. Settlement surveys were made periodically, and the longitudinal distances between reference bolts on each side of a wall joint were determined at intervals to determine the amount of joint opening or closing occurring after construction. Profiles of settlement

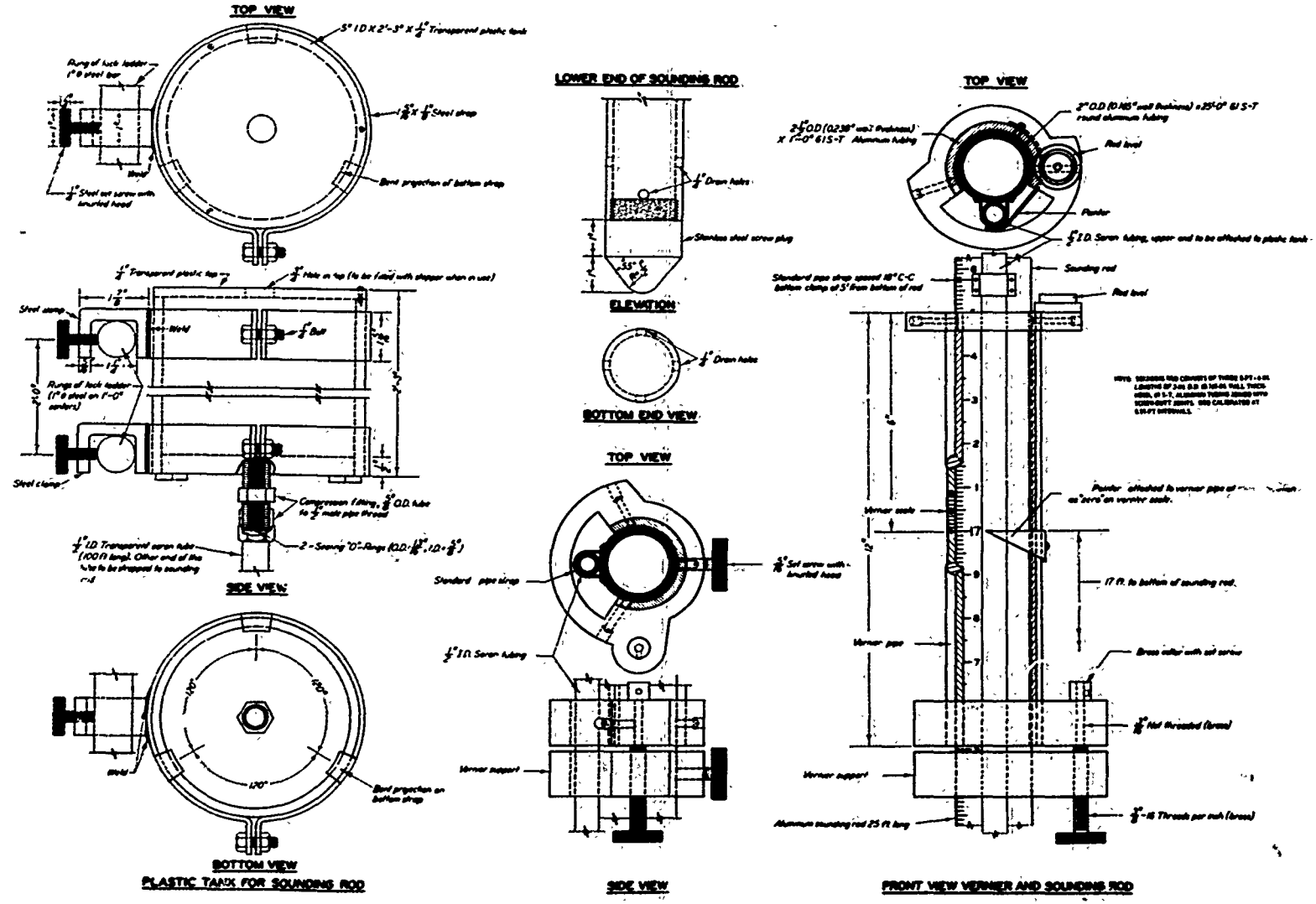

Fig. 12. Details of water-level device

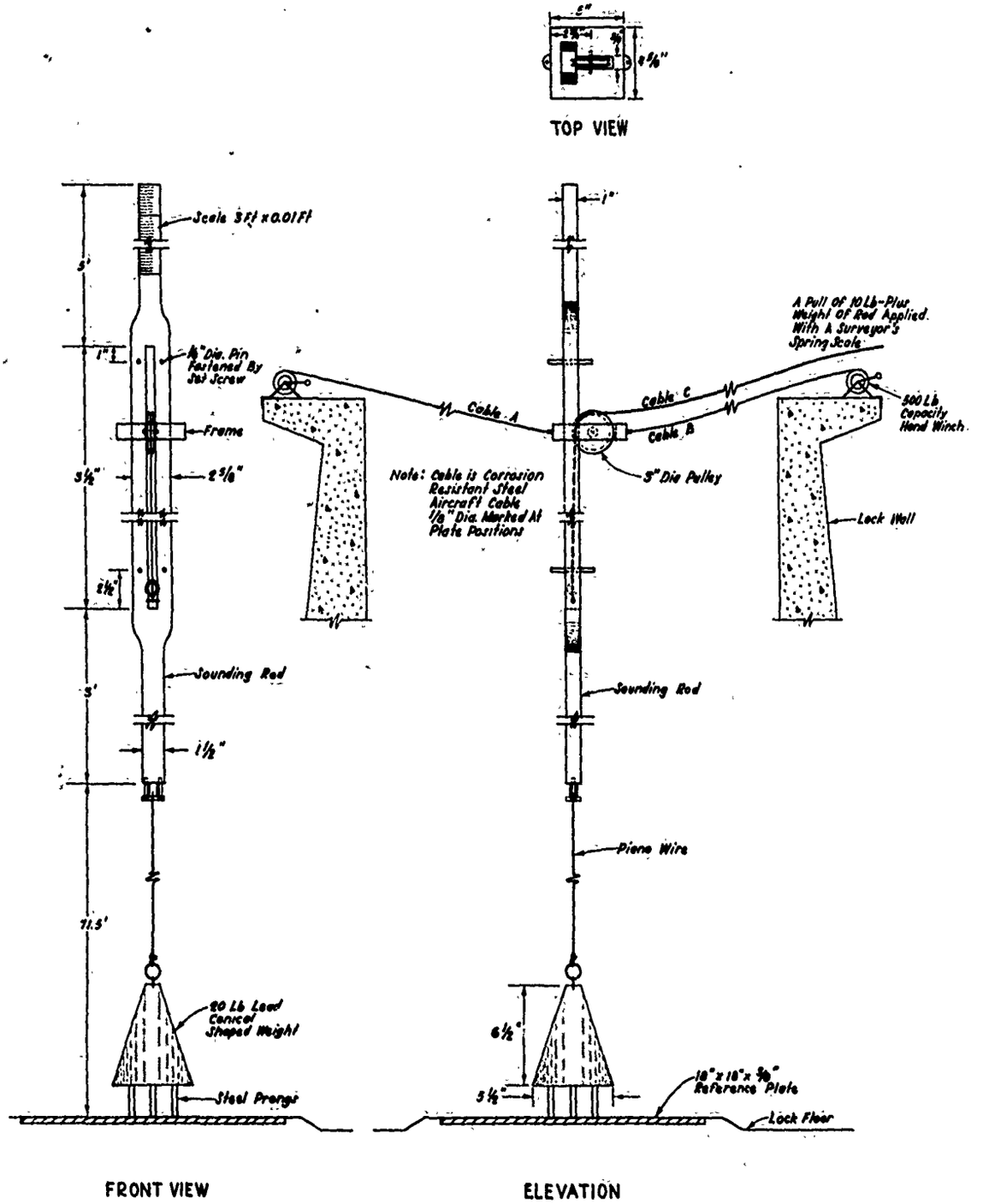

Fig. 13. Details of deepwater sounding device

of the tops of the lock walls and joint movements are shown in plate 22.

Sounding Wells and Piezometers

Sounding wells

47. Four sounding wells consisting of 3-in.-ID pipe were installed in the walls of the lock chamber and gate bays at locations shown in plate 12 to permit accurate determinations of the water levels inside and outside the lock chamber. Details of the sounding wells are shown in fig. 11. The wells were sounded by means of electrical sounding devices used also for sounding piezometers. A few months after water entered the lock, it became apparent that the water levels in the sounding wells were not the same as the water level in the lock, and it was concluded that the porous disks of the wells (see fig. 11) were clogged. Readings of the sounding wells were therefore discontinued.

Piezometers

48. Piezometers were installed beneath and adjacent to the lock structure at the locations shown in plate 13. The piezometers were designated as follows: "A" piezometers are those installed in the deep foundation sands, "B" piezometers are those installed in the foundation sands immediately beneath the lock, and "C" piezometers are those in the sand wedge backfill along the lock. Details of the piezometers are shown in fig. 14. As the earth pressure cells and stress meters record total pressures, a sufficient number of piezometers were installed adjacent to these devices to determine the hydrostatic pressures and thus make possible the determination of the effective pressures acting on the devices.

49. The stages of Old River during and after construction are shown in plate 5 along with the average piezometric head in the foundation sands and in the sand backfill at monolith 12. Time plots of the individual piezometers are shown in plates 23-26. Piezometric profiles along the center line of the lock for selected dates corresponding approximately to water levels assumed for the design cases are shown in plate 27.

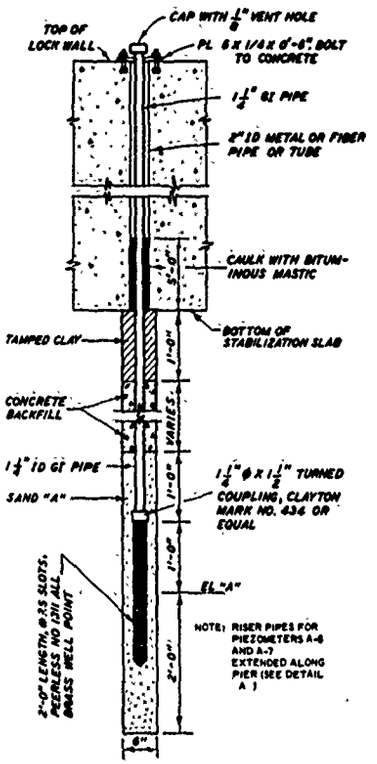

PIEZOMETER "A"

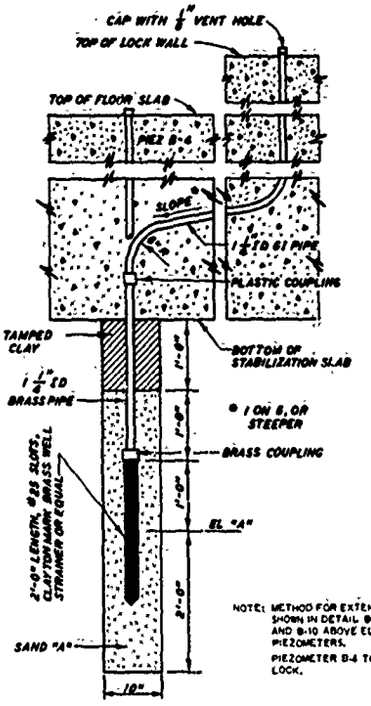

PIEZOMETER B

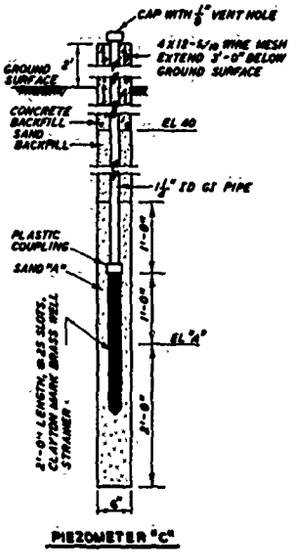

PIEZOMETER "C"

NOTE: METHOD FOR EXTENSION OF RISER PIPES FOR B PIEZOMETERS SHOWN IN DETAIL B. TOPS OF RISERS FOR PIEZOMETERS B-5 AND B-10 ABOVE EL 40 TO BE PROTECTED AS SHOWN FOR C PIEZOMETERS.

PIEZOMETER B-4 TO BE FILLED WITH GROUT PRIOR TO FLOODING LOCK.

LOCATION OF PIEZOMETERS

PIEZ NO.	MONOLITH NO.	LOCK STATION	OFFSET FROM ℄ LOCK, FT	EL "A"	DATE INSTALLED
A-1	22	90+35	39 S	+74.9	25 FEB, 1960
A-2	18	93+40	39 S	+40.0	25 FEB, 1960
A-3	12	96+93	39 S	+85.0	26 FEB, 1960
A-4	6	100+60	39 S	+43.0	20 FEB, 1960
A-5	1	104+45	39 S	+80.0	18 FEB, 1960
A-6	-	106+35	℄	+50.0	18 FEB, 1960
A-7	-	108+60	℄	+40.0	17 FEB, 1960
B-1	22	90+76	39 N	+90.5	7 MAR, 1960
B-2	22	90+76	℄	+90.5	7 MAR, 1960
B-3	22	90+76	39 S	+90.5	7 MAR, 1960
B-4	12	96+92	℄	+29.0	4 APR, 1960
B-5	12	95+89	66 N	+22.0	4 APR, 1960
B-6	12	95+89	39 N	+27.0	4 APR, 1960
B-7	12	96+89	℄	+27.0	4 APR, 1960
B-8	12	96+89	19 S	+27.0	4 APR, 1960
B-9	12	96+87	39 S	+27.0	4 APR, 1960
B-10	12	96+83	66 S	+22.0	4 APR, 1960
B-11	2	103+21	39 N	+35.5	10 MAR, 1960
B-12	2	103+21	℄	+35.5	10 MAR, 1960
B-13	2	103+21	39 S	+35.5	10 MAR 1960
C-1	23	89+78	70.5 N	2.0	22 JULY 1961
C-2	23	89+78	70.5 S	2.5	27 JULY 1961
C-3	22	90+77	74 N	2.0	18 JULY 1961
C-4	22	90+77	74 S	2.0	7 JULY 1961
C-5	12	96+83	46 N	21.0	28 SEPT, 1961
C-6	12	96+89	69 N	+4.0	29 MAY 1961
C-7	12	96+89	46 S	24.0	5 OCT, 1961
C-8	12	96+89	69 S	12.0	6 SEPT, 1961
C-9	12	96+90	69 S	3.0	24 JUNE 1961
C-10	12	96+89	69 S	+10.0	22 MAY 1961
C-11	2	103+22	74 N	2.0	5 JUNE 1961
C-12	2	103+22	74 S	2.0	5 JUNE 1961

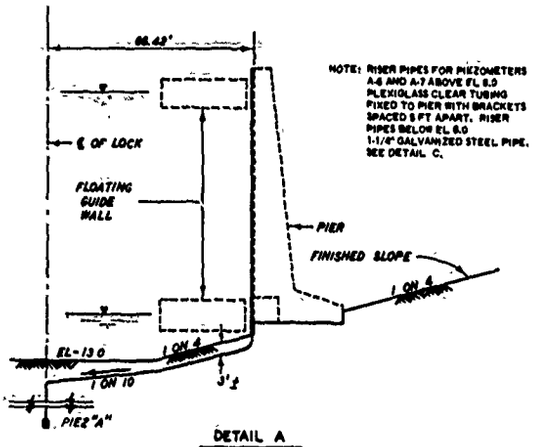

NOTE: RISER PIPES FOR PIEZOMETERS A-6 AND A-7 ABOVE EL 8.0 PLEXIGLASS CLEAR TUBING FIXED TO PIER WITH BRACKETS SPACED 8 FT APART. RISER PIPES BELOW EL 8.0 1-1/4" GALVANIZED STEEL PIPE. SEE DETAIL C.

DETAIL A

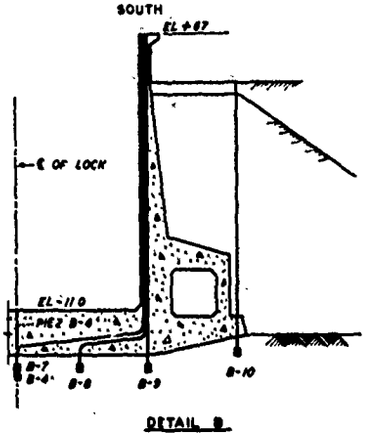

DETAIL B

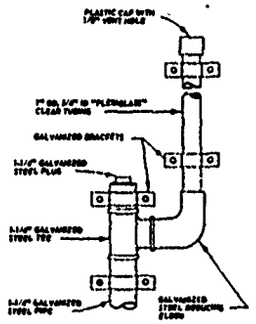

DETAIL C

Fig. 14. Piezometer details

Electrical Measuring Devices

Description and location

50. Electrical measuring devices consisted of soil stress meters, concrete stress meters, strain meters, a pore pressure cell, and resistance thermometers obtained from Dr. R. W. Carlson,[10] Berkeley, Calif., and WES pressure cells fabricated at WES. The devices are described in Appendix A. Additional details concerning the Carlson devices are given in reference 11. All electrical measuring devices were installed in the lock structure at monolith 12; the locations are shown in plate 13. All devices were carefully checked and calibrated in the laboratory prior to installation, and close control was maintained to ensure proper installation in the field. The results of the calibration tests and pertinent features of the installation of the devices are given in Appendix A.

Observations

51. All devices were read immediately before and after concrete had been placed around them. The devices were also read the following day; subsequently, until February 1962, the devices were read once a week and before and after each lift of concrete was placed in monolith 12. From March 1962 until about a month after the lock was flooded (October 1962), the devices were read every two weeks, and from November 1962 to June 1964, the devices were read once a month.

Carlson soil stress meters and WES pressure cells

52. Twenty-two Carlson soil stress meters were installed beneath the base slab and along the walls of the lock to measure base pressures and lateral earth pressures. Five WES pressure cells were installed adjacent to the soil stress meters to provide an additional check on observed pressures. The Carlson soil stress meters and WES pressure cells indicate the total pressure acting on the devices. As the design of base slab and walls is dependent on the assumed distribution of effective pressures, all observed pressures were converted to effective pressures (total pressure minus uplift). Appropriate calibration constants as discussed in Appendix A were used for each device in computing

the effect of uplift pressure determined from piezometers set beneath the lock and in the backfill. The resulting effective pressures at each device during and after construction are shown in plates 28-37. Also shown in these plates are the uplift pressures at the devices and pertinent features of construction. Computed pressures based on the weight of concrete in the base slab are shown for the period prior to construction of the walls. For the devices located in the walls, a time plot of elevations of top of backfill is shown. In those instances where a WES pressure cell was installed adjacent to a Carlson soil stress meter, the data for the two devices are shown in the same plot.

Carlson strain meters

53. Thirty-seven Carlson strain meters were installed to measure elastic strain of the concrete in the base slab and walls. Two "no stress" strain meters were installed in the base slab to measure strains that are independent of stress. The length changes indicated by the strain meters were converted into elastic strains by making proper corrections for thermal expansion or contraction of the meter frame and surrounding concrete. The elastic strains are plotted versus time in plates 38-54. Data from strain meters M-19, M-20, and M-25 are not shown, as the observed readings were well outside the range of readings indicated by the other meters.

54. The main purpose of the strain meters was to permit computation of concrete stresses that, in the case of tensile stresses, cannot be measured by available devices such as concrete stress meters. Under rapid conditions of loading, the change in stress is determined by multiplying the change in strain by the modulus of elasticity of the concrete. However, for loads applied over a relatively long period of time, consideration must be given to the change in the modulus of elasticity with time and to deformations resulting from creep and other causes. The magnitude of deformations resulting from creep and other causes was estimated from the laboratory tests described in Appendix B. The computed stresses for each regular strain meter are shown with the measured strains in plates 39-54. Stresses were computed using a method suggested in reference 10. The stress-time plots were used to determine

the distribution of internal stresses as described in subsequent analyses.

Concrete stress meters

55. Time plots for stresses indicated by the four Carlson concrete stress meters in the base slab are shown in plate 55.

Concrete pore pressure cell

56. A single pore pressure cell (PP-1) was installed in the concrete slab as described in Appendix A to measure pore pressures in the vicinity of the concrete stress meters. A week after its installation, the meter became inoperative; therefore, the pore pressure in the base slab could not be measured.

Resistance thermometers

57. No temperature-time plots were prepared for the two resistance thermometers located near the top of the south wall in monolith 12; the data pertinent to particular case analyses are presented with the analyses.

Wall Deflection Pipes

58. Four wall deflection pipes were installed, one in each wall of monolith 12 and two in the south wall of the river-side gate bay (see plate 12 for locations). Descriptions of the deflection pipes and the deflectometer used to read the pipes are given in Appendix A.

59. During wall construction, deflection pipes were read after each lift of concrete was placed in the monolith in which the pipes were located. The deflection pipes were also read when the backfill behind the lock walls was completed (August 1962), and they were subsequently read at the same time that settlement reference plates were read. Data from wall deflection pipes in terms of horizontal movement of the top of the wall and angular rotation of the top with respect to the base of the wall are shown in plates 56 and 57. Horizontal movements and deflections of the wall at various elevations are shown for selected dates in plates 20 and 21. As a check on the wall deflection pipe readings, the distances between reference points located on the top of each wall were

measured with a steel tape at periodic intervals of time after the walls were completed. A plot showing the comparison of the change in distance between the lock walls as measured by the steel tape and the change in distance as computed from deflection pipe data is shown in plate 58. The difference between the two types of measurements may reflect errors inherent in the measuring techniques.

PART IV: REBOUND, SETTLEMENT, AND DEFLECTIONS

Rebound and Settlement

Observed and predicted rebounds

60. The observed rebound of the foundation due to excavation at various sections perpendicular to the center line of the lock (at monoliths 2, 12, and 22) is shown in plates 14-16; the observed rebound along the center line of the lock is shown in plate 17. A maximum rebound of 0.48 ft was observed at the river-side gate bay (monolith 22). The rebound decreased along the length of the lock to a minimum value of 0.42 ft at the canal-side approach bay (monolith 1). At monolith 12, the observed rebound (0.45 ft) was approximately uniform across the width of the lock. Also shown in plates 14-17 are the rebounds predicted in design. The observed rebounds were considerably greater than the rebounds predicted in design. The predicted rebounds varied from 0.32 ft at the river-side gate bay to 0.17 ft at the downstream edge of the canal approach bay. The subsequent settlement at each monolith (2, 12, and 22) due to structural load was considerably less than the observed rebound, even though the structure load is approximately equal to the weight of the original overburden. From these observations, it appears that the observed rebounds are in error. It is probable that the bench marks were not set sufficiently deep and may have been affected by deep settlements caused by construction dewatering. As shown in plate 5, the piezometric head in the deep sands was lowered as much as 70 ft during construction and this may have caused significant settlement below the bottom of the bench marks. Furthermore, as previously mentioned, the bench marks were damaged or destroyed by the contractor during the early stages of construction.

Observed and predicted settlement

61. Foundation settlements at monoliths 2, 12, and 22 are shown in plates 14-16; settlements along the center line of the lock are shown in plate 17. All settlements are referred to the readings made just before the first lift of the base slab was placed. With only the base

slab in place, the settlement was fairly uniform across the width of the lock. At monolith 12, settlement at the center of the slab was only slightly (0.02 ft) greater than settlement at the edges of the slab. Subsequent placement of walls and backfill resulted in the edge of the lock settling more than the center. As in the case of the observed rebound, the observed settlement may be in error as a result of movements below the bench marks due to variations in groundwater level during construction (see plot of piezometer head in deep sands in plate 5).

62. All engineering measuring devices were read when conditions were similar to those assumed in the design of the lock. At monolith 12, the walls were brought up faster than walls in adjacent monoliths, as previously described. Just before the backfilling operations began in April 1961, the tops of the walls in monolith 12 were at el +52, or 15 ft below final height. The latter condition was somewhat similar to the Case I condition assumed in design (lock complete, no backfill). In August 1962, a condition existed that was very similar to the Case IA condition assumed in design (lock and backfill complete, no water in lock). Case II assumed that the lock was dewatered; this condition had not been realized as of the date of this report. During a high-water period in April 1963, the water level in the lock reached el 44.3, 20.7 ft below design flood stage of el 65.0 ft assumed in the lock for Case III. For simplicity in the following discussions, reference to Cases I, IA, and III will be used to designate loading conditions assumed in the design, and references to Cases I', IA', and III' will be used to designate corresponding cases but with actual loading conditions existing when the observations were made. A comparison of conditions for Cases I and I', IA and IA', and III and III' is shown below:

	Elevation, ft msl			
	Top of Wall	Water Level in Lock	Water Level in Backfill	Piezometric Level Beneath Lock
Case I	67.0	Empty	No backfill	-28.5
Case I'	52.0	Empty	No backfill	-26.4
Case IA	—	Empty	-13.0	-13.0
Case IA'	—	Empty	4.2	-7.0
Case III	—	65.0	43.0	53.0
Case III'	—	44.3	25.1	42.2

63. Observed settlements at monolith 12 for the conditions corresponding to Cases I', IA', and III' are shown in plate 15. There was very little settlement due to placement of concrete (Case I'). The greatest settlement occurred during placement of backfill behind the walls and over the culverts. The settlements predicted in design for Cases I, IA, and III are also shown in plate 15. The observed settlements for Cases I' and IA' were less than settlements predicted for design Cases I and IA, whereas the settlements observed for Case III' were greater than predicted settlements for design Case III. A comparison of predicted and observed settlements at monolith 12 is given in the following tabulation:

	Predicted Settlement, ft			Observed Settlement, ft	
	Center	Sides		Center	Sides
Case I	0.22	0.16	Case I'	0.08	0.05
Case IA	0.46	0.46	Case IA'	0.30	0.35
Case III	0.28	0.29	Case III'	0.34	0.37

64. Observed and predicted settlements at monoliths 2 and 22 are shown in plates 14 and 16, respectively. Case I was not realized at these monoliths because the backfill was placed at the same time that the walls were being constructed. Also, settlement plates on the lock floor at monolith 22 were not observed during the 1963 high-water period because the deepwater sounding device could not penetrate the sediments on top of the lock floor. A comparison of predicted and observed settlements for the two gate-bay monoliths is given below:

	Predicted Settlement, ft			Observed Settlement, ft	
	Center	Sides		Center	Sides
Monolith 2			Monolith 2		
Case IA	0.45	0.45	Case IA'	0.25	0.34
Case III	0.28	0.35	Case III'	0.31	0.39
Monolith 22			Monolith 22		
Case IA	0.49	0.46	Case IA'	0.29	0.34
Case III	0.29	0.28	Case III'	--	0.38

Here also the observed settlements for Case IA' were less than

settlements predicted for Case IA, and observed settlements for Case III' were greater than predicted settlements.

Settlement and
movement at wall joints

65. The settlement of the tops of the walls and the longitudinal movement at the wall joints as of January 1964 are shown in plate 22. The observed settlements of the walls varied from 0.05 ft at monolith 15 to 0.23 ft at monolith 12. Actually, settlements at the tops of the walls were relatively uniform; the apparent differential settlement between monoliths reflects differences in completion time for individual monoliths. For instance, monolith 12, which showed a settlement of 0.23 ft, was completed in August 1961, while adjacent monolith 13, which shows a settlement of 0.06 ft, was completed in March 1962.

66. Very little longitudinal movement at the wall joints occurred after the walls were completed. The data indicate that some joints are opening while others are closing. The maximum observed joint opening was 0.14 in. while the maximum closure was 0.19 in. The joints for the chamber monoliths were designed for a maximum closure of 0.5 in., and slightly larger movements were expected at the gate-bay joints. Consequently, the observed movements are not considered excessive.

Time rate of settlement

67. The foundation soils consist of sands to a depth of about 94 ft below the base of the lock except for a small stratum of clay between els 68 and 72; therefore, it was anticipated that settlement of the lock would be very rapid. By comparing the settlement of monolith 12 (plate 15) with the construction history (plate 5), it can be seen that settlement occurred quite rapidly as load was applied. For instance, from April 1961 to November 1961, sand backfill behind the lock walls was placed at a fairly uniform rate from el -18 to el +8, and the lock settled at a uniform rate of 0.03 ft per month. In July and August 1961, no backfill was placed and practically no settlement occurred. When backfilling resumed in September 1961, settlement resulted at a rate of 0.05 ft per month. When the sand backfill was completed (December 1961), the rate of settlement decreased sharply.

Placement of the 3-ft-thick clay blanket and flooding of the lock caused additional settlement. After the lock was flooded, very slight vertical movement occurred with rising and falling river stages. It appears from the time-settlement plots that settlement of the lock as of 1964 was almost complete, and no additional significant settlement is expected. As previously discussed, observed settlements could be in error because of changes that may have occurred in bench mark elevations due to variations in the groundwater level during construction.

Recomputed rebound and settlement

68. Purpose of computations. The rebound and settlement of the structure at monolith 12 were recomputed using the actual loading conditions, which in some instances differed appreciably from those assumed in design. The laboratory pressure-void ratio (p-e) curves that were used in the design settlement analysis were revised to represent more closely the actual loading conditions. The revised p-e curves for point A (center of the lock) are shown in fig. 15 together with the original laboratory curves.

69. Recomputed rebound. In recomputing the foundation rebound, the actual groundwater conditions were used in computing overburden pressures. When the heave plugs were installed (3-10 July 1958), the groundwater level was approximately at el +32.0, as compared with el +10 assumed in design. When the excavation was completed and just prior to placing the stabilization slab, actual groundwater level beneath the excavation was at el -38, as compared with el -28.5 assumed in design.

70. The recomputed rebounds were 0.09 ft at the center and 0.06 ft at the edges of the lock (fig. 16). These values are considerably less than the rebounds predicted in design (0.29 ft at the center and 0.21 ft at the edges), which in turn were considerably less than the observed rebound of 0.45 ft. However, as the observed rebounds are apparently in error, no comparison can be made between computed and actual rebound.

71. Recomputed settlement. In the computation of stresses in the foundation due to structure load for Case IA', the distribution of base pressures as indicated by observed soil stress meters (see plate 60) was

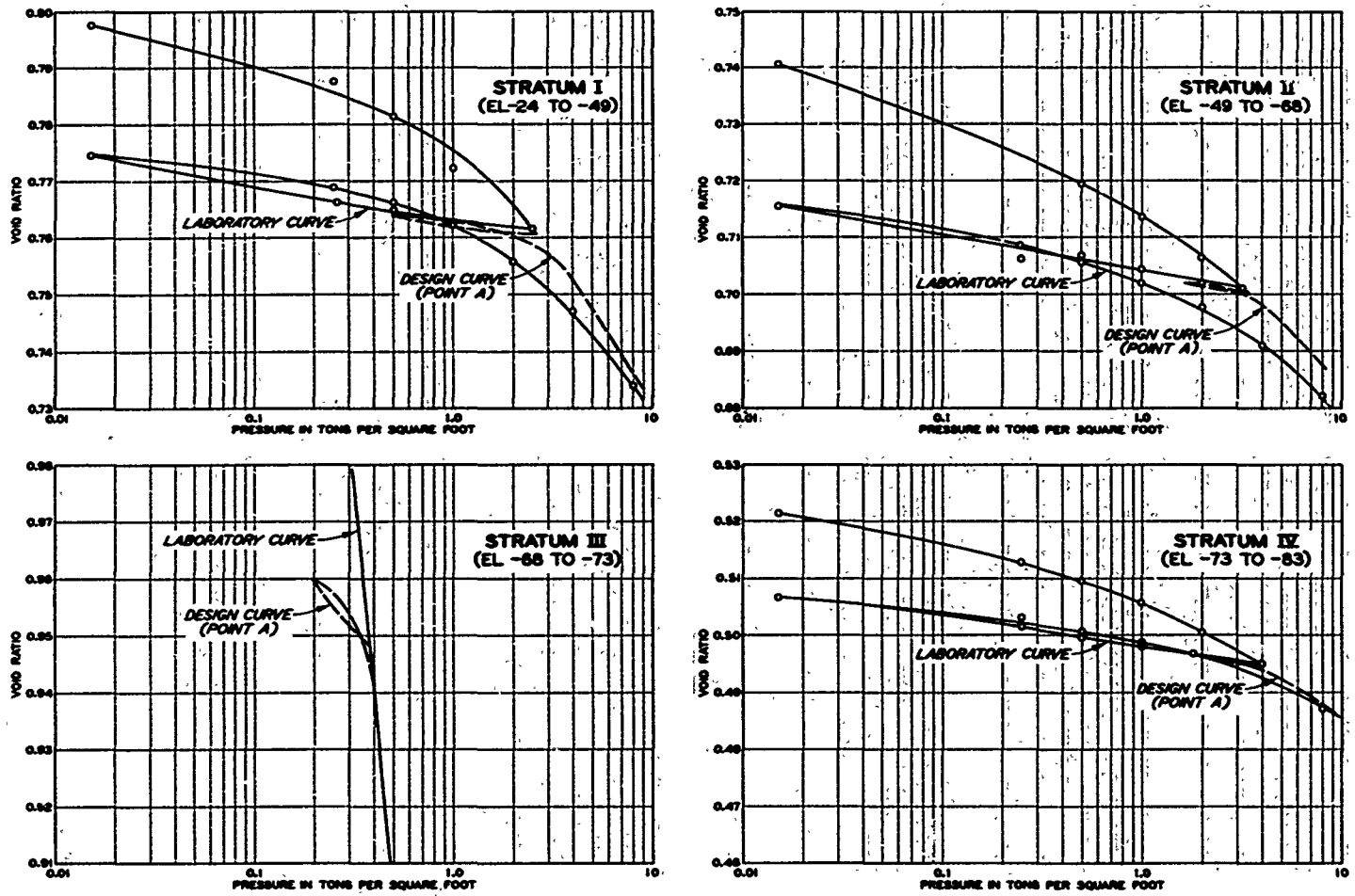

Fig. 15. Revised pressure-void ratio curves

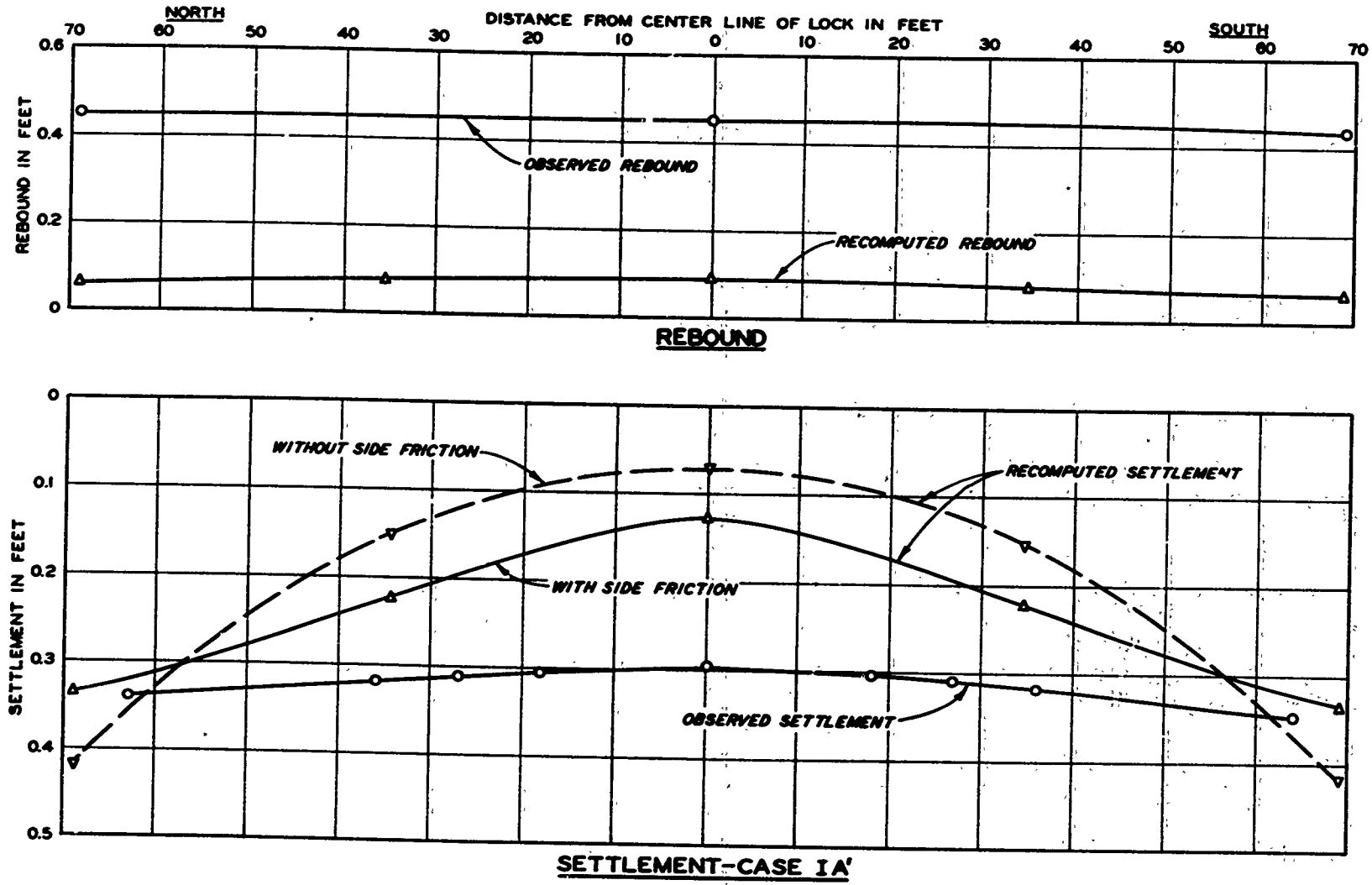

Fig. 16. Comparison of observed and recomputed rebound and settlement, monolith 12

used. As will be subsequently described, the observed base pressures (reaction) were greater than the actual structure load for Case IA' condition; this was due in part to frictional forces acting on the outer edges of the lock due to settlement of backfill relative to the lock. In the settlement analysis, two different assumptions were made as follows:

a. It was assumed that there were no frictional forces on the sides and that observed pressures were higher than actual; in this case, the observed effective base pressures (shown in plate 60) were proportionally reduced so that the total foundation pressure was equal to the actual structure load.

b. It was assumed that the observed pressures were correct and the difference between the reaction and actual structure load was due to frictional forces on the outer edges of the lock.

72. A comparison of the observed and recomputed settlements for Case IA' is shown in fig. 16 and the results are tabulated below:

Assumptions	Recomputed Settlement, ft		Observed Settlement, ft	
	Center	Sides	Center	Sides
Without frictional force	0.06	0.39	0.29	0.34
With frictional force	0.10	0.27	—	—

Note that computed settlements assuming frictional forces along the sides of the lock were slightly greater at the center and slightly less at the sides than settlements based on the assumption of no side friction. Computed settlements at the sides of the lock generally were in good agreement with observed settlements; however, computed settlements at the center of the lock were considerably less than the observed settlement. Although the magnitudes of the observed settlements are questionable because of probable movements of the bench marks, it may be concluded that settlement computations for similar structures on alluvial sands will give the general magnitude of settlement to be expected, but not an accurate estimate of the deflected shapes of the structures

73. Settlement of the structure was not recomputed for Case III'. Since the base pressure was less for Case III' than for Case IA', the lock should have rebounded. Instead, monolith 12 was observed to settle an additional 0.04 ft at the center line and 0.02 ft at the sides. The reason for this discrepancy is not known but may be related to movements of the bench marks.

Settlement of type A reference points

74. The observed settlements of deep reference points (type A) at monolith 12 and the gate bays are shown in plate 18. Also shown for comparison are the settlements of the center and sides of monolith 12. It can be seen that the settlements of deep reference points beneath monolith 12 followed very closely the trend of settlement of the structure.

75. A comparison of observed and computed foundation settlements at various depths below the side of monolith 12 for Case IA' is shown in fig. 17. Observations indicate that over 75 percent of the foundation settlement occurred below el -100, whereas computations indicate that most of the settlement should have resulted from the consolidation of the clay stratum between els -68 and -72 and the sand above the clay layer. It is believed that the observed settlements of the type A reference points are in error because the observations were referred to the bench marks that may have been affected by foundation rebound in the underlying soils as the groundwater level rose from el -40 to normal river stage levels (el 20 to 40), as shown in plate 5.

Deflection of Base Slab

Deflection determined from settlement observations

76. Despite uncertainties regarding the magnitude of the observed settlements, these data are useful in defining deflections. The deflected shape of the base slab was determined from the settlement profiles for monoliths 2, 12, and 22, as shown in plates 19-21. The deflections are shown for an initial condition after the slab was completed and just prior to wall construction. Also shown are the deflections of

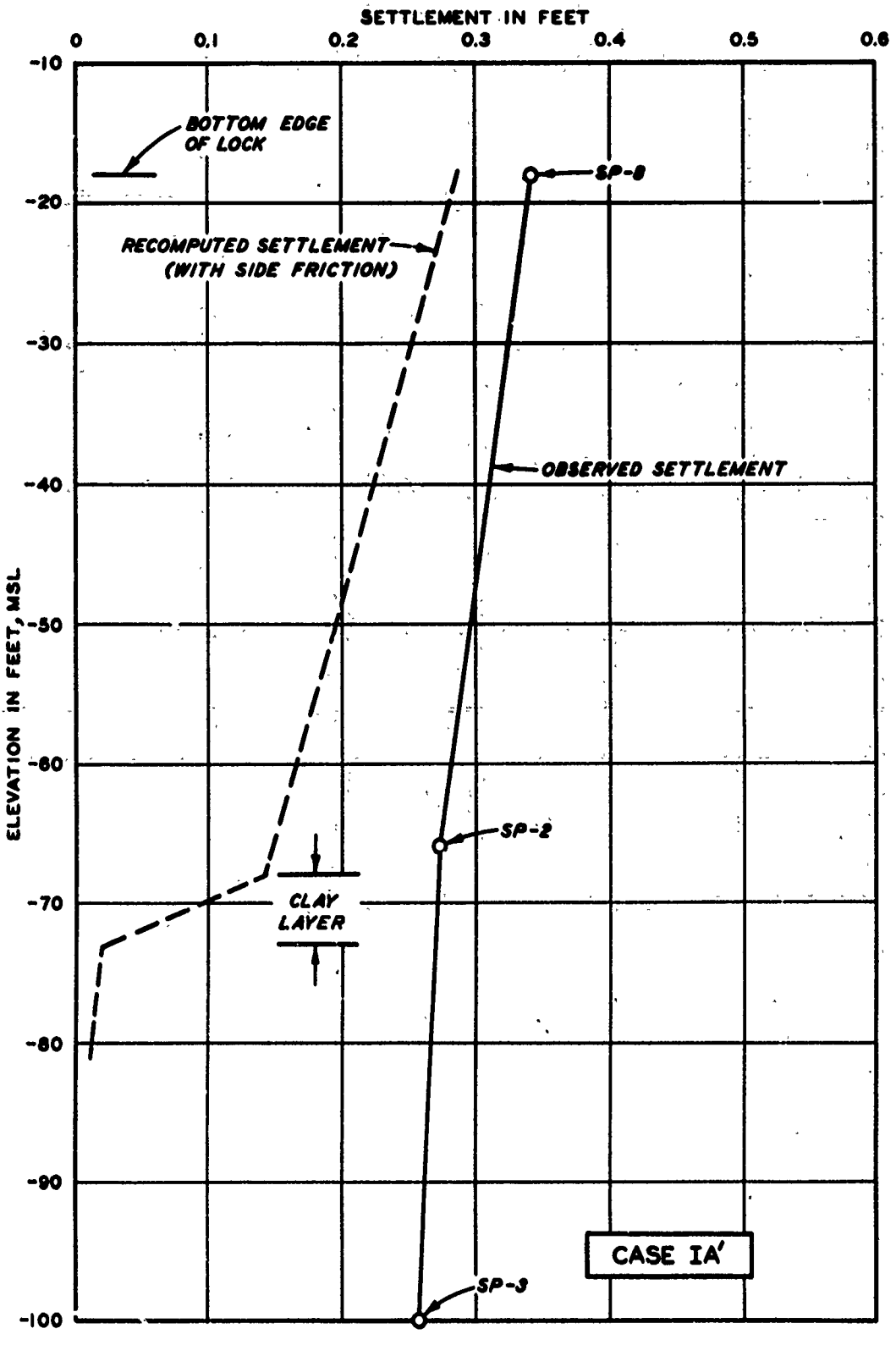

Fig. 17. Observed settlement versus depth

the slab from this initial condition to Case IA' and from the initial condition to Case III'. The deflected curves were drawn with respect to: (a) a straight line through the two points representing the settlement at the sides of the lock for the case of greater settlement at the center, and (b) a horizontal line through the point of minimum settlement for the case of greater settlement at the sides of the lock.

77. At monoliths 12 and 22, before wall construction began, the center of the slab deflected slightly downward with respect to the sides. The maximum deflections at the center were 0.014 and 0.021 ft for monoliths 12 and 22, respectively. At monolith 2, there were no temporary settlement reference points at the sides of the structure; therefore, the deflection prior to wall construction was estimated by extrapolating data from reference points. At this monolith, it was estimated that the sides of the slab deflected downward about 0.02 ft with respect to the center prior to wall construction.

78. As shown in plates 19-21, construction of the walls and backfill resulted in the sides of the lock deflecting downward with respect to the center (see Case IA' conditions). It may be noted that the deflection was slightly less for Case III' than for Case IA'. At monolith 12, deflections of the sides of the lock with respect to the center were about 0.08 ft for Case IA' and 0.06 ft for Case III'.

PART V: LATERAL EARTH PRESSURES AND WALL MOVEMENTS

Sand Backfill

79. A description of the sand backfill material behind the lock walls, placement procedures, and results of laboratory tests on representative samples of the sand backfill are given in Appendix B. Laboratory tests on drive cylinder samples indicated that the sand backfill behind monolith 12 was placed at an average dry density of 102 lb/cu ft, corresponding to a relative density of 74 percent. However, as discussed in Appendix B, it is probable that because of errors inherent in the drive cylinder method of sampling, the actual and relative densities were somewhat higher than indicated above. On the basis of correlations between relative density and angle of internal friction (described in fig. B13), it was estimated that the angle of internal friction of the sand backfill behind monolith 12 was about 40 deg.

Observed Earth Pressures

Earth pressures versus time

80. Time plots of earth pressures against the lock walls as measured by soil stress meters S-12, S-13, and S-15 through S-20 and WES pressure cells W-4 and W-5 are shown in plates 35-37. It can be seen in these plates that soil pressures increased as backfill was placed. The readings of WES pressure cells W-4 and W-5 were about the same as readings of adjacent Carlson soil stress meters S-15 and S-17, respectively. However, the readings of meters S-19 and S-20 on the north wall were lower than the readings of the meters at similar locations on the south wall (S-15 and S-17), e.g., the earth pressures indicated by S-19 were about half as great as those indicated by S-15. The reason for this difference is not known. It is also noted that the pressures indicated by S-13 were considerably less than the pressures indicated by the meters below it (S-12) and above it (S-15). Pressure indicated by S-13 became progressively smaller until the meter ceased to function about

7 years after its installation. It is believed that data from this meter are of questionable value.

Distribution of
lateral earth pressures

81. Case IA'. The observed distribution of lateral earth pressures for Case IA' is shown in plate 60 together with earth pressures assumed for design Case IA. It can be seen in this plate that observed earth pressures were considerably less than those assumed in design. For Case IA, the design earth pressures were based on an at-rest earth pressure coefficient of 0.5. The coefficient of lateral earth pressure k was computed directly from observed pressures according to the expression

$$k = \frac{p_h}{p_v} \tag{1}$$

where

p_h = the effective earth pressure in a horizontal direction as measured by soil stress meters

p_v = the computed effective overburden pressure at the elevation of the meter

The distribution of coefficients of lateral earth pressures along the wall for Case IA is shown in fig. 18. The k values vary from about 0.31 along the culvert wall to slightly more than 0.2 along the wall stem. The k values along the culvert wall are approximately the same as those observed at Port Allen Lock, whereas the k values along the wall stem are considerably smaller than those observed at Port Allen Lock where wall movements were correspondingly larger.

82. Case III. The observed distribution of lateral earth pressures for Case III' is shown in plate 61 together with lateral earth pressures assumed in design. For design purposes, a coefficient of earth pressure of 1.0 was assumed acting from the ground surface to the top of the culvert, below which the coefficient was assumed to decrease linearly to a value of 0.5 (assumed at-rest pressure) at the base of the wall. The k value of 1.0 was considered to be conservative since it

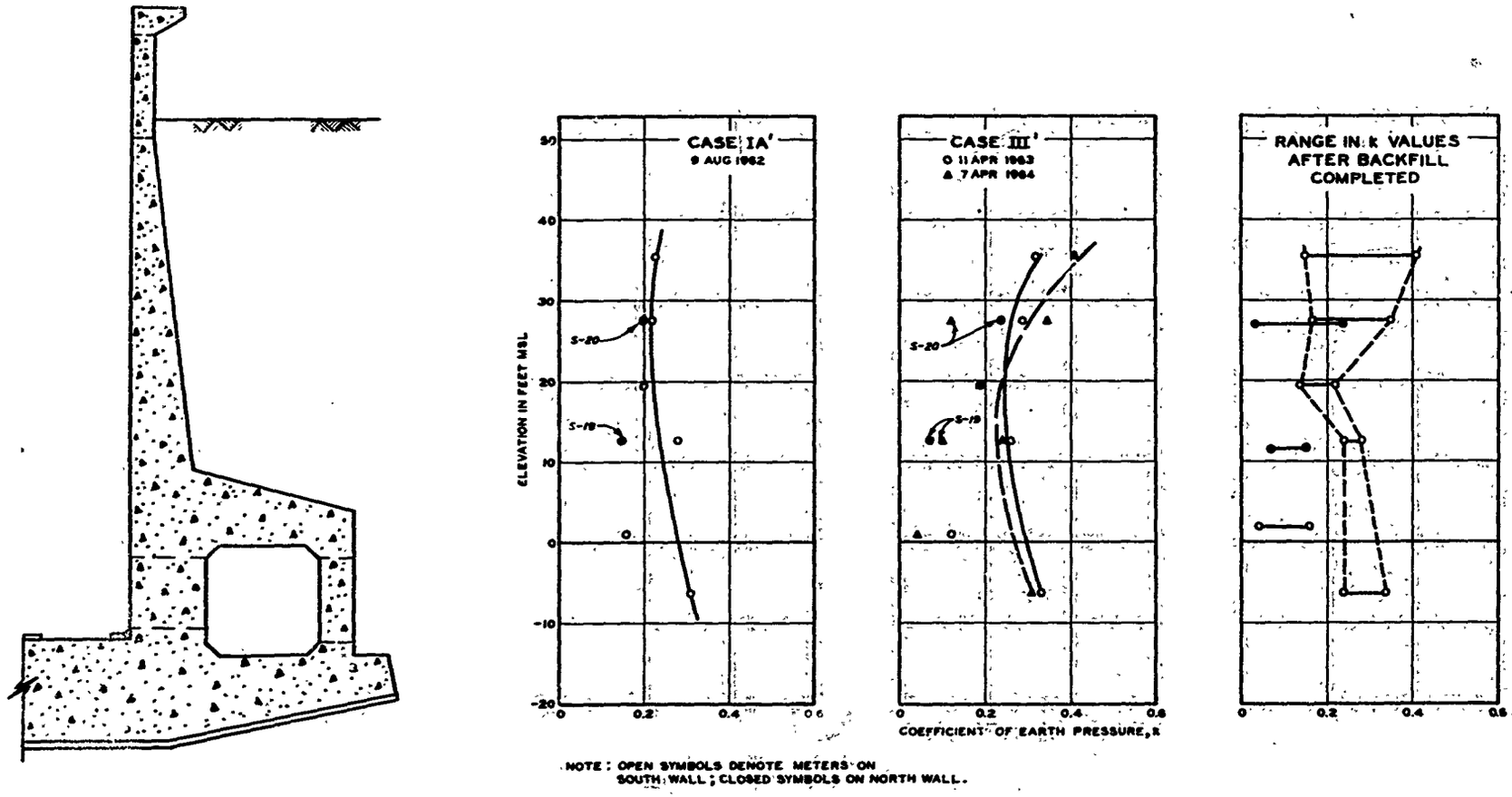

Fig. 18. Distribution of coefficients of lateral earth pressures

would not require mobilization of shearing stresses in the backfill and thus would be developed without excessive wall deflection. As shown in plate 62, the observed lateral earth pressures were considerably less than those assumed for design.

83. The distribution of coefficients of lateral earth pressures for Case III' are shown in fig. 18. The values of k for Case III' were similar to the k values for Case IA' except that they were slightly higher near the upper portion of the wall stem. During the 1963 high-water season (April 1963), the coefficient of earth pressure near the top of the wall, as indicated by meter S-18, reached a maximum value of 0.32; during the 1964 high-water season, the meter indicated a value of k of 0.41. At no time did the coefficient of earth pressure near the top of the wall approach the value of 1.0 assumed in design Case III. However, it should be pointed out that during the 1963 and 1964 high-water periods, the water level in the lock was about 20 ft lower than the water level assumed for Case III'. Also, the uppermost meter (S-18) is 17.5 ft below the top of the backfill, and it is possible that a higher value of k may develop above this meter during high-water periods.

Wall Movements

84. During and after construction, wall movements were measured by means of wall deflection pipes and a deflectometer (see Appendix A). In order to correlate wall movement and lateral earth pressures, wall displacement at each soil stress meter was determined assuming a zero reference at the time when the backfill reached the level of the particular meter. Time plots of wall displacement at each meter along the wall are shown in plates 62 and 63. During placement of backfill, the wall moved toward the backfill. The maximum displacement at each meter occurred when the backfill was completed. After the backfill was completed (July 1962), the wall moved away from the backfill. After the lock was flooded (September 1962), wall movement appeared to vary seasonally, i.e., the walls moved toward the backfill during warmer months

and away from the backfill during cooler months. There appears to be no definite relationship between wall movement and water level in the locks. For instance, at stress meters S-17 and S-18, the position of the wall during January 1963, when there was low water in the lock, was about the same as the position of the wall during the crest of the 1963 high water (April 1963). It appears then that movement of the walls is more closely related to seasonal temperature variations than to the water level in the lock. No analyses were made for this report of temperature effects on wall movement. However, Duncan and Clough[12] analyzed temperature effects using the finite element method. Their computed wall movements due to temperature changes agreed well with observed movements.

85. Time plots of coefficients of earth pressure k are shown in plates 62 and 63 with the time plots of wall movements. An attempt was made to correlate wall movement with coefficient of earth pressure, but the results indicated that there was no direct relationship. There appears to be only a general relationship between k and wall movement, i.e., the values of k generally increase when the walls move toward the backfill and decrease when the walls move away from the backfill. Some exception can be noted. At meter S-18 (see plate 63), there was a large increase in k from January to April 1963, although there was apparently no wall movement during that time. Between April 1963 and June 1963, the wall moved toward the backfill about 0.1 in., whereas the k value remained about the same.

PART VI: FOUNDATION BASE PRESSURES AND UPLIFT

Foundation Base Pressures

Effective base pressures

86. Based on the time plots of observed base pressures shown in plates 28-34, profiles were constructed of effective base pressures and uplift pressures beneath the lock for (a) a condition just before wall construction was begun, (b) Case I', (c) Case IA', and (d) Case III'. These profiles, which are shown in plates 59, 60, and 61, are not precisely defined by the observed data and represent the best estimate, assuming all of the meters provided reasonably accurate indications of the pressure. The scatter of data indicated that in future installations on sand foundations, a considerably greater number of devices should be installed to define the effective base pressure distribution. A distinguishing feature of the effective base pressure profiles is the high base pressure near the south side of the lock, as indicated by stress meters S-9, S-10, and S-11. These high pressures were also assumed to act on the north side of the lock. It may be noted that the readings of stress meter S-7 are not consistent with readings of adjacent meters and indicate pressures slightly higher than expected. As mentioned in Appendix A, meter S-7 was installed adjacent to a pocket of organic material. There is probably very little pressure exerted on the base slab at the location of the organic deposit, and the excess pressure is probably taken up by areas adjacent to the soft spot, which may be why S-7 indicates a higher pressure than expected.

87. Plate 64 presents a time plot showing the actual weight* of the structure (including the weight of backfill above the culverts and water in the lock and culvert) and the measured effective base pressures (computed from profiles described above), uplift pressures, and measured

---

* Weights and moments referred to in subsequent paragraphs and in the plates are derived for a 1-ft-wide section of lock, foundation, and backfill normal to the lock center line.

total base pressures for the south half of monolith 12 on selected days. In computing the weight of the structure, the average density of the concrete, adjusted for the presence of steel, was taken as 150 lb/cu ft. The density (saturated unit weight) of the sand backfill was taken as 125 lb/cu ft. The measured effective base pressure is equal to the area under the effective pressure diagram. (See plates 59-61 for examples of the base pressure diagrams.) The measured total base pressure corresponds to the foundation reaction and is equal to the measured effective base pressure plus the uplift pressure (area under uplift diagram).

88. At the beginning of construction, the effective base pressures increased with increasing structure load (weight of concrete and backfill). The pressure increased to a maximum of 450 kips in December 1961, when the sand backfill was completed. After December 1961, the effective base pressure showed a slight decrease due to an increase in uplift pressures beneath the lock. After the lock was flooded, the effective base pressure varied with changes in uplift pressure. When the uplift pressure increases during high-water periods, the effective base pressure decreases; when the uplift pressure decreases during low-water periods, the effective pressure increases.

Difference between weight of
structure and measured reaction

89. For analysis of data, it was assumed that the base pressures beneath the north half of monolith 12 were the same as base pressures beneath the south half. The time plot in plate 64 shows a difference between the actual weight of the structure and the measured reaction for the south half of monolith 12. This difference, expressed both in kips and in percent of actual weight, is also plotted versus time in plate 64. The difference in the reaction and actual weight during the early stage of construction (before the base slab was completed) is not considered significant because the actual pressures were relatively small. After the base slab was placed, the difference varied from 0 to 33 percent of the actual weight.

90. The difference between the measured total pressure and actual weight of the structure could be due to: (a) errors in constructing

accurate soil pressure diagrams, (b) overregistration of soil stress meters and time effects, and (c) frictional forces acting along the sides of the lock generated by settlement of backfill with respect to the lock. The effect of errors in drawing the soil pressure diagrams was minimized by drawing all soil pressure diagrams with respect to the plotted points in as similar a manner as possible so that the resulting error, if any, would be a constant percentage of the reaction.

91. Changes in meter readings with time are demonstrated by the observations during placement of the three lifts of the base slab (see plates 28-34). It can be seen that in some cases, meters reacted relatively slowly and did not register a stable pressure until a week after a lift was placed. Measured reactions for the time plots in plate 64 were generally selected during periods of construction inactivity to reduce time effects; however, any errors due to possible overregistration or underregistration are still included in the measured values.

92. A significant percentage of the difference between the measured base pressures and actual weight of the structure is most probably due to frictional forces acting along the sides of the structure. Placement of sand backfill behind the lock walls resulted in a greater load existing under the backfill than under the lock; consequently, the backfill settled more than the lock. Also, placement of the sand backfill probably caused the 5-ft-thick clay blanket at the bottom of the excavation to consolidate, thereby increasing the differential settlement between the backfill and the lock. This difference in settlement was probably effective in creating a downward drag on the sides of the lock, which in turn resulted in the foundation reaction being progressively greater than the actual structure load. It can be seen in plate 64 that the difference between measured reaction and actual weight of the structure increased as the sand backfill was placed (April to December 1961). Flooding of the lock caused an increase in structure load and resulted in a decrease in frictional drag on the sides of the lock, as indicated by a decrease in the difference between foundation reaction and actual load. The difference between the reaction and actual load decreased to 10 percent of the actual load during the crest

of the 1963 high water (April 1963), increased during the low-water season (July 1963 to January 1964), and decreased again during the 1964 high water. This would indicate that the frictional drag decreases when structure load increases and increases when the structure load decreases.

Comparison of Observed and Predicted Base Pressures

93. The effective base pressures and uplift pressures observed at monolith 12 for Case I', IA', and III' conditions are shown in plates 59, 60, and 61, respectively, together with the base pressures and uplift pressures assumed for design Case I, IA, and III conditions. As shown in these plates, the observed effective base pressure distributions are considerably different from those assumed in design. The observed distribution is similar in shape to the observed distribution of base pressures of Port Allen Lock except that pressures were much greater beneath the culverts and smaller near the center than those observed at Port Allen. For all cases, the maximum pressures developed about 55 ft on either side of the center line of the lock (near the center of the culverts), the minimum pressure occurred from 15 to 25 ft on either side of the center line, and the pressure at the center line was only slightly greater than the minimum observed pressure. A summary of base pressures assumed in design for the center and outer edge of the lock and the observed pressures at the center and maximum observed pressure (55 ft on either side of the center) expressed in percent of uniform base pressure is given in the following tabulation:

	Percent of Uniform Base Pressure Assumed in Design			Percent of Uniform Base Pressure Observed	
	Center	Sides		Center	Under Culverts (Max)
Case I	68	132	Case I'	69	220
Case IA	128	72	Case IA'	47	202
Case III	104	96	Case III'	41	223

94. As shown in plate 60, the uplift pressure observed for Case IA' was somewhat greater than uplift pressures assumed for design Case IA. The observed uplift was about 8.2 psi, as compared with 4.6 psi assumed in design. The observed uplifts for Case III' (see plate 61) were somewhat less than those assumed for design Case III, principally because the river stage assumed for design Case III (el 65.0) was much higher than the river stage observed for Case III'. The uplift pressure assumed for design Case III was 33.2 psi, whereas during the 1963 high water (Case III'), an uplift pressure of 28.6 psi was observed.

95. As previously mentioned, it is probable that significant frictional force was developed on the sides of the lock. However, in moment calculations for Cases IA' and III', the two following assumptions were made:

a. There were no frictional forces on the sides of the lock, as the observed pressures were greater than actual loads. The observed pressures were reduced proportionally so that the total base pressure was equal to the structure load.

b. The observed base pressures were correct and the difference between the reaction and the structure load was due to friction on the sides of the lock.

96. Applying assumption b to Case IA', the resulting side frictional force was found to be extremely large. This force (110,740 lb on each side of the lock) was about 30 percent of the structural load and was greater than the total effective lateral earth pressure against the walls (85,910 lb). For a similar condition at Port Allen Lock, the side friction was only about 11 percent of the structure load. It was therefore concluded that for Old River Lock, the difference between the observed base pressure and structure load may not have been entirely due to side friction. Therefore, for Case IA', a third assumption (assumption c) was made that considered the soil stress meter overregistering by 10 percent. In this analysis, the observed effective earth pressures beneath the lock were arbitrarily reduced by 10 percent, and the resulting difference between base pressures and structure load was considered to be due to side friction.

97. For Case III', the difference between observed base pressures

and structure load was nearly 10 percent (see plate 64). Assuming that the meters overregistered by 10 percent (assumption c) would give the same results assuming no side friction (assumption a). Therefore, moments for Case III' were computed only for assumptions a and b.

PART VII: BENDING MOMENTS IN BASE SLAB AND WALLS

98. In order to determine the actual bending moments imposed on the lock, moments in the base slab and walls were recomputed on the basis of the observed data, and a comparison was made of the recomputed moments and those computed for design. Moments were recomputed only for monolith 12 and were based on externally applied loads on the structure as measured by soil stress meters and piezometers. In order to verify the recomputed moments, deflections of the base slab were computed from the moment curves and compared with observed deflections of the structure. It was planned also to recompute moments from the internal stresses measured by concrete stress meters and computed from concrete strain meters. However, data from these meters indicated that the distribution of internal stresses was extremely complex; therefore, no attempt was made to compute moments from internal stresses.

Moments Based on Applied Loads

Moments in the base slab

99. Moments in the base slab were computed for Cases IA' and III' using the external load distributions shown in plates 60 and 61, respectively. Moments for Case IA' were computed for the following assumptions:

a. No frictional forces on the sides of the lock and observed pressures greater than actual. Here, the observed effective base pressures (shown in plate 60) were reduced proportionally so that total measured reaction was equal to the structure load.

b. The total difference between the observed base pressures and structure load was due to friction on the sides of the lock.

c. The observed effective base pressures were reduced by 10 percent and the resulting difference between base pressures and structure load was considered to be due to friction on the sides of the lock.

100. Moments computed on the basis of the above three assumptions are shown in fig. 19. It can be seen that there is a large difference

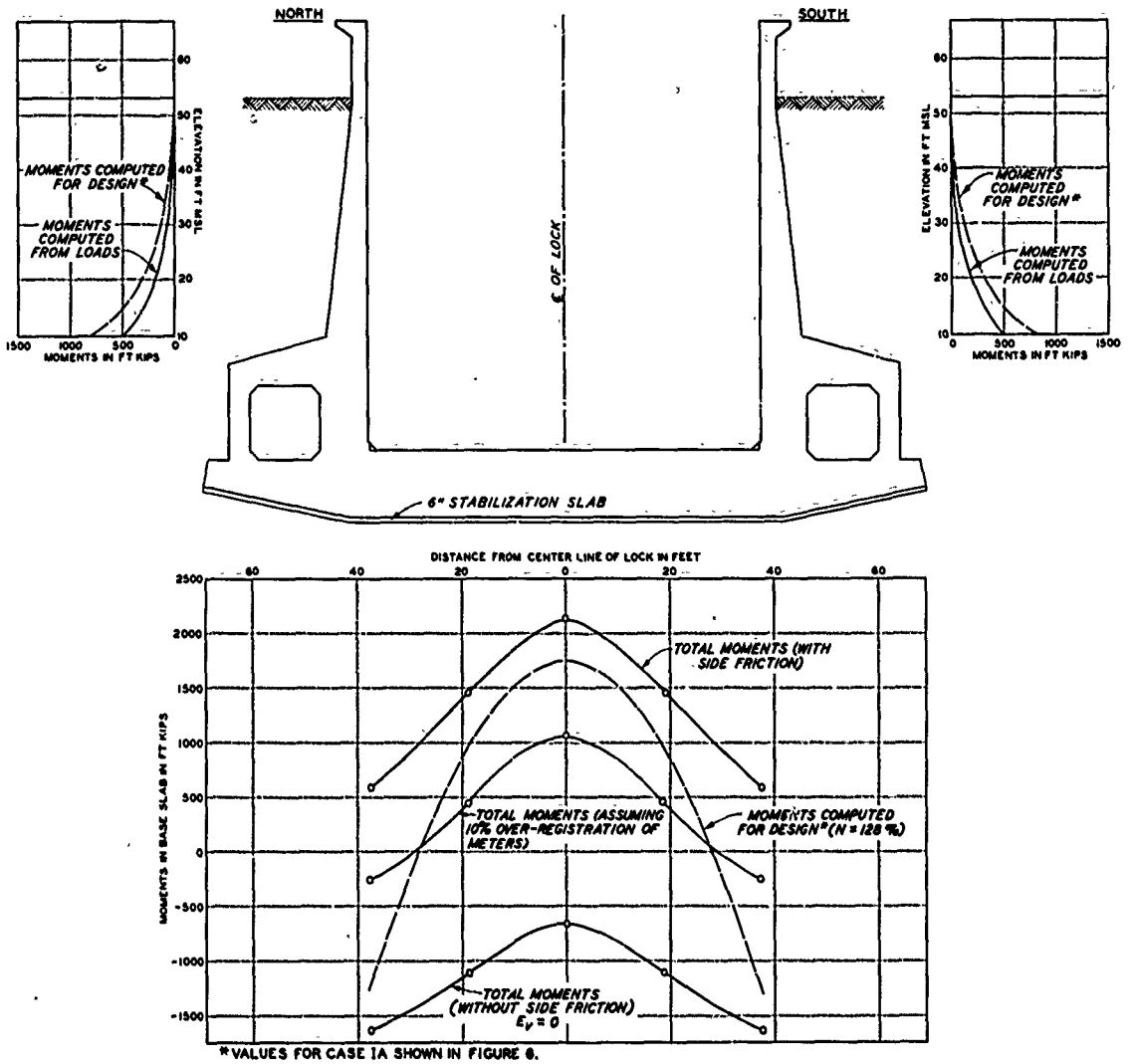

Fig. 19. Summary of moments computed for Case IA' loading conditions, monolith 12

between the moments computed from the assumptions above. A summary of moments computed for the three assumptions is given below along with the moments computed for design:

	Computed Moments, ft-kips	
	At Center Line of Lock	At Sides of Lock
Case IA'		
Assumption a	-654	-1634
Assumption b	2135	597
Assumption c	1075	-252
Design Case IA	1734	-1266

From the comparison above, it can be seen that the assumption of magnitude of side friction has a considerable effect on computed moments. As previously mentioned, it appears that friction does act on the sides of the walls; however, the magnitude of this frictional force cannot be accurately determined from available data. Assuming that the entire difference in observed base pressure and structure load is due to side friction (assumption b), the computed moment at the center of the lock is about 23 percent greater than the moment computed for design. If the soil stress meters are assumed to overregister by 10 percent (assumption c), the computed moment at the center is 38 percent less than the moment computed for design. Assuming no side friction (assumption a) would result in negative moments along the entire length of the base slab.

101. Moments for Case III' (high water in the lock) are shown in fig. 20. There was high water in the lock both in April 1963 and April 1964; moments were computed for both of the conditions. The major difference between the 1963 and 1964 high-water observations was that uplift pressures beneath the lock in 1964 were less than those observed in the 1963 high-water period. Moments for the high-water conditions were computed for assumptions a and b above. Assuming that the soil stress meter overregistered by 10 percent (assumption c) would be the same as assuming no side friction (assumption a), because the difference between the total observed base pressures and the structure load was nearly 10 percent for both high-water conditions. A summary of the

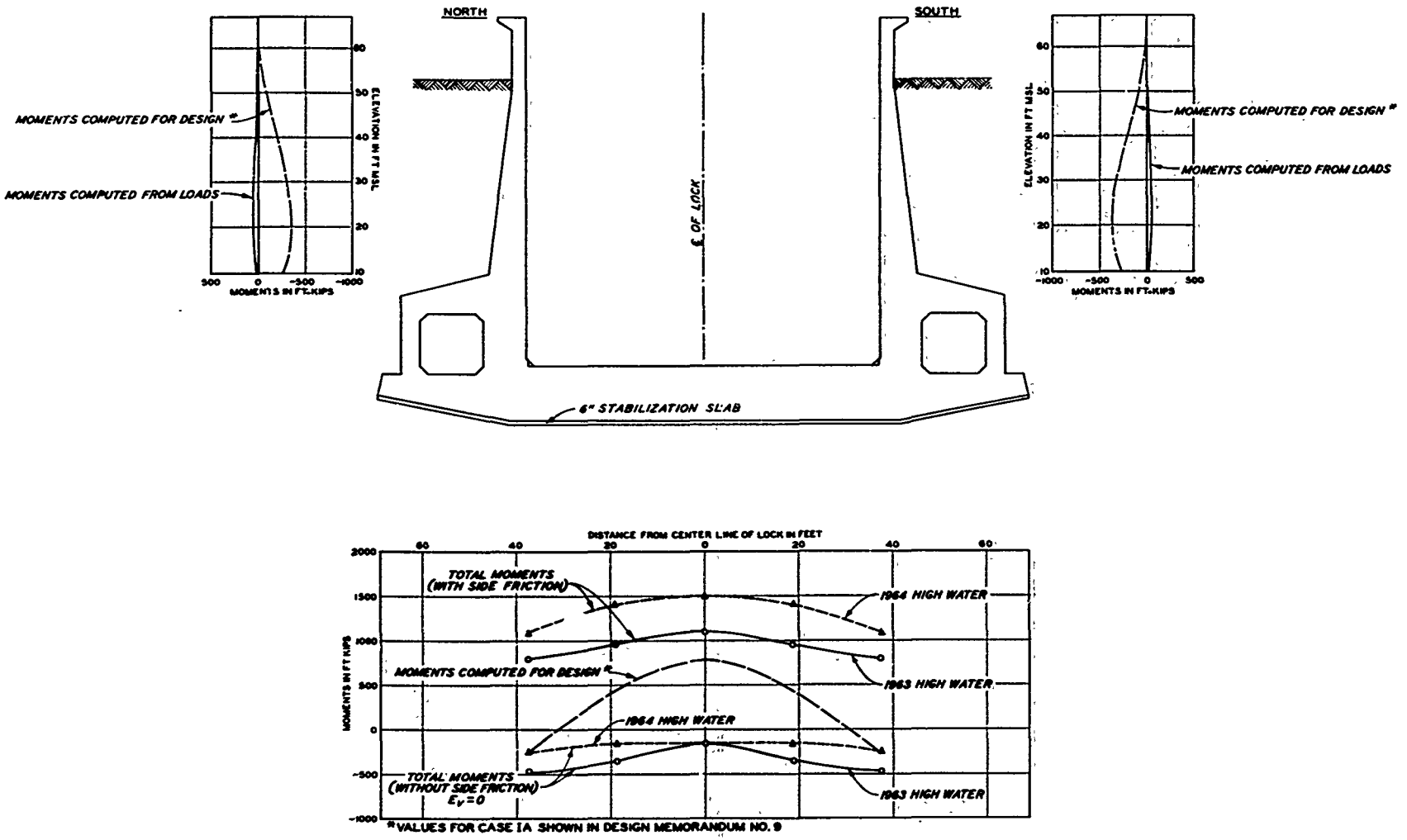

Fig. 20. Summary of moments computed for Case III' loading conditions, monolith 12

moments computed from observed loads is shown in the following tabulation along with moments computed for design:

	Computed Moments, ft-kips	
	At Center Line of Lock	At Sides of Lock
1963 high water		
Assumption a	-145	-470
Assumption b	1119	802
1964 high water		
Assumption a	-159	-254
Assumption b	1515	1082
Design Case III	786	-275

102. Here again there is a large difference between moments computed for assumption a and those computed for assumption b, assumption b giving larger positive moments (tension on the top of the base slab) than assumption a. Also, there is a considerable difference between moments computed from observed loads and those computed in design.

Moments in the walls

103. Moments in the walls computed from observed lateral pressures for Cases IA' and III' are shown in figs. 19 and 20. Observed lateral earth pressures for Case IA' were less than those assumed for design Case IA (see plate 19). Consequently, moments computed from observed loads were less than moments computed for design. The maximum moment computed from observed loads on the walls (just above the culvert) was 467 ft-kips (tension on the backfill side of the wall), whereas the maximum moment computed for design was 823 ft-kips.

104. The loading conditions on the walls for Case III' were considerably different from conditions assumed for design Case III, as the water level in the lock was 22.6 ft lower than the water level assumed in design. For that reason, moments in the walls for Case III' were considerably different from moments computed for design. The maximum moment in the walls computed for Case III' (shown in fig. 20) was about 50 ft-kips (tension on the backfill side of the lock). The maximum

moment computed for design was 356 ft-kips (tension on the inside of the wall).

Computation of Deflections from Moments

105. In order to verify the values of base pressure bending moments at monolith 12, deflections of the base slab were computed from the moment curves, and the computed deflections were compared with the observed deflection of the base slab. To permit an accurate comparison, the condition of the base just prior to placement of the wall (November 1961) was assumed as a zero reference. The net moments from this initial condition to Case IA' and from the initial condition to Case III' were determined. An equation was determined for each of the moment curves, and deflections were computed from the general equation:

$$y = \frac{1}{EI} \int_o^x \int_o^x M \, dx^2 \qquad (2)$$

Where

y = deflection at horizontal distance x from the center line of the lock

E = modulus of elasticity of concrete

I = moment of inertia of the base slab

M = moment

The electronic computer was utilized in determining an equation for the moment curve. In the computation, it was assumed that zero deflection occurred at the center of the lock. The value of E is the sustained modulus of elasticity (instantaneous modulus corrected for deformation due to creep) and was determined from values obtained in creep tests reported in Appendix B. An E value of 4.2×10^6 psi was used for Case IA', and an E value of 4.1×10^6 psi was used for Case III'. The value of I (moment of inertia of the base slab) was computed for a cracked section.

106. A comparison of the observed deflections of monolith 12 with deflections computed from moments is shown in fig. 21. For Case IA',

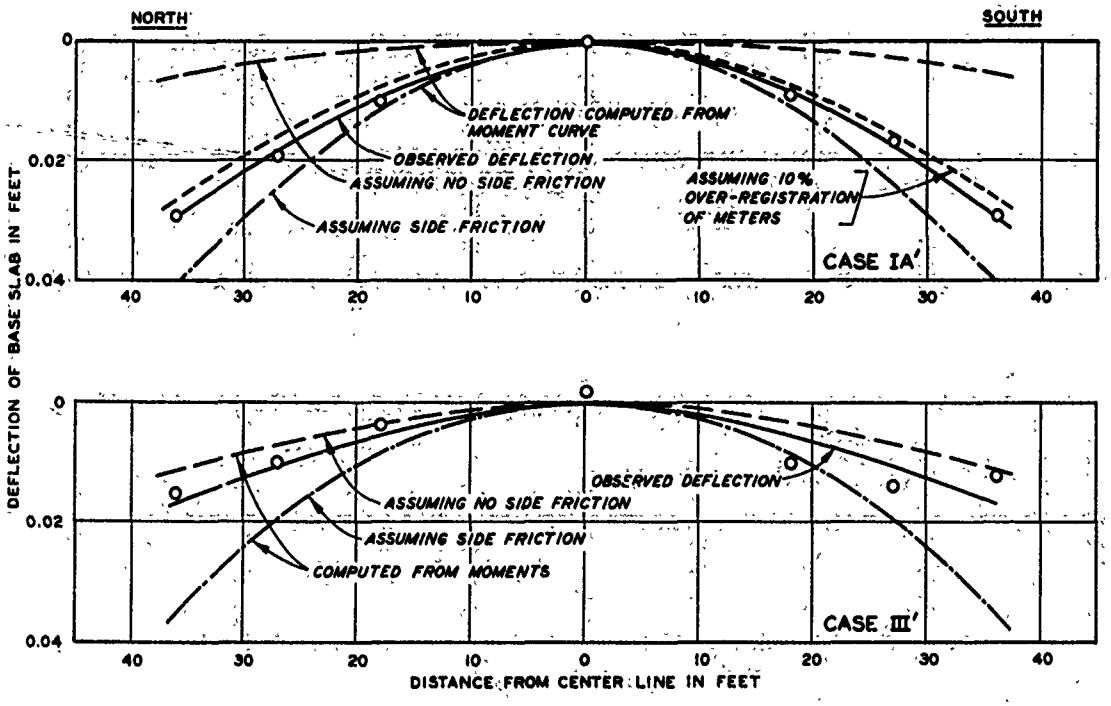

Fig. 21. Observed and computed deflections of base slab

deflections were computed for three moment curves: one moment curve was computed for assumption a, one for assumption b, and one for assumption c. As shown in fig. 21, there is a good agreement between observed deflections and deflections computed from moments for assumption c. For assumption a, the computed deflection is about 20 percent of the observed deflection, and for assumption b, the computed deflection is about 140 percent of the observed deflection.

107. A similar comparison was made of deflections computed from moment curves and observed deflections for Case III', as shown in fig. 21. For this case, deflections were computed from moment curves for assumptions a and b. There is good agreement between observed deflection and deflection computed from moments for assumption a, whereas deflection computed from moments for assumption b is slightly higher than observed deflection.

Internal Stresses and Strains

108. Summaries of the internal strains, as measured by the

concrete strain meters for Cases IA' and III', are given in plates 65 and 66, respectively. Stresses were computed from observed strains as previously described, and summaries of computed stresses for Cases IA' and III' are shown in plates 67 and 68, respectively. At the center line of the lock, nine strain meters were installed at various elevations in the base slab to observe the distribution of stresses and strains at that location. It was considered that moments could be computed at the center line from the stresses computed from observed strain. As experienced at Port Allen Lock, the stress distribution in the base slab at Old River Lock prior to placement of walls was very complex, and no attempt was made to compute moments in the base slab prior to this time. Instead, an attempt was made to employ the same method of analysis as was used for Port Allen, i.e., use the internal stresses just prior to placement of walls as a zero reference and compute moments caused by subsequent load. The distribution of stresses in the base slab caused by the subsequent loads is shown in plate 67 for Case IA' and in plate 68 for Case III'. It can be seen that these distributions of stresses are still very complex; it appears that the base slab is acting as three separate beams instead of as a single beam. Because of this complex distribution of stresses, the attempt to compute moment in the base slab from internal stress was abandoned.

Finite Element Analysis

109. In 1968-1969, the University of California, Berkeley, under contract with WES conducted a study to develop a procedure for finite element analysis of reinforced concrete U-frame structures and applied the analysis to Port Allen and Old River Locks. Detailed results of the study are reported in reference 12, and a summary of the results of the Old River Lock analysis is given below.

110. In the study, various finite element design procedures were employed, and results of computed displacements and soil pressures were compared with instrumentation observations from Port Allen Lock. The procedure was refined until good agreement was obtained between

computed and observed displacements and soil pressures. After the procedure was developed for Port Allen Lock, it was used to analyze Old River Lock as a means of verifying the procedure.

111. The procedure simulates the actual sequence of construction operations such as excavation, dewatering, placement of concrete and backfill, etc. The incremental finite element analysis was employed with nonlinear, stress-dependent, inelastic soil stress-strain behavior as developed by Duncan and Chang.[13] Soil parameters required in the analyses were obtained from the results of consolidated-drained triaxial tests. The reinforced concrete lock was treated as a linear elastic structure; the sustained modulus of the concrete was obtained from results of the creep tests described in Appendix B. Special one-dimensional interface elements developed by Goodman et al.,[14] were used to simulate the interface behavior between the concrete lock walls and sand backfill.

112. Results of the computed deflections of the base slab and walls of the lock (see figs. 22 and 23) agree fairly well with observed deflections. Computed and observed effective earth pressures are shown in figs. 24 and 25. The computed lateral earth pressures along the lock wall and culvert are generally in good agreement with observed earth pressures; however, computed base pressures are much more uniform than observed base pressures. Observed base pressures are lower at the center and higher under the culverts than the computed base pressures. The computed friction on the sides of the walls was much less than the difference between observed base pressure and structure load. For Case IA', the computed side friction was 9.5 percent of the structure load (weight of structure and backfill above culverts); the difference between observed base pressures and structure load was 30 percent of the structure load. For Case III', the computed side friction was 6.5 percent of the structure load; the difference between observed base pressures and structure load was 10 percent of the structure load.

113. Moments in the base slab based on the finite element analysis are shown with the moments from observed external pressures in figs. 26 and 27, for Cases IA' and III', respectively. Although the

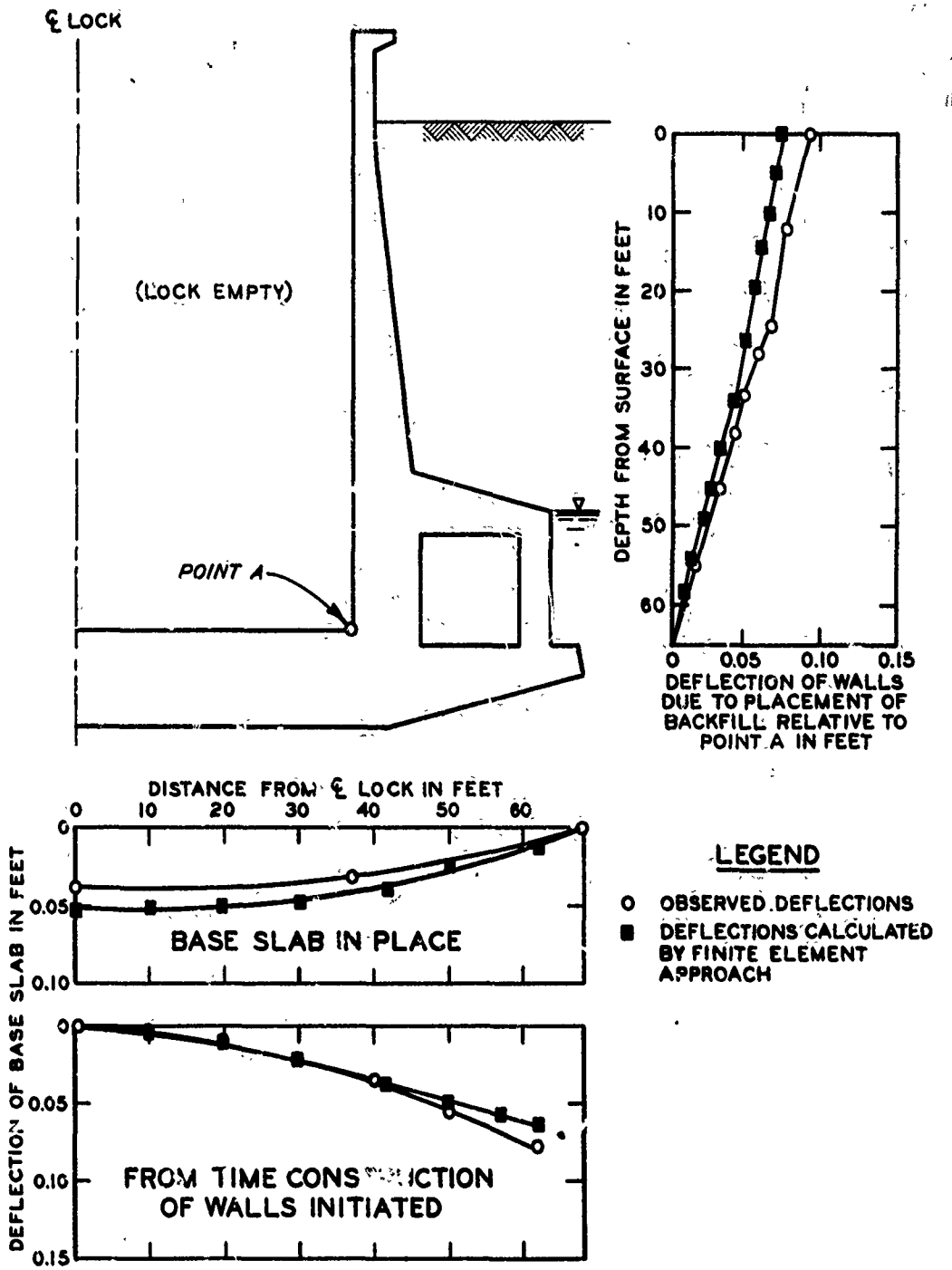

Fig. 22. Deflections of base slab and walls computed by finite element method, Case IA'

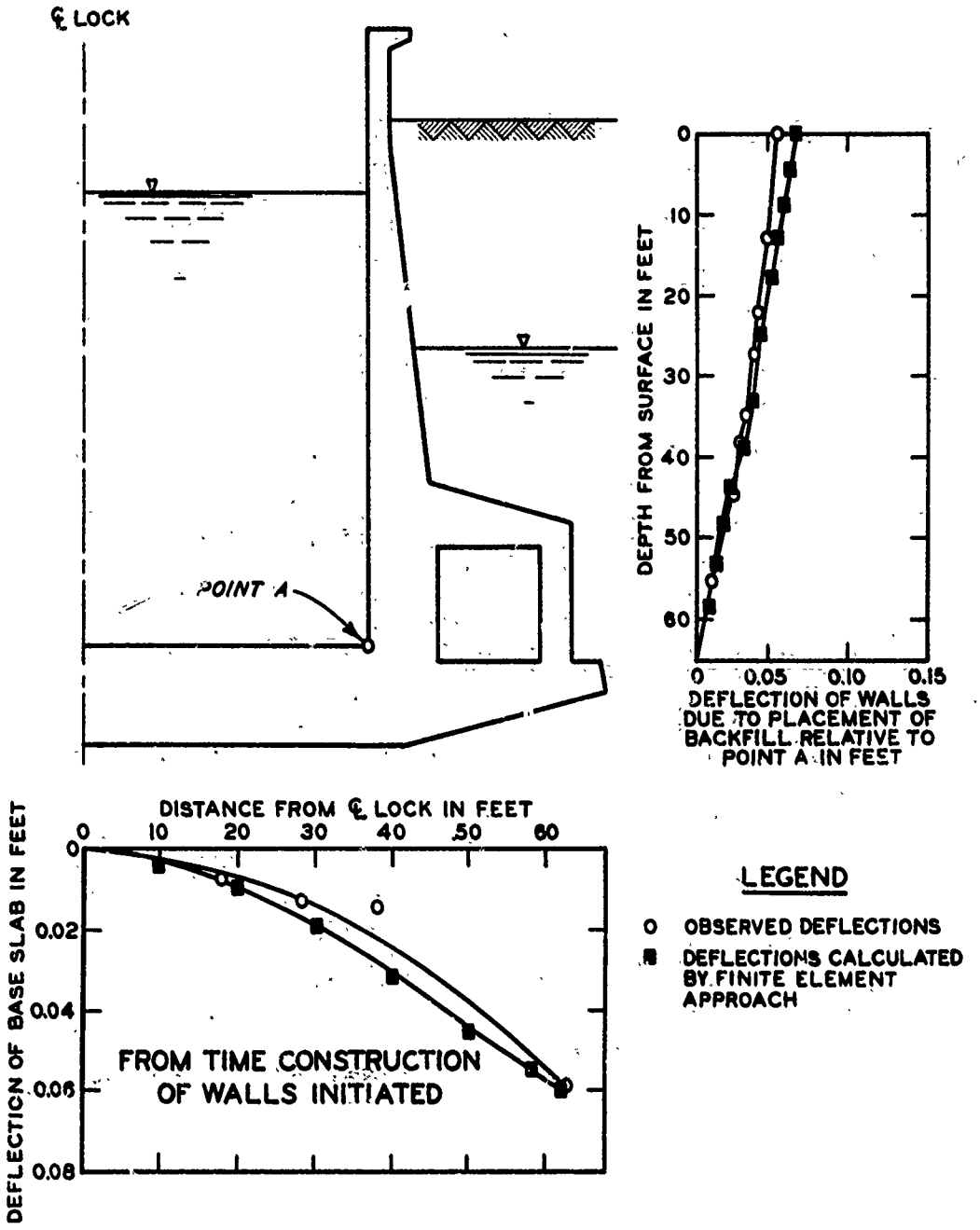

Fig. 23. Deflections of base slab and walls computed by finite element method, Case III'

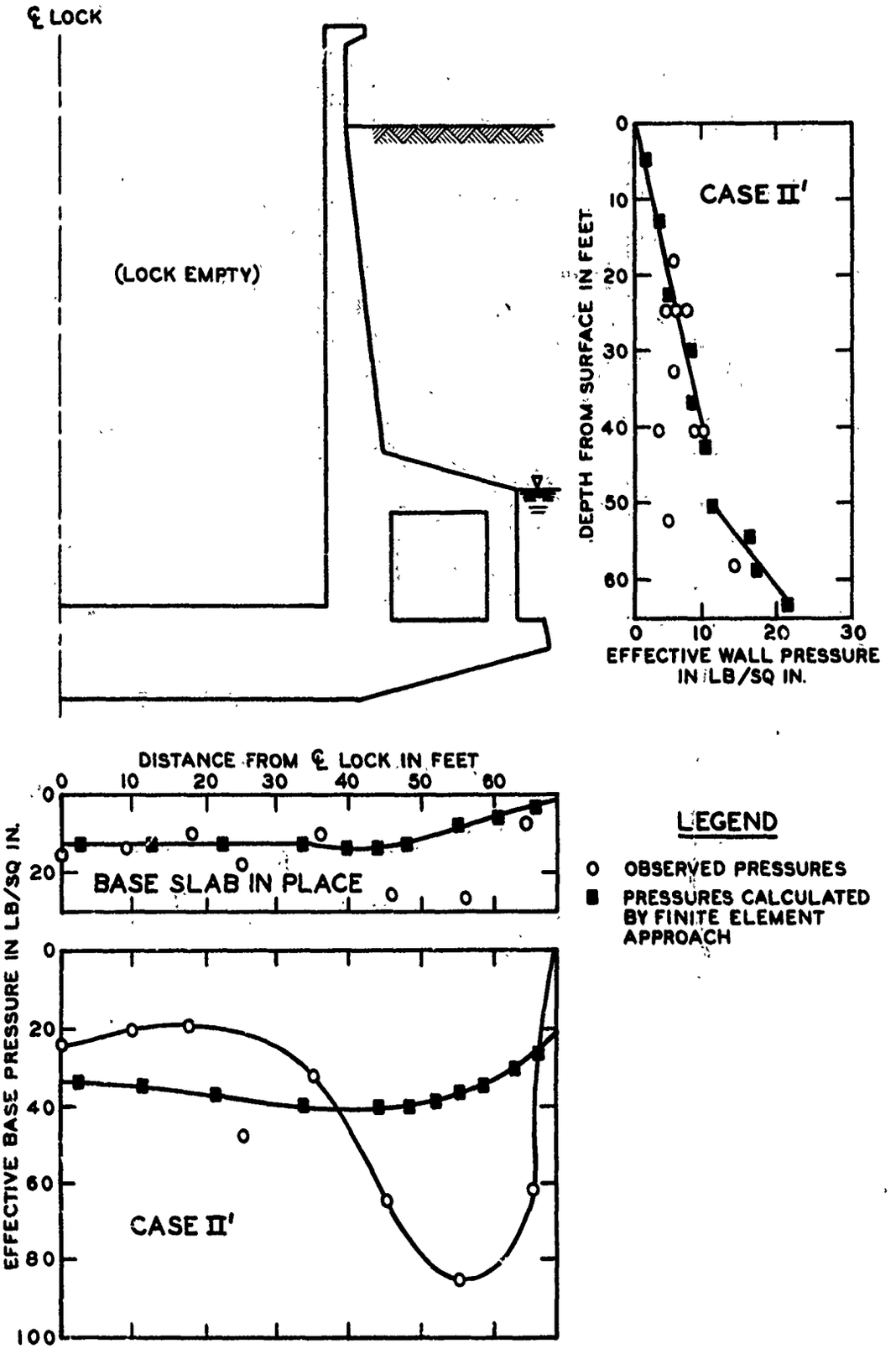

Fig. 24. Effective base and wall pressures observed and computed by finite element method, Case IA'

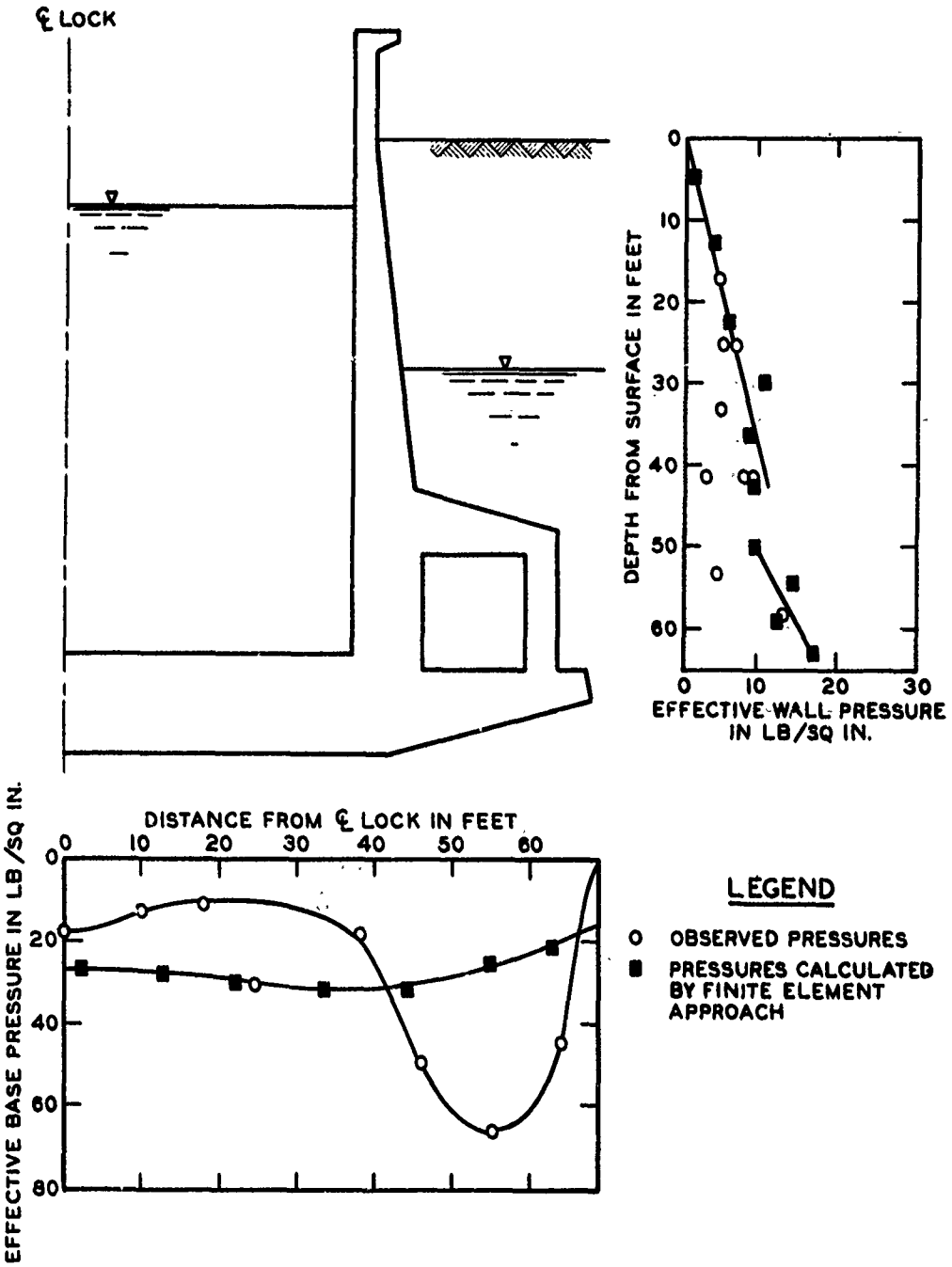

Fig. 25. Effective base and well pressures observed and computed by finite element method, Case III'

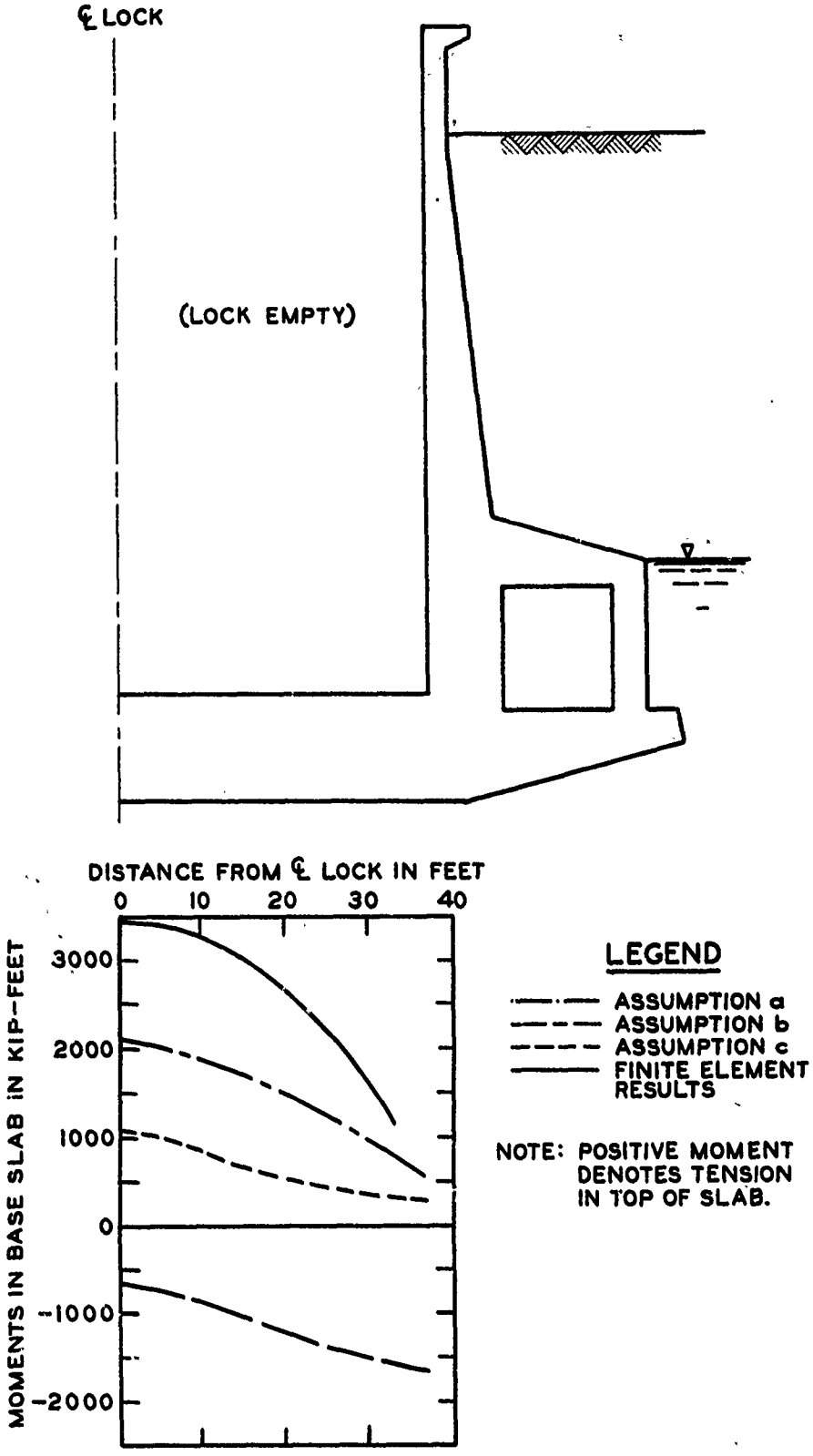

Fig. 26. Moments in base slab from finite element method, Case IA'

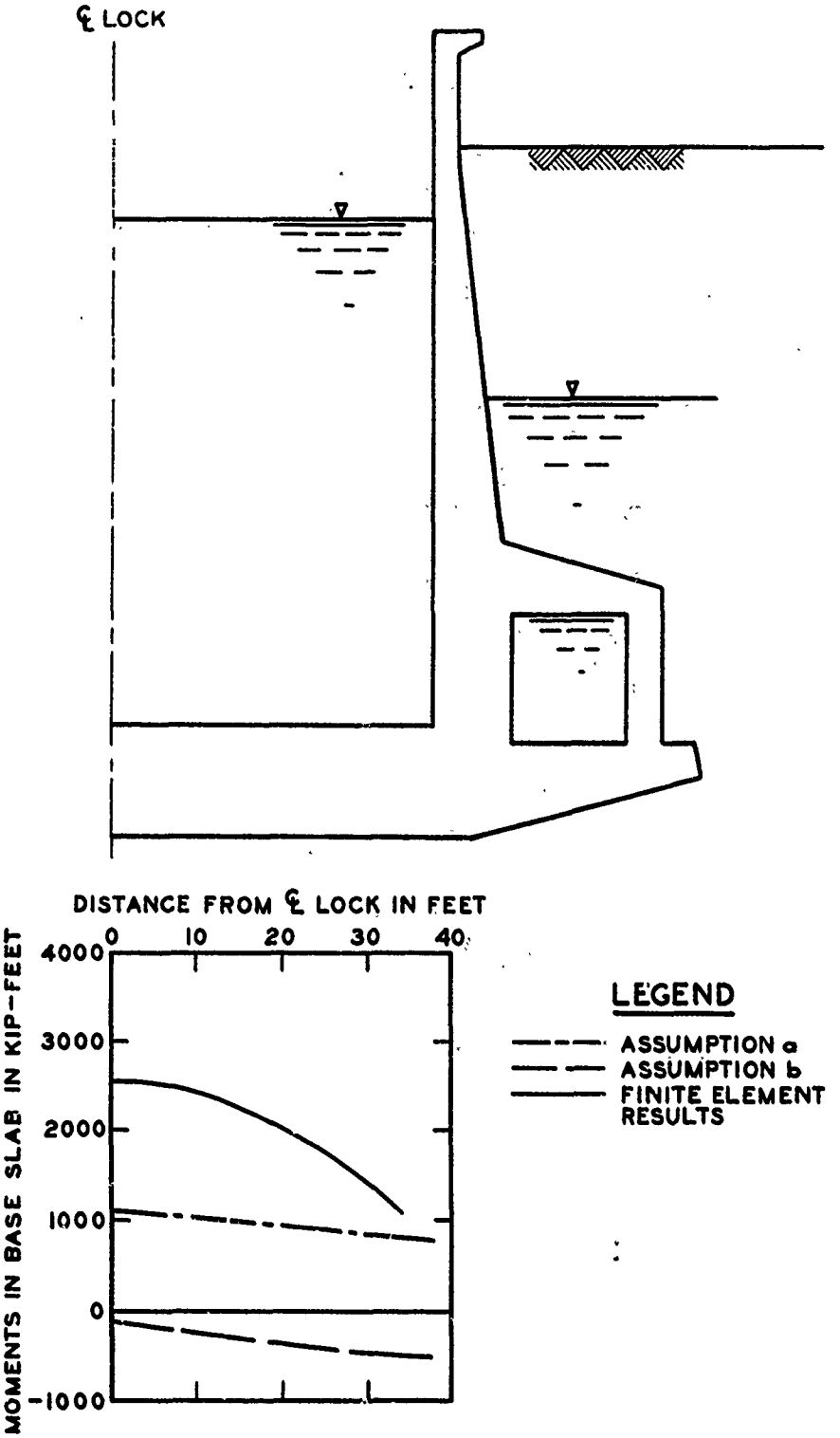

Fig. 27. Moments in base slab from finite element method, Case III'

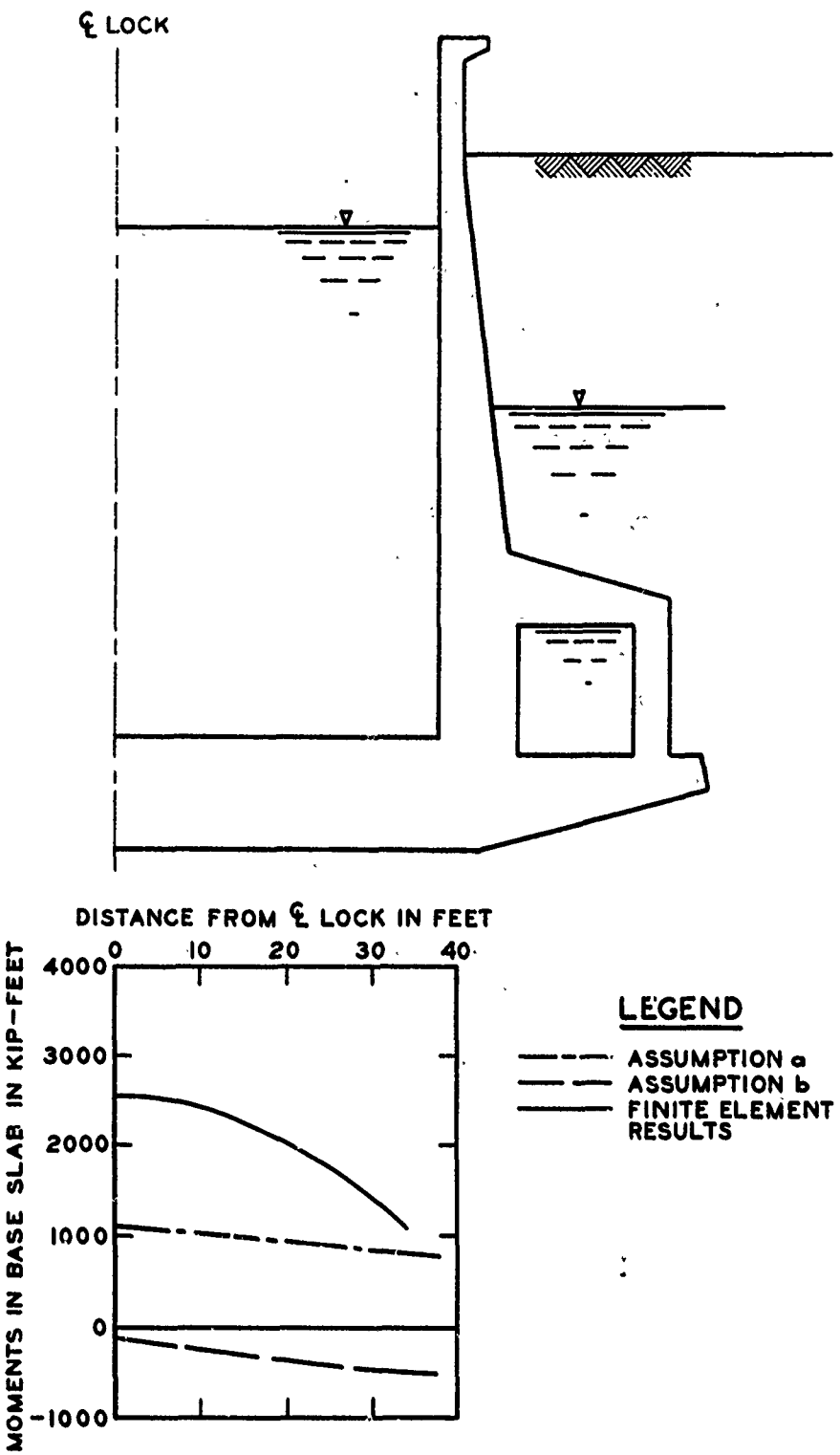

Fig. 27. Moments in base slab from finite element method, Case III'

computed side friction is considerably less than the difference between observed base pressures and structure load, moments based on the finite element method are significantly greater than moments based on observed loads. The reason for this is that observed base pressures, which are characterized by high pressures under the culvert, are more similar to the distribution of structure weight and thus will cause lower moments than the more uniformly distributed computed pressures.

114. For Case IA', maximum moment in the walls computed by the finite element analysis was 330 ft-kips, as compared with 467 ft-kips computed from observed pressures. For Case III', maximum wall moment computed from the finite element method was about 100 ft-kips, as compared with approximately 50 ft-kips computed from observed loads.

PART VIII: CONCLUSIONS AND RECOMMENDATIONS

Conclusions

115. Based on the analyses and observations of engineering measuring devices at Old River Lock, the following conclusions are believed warranted.

Instrumentation

116. The electrical measuring devices performed satisfactorily and constitute an accurate and reliable means of obtaining field measurements provided they are properly checked and tested prior to installation and are installed by qualified instrumentation technicians. With the exception of the Carlson pore pressure cell, all electrical devices were functioning when construction was completed. After approximately nine years of service, all devices except the pore pressure cell, a soil stress meter, and a concrete strain meter were functioning.

117. The wall deflection pipes provided a simple means of determining accurate measurements of the rotation and deflection of lock walls.

118. The water-level device operated satisfactorily for measuring settlements of the lock floor. The deep-water sounding device performed satisfactorily until the accumulation of sediment over the settlement plates in both gate bays became too deep to be penetrated by the device.

119. The engineering measuring devices performed as intended with the following exceptions:

a. The sounding wells became inoperative a few months after water entered the lock due to clogging of the inlets at the bottoms of the wells.

b. One bench mark was destroyed and the other was damaged and subsequently repaired; as a result, doubtful measurements of foundation rebound were obtained. Bench marks were not set sufficiently deep and were probably affected by changing stress conditions resulting from groundwater lowering during construction.

Observations and analysis

120. Observed rebounds ranged from 0.48 to 0.42 ft and were

considerably greater than rebound predicted in design. However, bench mark elevations are questionable, and it is believed that observed rebounds are in error. For the same reason, the magnitudes of the observed settlements are questionable. It is believed that the observed settlements provide a reasonable indication of the deflected shape of the lock.

121. The lock settled at a relatively uniform rate during construction, and, as of 1964, settlement appeared to be essentially complete. The lock still tends to settle and rebound a minor amount with rising and falling river stages.

122. The observed base pressure distribution curves differed in shape from the distribution curve assumed in design. The distribution curve for effective base pressures beneath Old River Lock was similar in shape to the pressure distribution curve for effective base pressure beneath Port Allen Lock except that observed pressures at Old River Lock were greater beneath the culverts and smaller beneath the center line than the base pressures observed at Port Allen.

123. Differences in magnitude between measured total base pressures and the actual structure load for Case IA' are attributed mainly to frictional drag on the sides of the lock, which was probably caused by greater settlement beneath the backfill than beneath the lock itself. With high water in the lock (Case III'), the lock settled with respect to the backfill, and side friction was reduced. The actual magnitude of frictional forces cannot be accurately determined from available data.

124. The observed lateral earth pressures along the lock walls were considerably less than those assumed in design. For Case IA', coefficients of earth pressure k varied from 0.31 along the culvert wall to 0.21 along the wall stem. The values of k for Case III' were similar to the k values for Case IA' except that values were slightly higher near the upper portion of the wall stem. The walls moved toward the backfill during construction. After construction, movements of the wall were affected more by seasonal temperature variation than by water levels in the lock.

125. In computing moments in the base slab from observed external

loads, the assumed magnitude of side friction has a considerable effect. Assuming that the total difference between observed base pressures and actual structure load is due to side friction, the computed moment at the center of the base slab was 2135 ft-kips, which is 22 percent greater than the moment computed in design; assuming the meters overregister by 10 percent, the moment computed at the center is 1705 ft-kips, or 38 percent less than the design moment; and assuming no side friction results in negative moments at the center. In computing deflections of the base slab from moments, the computed deflection assuming 10 percent overregistration of meters gave the best agreement with observed deflections.

126. Although the finite element method of analysis resulted in good agreement between computed and observed earth pressures beneath the base slab and along the walls of Port Allen Lock and along the walls of Old River Lock, the base pressures beneath Old River Lock computed by this method were in poor agreement with observed base pressures. Moments in the base slab computed from the finite element method were much greater than moments computed from observed loads. Despite the lack of agreement between observed base pressures and those computed by the finite element method, the finite element analysis is considered to be markedly superior to other existing design procedures.

Recommendations

Old River Lock

127. It is recommended for Old River Lock that:

a. All electrical measuring devices, settlement reference points and plates, and wall deflection pipes be read once a year during low-water season. All devices should be read when the lock is dewatered.

b. At the time the data presented in this report were analyzed, it was considered that the observed internal stresses and strains in the concrete were too complex to be analyzed by conventional methods and that such an analysis was beyond the scope of this report. In recent years, advances have been made in structural analysis using the finite element method. It is therefore

recommended that additional studies be made to analyze the observed internal stresses and strains using the finite element method.

Similar Structures

128. For instrumentation of similar structures, it is recommended that:

a. Bonded strain gages be used to measure strain in the reinforcing steel in the concrete base slab.

b. Settlement plates be installed in the backfill behind the lock walls. Observed settlements of the backfill may contribute to a better understanding of the development of frictional forces on the sides of the lock.

c. Pressure cells capable of measuring both normal and shear stresses be utilized along the lock walls if such cells become commercially available.

d. Additional pressure cells at closer spacing be installed on both sides of the lock to provide a more accurate assessment of the pressure distribution beneath the slab.

e. Bench marks be installed at sufficient depth to minimize the effects of movements from stress changes caused by groundwater lowering during construction.

129. On the basis of data obtained from the instrumentation program at Old River Lock, the following recommendations are made with regard to the design of similar structures having the same width-depth ratio and having similar foundation soils, backfill materials, and clay blankets at the base of the backfill:

a. The lateral earth pressures be selected on the basis of observed k values presented in this report (see fig. 18), providing that the relation of sequence of wall construction to backfill placement is similar to that employed at Old River Lock.

b. A rectangular distribution of base pressure be used beneath the lock with 175 percent of the average base pressure acting beneath the culverts and lock walls and the remainder of the pressure distributed uniformly beneath the lock chanber. The finite element analysis described in reference 12 should be used to check design procedures for future similar structures.

LITERATURE CITED

1. U. S. Army Engineer Division, Lower Mississippi River Valley, CE, "Mississippi River and Tributaries, Old River Navigation Lock; Lock Masonry," Design Memorandum No. 9, Jun 1958 (Revised Jul 1959), Vicksburg, Miss.; prepared by Bedell and Nelson Engineers, Inc., and A. W. Thompson and Assoc., New Orleans, La.

2. _____, "Mississippi River and Tributaries, Old River Navigation Lock; Instrumentation," Design Memorandum No. 9B, Nov 1958 (Revised Jan 1959), Vicksburg, Miss.; prepared by U. S. Army Engineer Waterways Experiment Station, CE, Vicksburg, Miss.

3. Trahan, C. C., "Instructions for Installation and Observations of Engineering Measurement Devices, Old River Navigation Lock," Instruction Report No. 5, Nov 1959, U. S. Army Engineer Waterways Experiment Station, CE, Vicksburg, Miss.

4. _____, "Calibration and Installation of Electrical Measuring Devices and Results of Tests on Concrete and Sand Backfill, Old River Lock," Miscellaneous Paper No. 3-554, Jan 1963, U. S. Army Engineer Waterways Experiment Station, CE, Vicksburg, Miss.

5. Goode, T. B., "Undisturbed Sand Sampling Below the Water Table," Bulletin No. 35, Jun 1950, U. S. Army Engineer Waterways Experiment Station, CE, Vicksburg, Miss.

6. Garber, P. K., "Potamology Investigation, Summary Report of Soils Data," Potamology Investigation Report No. 12-2, Oct 1952, U. S. Army Engineer Waterways Experiment Station, CE, Vicksburg, Miss.

7. Sherman, W. C., Jr., and Trahan, C. C., "Analysis of Data from Instrumentation Program, Port Allen Lock," Technical Report S-68-7, Sep 1968, U. S. Army Engineer Waterways Experiment Station, CE, Vicksburg, Miss.

8. Kaufman, R. I. and Webb, R. R., "Review of Soils Design, Construction, and Performance Observations, Bayou Boeuf Lock," Technical Report No. 3-458, Jun 1957, U. S. Army Engineer Waterways Experiment Station, CE, Vicksburg, Miss.

9. Terzaghi, K., "Large Retaining Wall Tests," Engineering News-Record, Vol 112, Nos. 5, 8, 10, 13, 16, and 23, and Vol 113, Nos. 2 and 17, 1934.

10. Carlson, R. W., Manual for the Use of Stress Meters, Strain Meters, and Joint Meters in Mass Concrete, 3d ed., Gillick, Berkeley, Calif., 1966.

11. Raphael, J. M. and Carlson, R. W., Measurement of Structural Action in Dams, 3d ed., Gillick, Berkeley, Calif., 1965.

12. Clough, C. W. and Duncan, J. M., "Finite Element Analyses of Port Allen and Old River Locks," Contract Report S-69-6, Sep 1969, U. S. Army Engineer Waterways Experiment Station, CE, Vicksburg, Miss.; Prepared by University of California, Soil Mechanics and Bituminous Materials Laboratory, Berkeley, Calif., under Contract No. DACW39-68-C-0040.

13. Duncan, J. M. and Chang, C. Y., "Nonlinear Analysis of Stress and Strain in Soils," Journal, Soil Mechanics and Foundations Division, American Society of Civil Engineers, Vol 96, No. SM5, Sep 1970, pp 1629-1653.

14. Goodman, R. E., Taylor, R. L., and Brekkle, T. L., "A Model for the Mechanics of Jointed Rock," Journal, Soil Mechanics and Foundations Division, American Society of Civil Engineers, Vol 94, No. SM3, May 1968, pp 637-659.

15. Woodman, E. H., "Pressure Cells for Field Use," Bulletin No. 40, Jan 1955, U. S. Army Engineer Waterways Experiment Station, CE, Vicksburg, Miss.

16. Pant, B. and Patil, S. S., "Two Dimensional Photoelastic Analysis of Stresses in the Vicinity of 'No Stress Meters' Installed in Dams," Irrigation and Power, Journal of Central Board of Irrigation and Power, Vol 18, No. 10, New Delhi, India, Oct 1961.

17. U. S. Army Engineer Waterways Experiment Station, CE, "Handbook for Concrete and Cement," Aug 1949 (with quarterly supplements), Vicksburg, Miss.

18. American Society for Testing and Materials, "Standard Methods of Tension Testing of Metallic Materials," Designation: E 8-69, 1970 Book of ASTM Standards, Part 31, 1970, Philadelphia, Pa., pp 194-213.

Table 1

Heave Point Installation Data

Heave Point No.	Date Installed	As-Installed Position			Offset in Plan of As-Installed Position from True Position, ft	Corrected Initial Elevation ft msl
		Station	Offset from ℄ ft	Elevation ft msl		
H-1	2 Jul 58	90+80.00	0	-31.003	1.95	-30.978
H-2*	--	90+80.00	70.00 S	--	--	--
H-3	8 Jul 58	96+95.00	0	-26.016	1.22	-26.006
H-4	3 Jul 58	97+00.00	70.00 S	-21.010	1.00	-21.003
H-5	10 Jul 58	97+00.00	70.00 N	-20.996	0.68	-20.993
H-6	11 Jul 58	1044+10.00	0	-35.569	1.73	-35.559
H-7	23 Jul 58	1044+10.00	70.00 N	-31.004	1.58	-30.988
H-8	23 Oct 58	103+20.00	0	-34.530	1.47	-34.517
H-9*	--	103+20.00	70.00 S	--	--	--

* Destroyed during excavation.

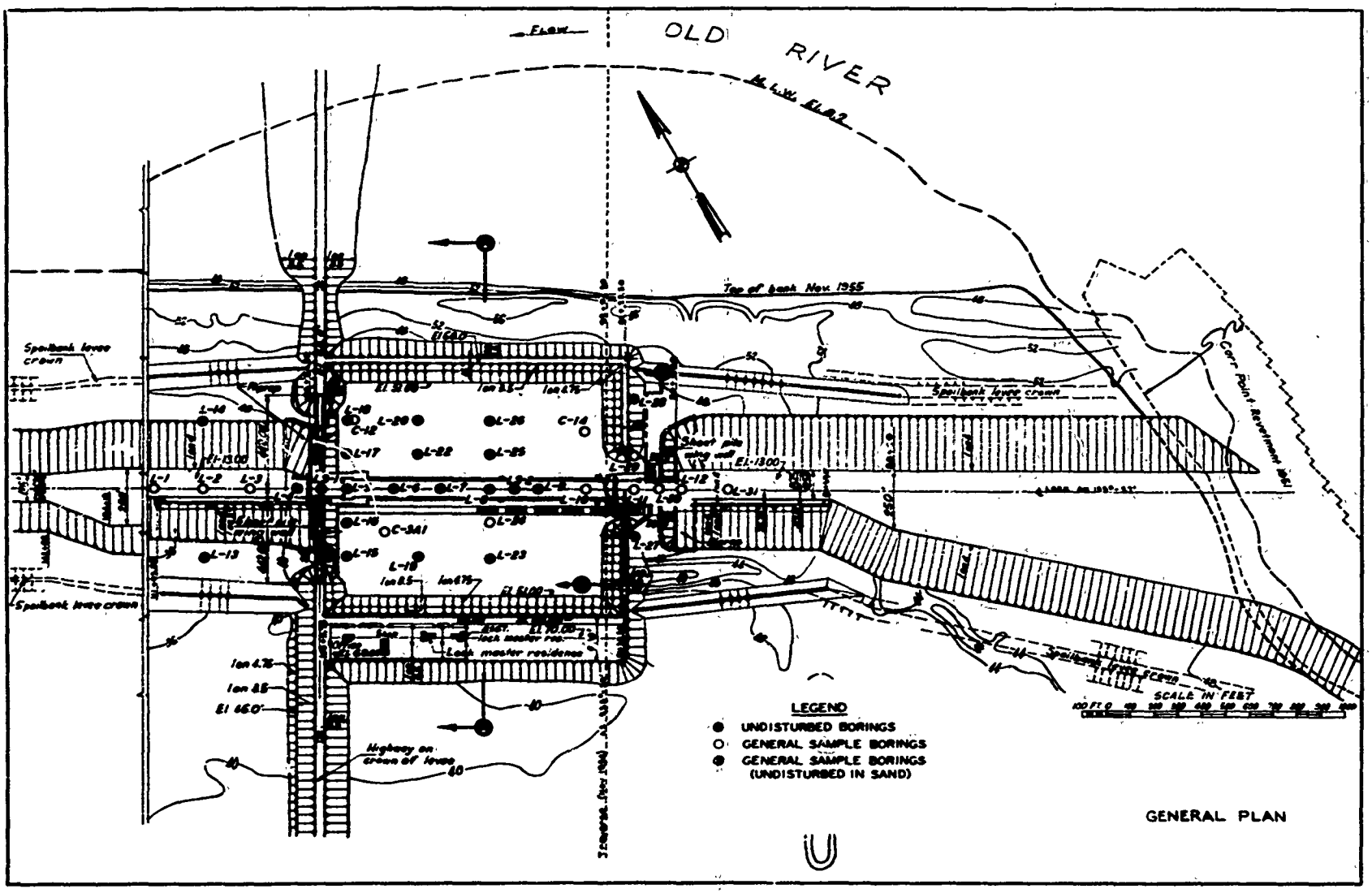
OLD RIVER
Flow
Top of bank Nov. 1955
Spoilbank levee crown
Corr. Point Revetment
Sheet pile wing wall
EL. 13.00
Lock master residence
Highway on crown of levee
Levee toe (low water)
LEGEND
UNDISTURBED BORINGS
GENERAL SAMPLE BORINGS
GENERAL SAMPLE BORINGS (UNDISTURBED IN SAND)
SCALE IN FEET
GENERAL PLAN

PLATE 1

PLATE 2

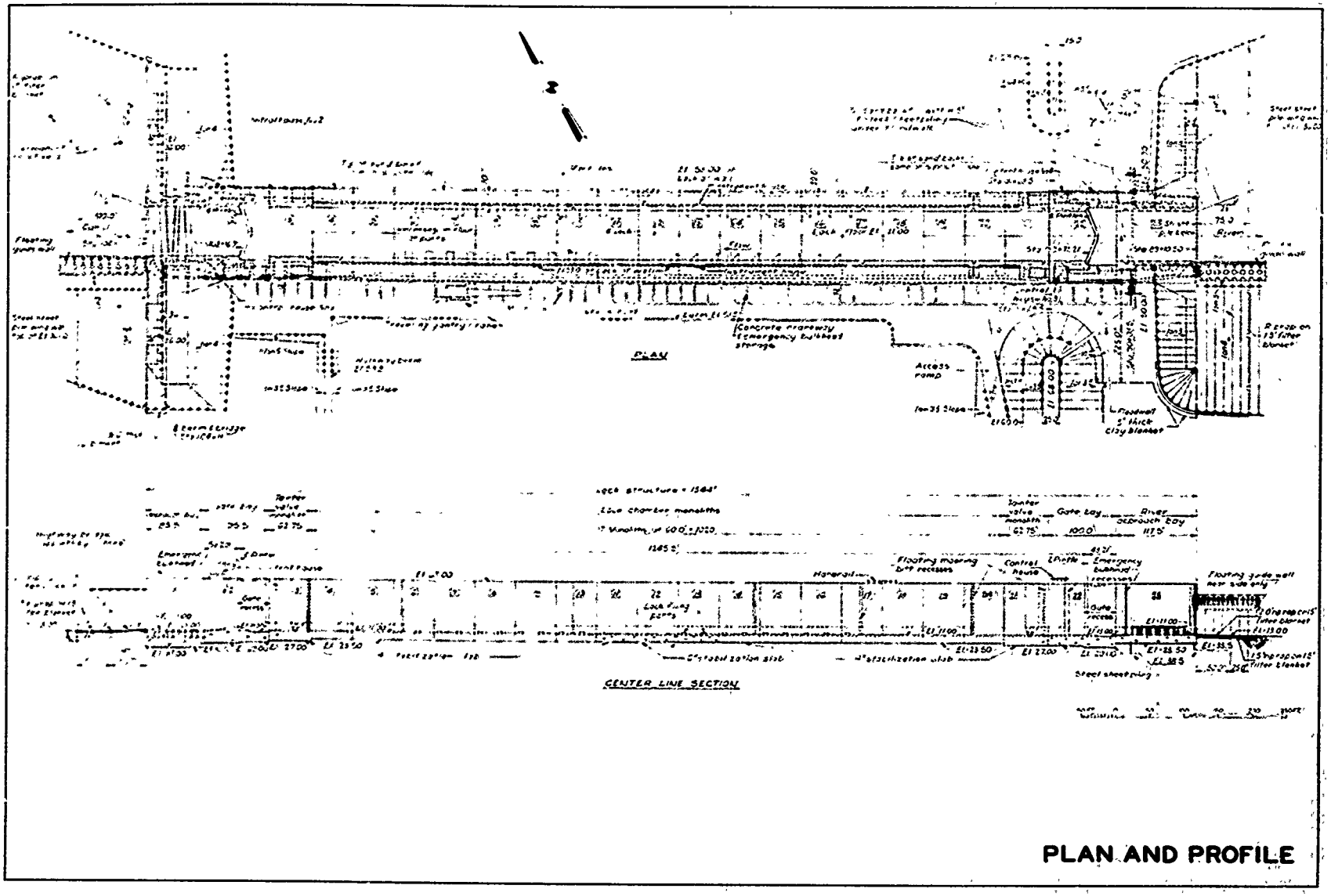

PLAN AND PROFILE

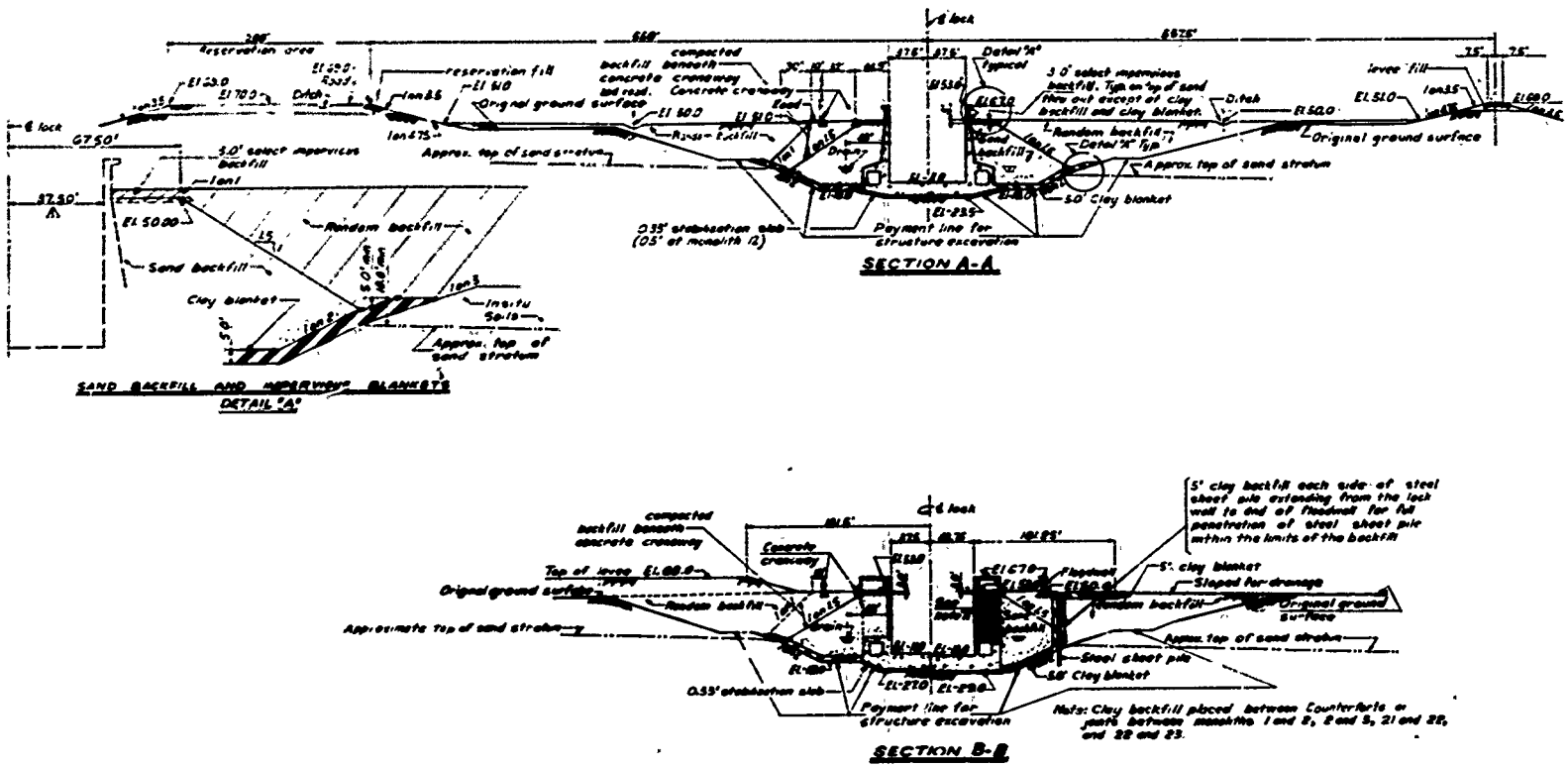

NOTE: SEE PLATE 1 FOR LOCATIONS OF SECTIONS.

TYPICAL SECTIONS

PLATE 3

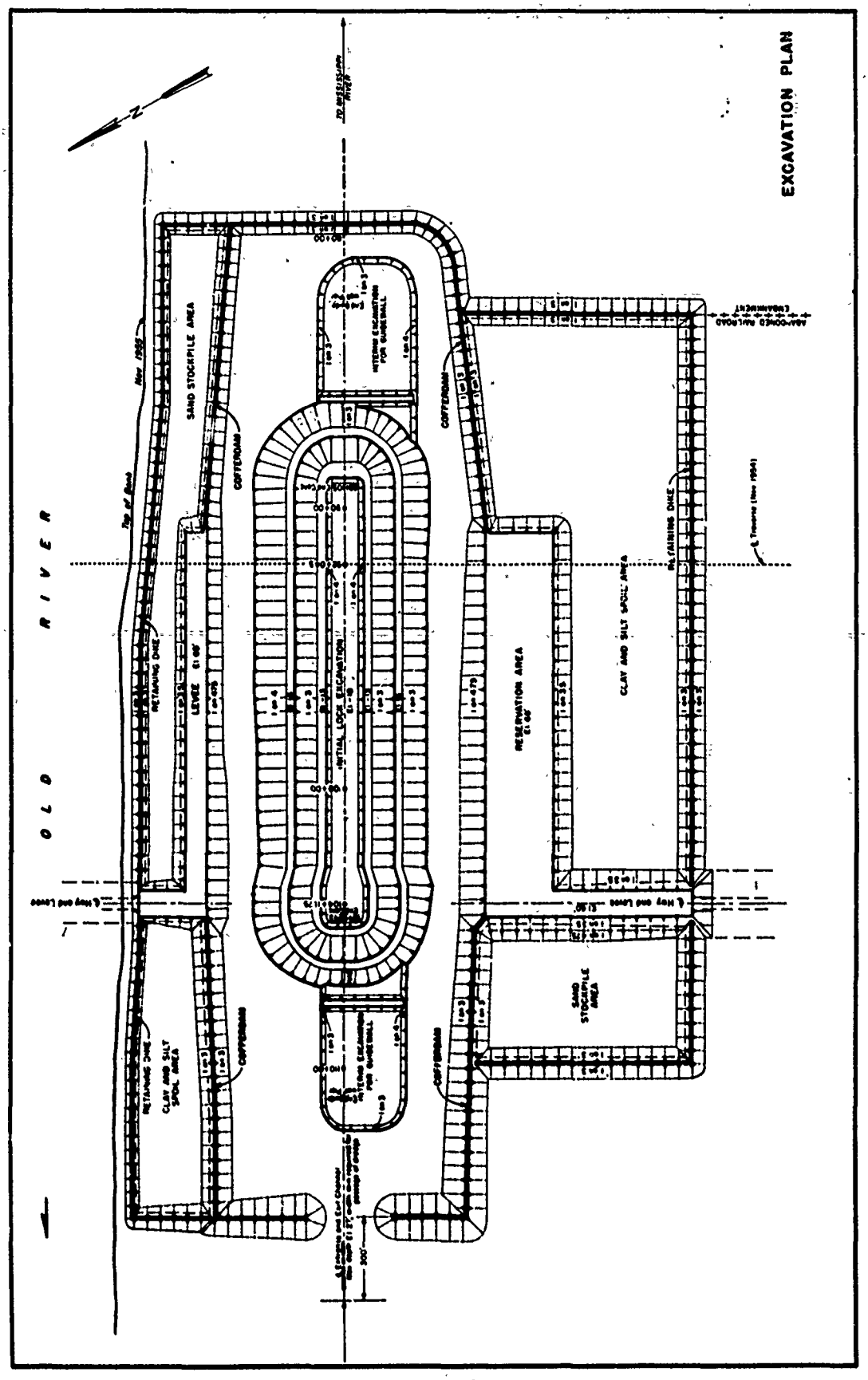
EXCAVATION PLAN
OLD RIVER
SAND STOCKPILE AREA
COFFERDAM
LEVEE
RETAINING DIKE
INITIAL LOCK EXCAVATION
RESERVATION AREA
CLAY AND SILT SPOIL AREA
REFAIRING DIKE
CLAY AND SILT SPOIL AREA
SAND STOCKPILE AREA

PLATE 4

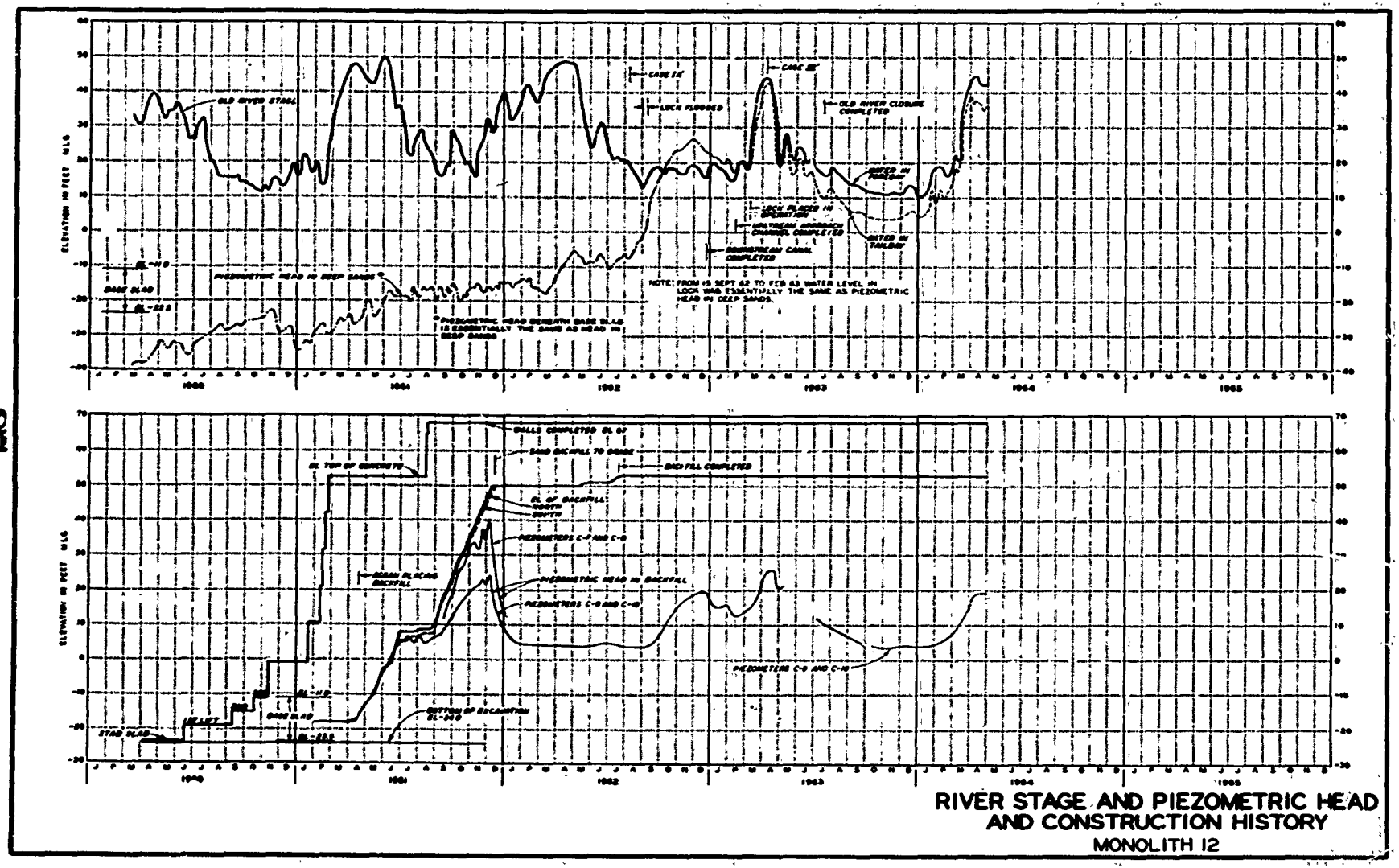

RIVER STAGE AND PIEZOMETRIC HEAD AND CONSTRUCTION HISTORY

MONOLITH 12

PLATE 5

87

PLATE 6

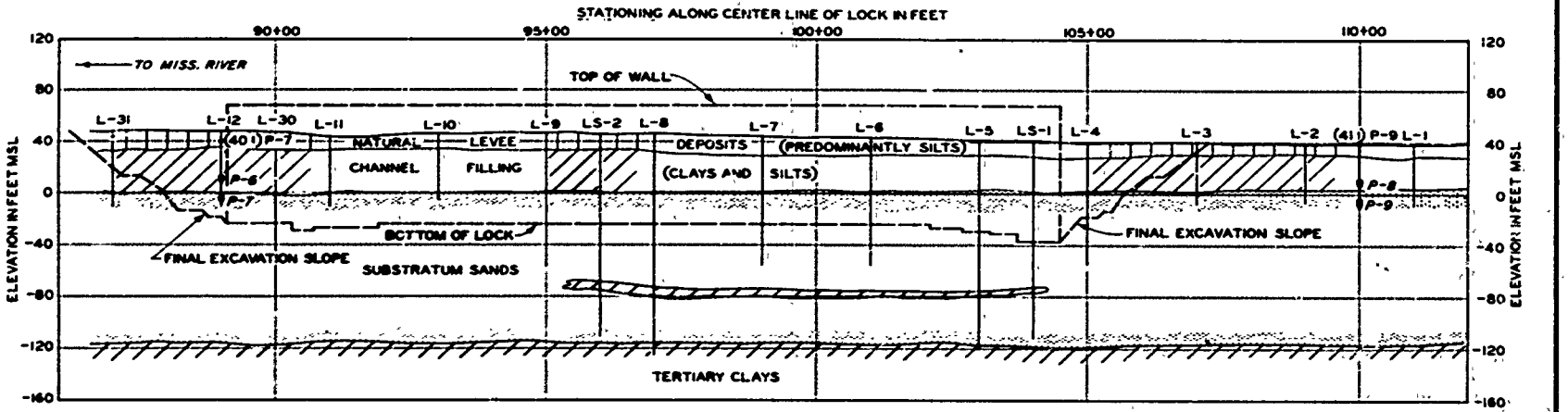

GENERALIZED SOIL PROFILE ALONG BASE LINE AND CENTER LINE OF LOCK

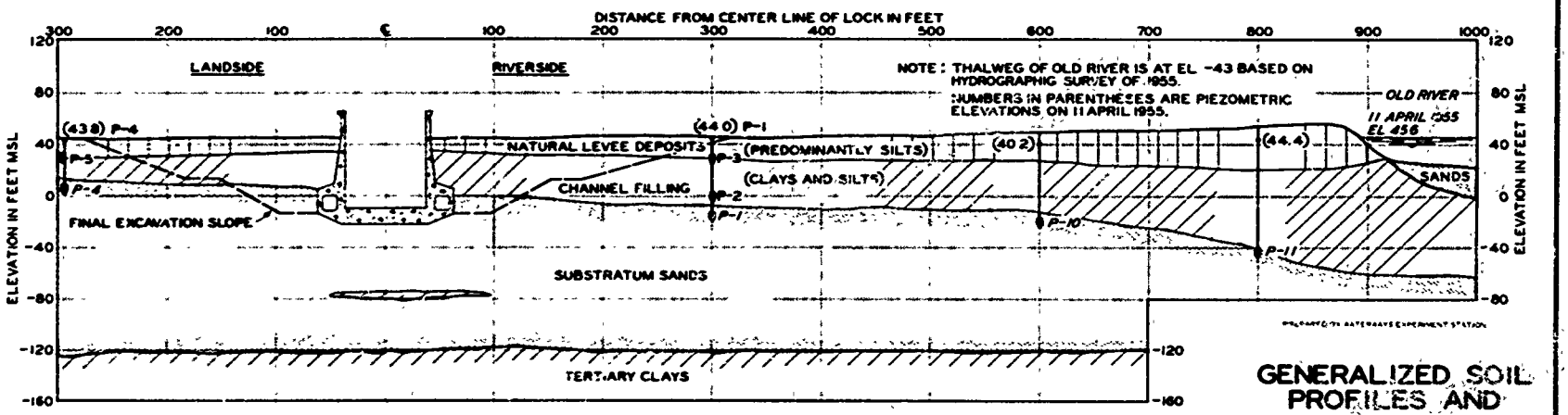

GENERALIZED SOIL PROFILE PERPENDICULAR TO RIVER AND LOCK

GENERALIZED SOIL PROFILES AND LOCATIONS OF PIEZOMETERS

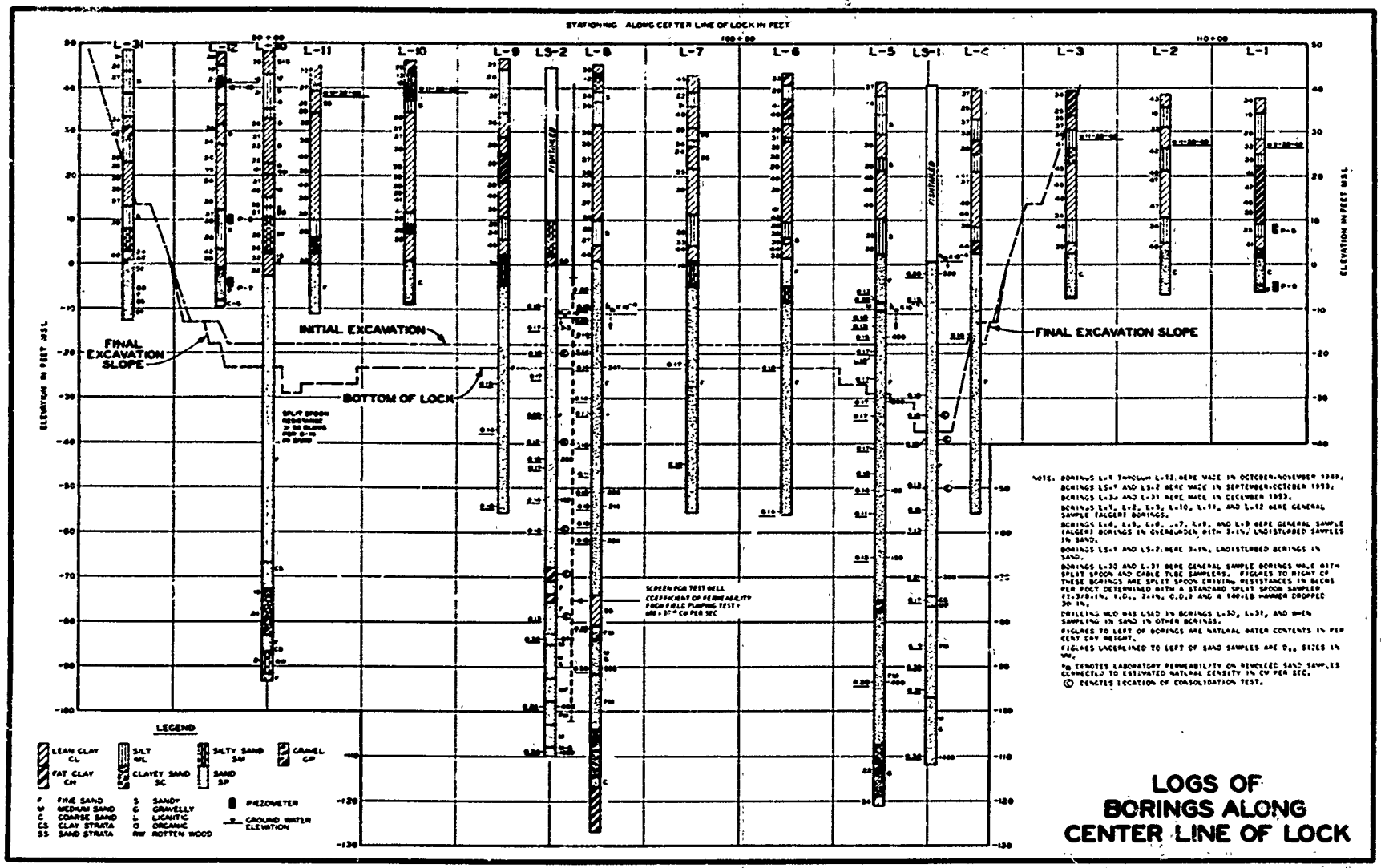

LOGS OF BORINGS ALONG CENTER LINE OF LOCK

PLATE 7

PLATE 8

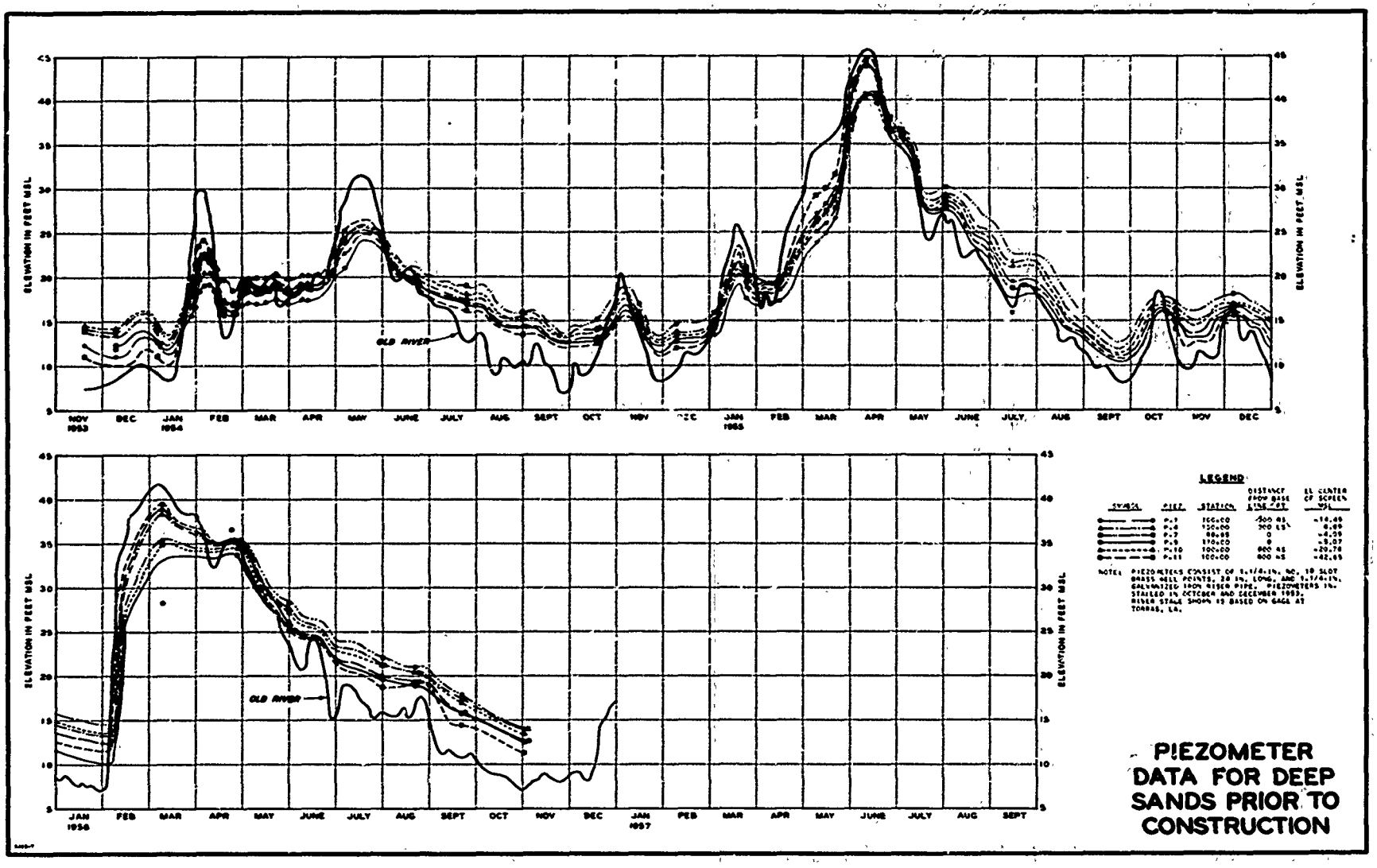

PIEZOMETER DATA FOR DEEP SANDS PRIOR TO CONSTRUCTION

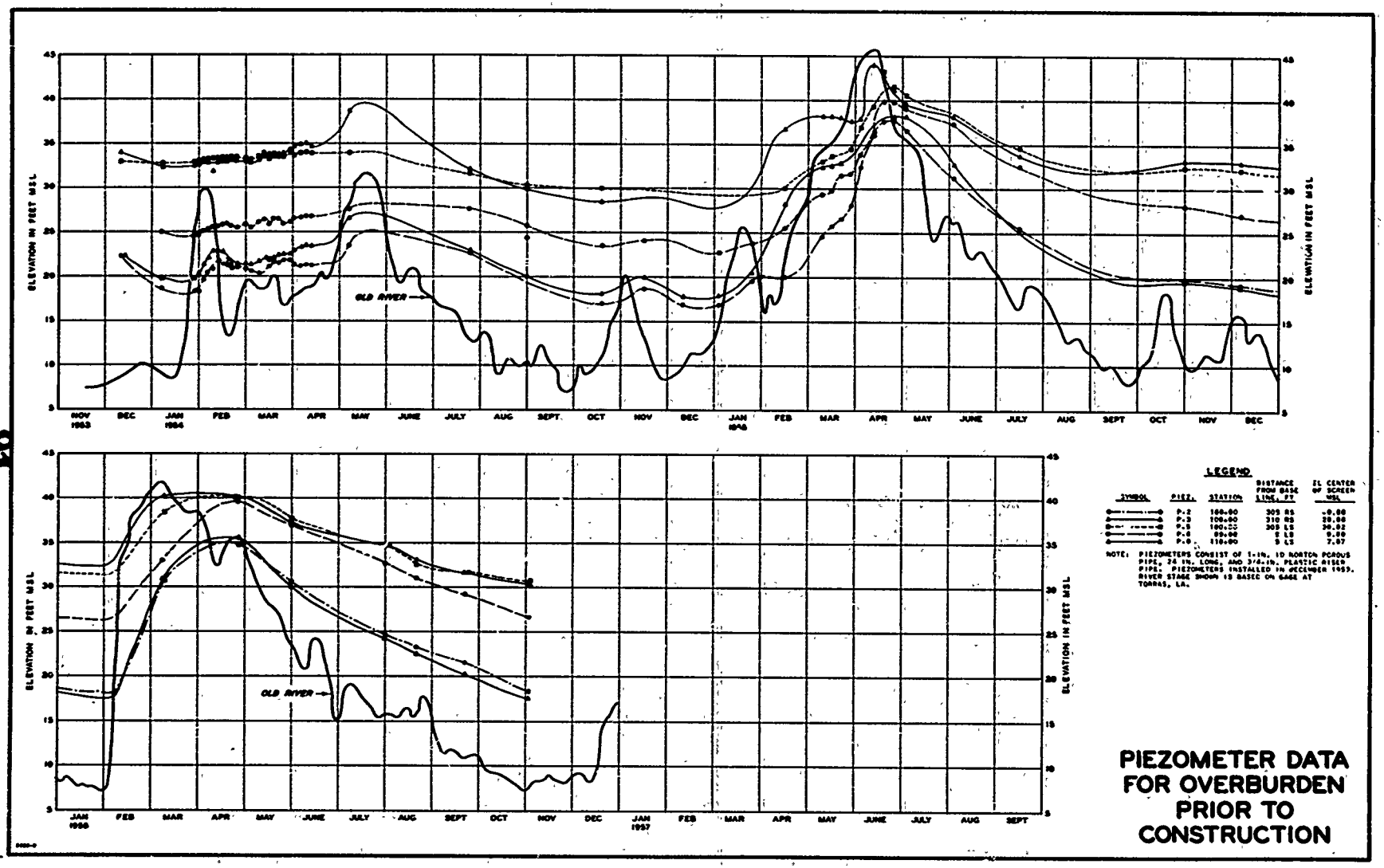
ELEVATION IN FEET MSL
OLD RIVER
NOV 1963
DEC
JAN 1964
FEB
MAR
APR
MAY
JUNE
JULY
AUG
SEPT
OCT
NOV
DEC
JAN 1965
FEB
MAR
APR
MAY
JUNE
JULY
AUG
SEPT
OCT
NOV
DEC
JAN 1966
FEB
MAR
APR
MAY
JUNE
JULY
AUG
SEPT
OCT
NOV
DEC
JAN 1967
FEB
MAR
APR
MAY
JUNE
JULY
AUG
SEPT
LEGEND
SYMBOL
PIEZ.
STATION
DISTANCE FROM BASE LINE, FT
EL CENTER OF SCREEN MSL
P-2
P-3
P-5
P-6
P-8
NOTE: PIEZOMETERS CONSIST OF 1-IN., 10 MICRON POROUS PIPE, 24 IN. LONG, AND 3/4-IN. PLASTIC RISER PIPE. PIEZOMETERS INSTALLED IN DECEMBER 1963. RIVER STAGE SHOWN IS BASED ON GAGE AT TORRAS, LA.
PIEZOMETER DATA FOR OVERBURDEN PRIOR TO CONSTRUCTION

PLATE 9

PLATE 10

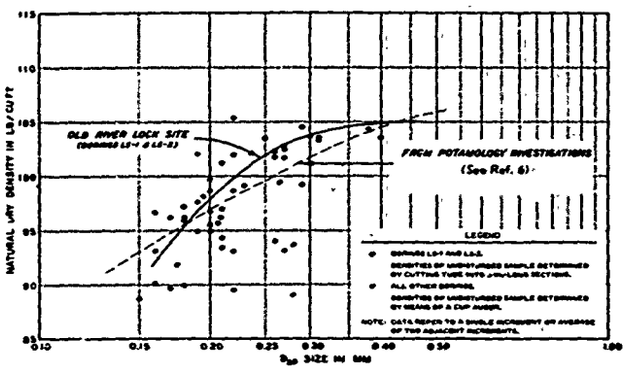

NATURAL DENSITY OF SAND VS GRAIN SIZE

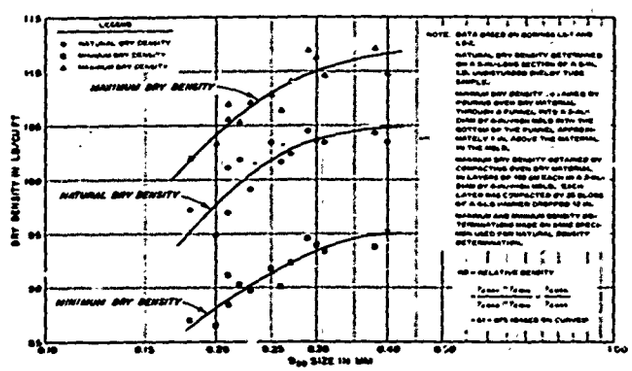

MAXIMUM, MINIMUM AND NATURAL DRY DENSITY OF SAND VS GRAIN SIZE

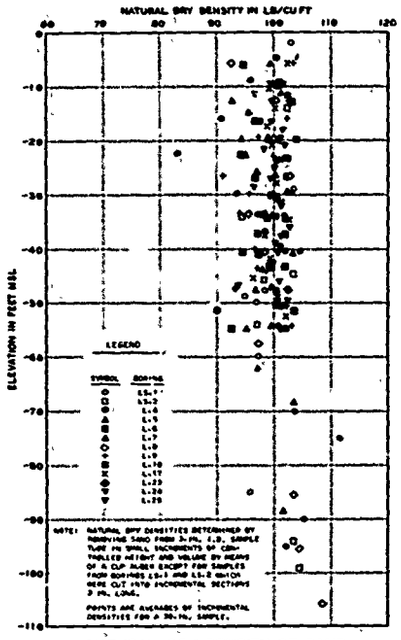

NATURAL DRY DENSITY OF SAND VS ELEVATION

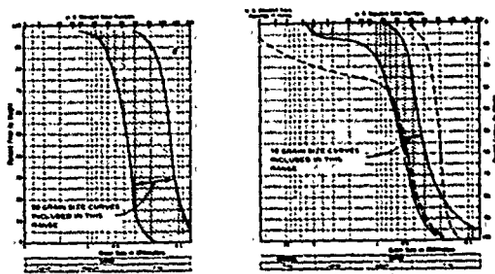

GRAIN SIZE DISTRIBUTION OF SANDS

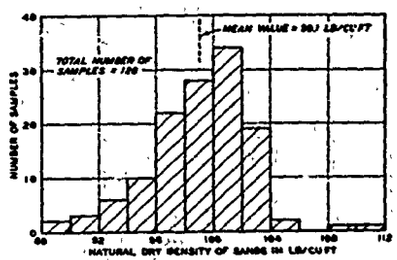

FREQUENCY DISTRIBUTION OF NATURAL DRY DENSITIES OF SANDS

CLASSIFICATION AND DENSITY DATA OF FOUNDATION SANDS

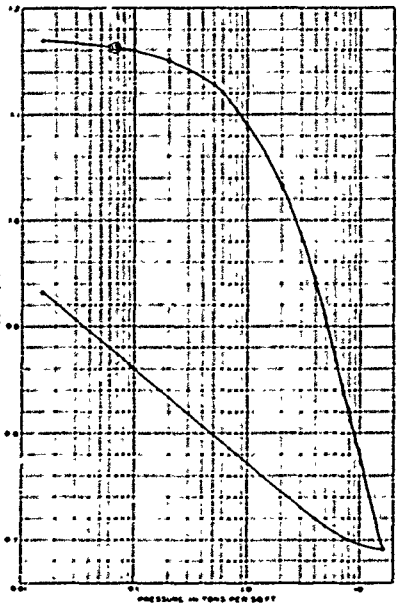

CLAYS AND SILTS

PRESSURE-VOID RATIO CURVES

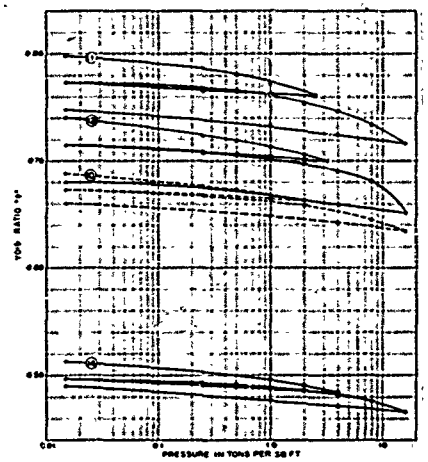

SANDS- UNDISTURBED

PRESSURE-VOID RATIO CURVES

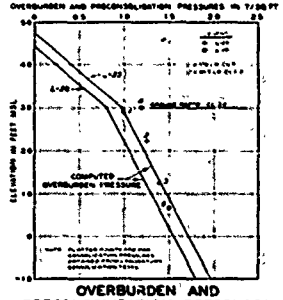

OVERBURDEN AND PRECONSOLIDATION PRESSURES

GRAIN SIZE CURVES

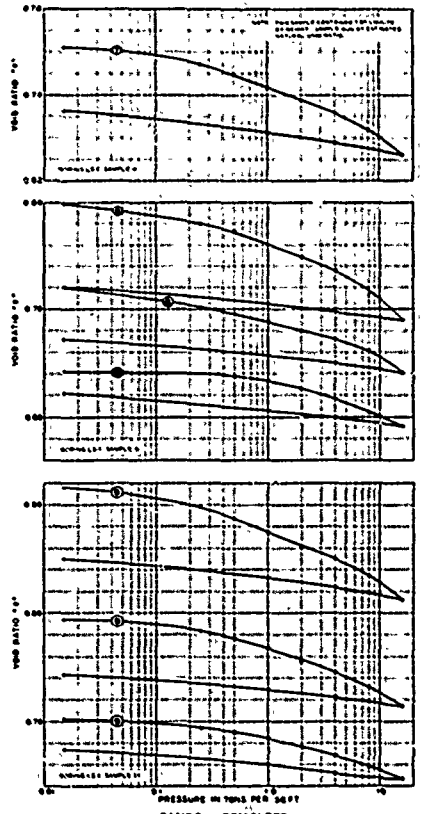

SANDS— REMOLDED

PRESSURE-VOID RATIO CURVES

Summary of Consolidation Test Data

Ref No.	Boring	Sample	Depth ft	El msl	Classification	Atterberg Limits LL	Atterberg Limits PL	Atterberg Limits PI	Mechanical Analysis % Sand	Mechanical Analysis % Fines	Before Test w, %	Before Test γ_d lb/cu ft	Before Test e_o	Before Test S_o, %	Sp Gr	P_c' tons/sq ft	P_o tons/sq ft	C_c
7	LS-1	8	73.4	-33.9	Fine sand w/lignite	NP	--	--	100	0	--	94.9	0.745	96	2.65	--	---	----
8		9	78.9	-39.4	Fine sand	NP	--	--	99	1	--	91.4	0.798	89	2.63	--	---	----
											--	95.5	0.720	94				
											--	100.0	0.682	95				
9		11	89.4	-49.9	Fine sand	NP	--	--	100	0	--	87.3	0.916	88	2.68	--	---	----
											--	93.3	0.793	98				
											--	98.3	0.702	100				
10	LS-2	4	64.5	-20.0	Fine sand	NP	--	--	99	1	--	98.7	0.689	88	2.67	--	---	----
11		8	83.5	-39.0	Fine sand	NP	--	--	98	2	10	91.0	0.798	90	2.68	--	---	----
12		12	103.5	-59.0	Fine sand	NP	--	--	99	1	4	95.8	0.740	94	2.67	--	---	----
13		14	113.5	-69.0	Clay	CH	52	21	31	14	86	43	78.0	1.167	100	2.71	3.8	2.0	0.49
14		16	123.5	-79.0	Fine sand	NP	--	--	--	94	5	18	110.2	0.513	95	2.67	--	---	----

Note: Tests on samples 9 and 11, Boring LS-1, were performed on specimens remolded at three different void ratios. Test on sample 8, Boring LS-1, performed on specimen remolded at estimated natural void ratio. Tests on samples 4, 8, 12, and 16, Boring LS-2, were performed on samples that were frozen immediately after sampling to minimize disturbance during handling and preparation of test specimens. The specimens were permitted to thaw before testing.

RESULTS OF LABORATORY CONSOLIDATION TESTS

PLATE 11

PLATE 12

94

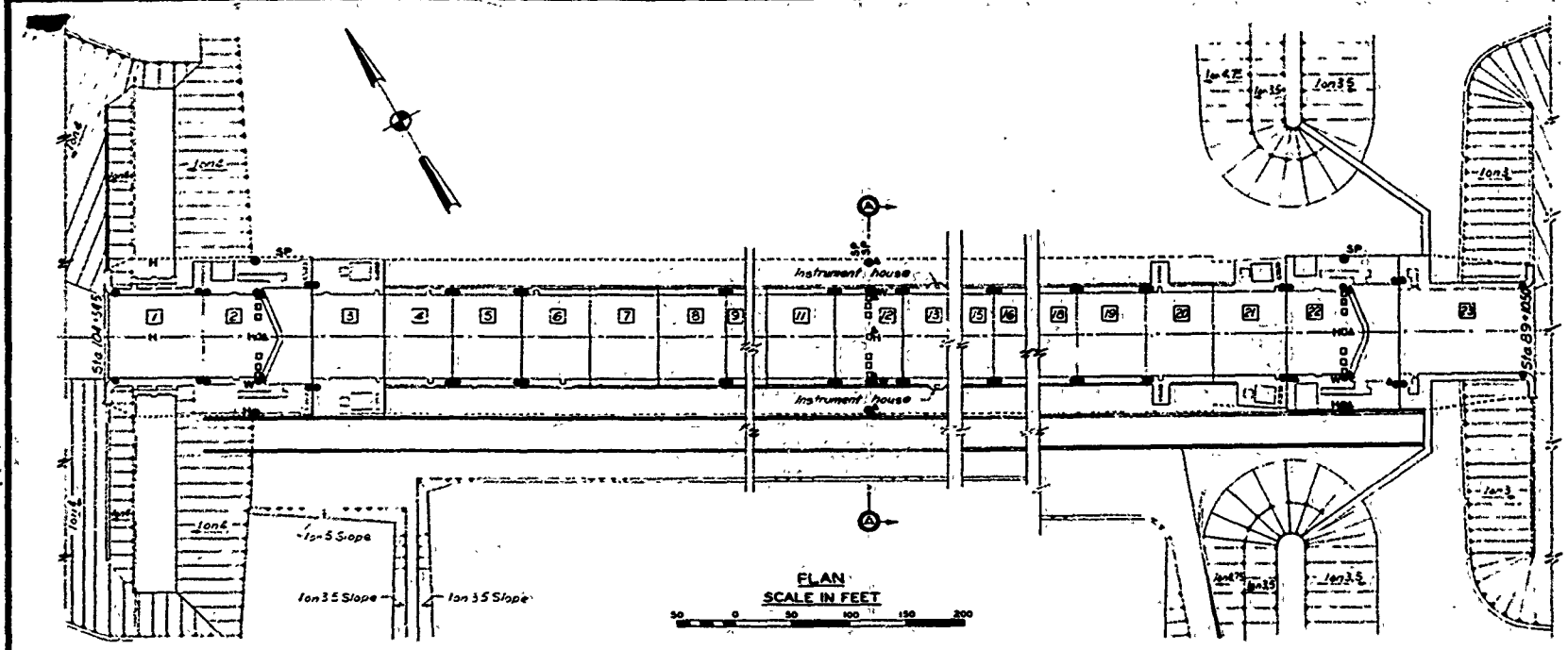

SUMMARY OF ENGINEERING MEASUREMENT DEVICES

SYMBOL SEC	SYMBOL PLAN	SYMBOL EL	DEVICE	NUMBER INSTALLED MON 2	MON 12	MON 22	TOTAL
●			PIEZOMETER[2] TYPE A	---	1	1	2[3]
●			PIEZOMETER[2] TYPE B	3	7	3	13
●			PIEZOMETER[2] TYPE C	2	6	2	10[4]
●			CARLSON PORE PRESSURE CELL	---	1	---	1
○		○	SEQ PRESSURE CELL	---	3	---	3
●		●	CARLSON SOIL STRESS METER	---	20	---	20
●			CARLSON CONCRETE STRESS METER	---	6	---	6
●			CARLSON STRAIN METER	---	37	---	37
●	H		WALL DEFLECTION PIPE	---	2	2	4
●	H		HEAVE POINT	2	3	2	9[4]
●	H		TEMPORARY SETTLEMENT REFERENCE POINT	3	5	4	12
●	H	•	SETTLEMENT REFERENCE BOLT	6	6	6	18[5]
●	T		RESISTANCE THERMOMETER	---	2	---	2
●	W		SOUNDING WELL	1	2	1	4
SP	SP		SETTLEMENT REFERENCE POINT (TYPE "A")	1	2	1	4
◻	◻		SETTLEMENT REFERENCE POINT (TYPE "B")	2	2	2	6
◻	◻		18" x 18" x 3" REFERENCE PLATE	7	7	7	21

[2] FOR DESIGNATION OF PIEZOMETERS, SEE FIGURE 16.
[3] INCLUDES "A" PIEZOMETERS AT STA 108+60 AND 101+35 AND MONOLITHS 1, 6 AND 10.
[4] INCLUDES "C" PIEZOMETERS AT MONOLITH 23
[5] INCLUDES BOLTS ON MONOLITHS 1-23, INCLUSIVE
[6] TWO HEAVE POINTS IN MONOLITH NO. 7, STA 104+10

PLAN OF INSTRUMENTATION

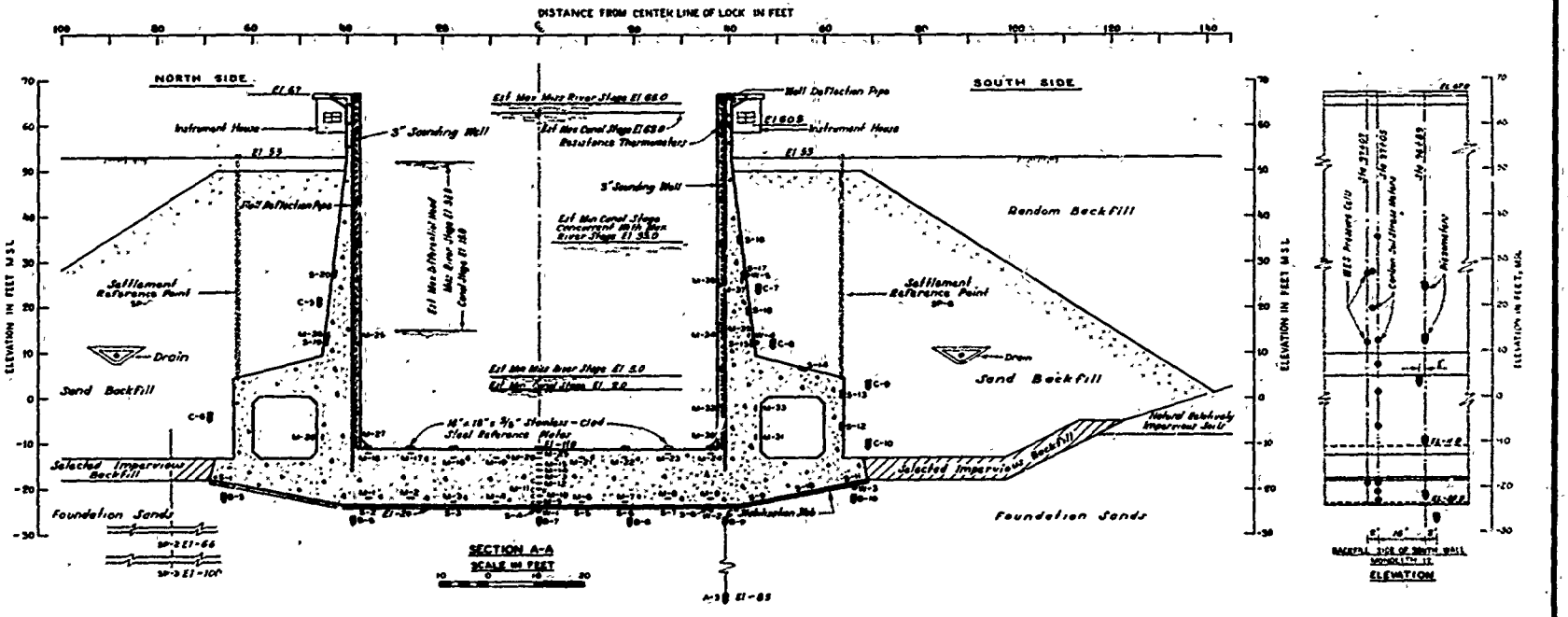

NOTE: SEE PLATE 12 FOR LEGEND.

INSTRUMENTATION FOR MONOLITH 12

PLATE 13

PLATE 14

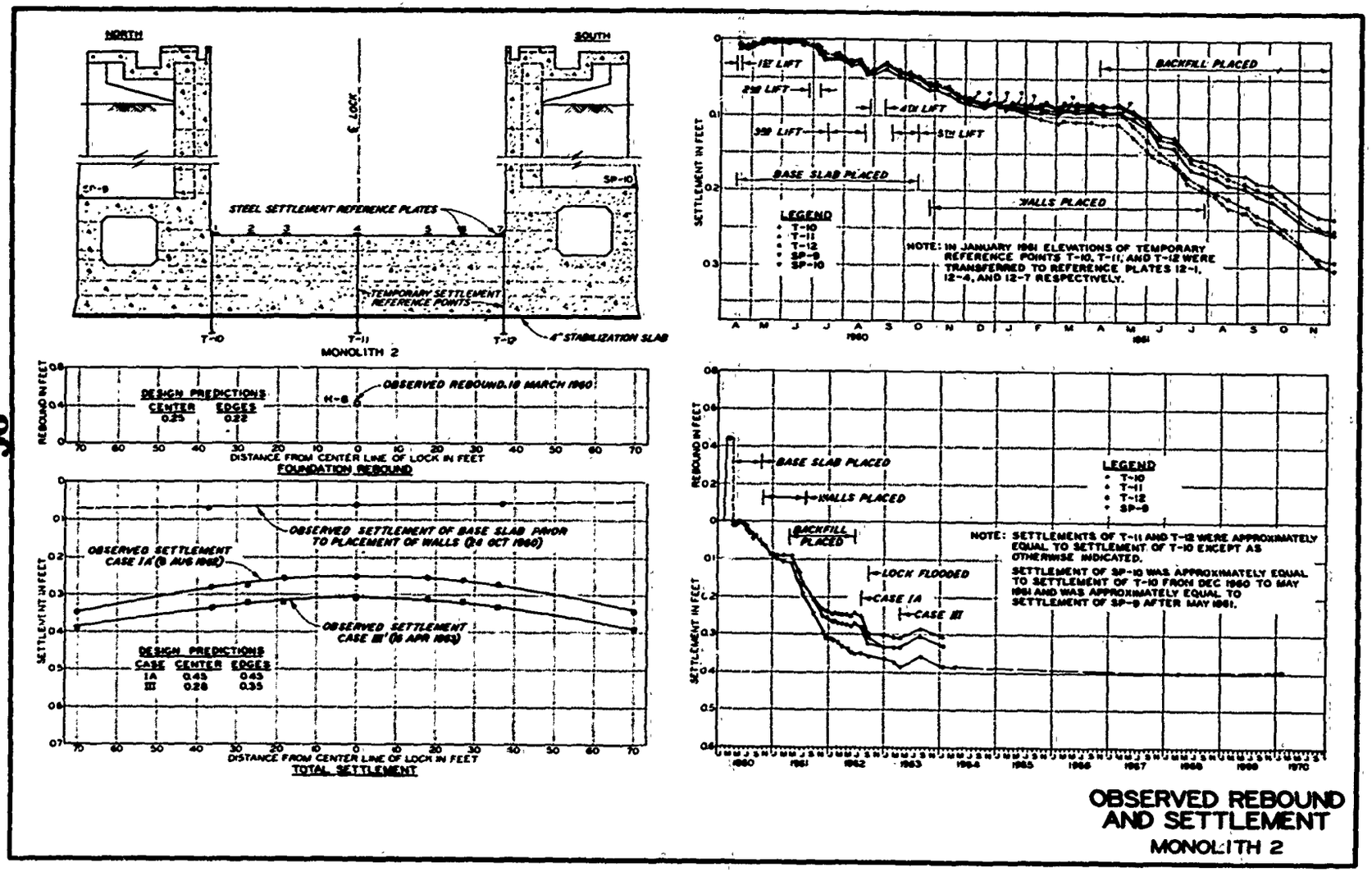

OBSERVED REBOUND AND SETTLEMENT

MONOLITH 2

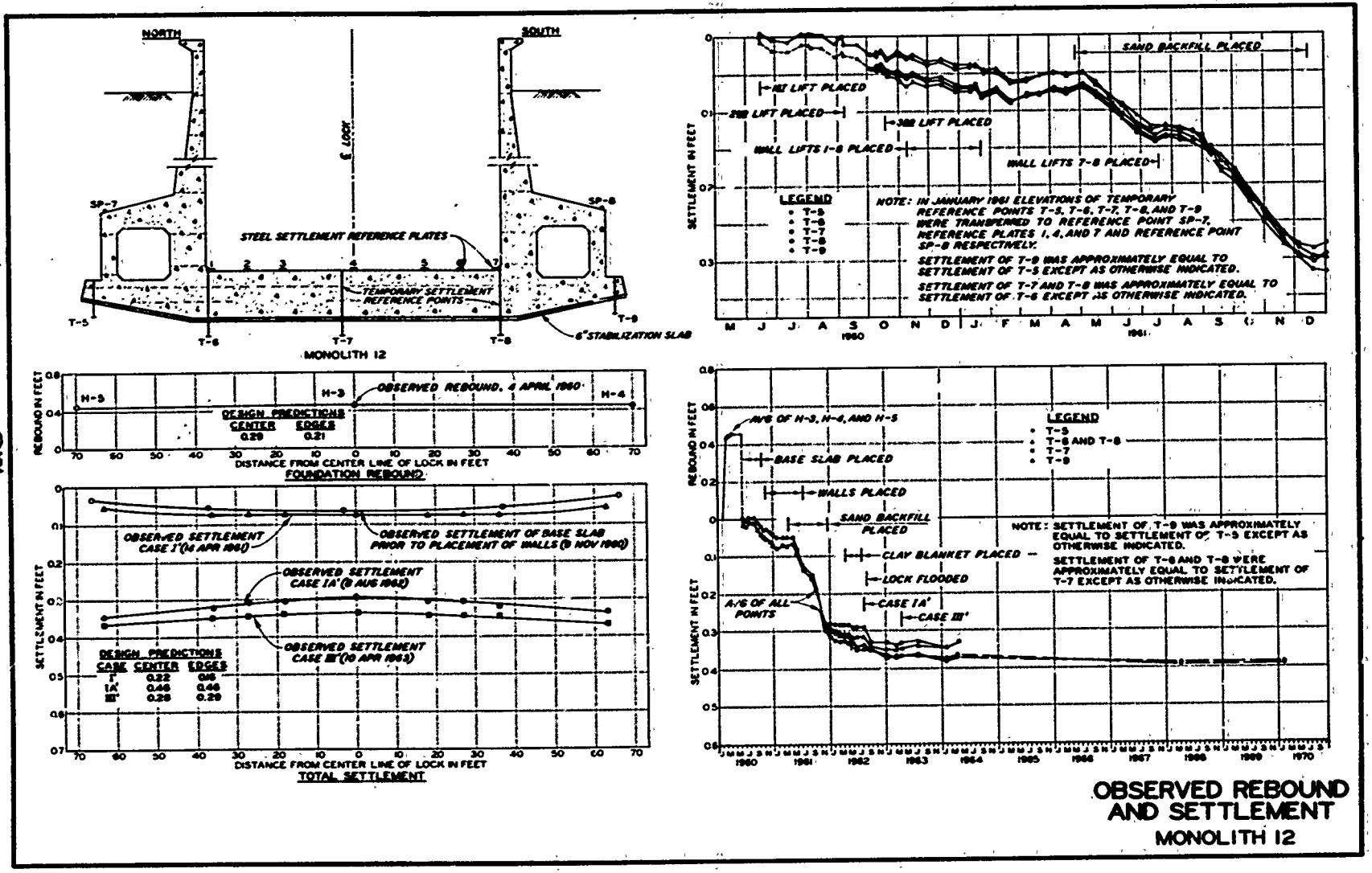

OBSERVED REBOUND AND SETTLEMENT
MONOLITH 12

PLATE 15

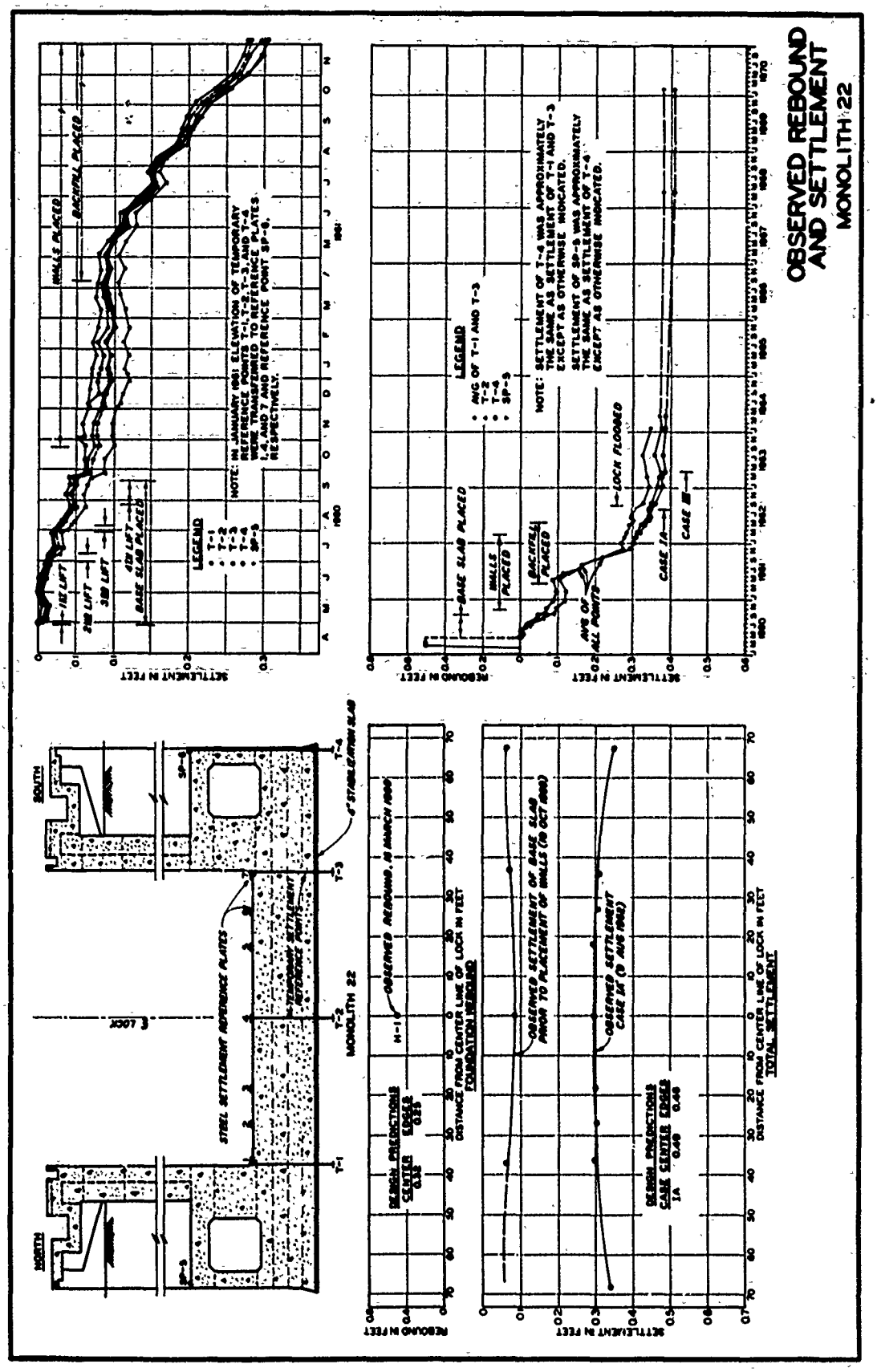
OBSERVED REBOUND AND SETTLEMENT
MONOLITH 22
WALLS PLACED
BACKFILL PLACED
1ST LIFT
2ND LIFT
3RD LIFT
4TH LIFT
BASE SLAB PLACED
LEGEND
T-1
T-2
T-3
T-4
SP-5
NOTE: IN JANUARY 1951 ELEVATION OF TEMPORARY REFERENCE POINTS T-1, T-2, T-3, AND T-4 WERE TRANSFERRED TO REFERENCE PLATES 1, 4, AND 7 AND REFERENCE POINT SP-6, RESPECTIVELY.
SETTLEMENT IN FEET
REBOUND IN FEET
BASE SLAB PLACED
WALLS PLACED
BACKFILL PLACED
AVG OF ALL POINTS
LOCK FLOODED
CASE IA
CASE III
AVG OF T-1 AND T-3
NOTE: SETTLEMENT OF T-4 WAS APPROXIMATELY THE SAME AS SETTLEMENT OF T-1 AND T-3 EXCEPT AS OTHERWISE INDICATED.
SETTLEMENT OF SP-5 WAS APPROXIMATELY THE SAME AS SETTLEMENT OF T-4 EXCEPT AS OTHERWISE INDICATED.
SOUTH
NORTH
STEEL SETTLEMENT REFERENCE PLATES
TEMPORARY SETTLEMENT REFERENCE POINTS
JOINT
MONOLITH 22
6" STABILIZATION SLAB
OBSERVED REBOUND, 10 MARCH 1950
REBOUND PREDICTIONS
CENTER EDGE
0.55 0.35
DISTANCE FROM CENTER LINE OF LOCK IN FEET
FOUNDATION REBOUND
OBSERVED SETTLEMENT OF BASE SLAB PRIOR TO PLACEMENT OF WALLS (10 OCT 1950)
OBSERVED SETTLEMENT CASE IA (5 AUG 1952)
REBOUND PREDICTIONS
CASE CENTER EDGE
IA 0.40 0.46
TOTAL SETTLEMENT

PLATE 16

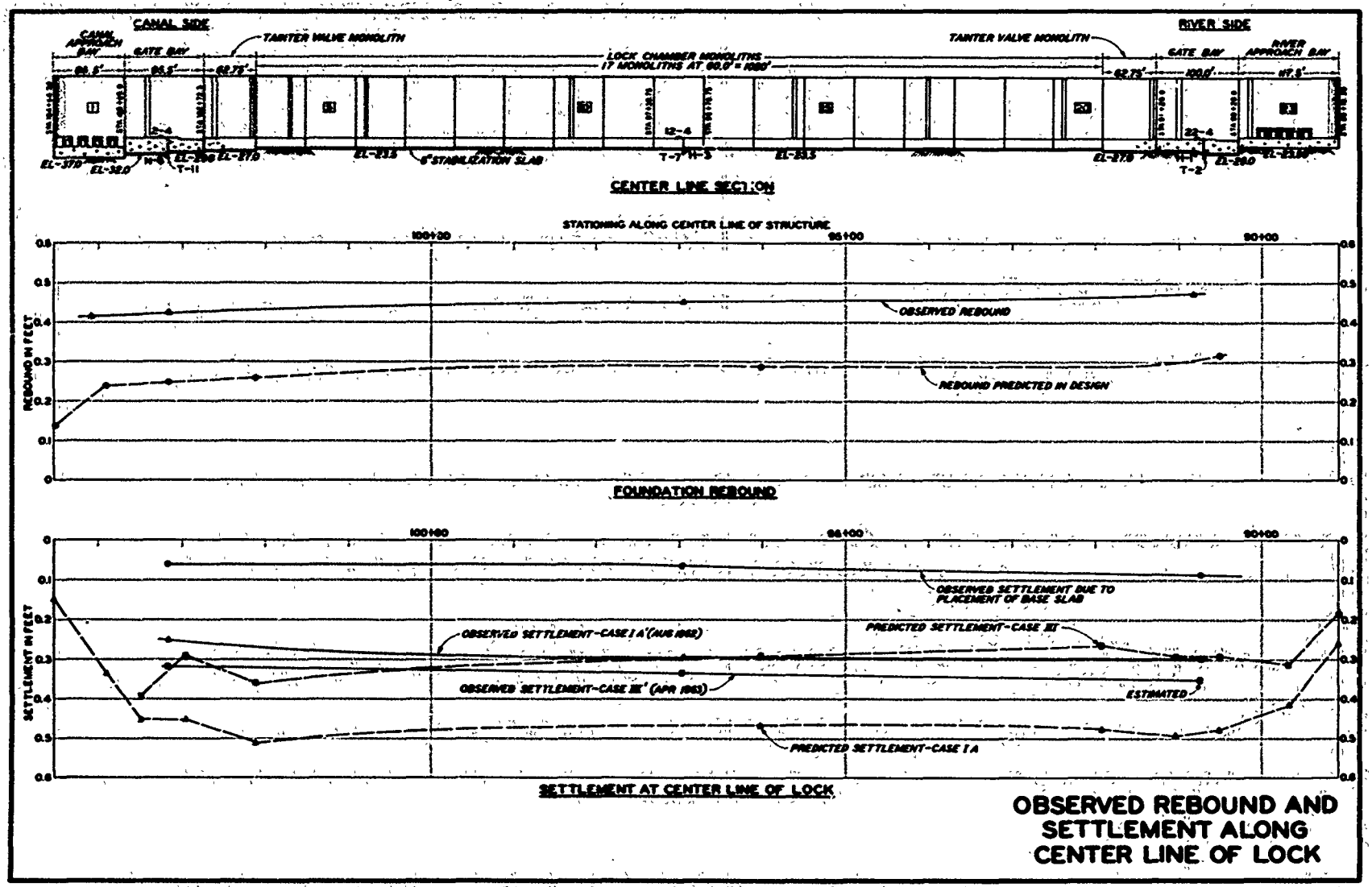

OBSERVED REBOUND AND SETTLEMENT ALONG CENTER LINE OF LOCK

PLATE 17

PLATE 18

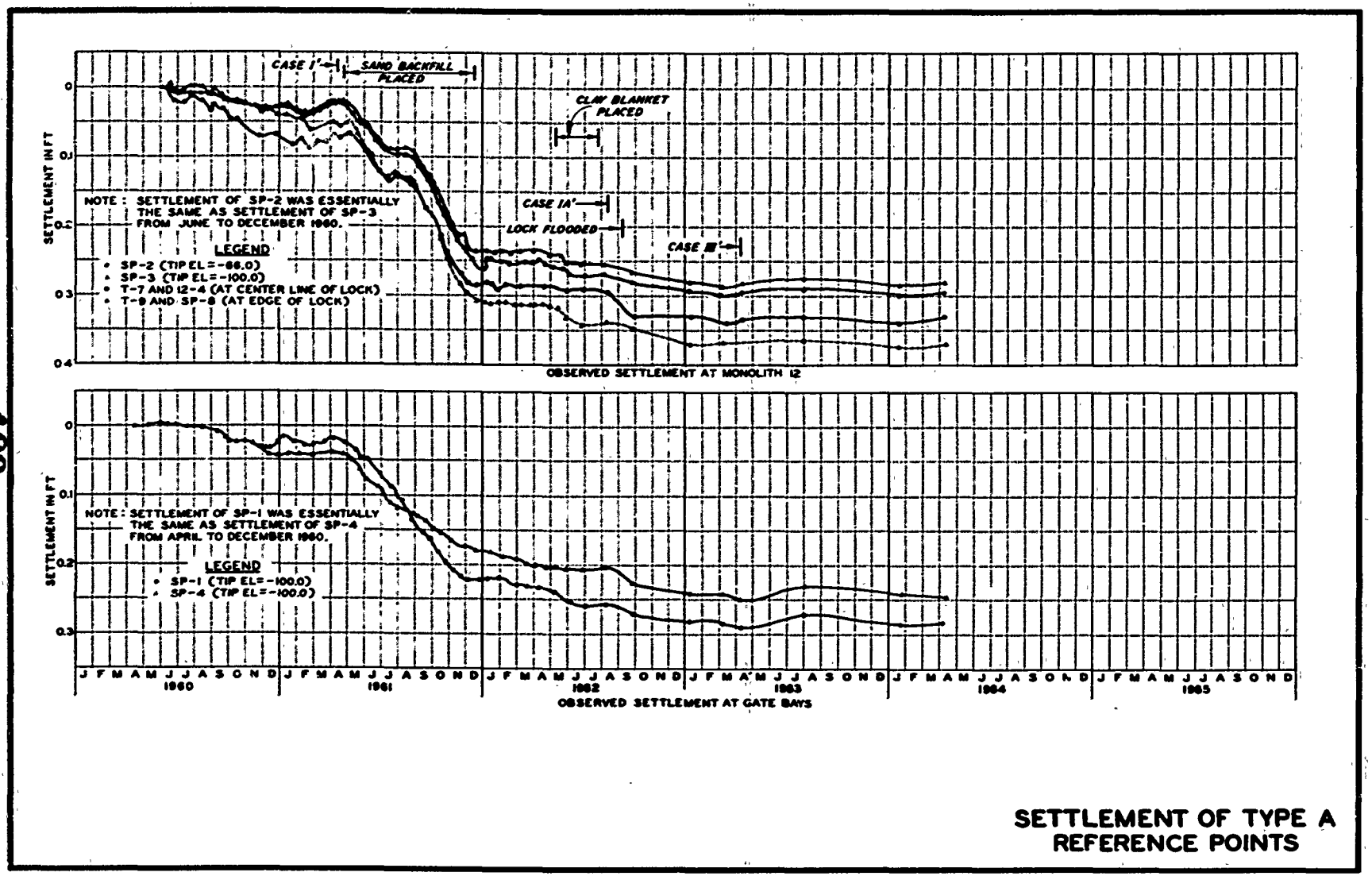

SETTLEMENT OF TYPE A REFERENCE POINTS

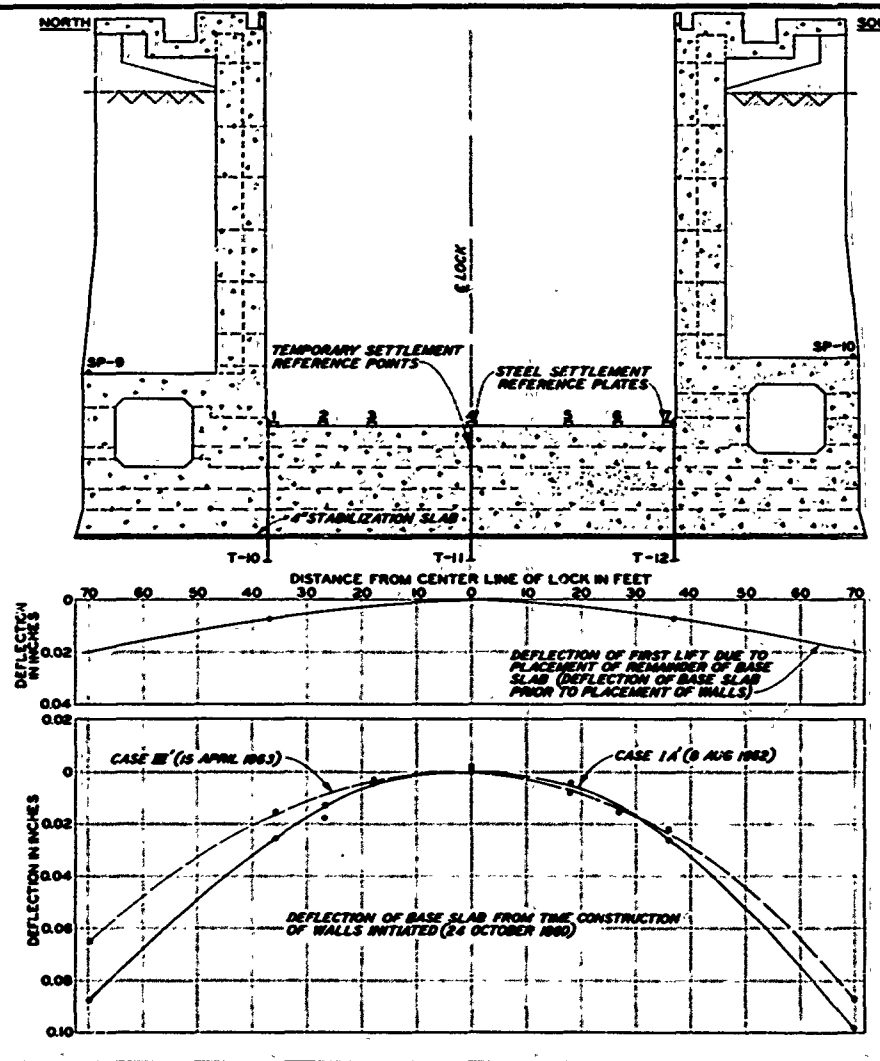

DEFLECTION OF BASE SLAB AND WALLS
MONOLITH 2

PLATE 19

PLATE 20.

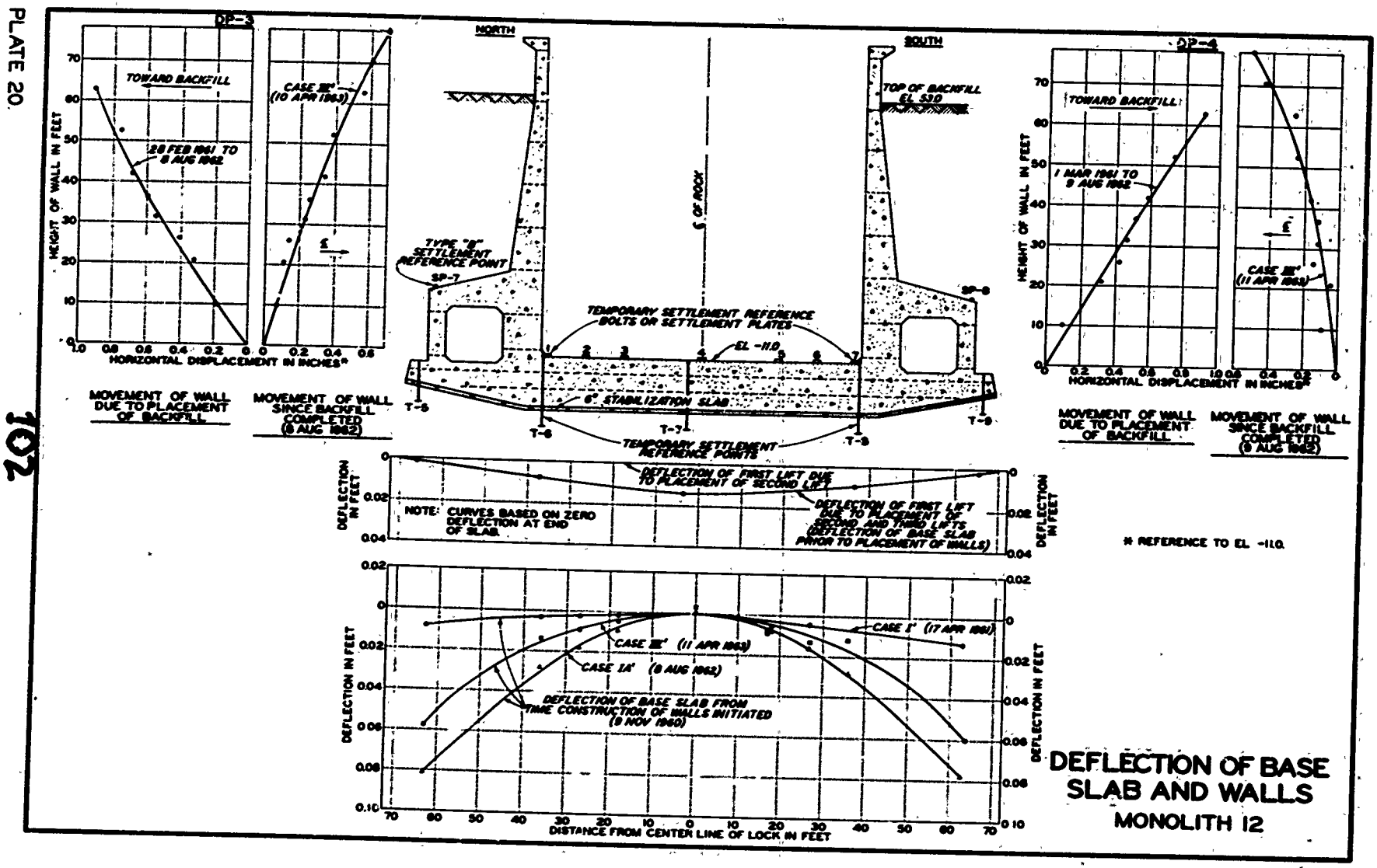

DEFLECTION OF BASE SLAB AND WALLS
MONOLITH 12

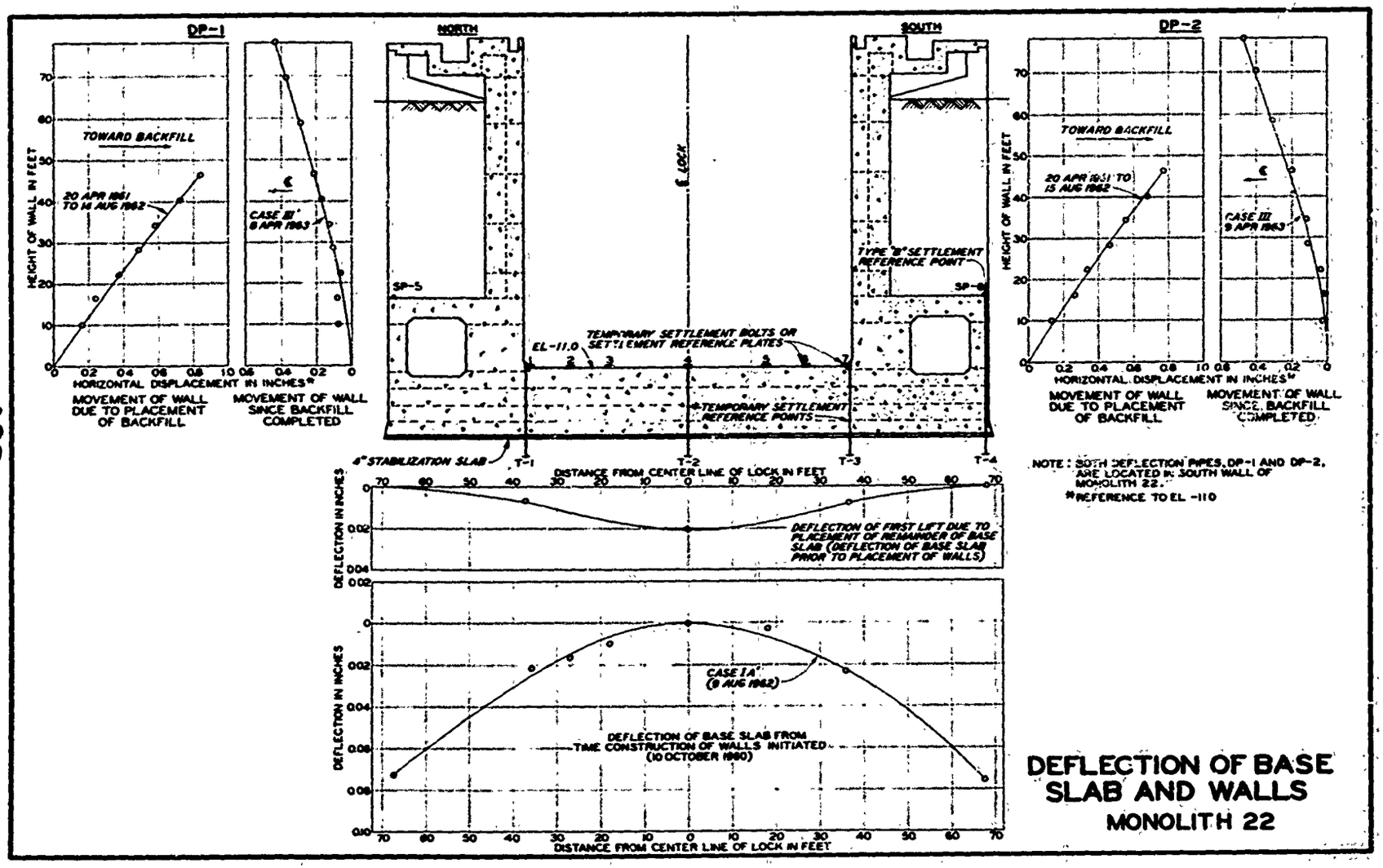

DEFLECTION OF BASE SLAB AND WALLS
MONOLITH 22

PLATE 21

PLATE 22

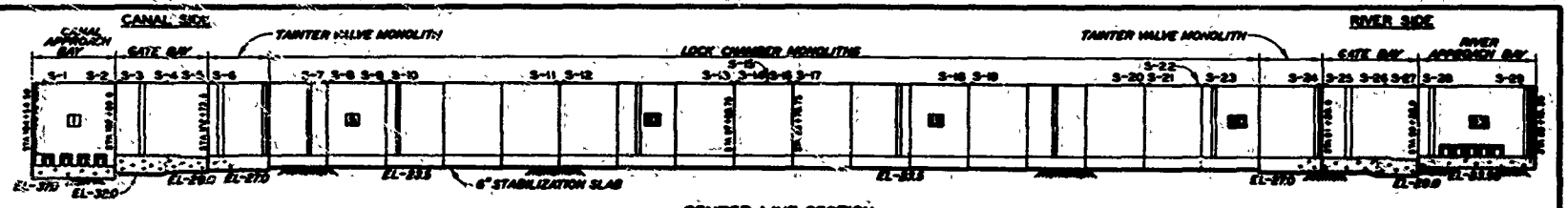

CENTER LINE SECTION

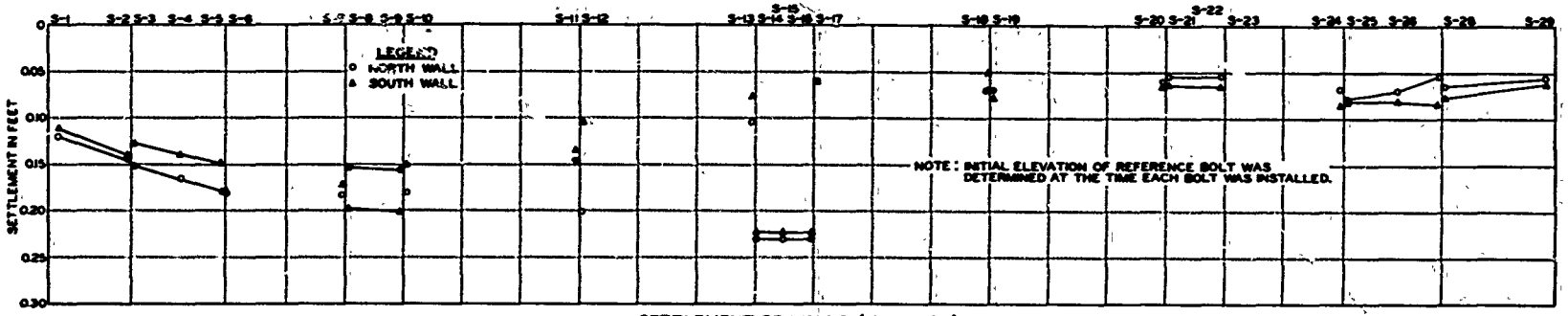

SETTLEMENT OF WALLS (JAN 1964)

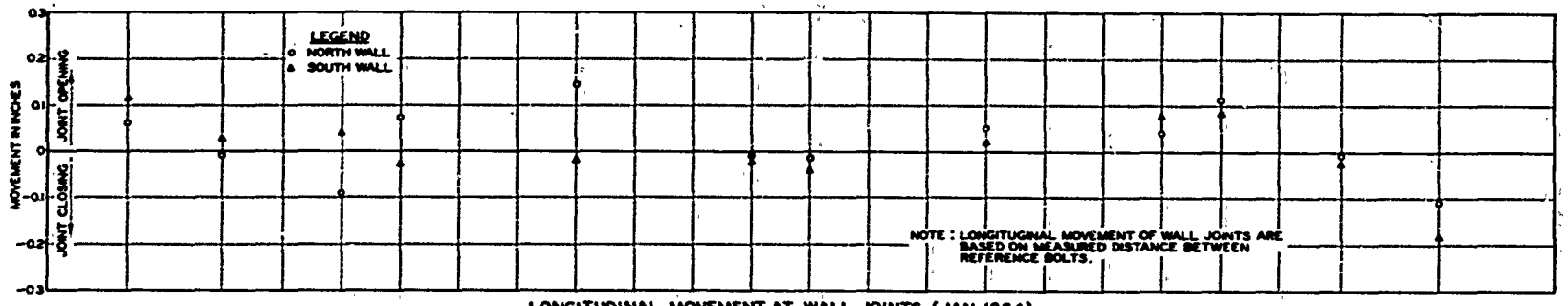

LONGITUDINAL MOVEMENT AT WALL JOINTS (JAN 1964)

SETTLEMENT OF LOCK WALLS AND MOVEMENT AT JOINTS

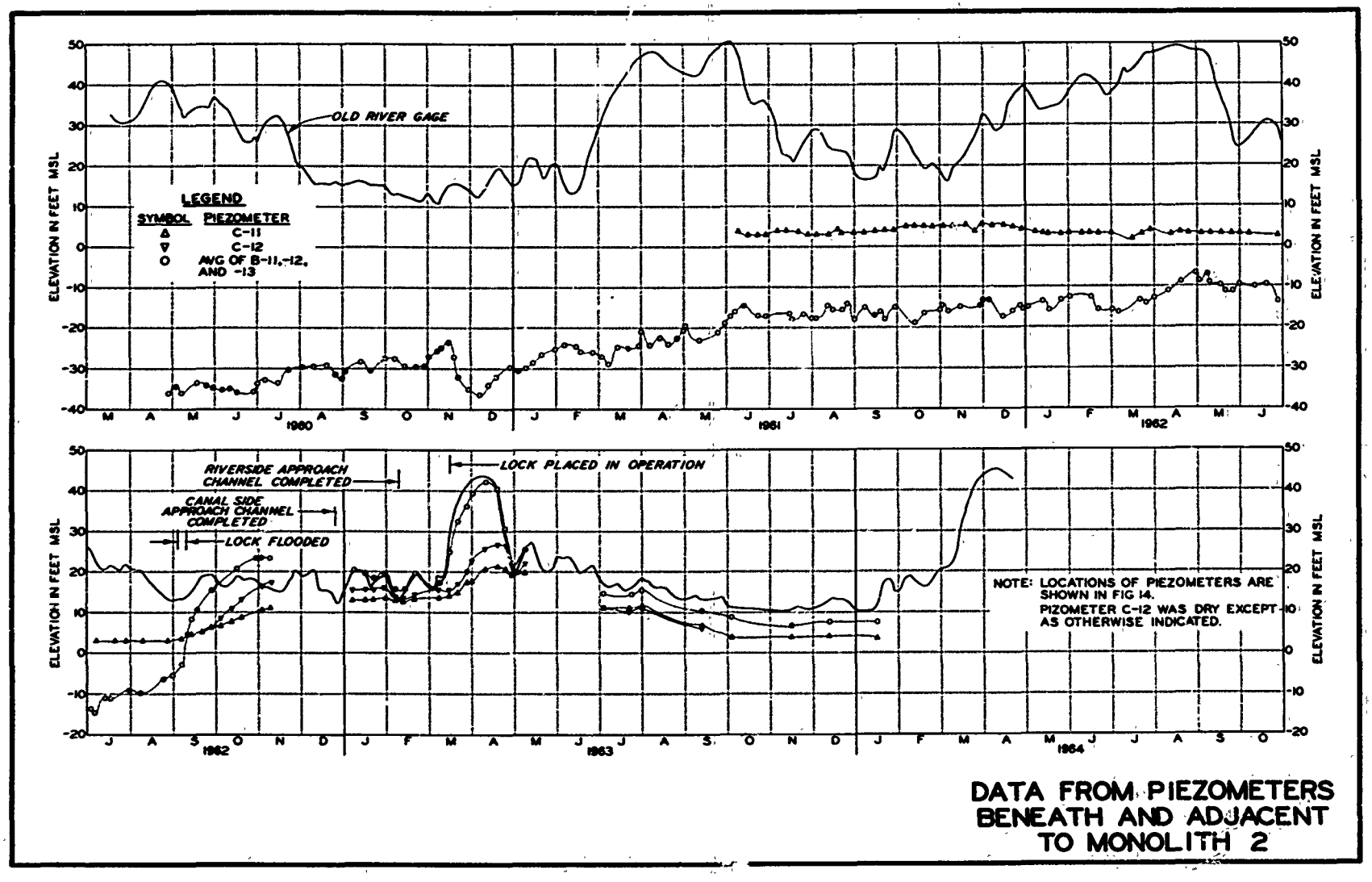

DATA FROM PIEZOMETERS BENEATH AND ADJACENT TO MONOLITH 2

PLATE 23

PLATE 24.

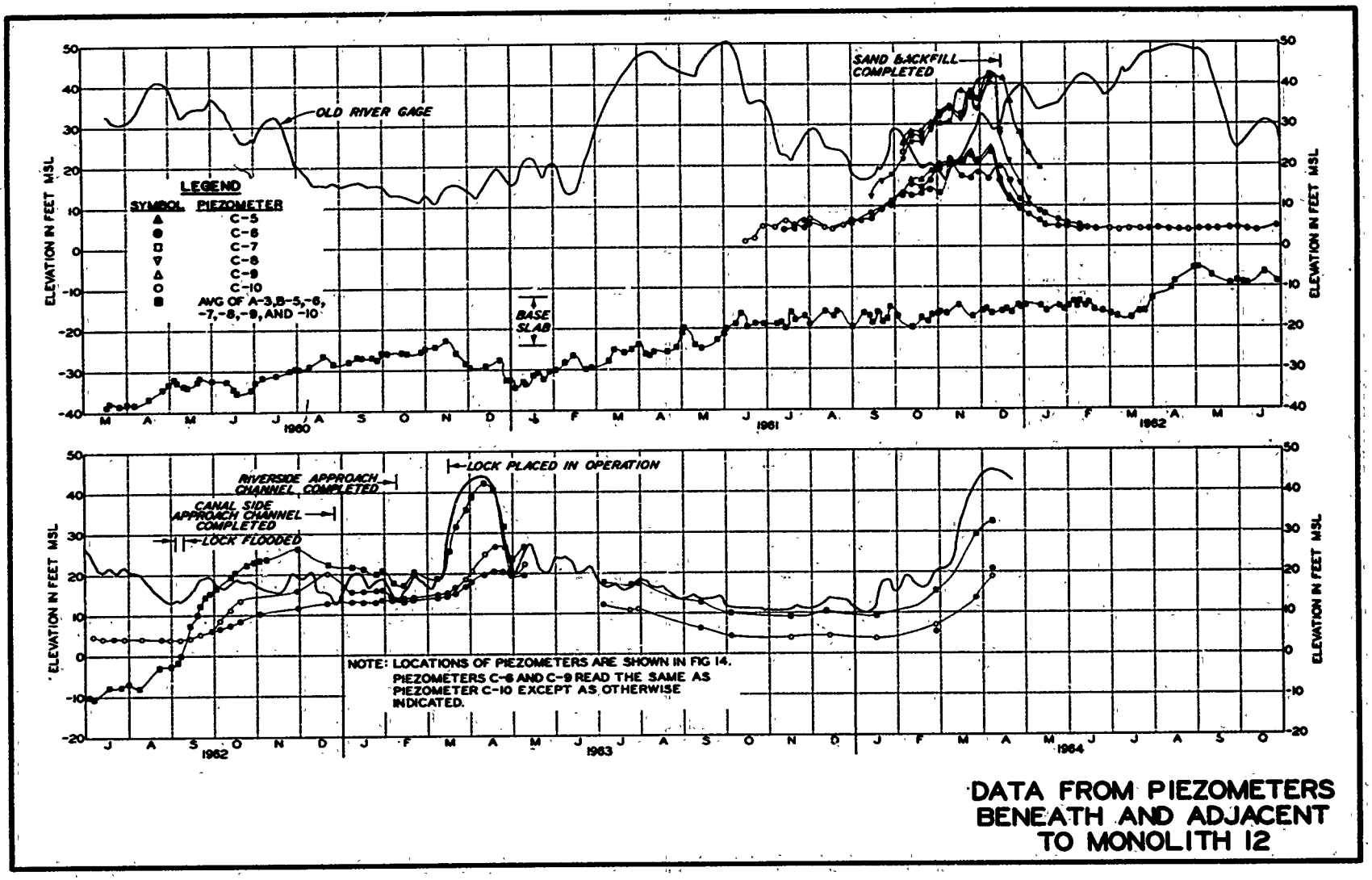

DATA FROM PIEZOMETERS BENEATH AND ADJACENT TO MONOLITH 12

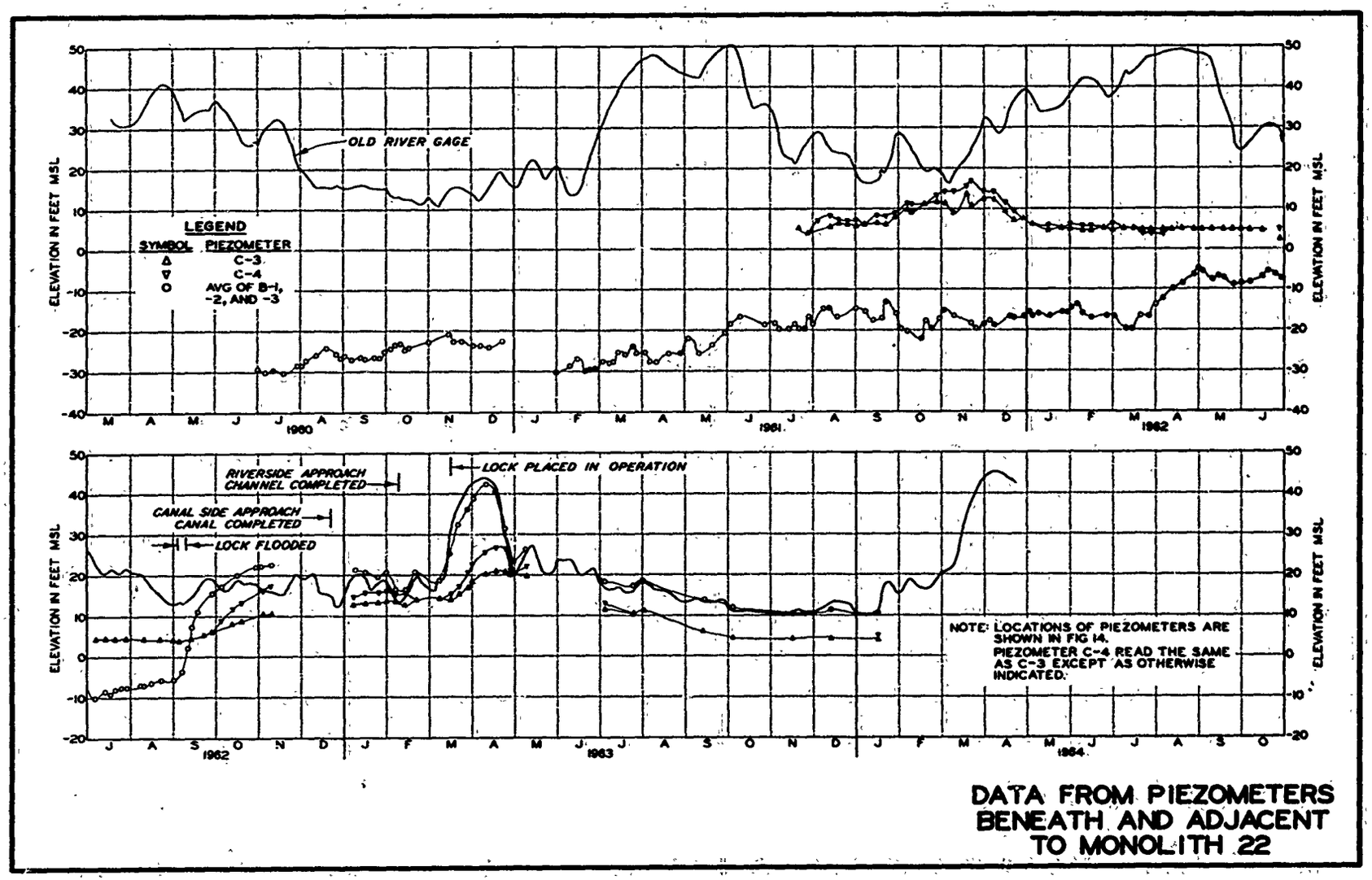

DATA FROM PIEZOMETERS BENEATH AND ADJACENT TO MONOLITH 22

PLATE 25

PLATE 26

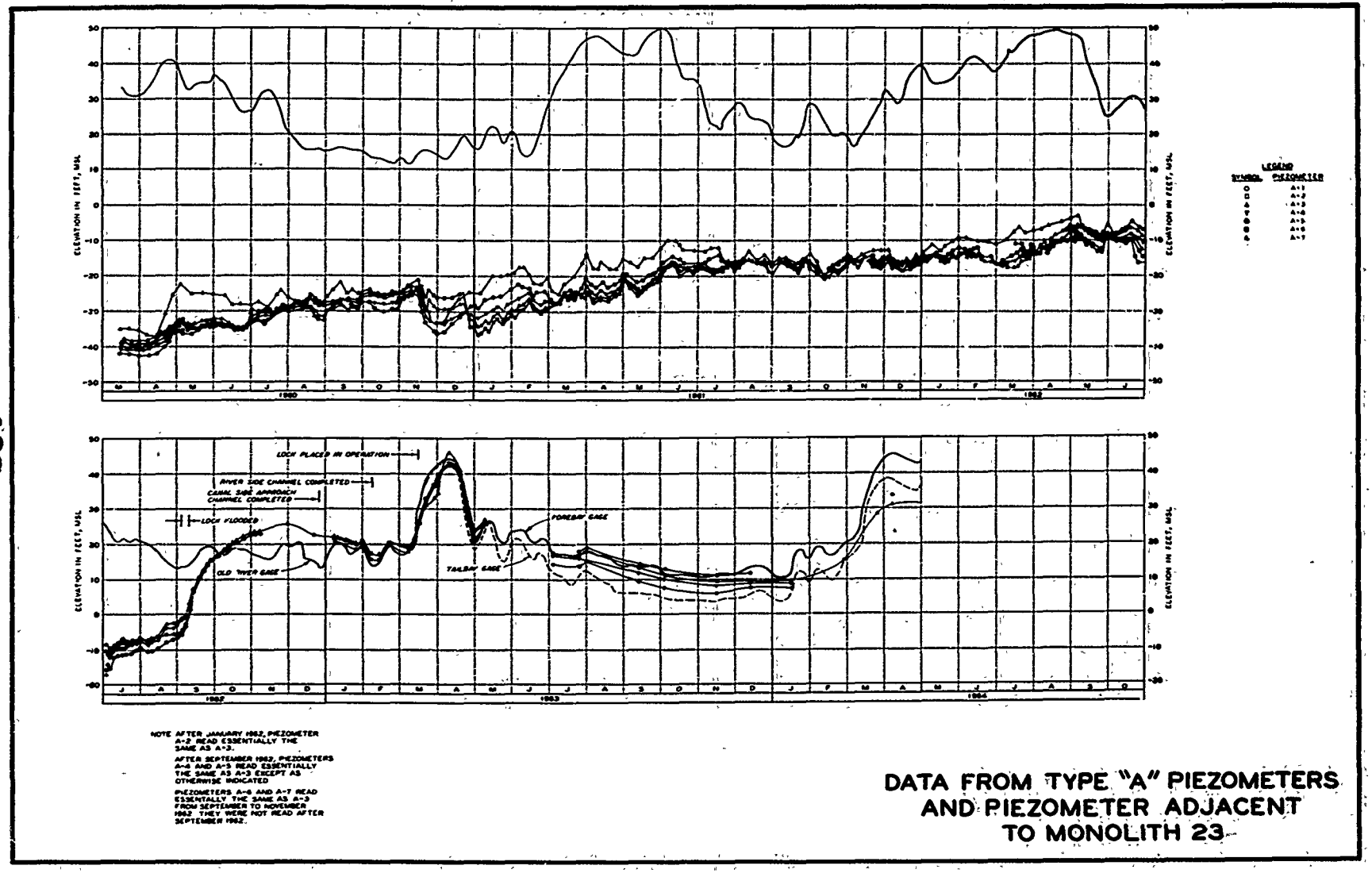

NOTE AFTER JANUARY 1962, PIEZOMETER A-2 READ ESSENTIALLY THE SAME AS A-3.

AFTER SEPTEMBER 1962, PIEZOMETERS A-4 AND A-5 READ ESSENTIALLY THE SAME AS A-3 EXCEPT AS OTHERWISE INDICATED.

PIEZOMETERS A-6 AND A-7 READ ESSENTIALLY THE SAME AS A-3 FROM SEPTEMBER TO NOVEMBER 1962. THEY WERE NOT READ AFTER SEPTEMBER 1962.

DATA FROM TYPE "A" PIEZOMETERS AND PIEZOMETER ADJACENT TO MONOLITH 23

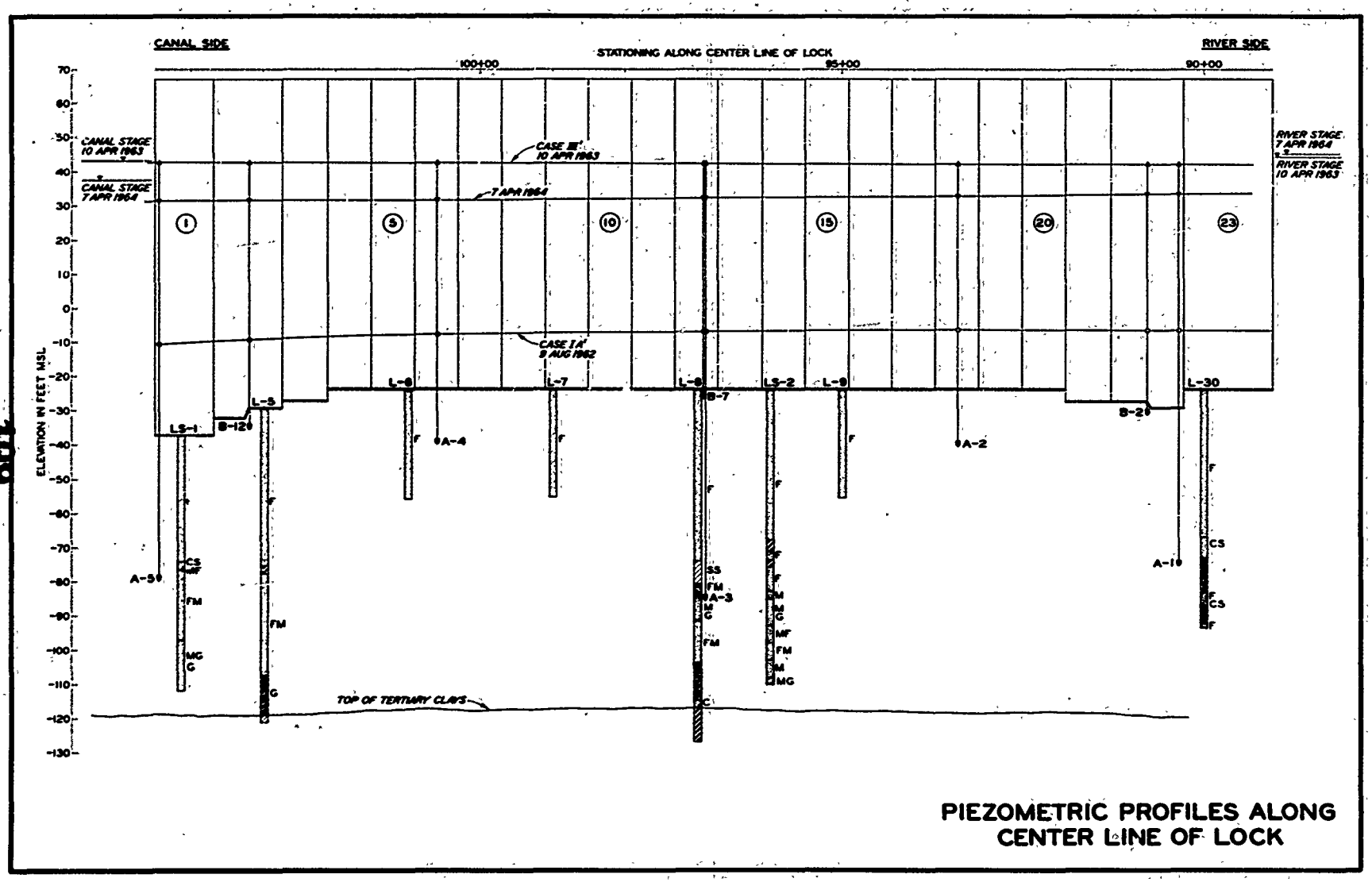

PLATE 27

PIEZOMETRIC PROFILES ALONG CENTER LINE OF LOCK

PLATE 28

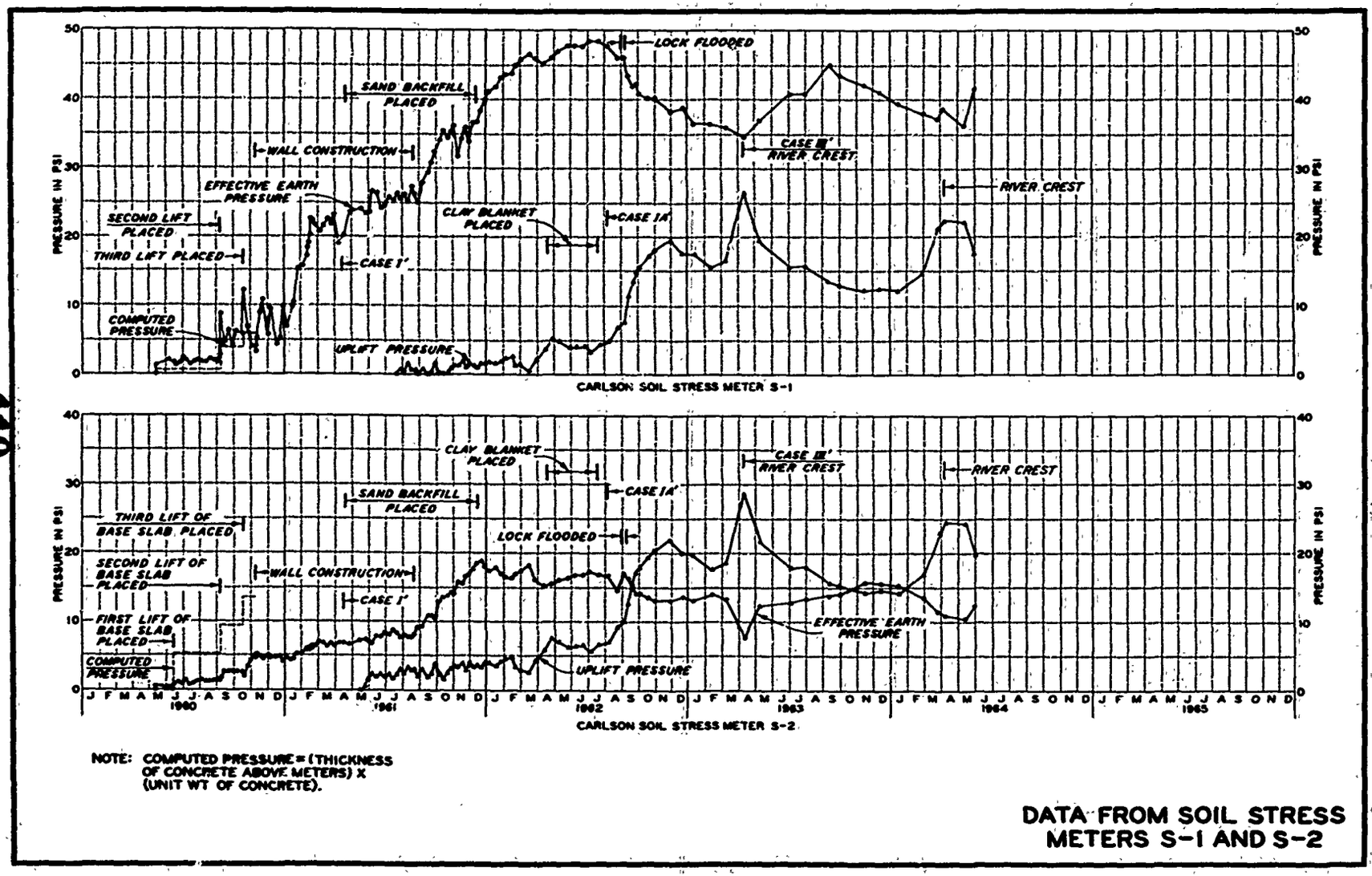

NOTE: COMPUTED PRESSURE = (THICKNESS OF CONCRETE ABOVE METERS) X (UNIT WT OF CONCRETE).

DATA FROM SOIL STRESS METERS S-1 AND S-2

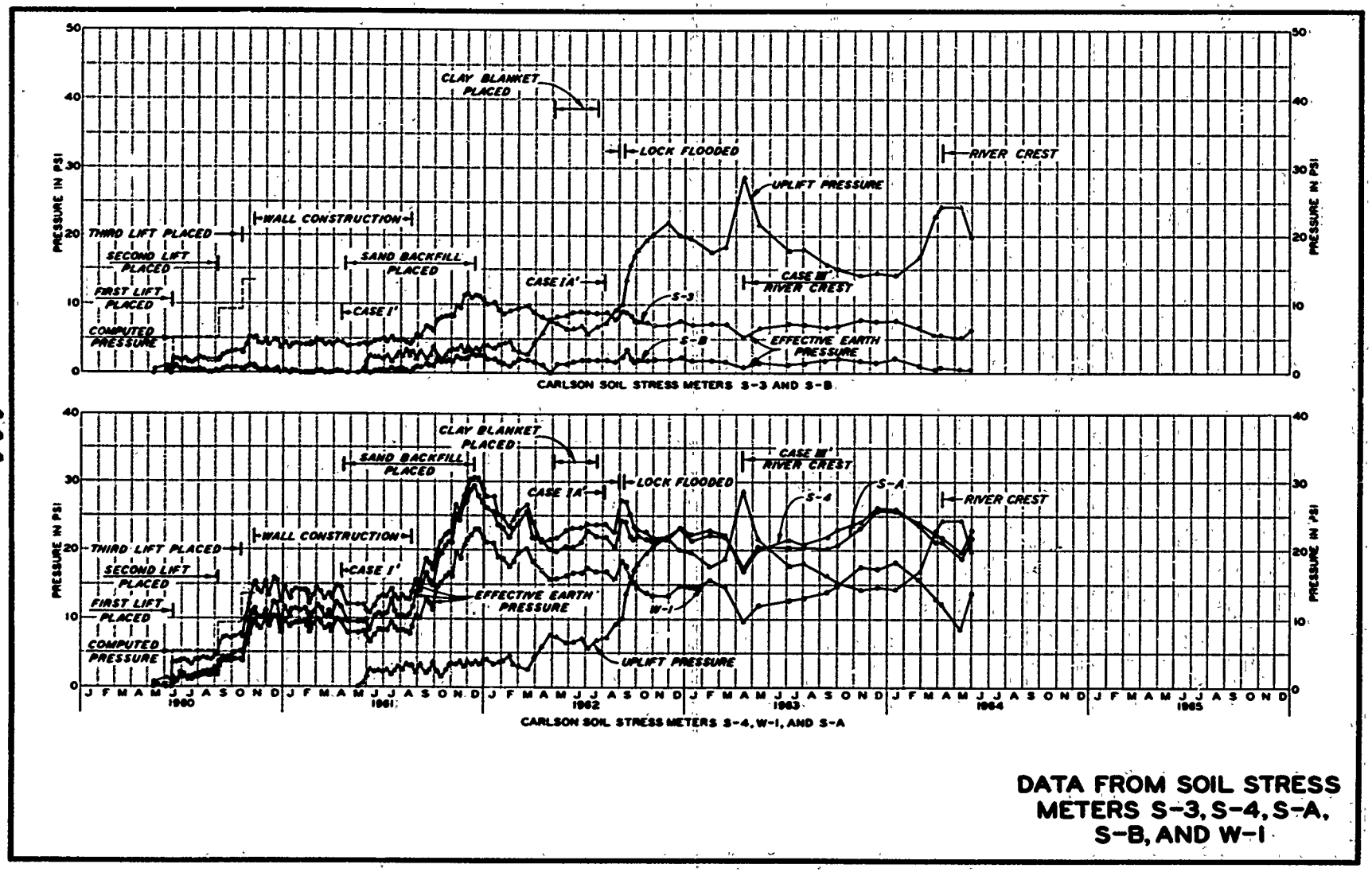

DATA FROM SOIL STRESS METERS S-3, S-4, S-A, S-B, AND W-1

PLATE 29

PLATE 30

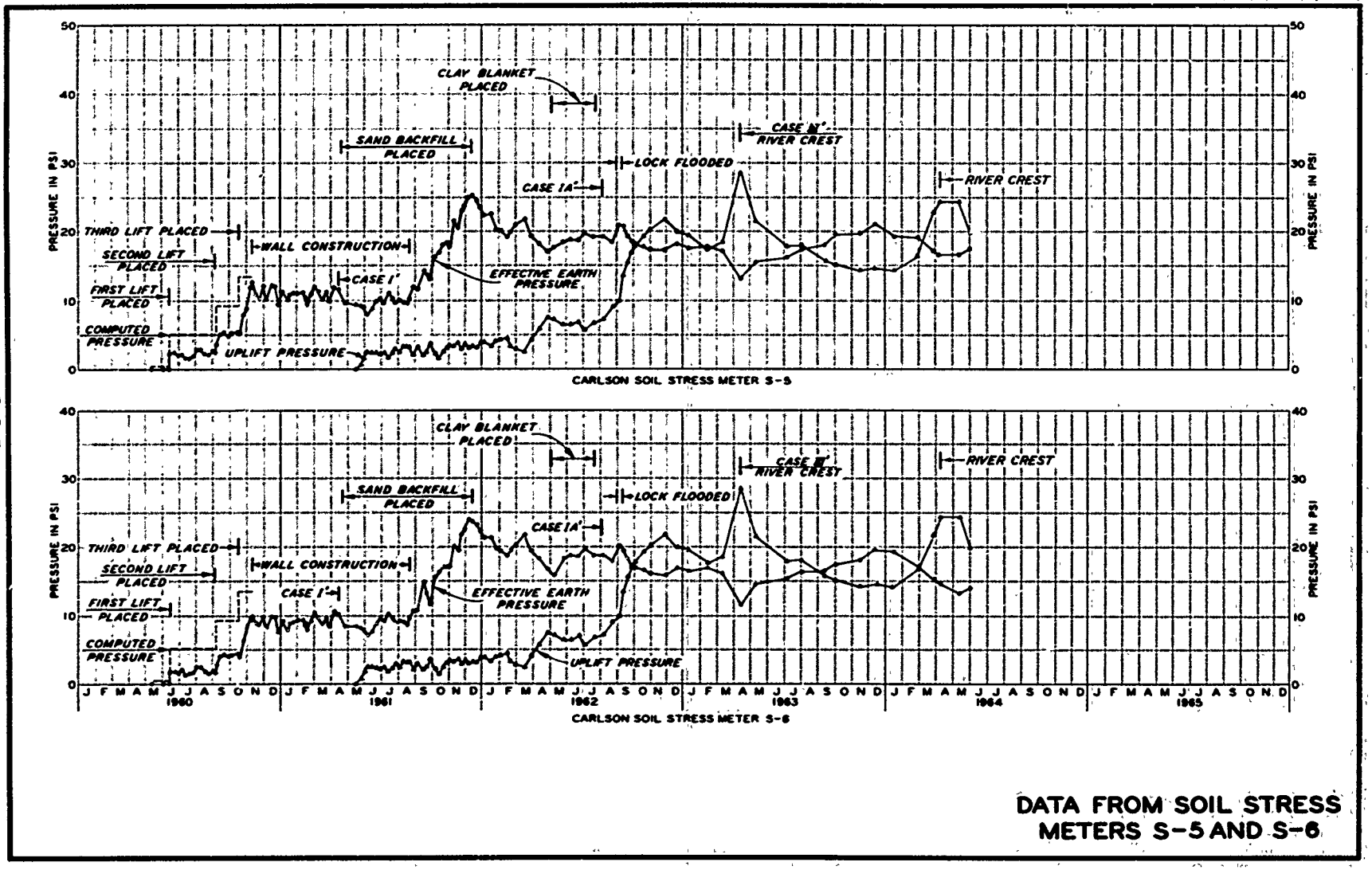

DATA FROM SOIL STRESS METERS S-5 AND S-6

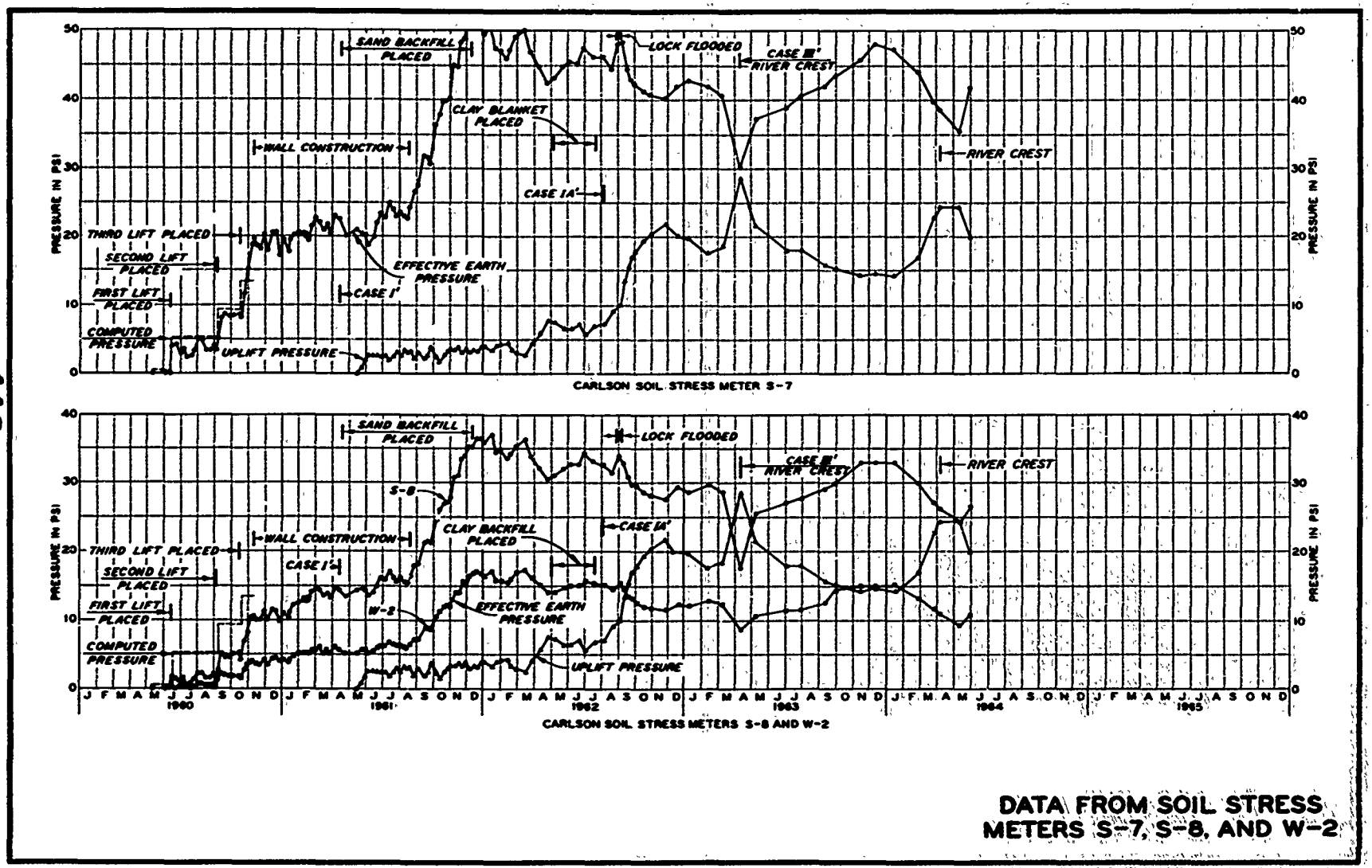

PLATE 31

DATA FROM SOIL STRESS METERS S-7, S-8, AND W-2

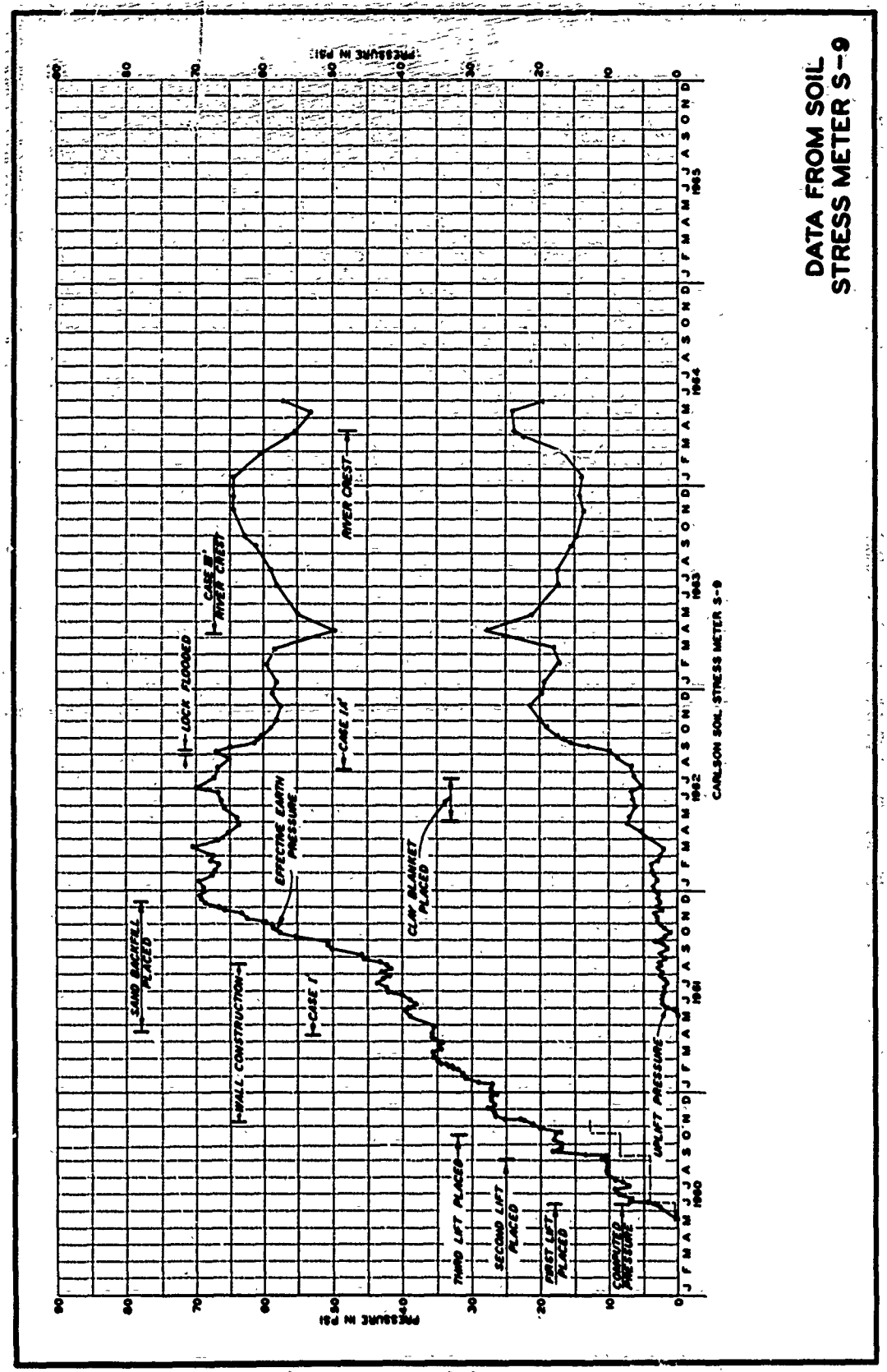
DATA FROM SOIL
STRESS METER S-9
PRESSURE IN PSI
CARLSON SOIL STRESS METER S-9
SAND BACKFILL PLACED
WALL CONSTRUCTION
CASE I
LOCK FLOODED
CASE II
RIVER CREST
EFFECTIVE EARTH PRESSURE
CASE III
RIVER CREST
CLAY BLANKET PLACED
THIRD LIFT PLACED
SECOND LIFT PLACED
FIRST LIFT PLACED
COMPUTED PRESSURE
UPLIFT PRESSURE
J F M A M J J A S O N D J F M A M J J A S O N D J F M A M J J A S O N D
1960
1961
1962
1963
1964
1965

PLATE 32

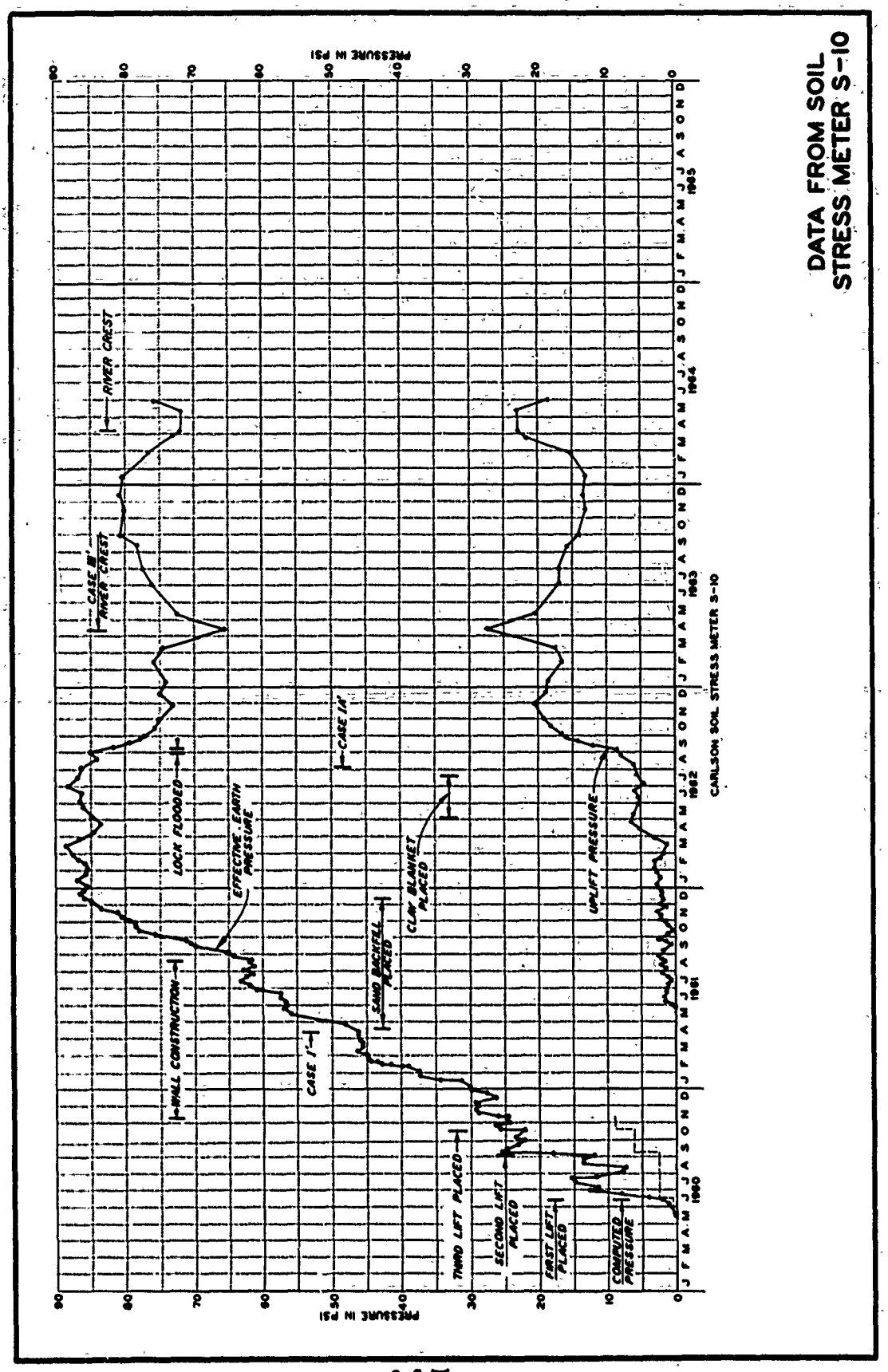

DATA FROM SOIL
STRESS METER S-10

PLATE 33

PLATE 34

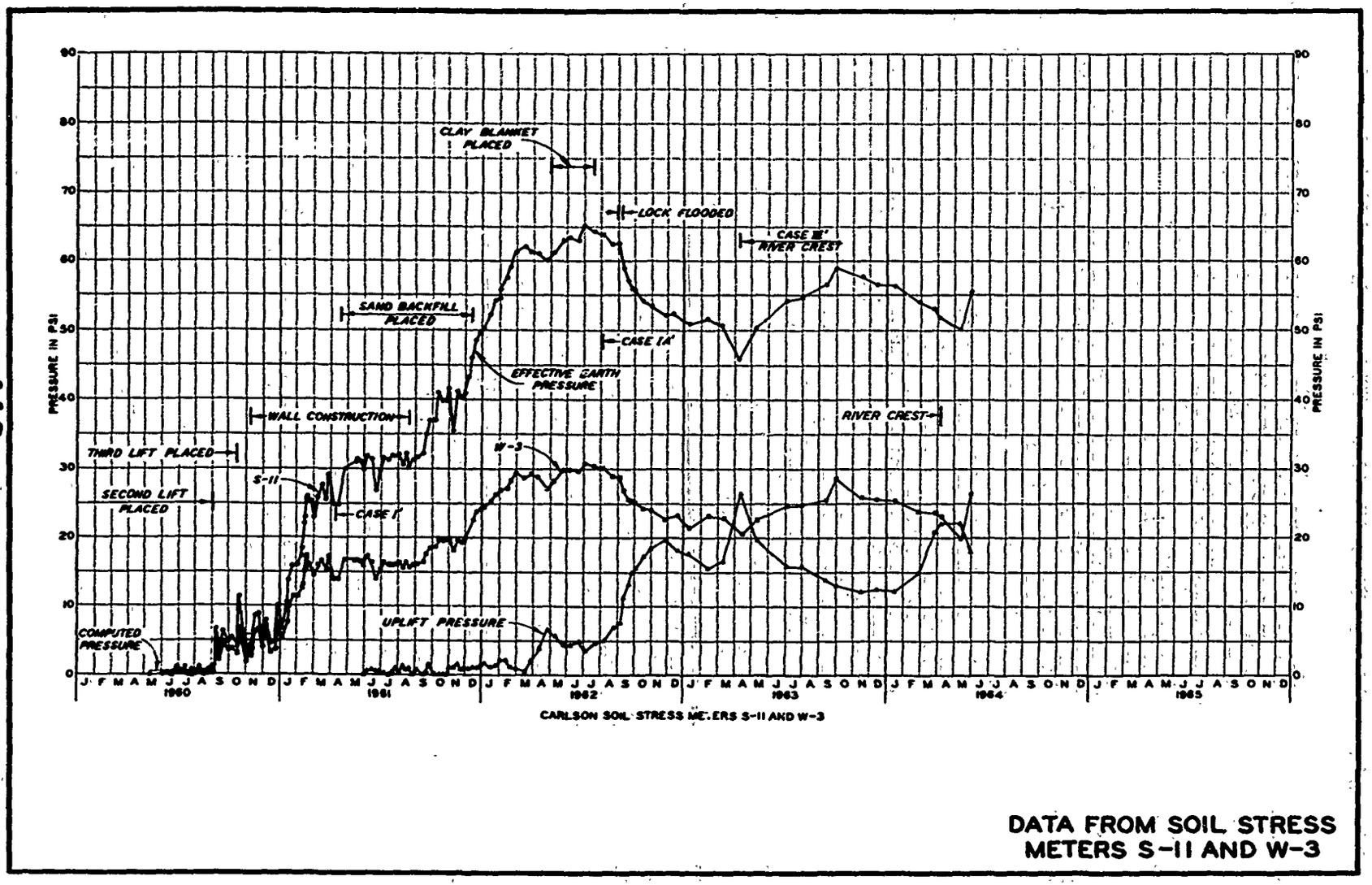

CARLSON SOIL STRESS METERS S-11 AND W-3

DATA FROM SOIL STRESS METERS S-11 AND W-3

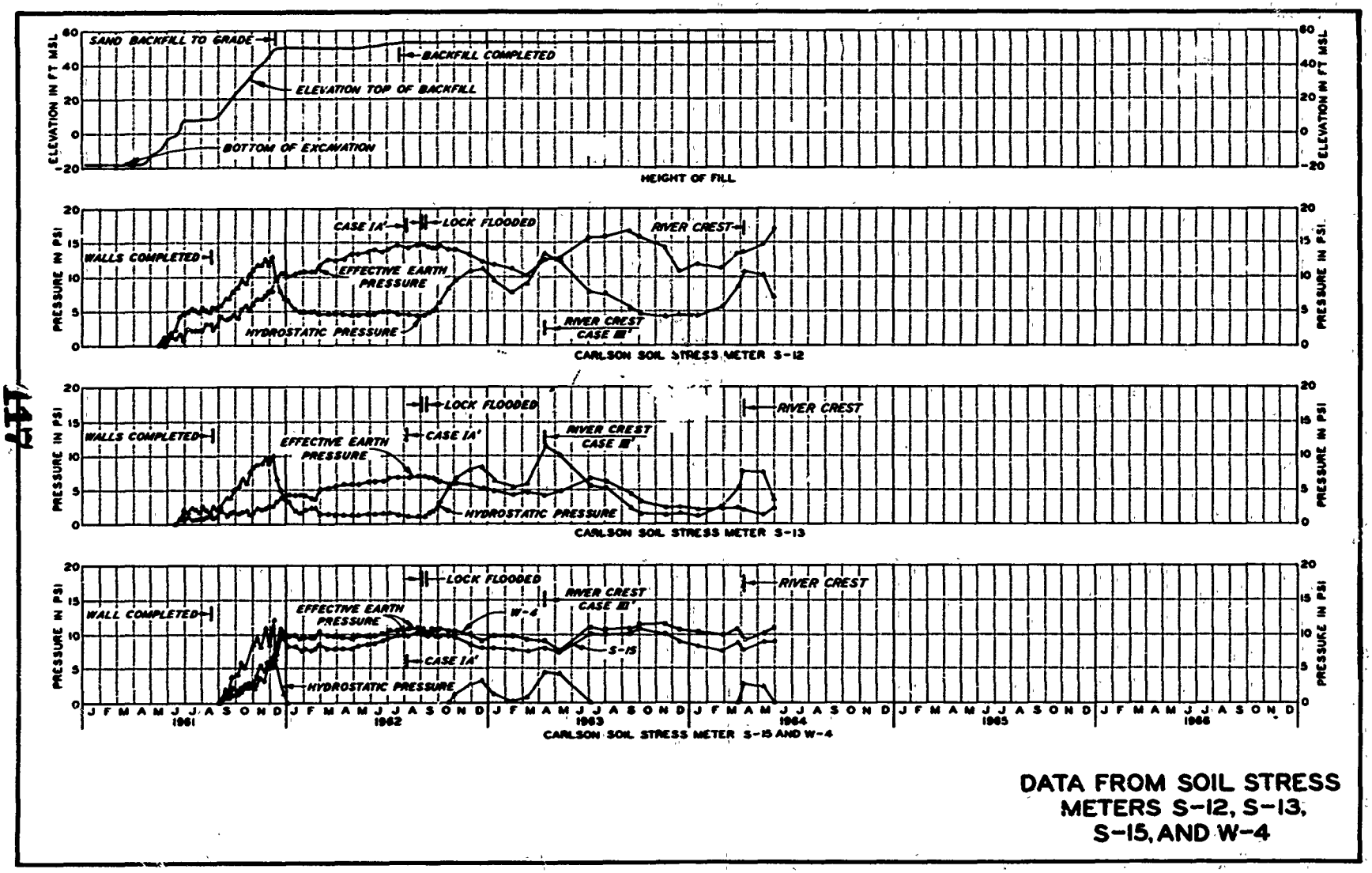

DATA FROM SOIL STRESS METERS S-12, S-13, S-15, AND W-4

PLATE 35

PLATE 36

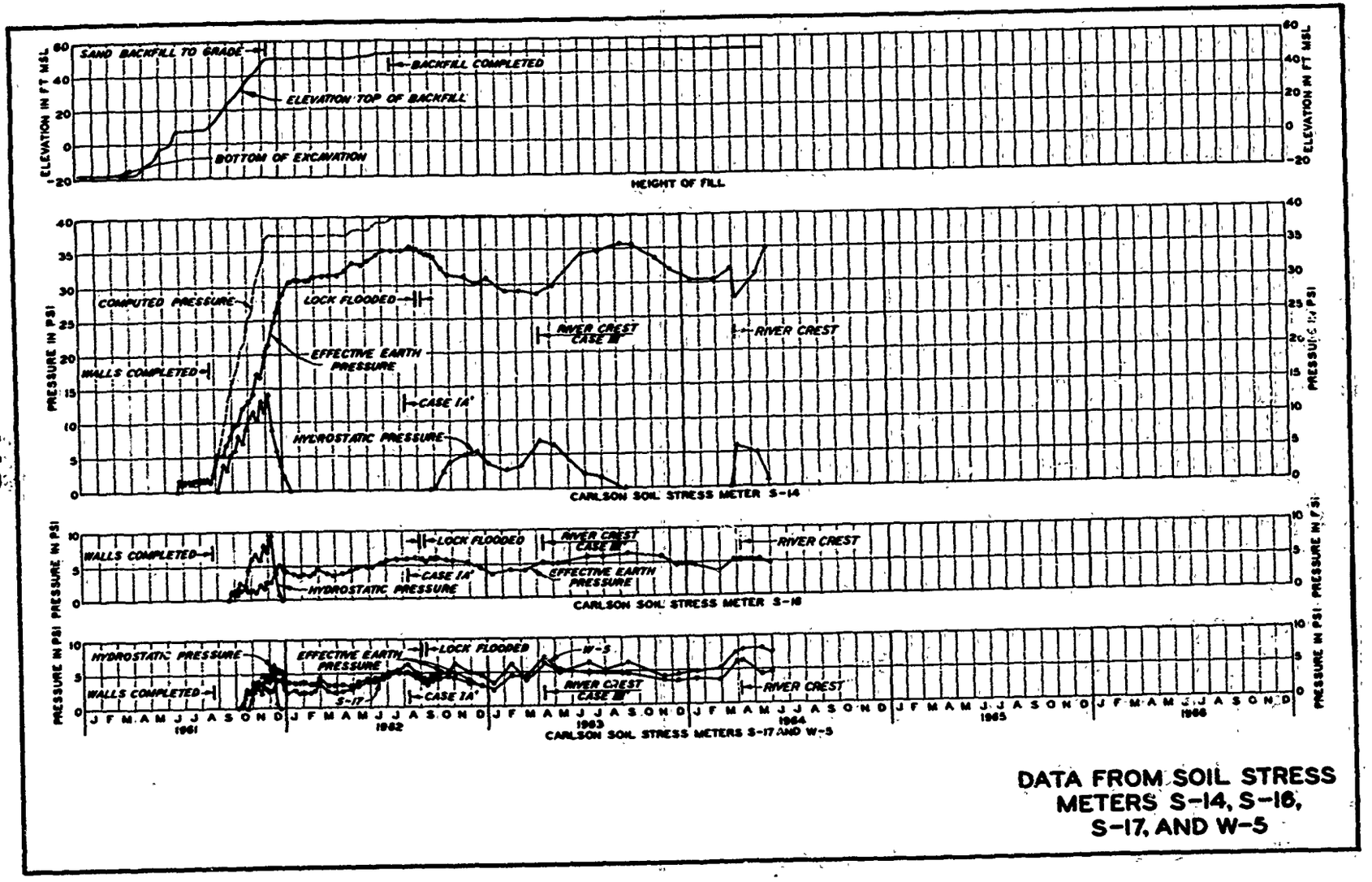

DATA FROM SOIL STRESS METERS S-14, S-16, S-17, AND W-5

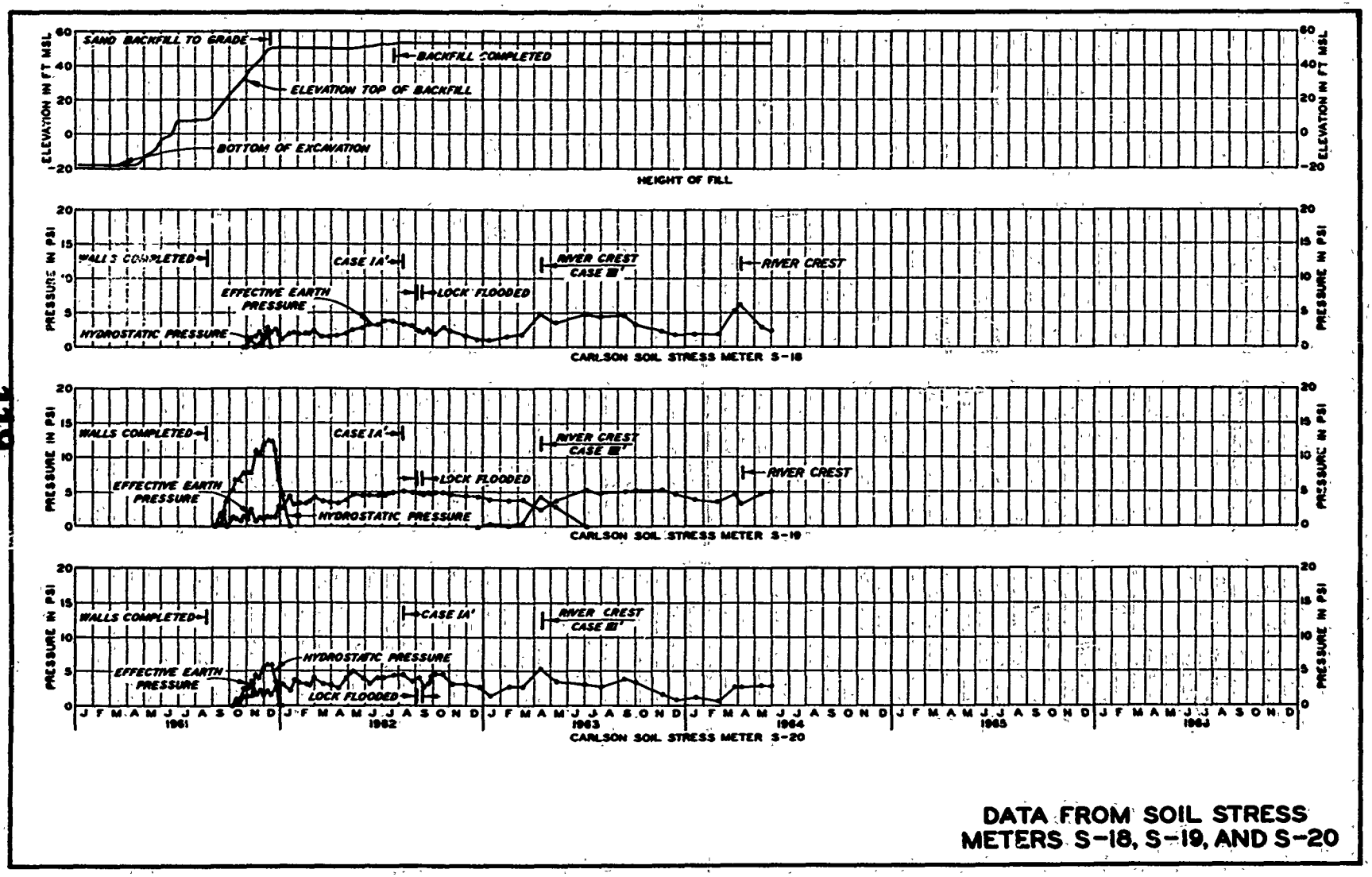

PLATE 37

DATA FROM SOIL STRESS METERS S-18, S-19, AND S-20

PLATE 38

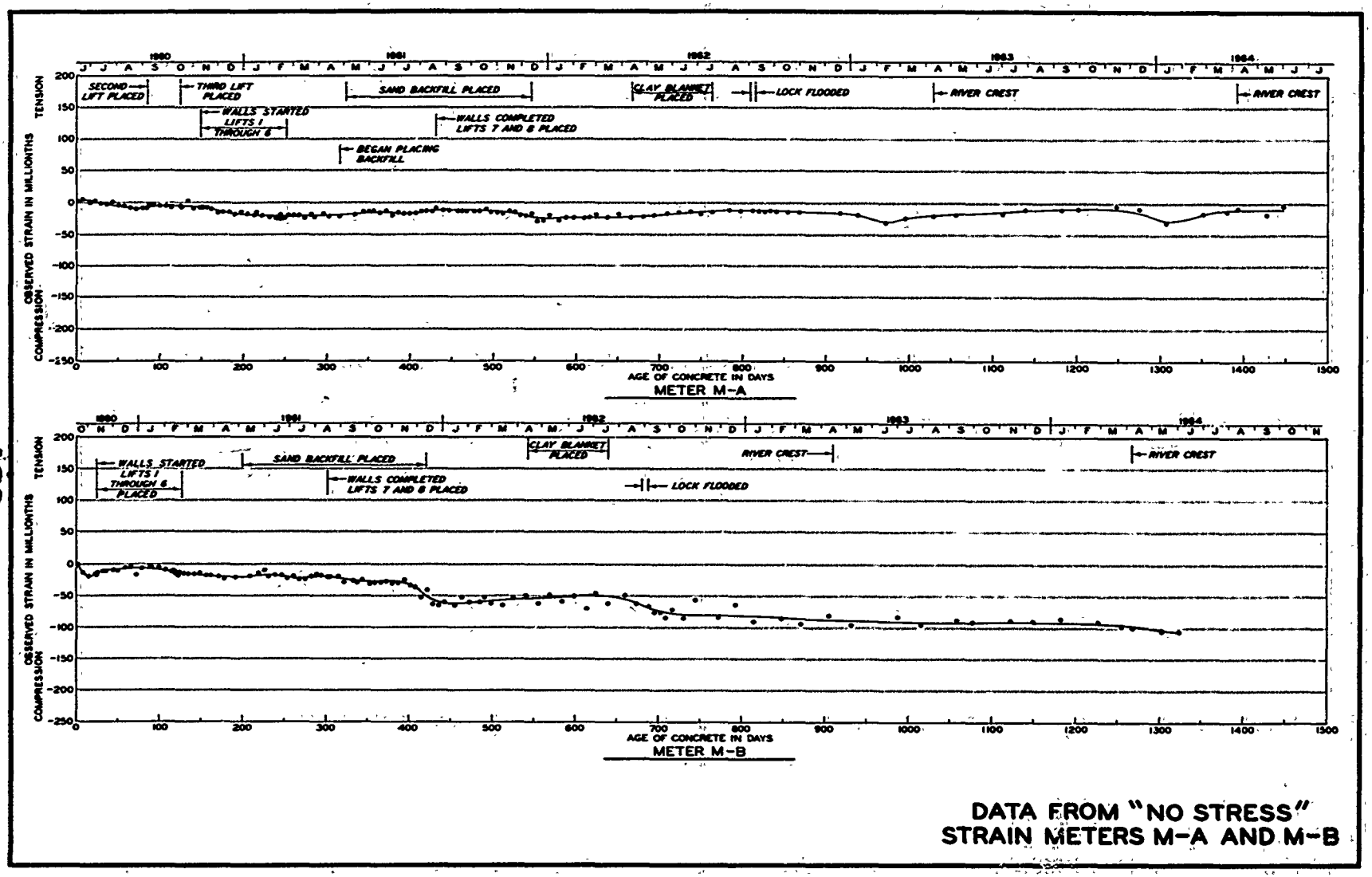

DATA FROM "NO STRESS" STRAIN METERS M-A AND M-B

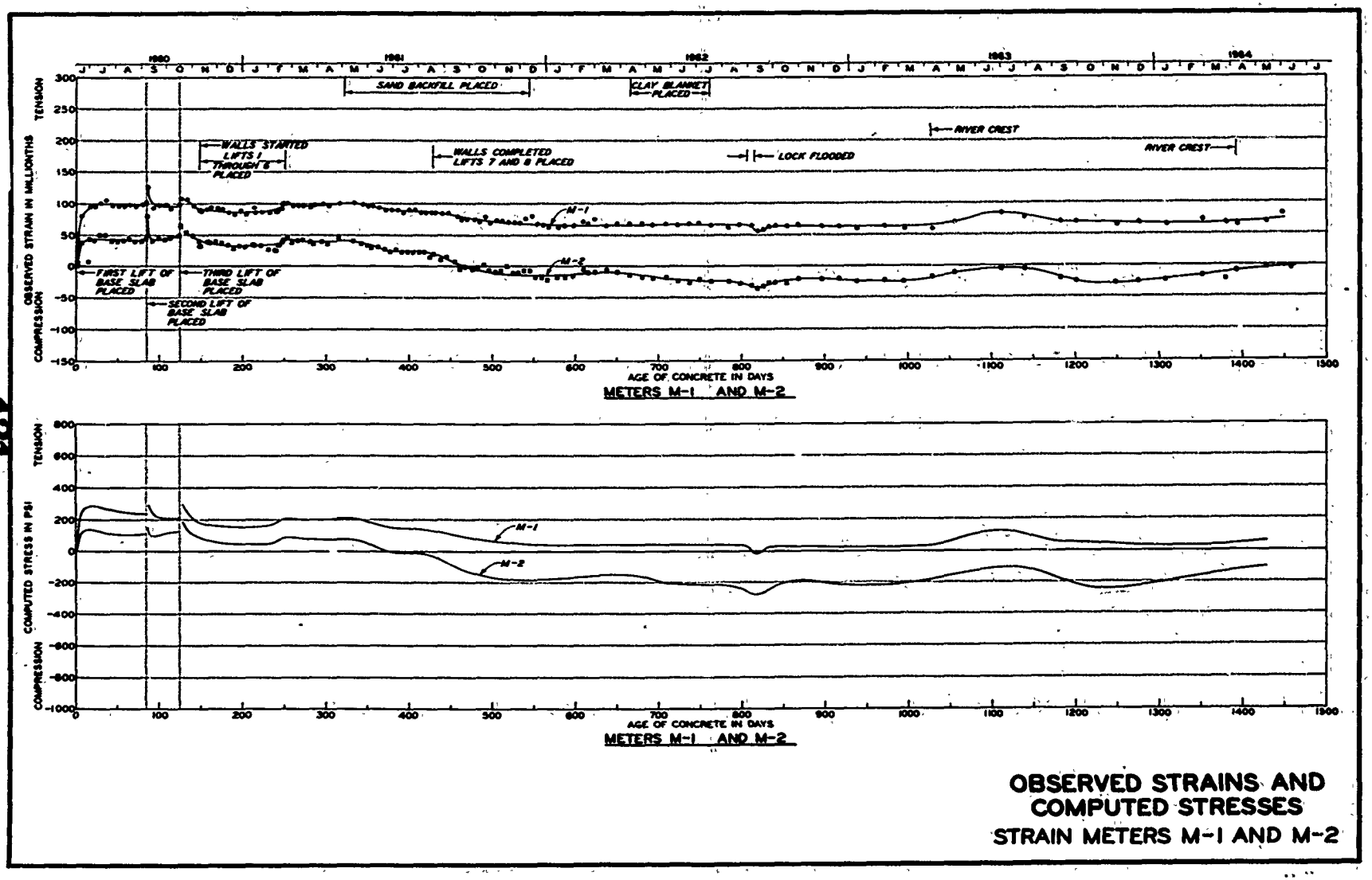

OBSERVED STRAINS AND COMPUTED STRESSES
STRAIN METERS M-1 AND M-2

PLATE 39

PLATE 40

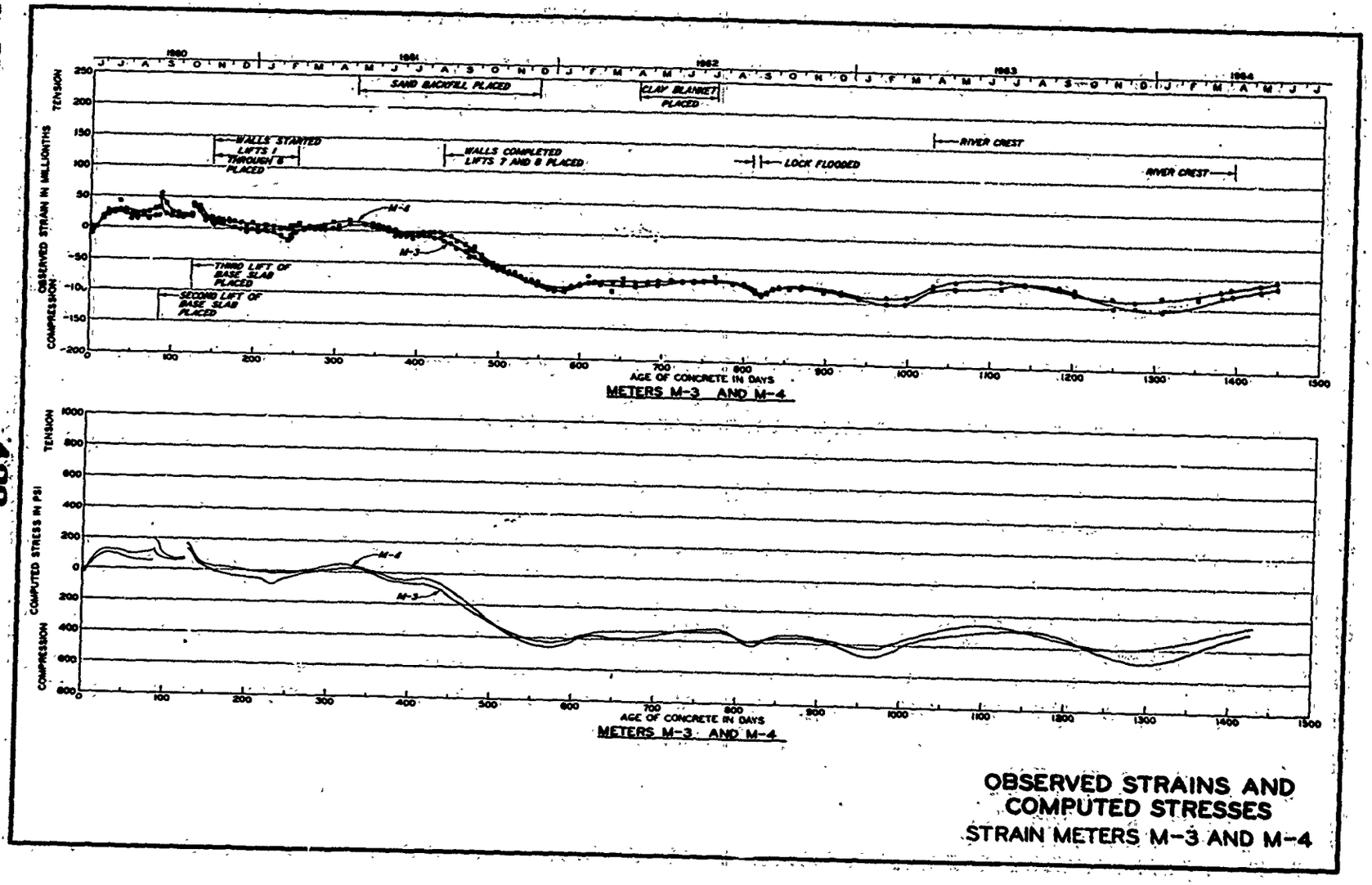

OBSERVED STRAINS AND COMPUTED STRESSES
STRAIN METERS M-3 AND M-4

122

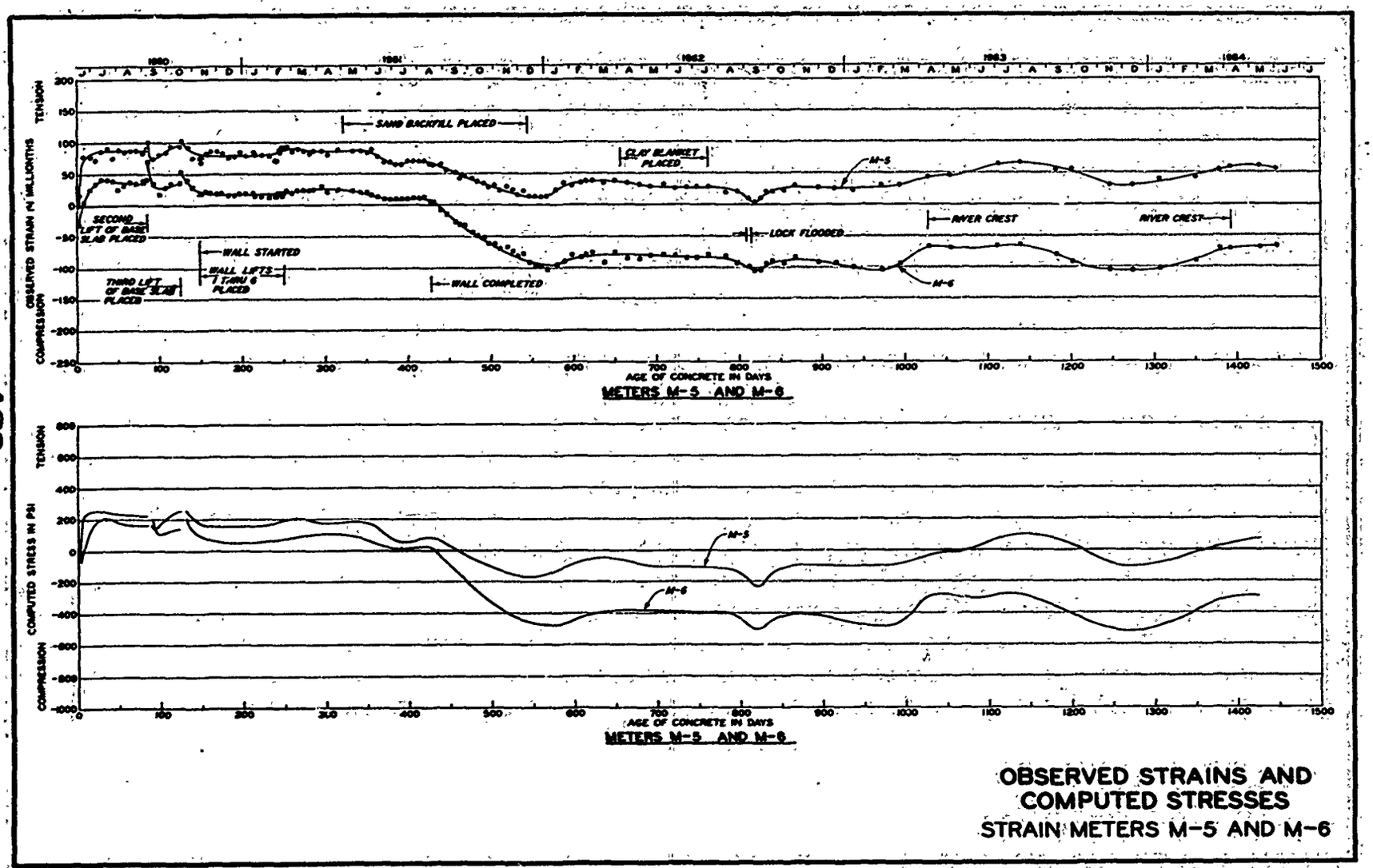

OBSERVED STRAINS AND COMPUTED STRESSES
STRAIN METERS M-5 AND M-6

PLATE 41

PLATE 42

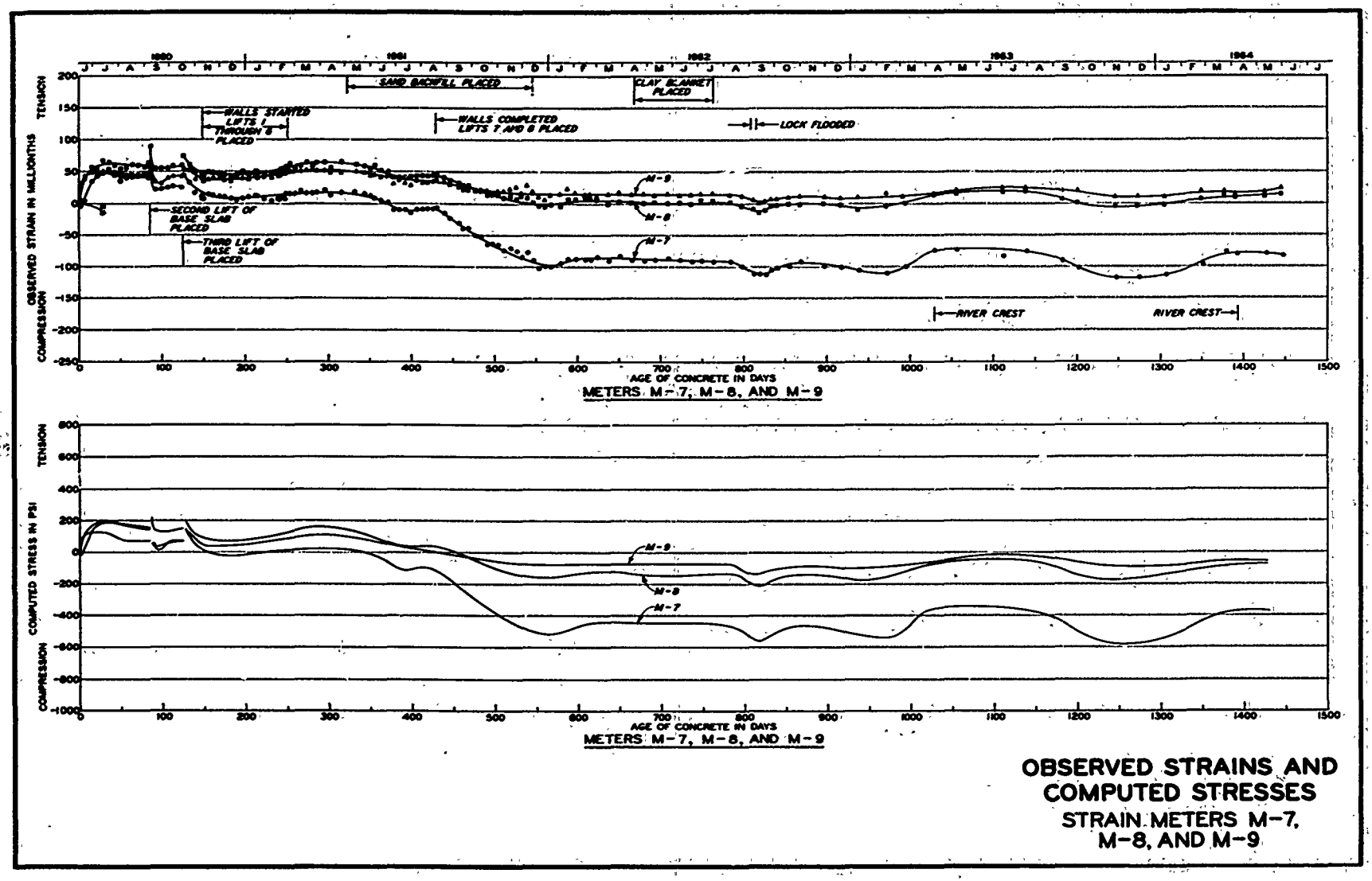

OBSERVED STRAINS AND COMPUTED STRESSES
STRAIN METERS M-7, M-8, AND M-9

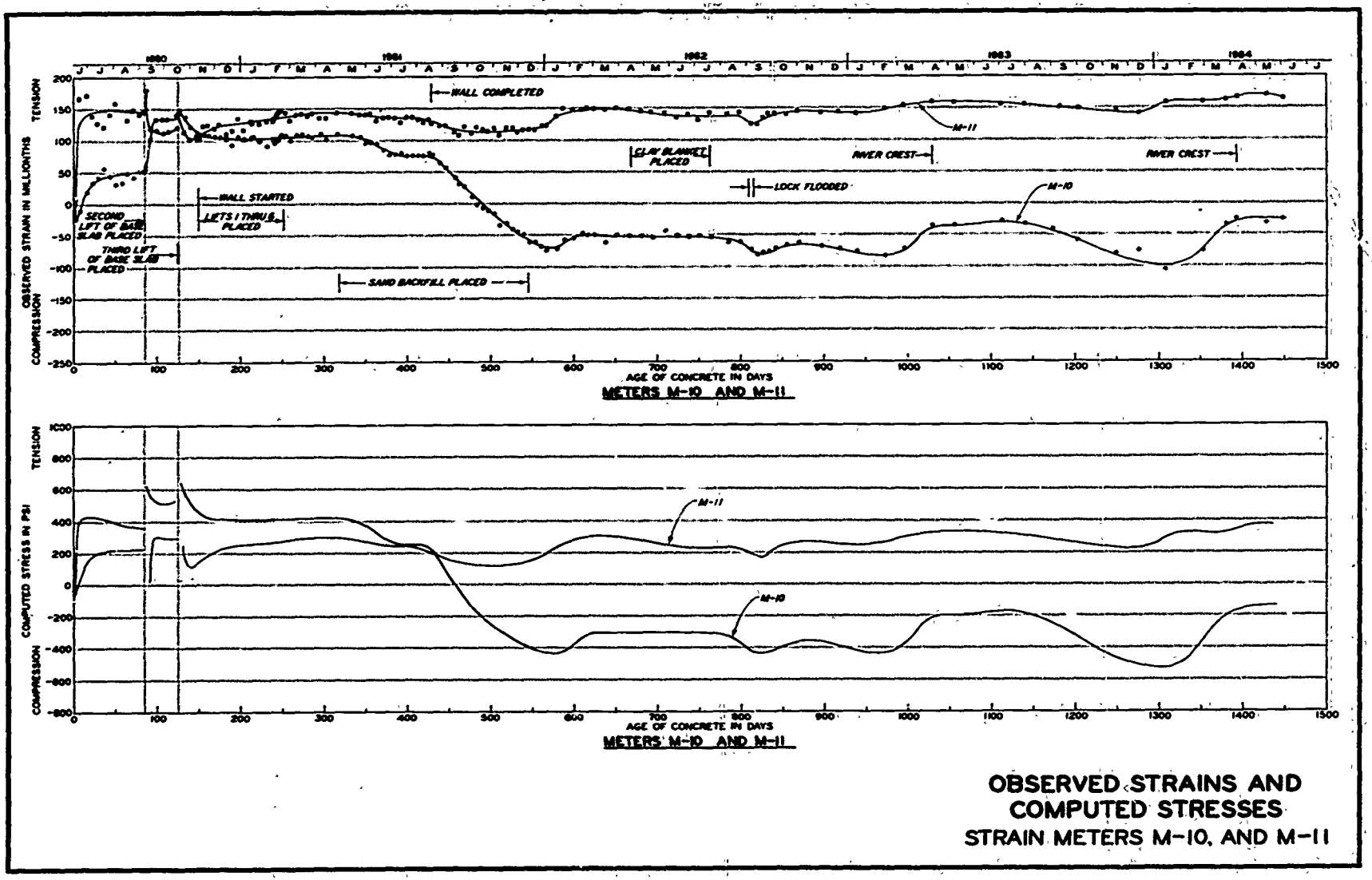

OBSERVED STRAINS AND COMPUTED STRESSES
STRAIN METERS M-10, AND M-11

PLATE 43

PLATE 44

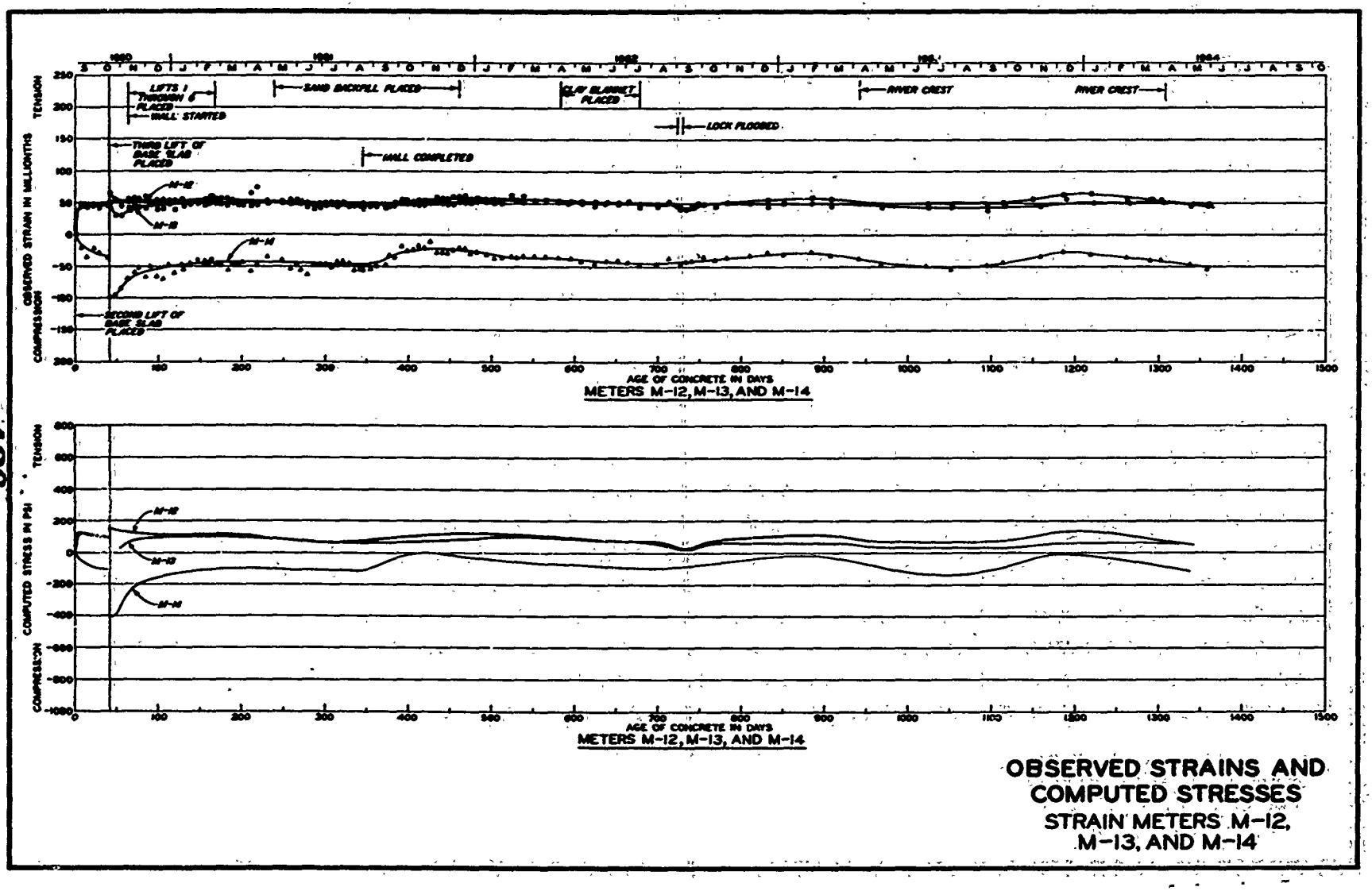

OBSERVED STRAINS AND COMPUTED STRESSES
STRAIN METERS M-12, M-13, AND M-14

126

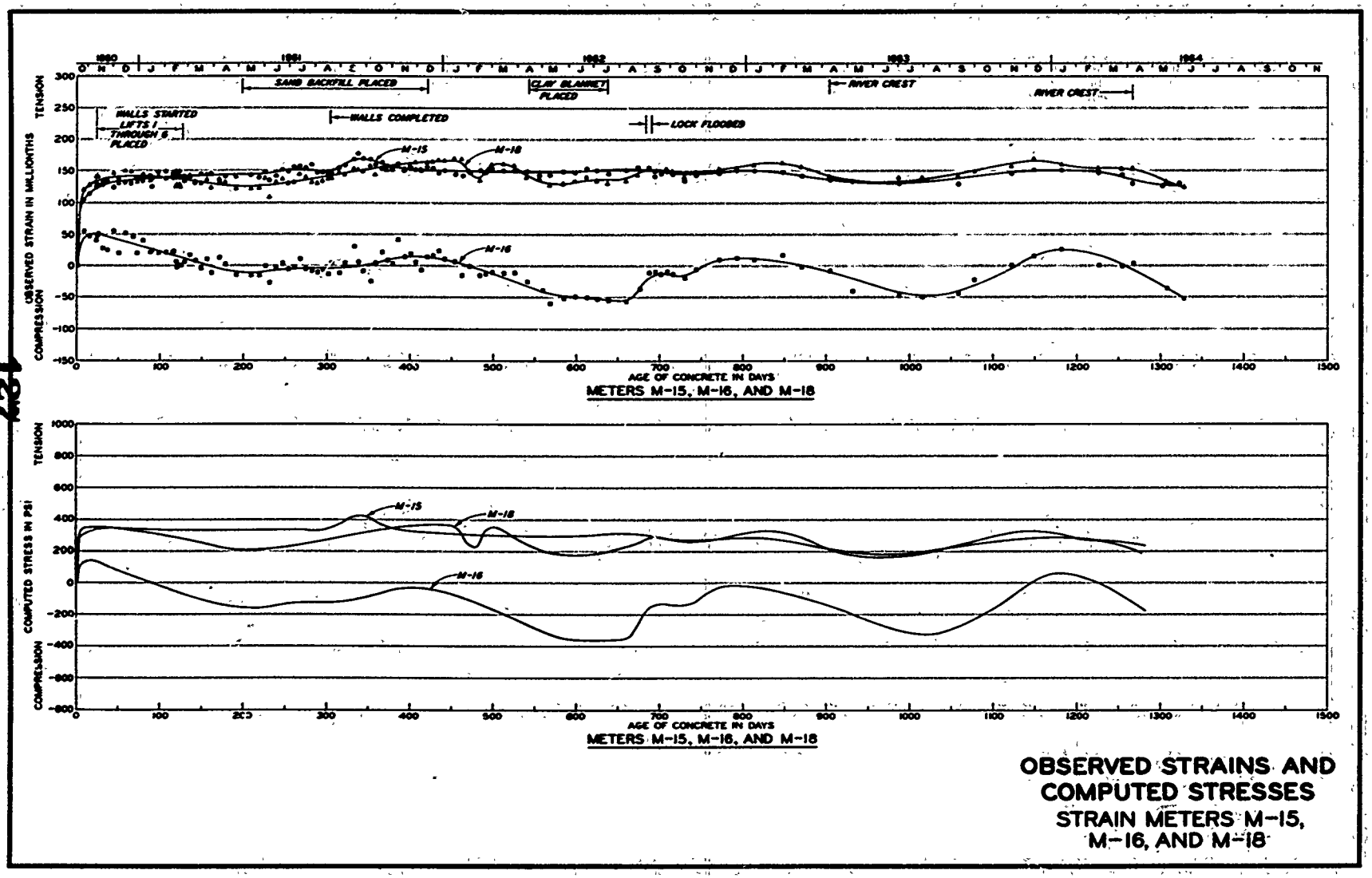

PLATE 45

OBSERVED STRAINS AND COMPUTED STRESSES

STRAIN METERS M-15, M-16, AND M-18

PLATE 46

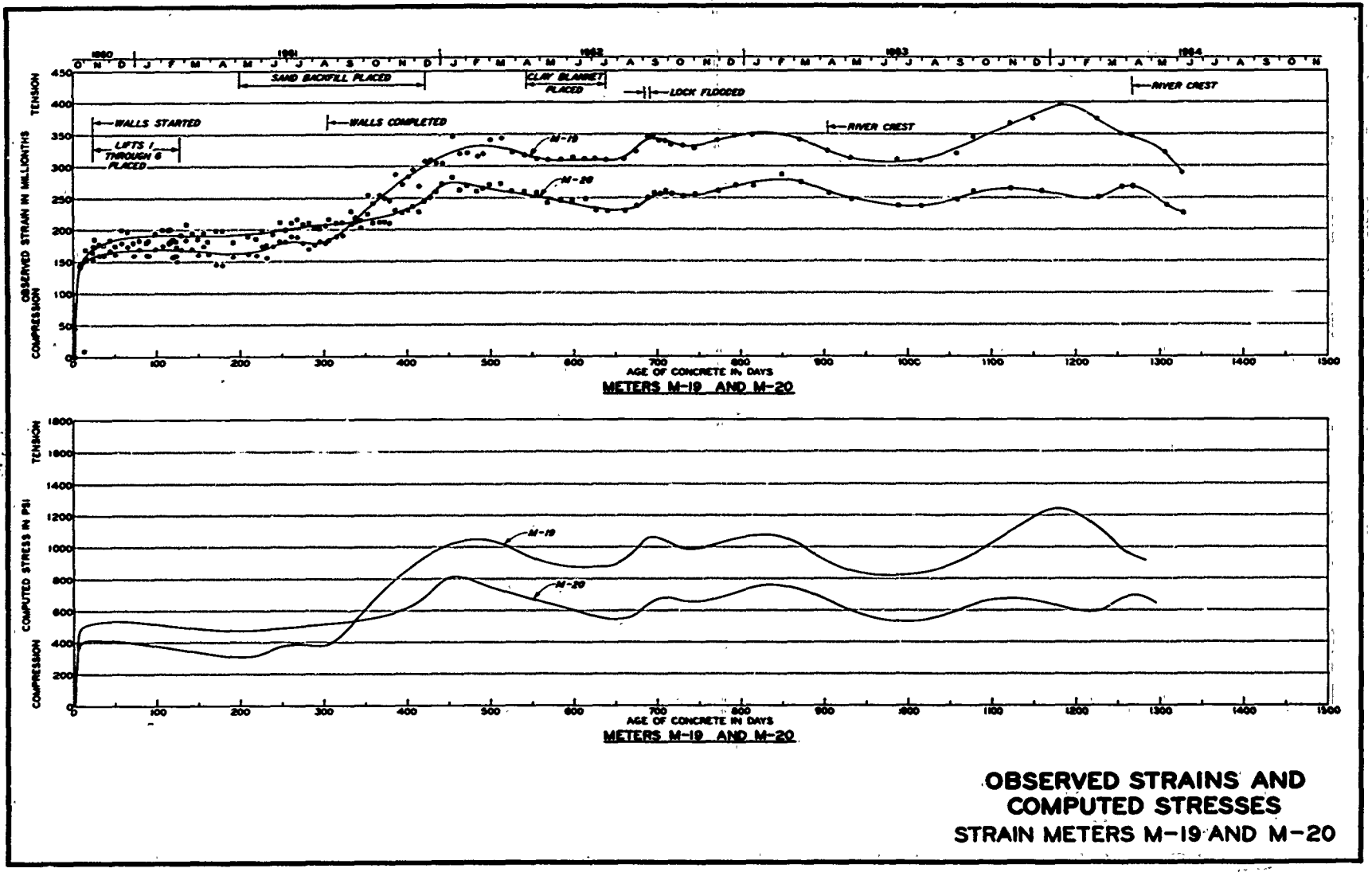

OBSERVED STRAINS AND COMPUTED STRESSES

STRAIN METERS M-19 AND M-20

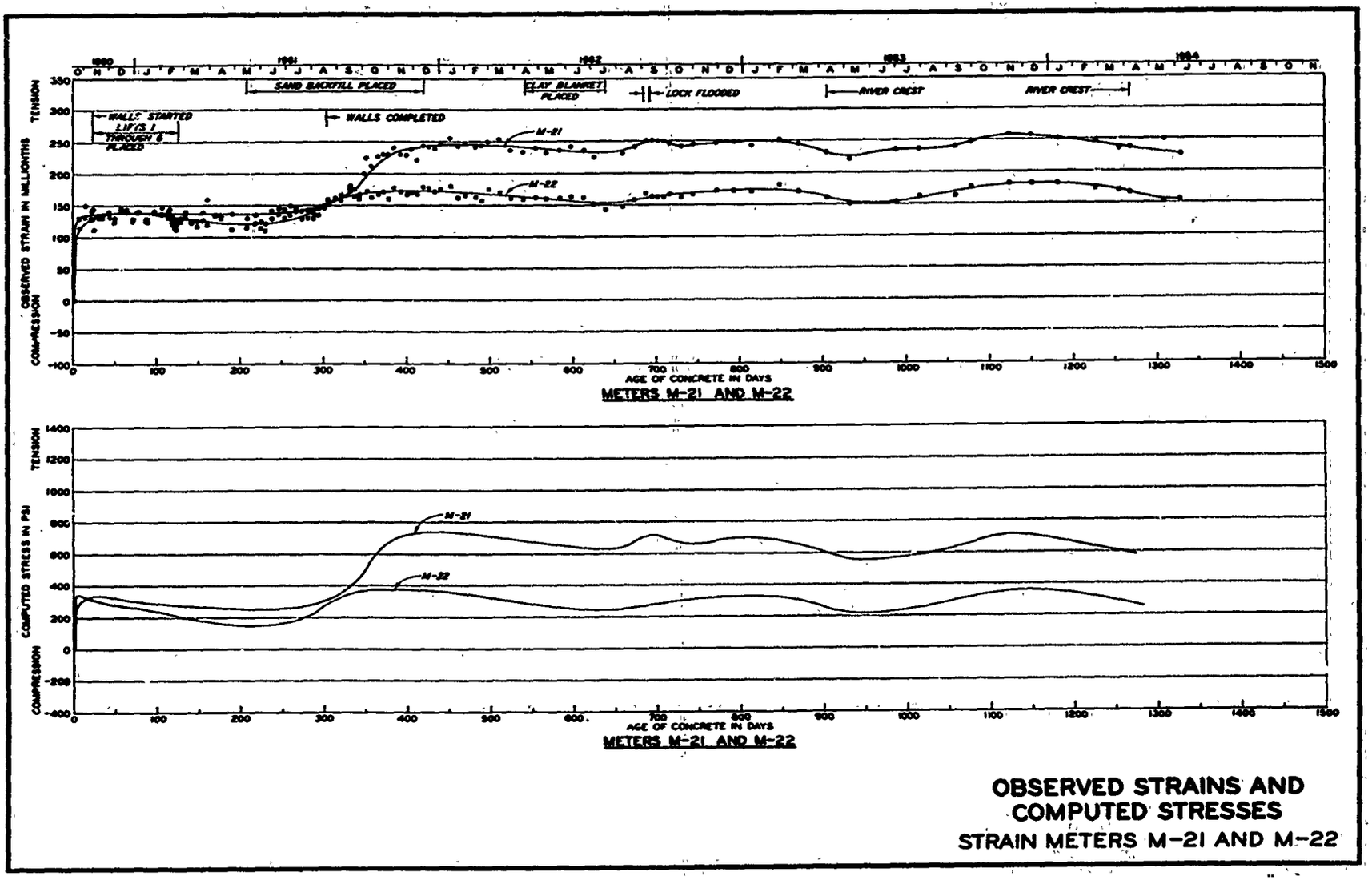

OBSERVED STRAINS AND COMPUTED STRESSES

STRAIN METERS M-21 AND M-22

PLATE 47

PLATE 48

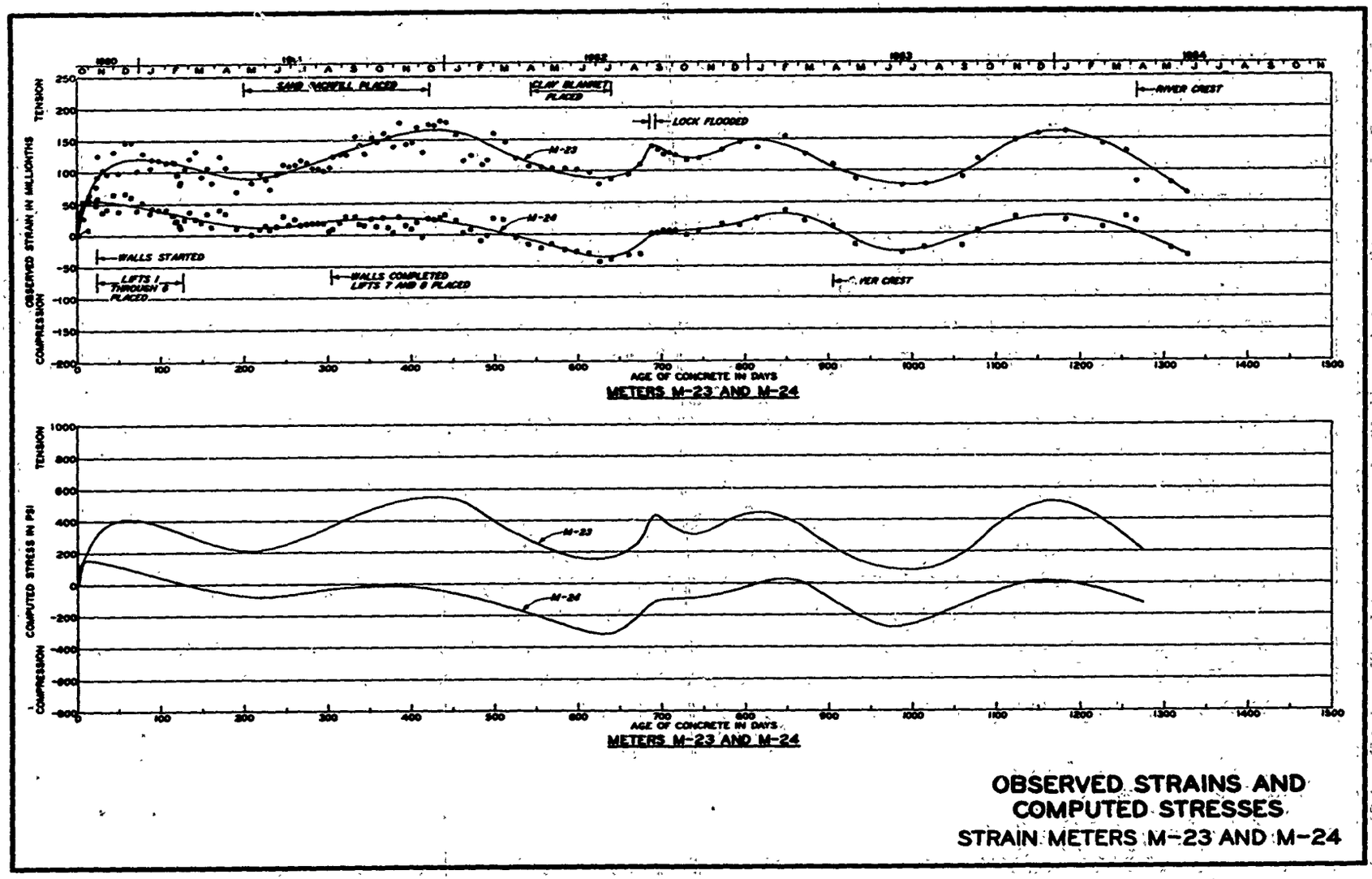

OBSERVED STRAINS AND COMPUTED STRESSES
STRAIN METERS M-23 AND M-24

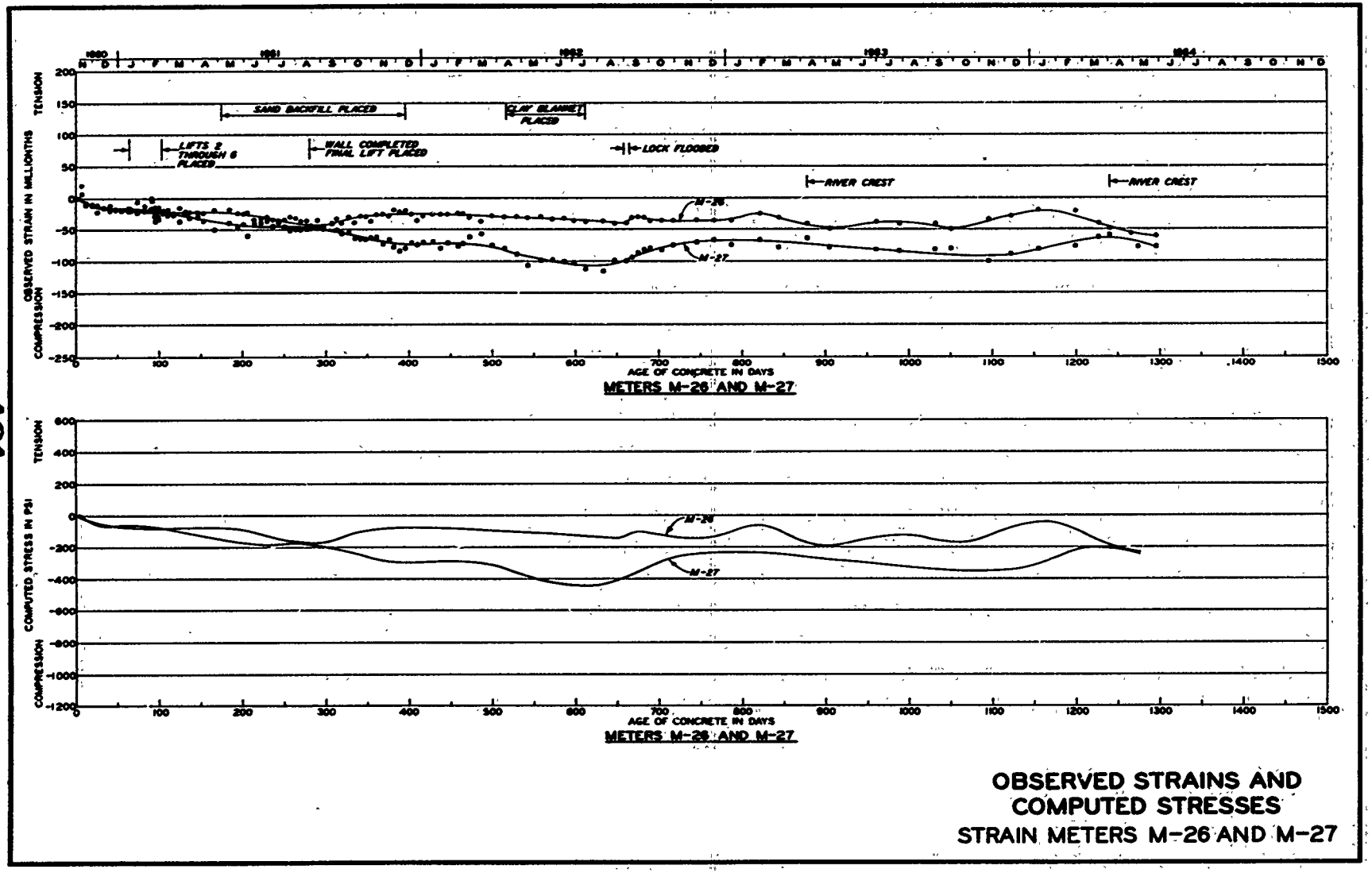

OBSERVED STRAINS AND COMPUTED STRESSES
STRAIN METERS M-26 AND M-27

PLATE 49

PLATE 50

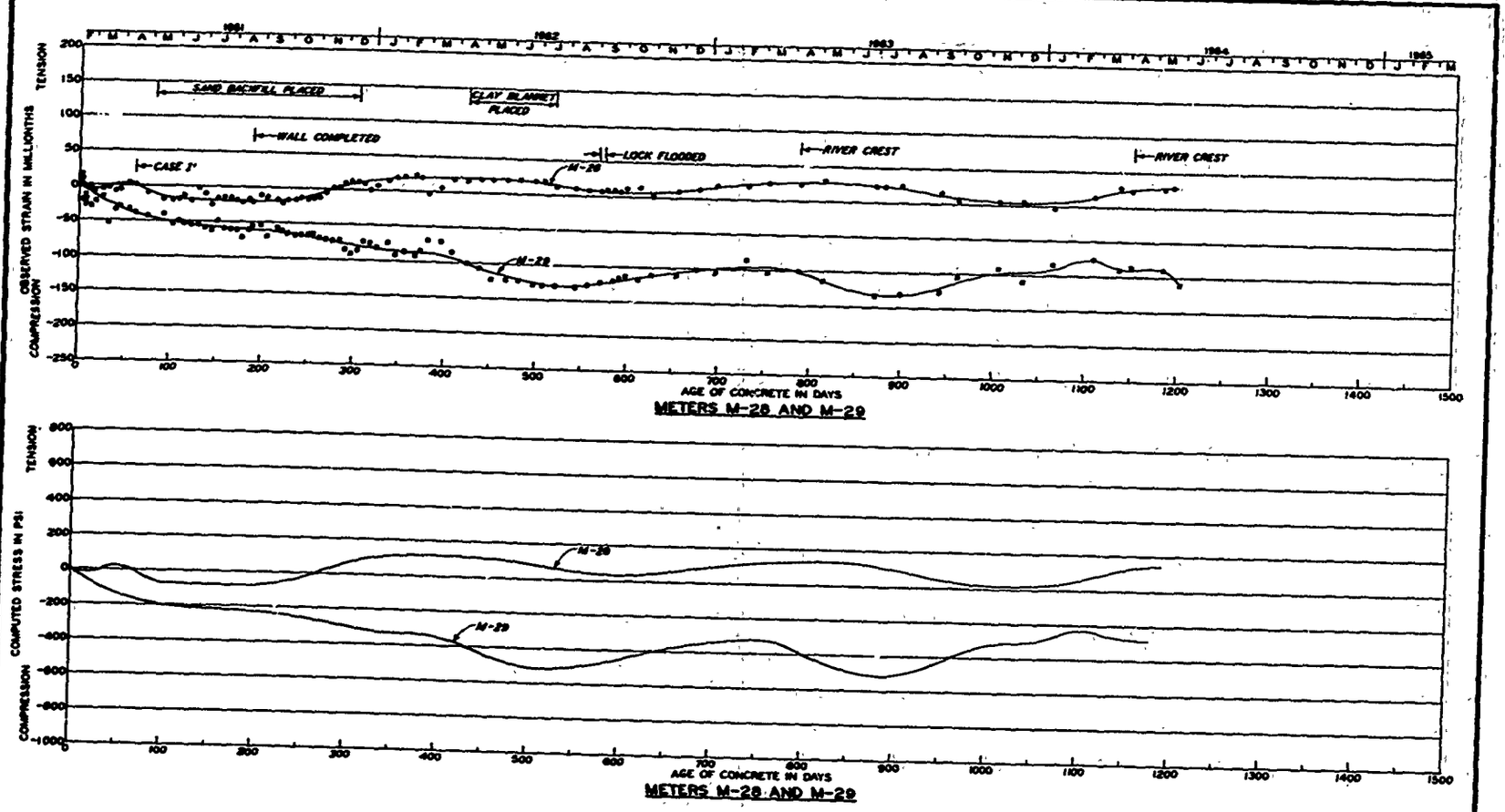

OBSERVED STRAINS AND COMPUTED STRESSES

STRAIN METERS M-28 AND M-29

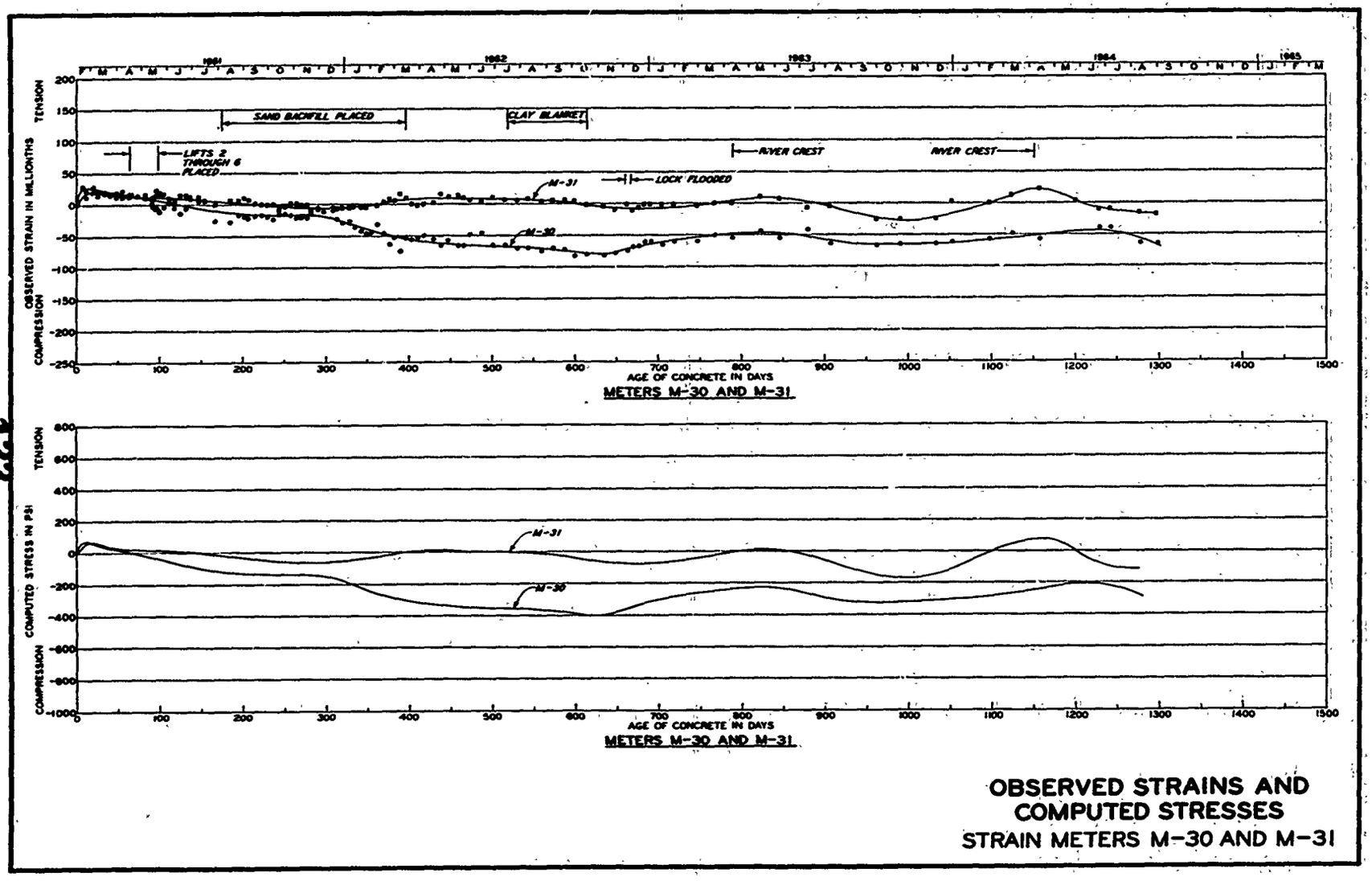

OBSERVED STRAINS AND COMPUTED STRESSES
STRAIN METERS M-30 AND M-31

PLATE 51

PLATE 52

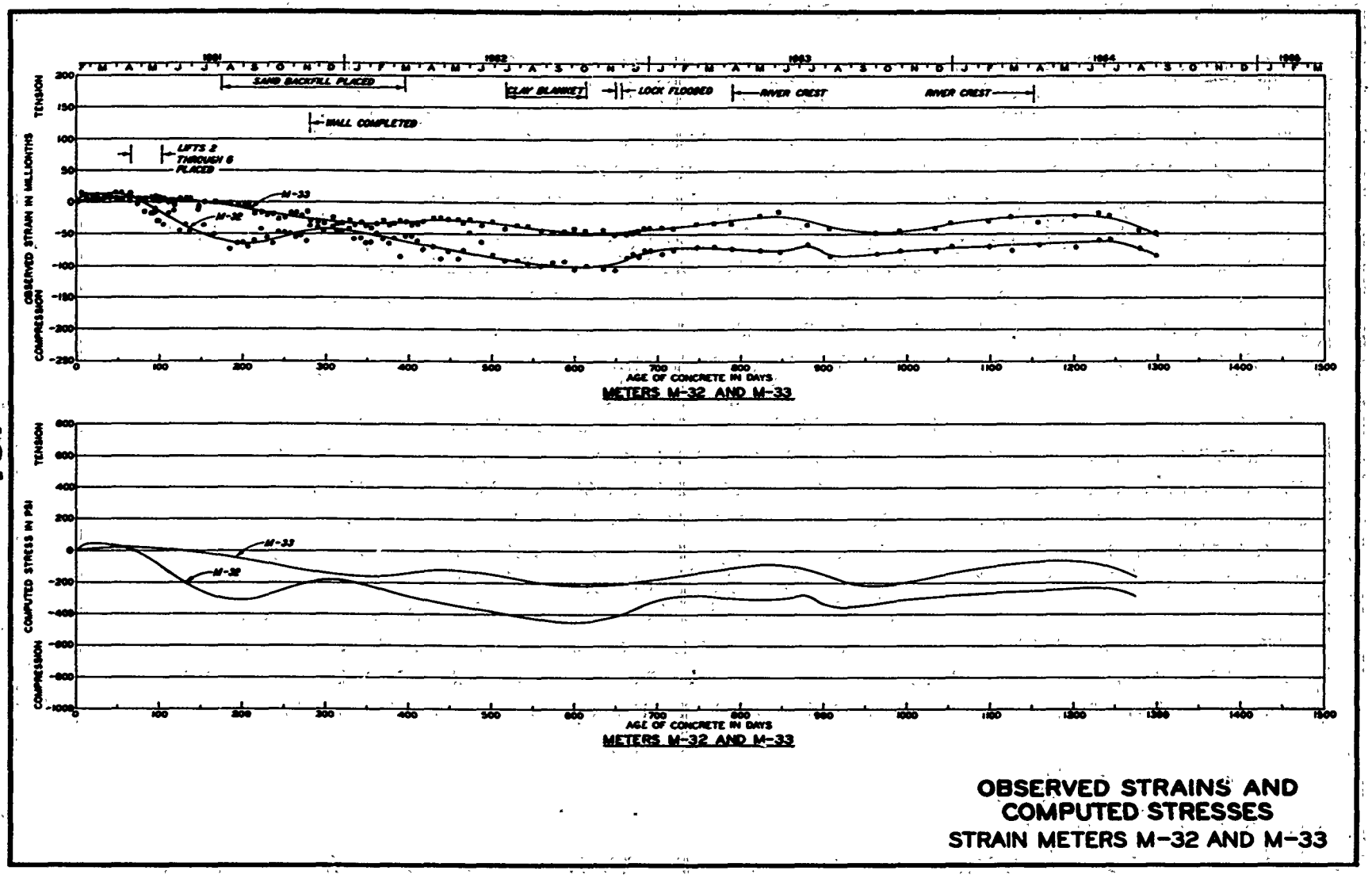

OBSERVED STRAINS AND COMPUTED STRESSES
STRAIN METERS M-32 AND M-33

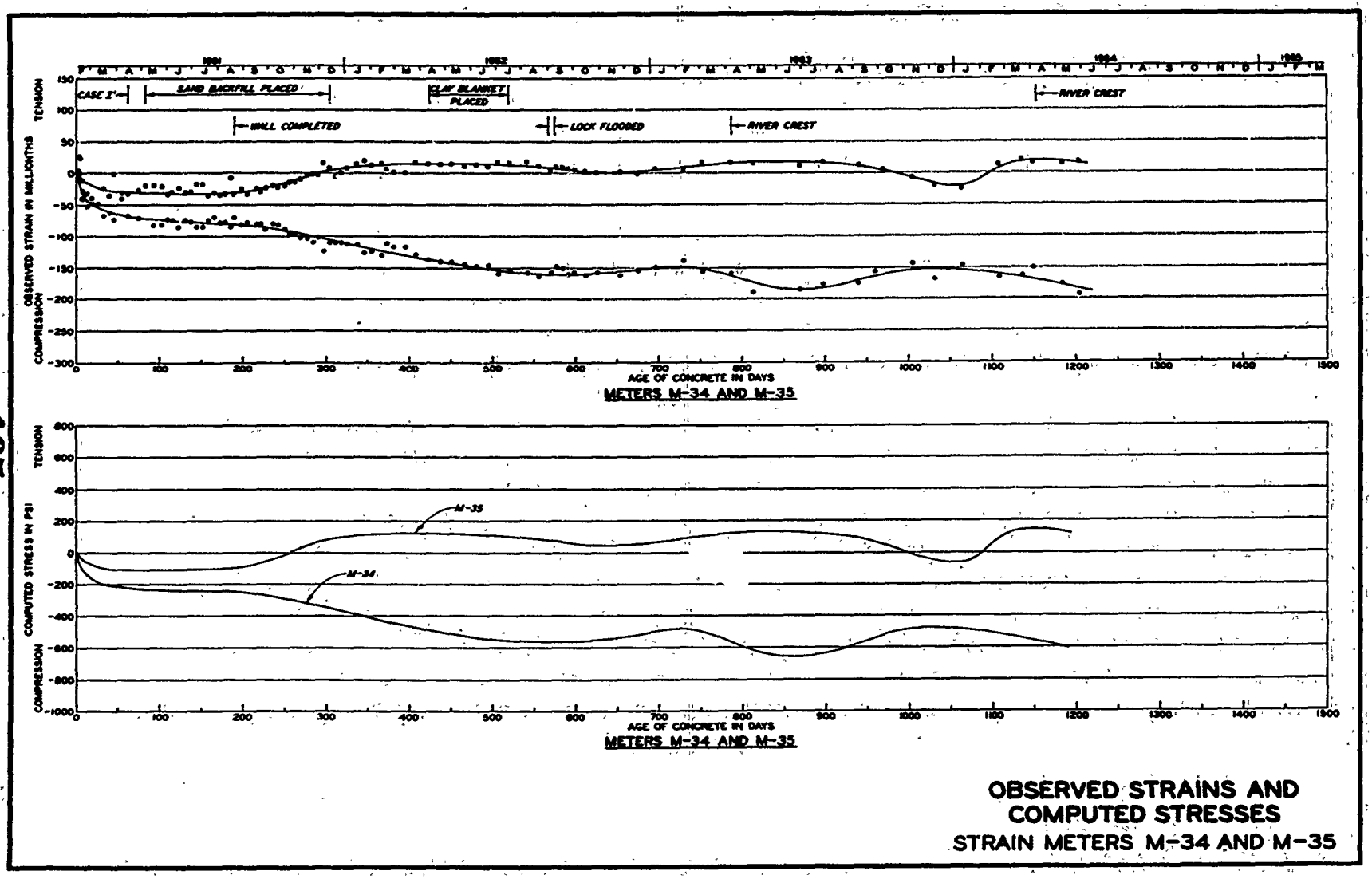

OBSERVED STRAINS AND COMPUTED STRESSES
STRAIN METERS M-34 AND M-35

PLATE 53

PLATE 54

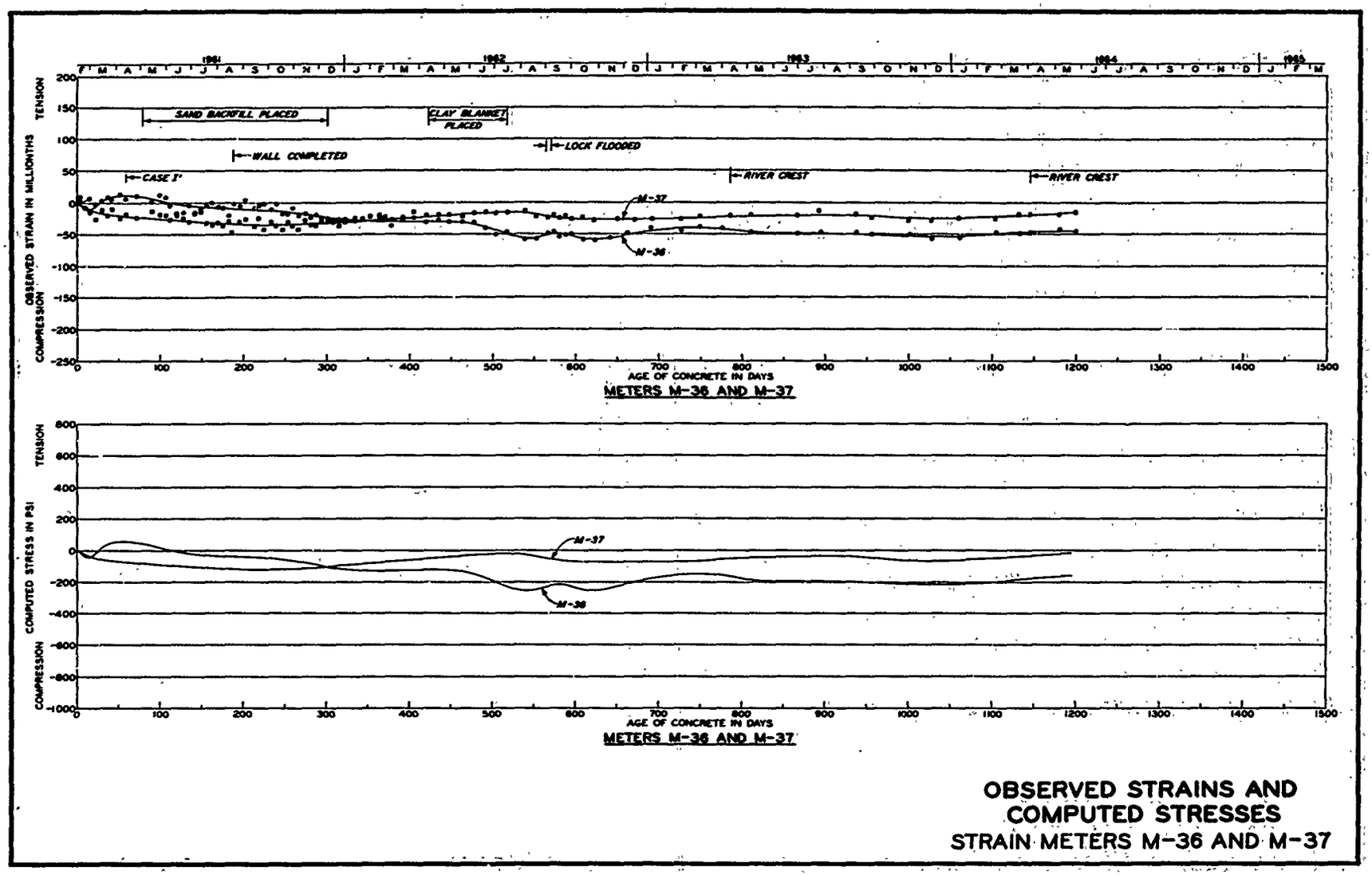

OBSERVED STRAINS AND COMPUTED STRESSES
STRAIN METERS M-36 AND M-37

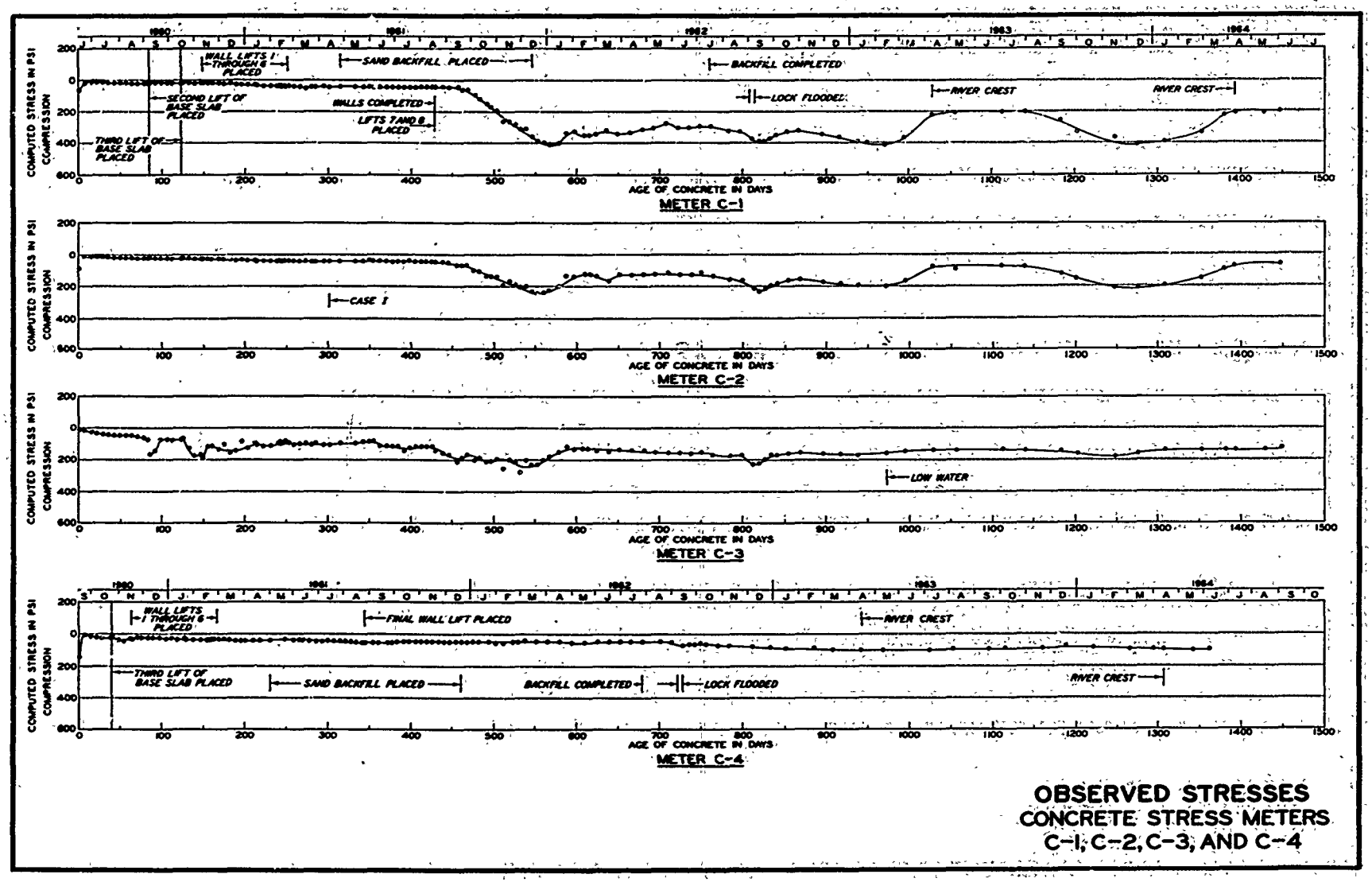

OBSERVED STRESSES
CONCRETE STRESS METERS
C-1, C-2, C-3, AND C-4

PLATE 55

PLATE 56

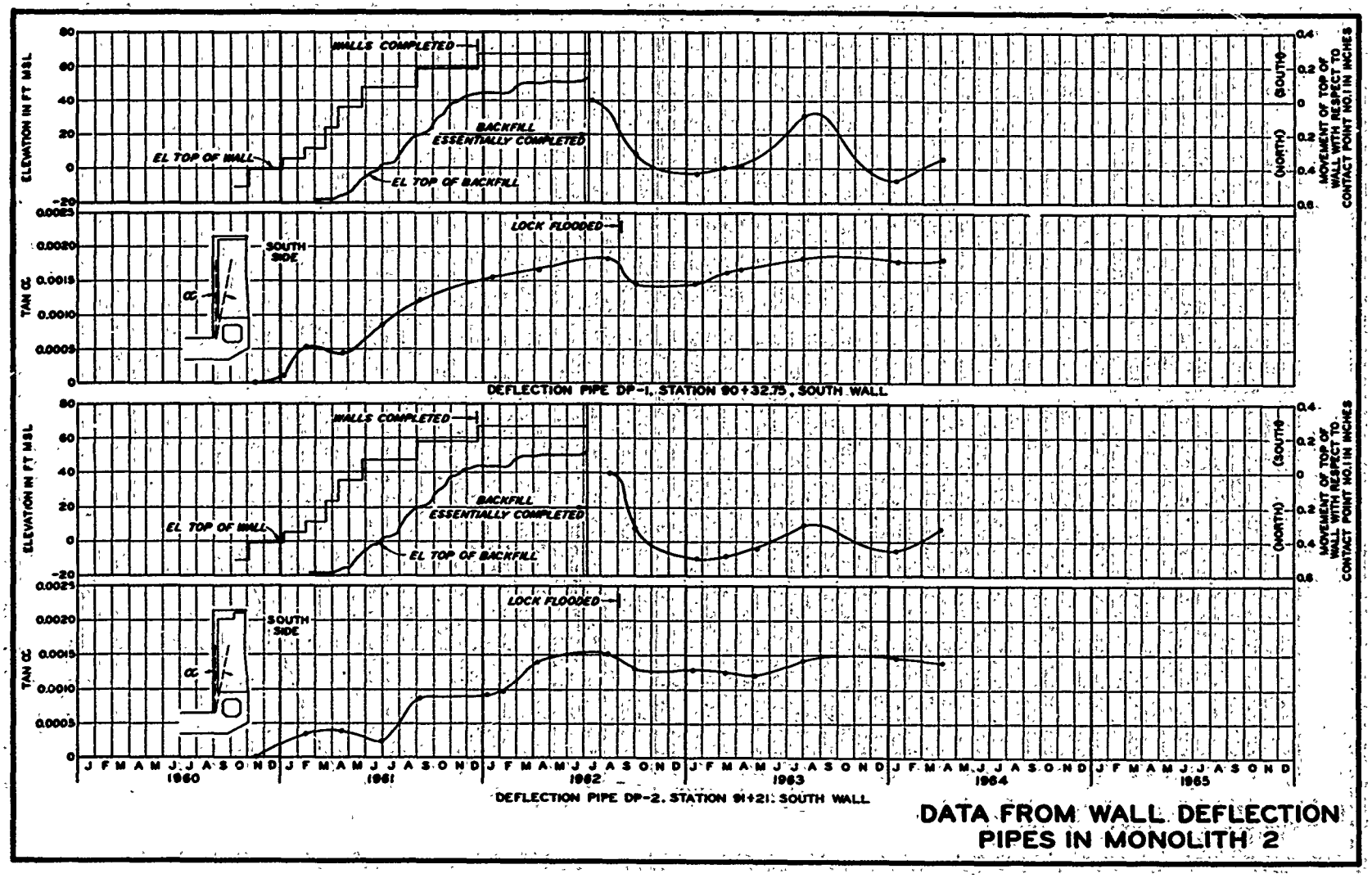

DATA FROM WALL DEFLECTION PIPES IN MONOLITH 2

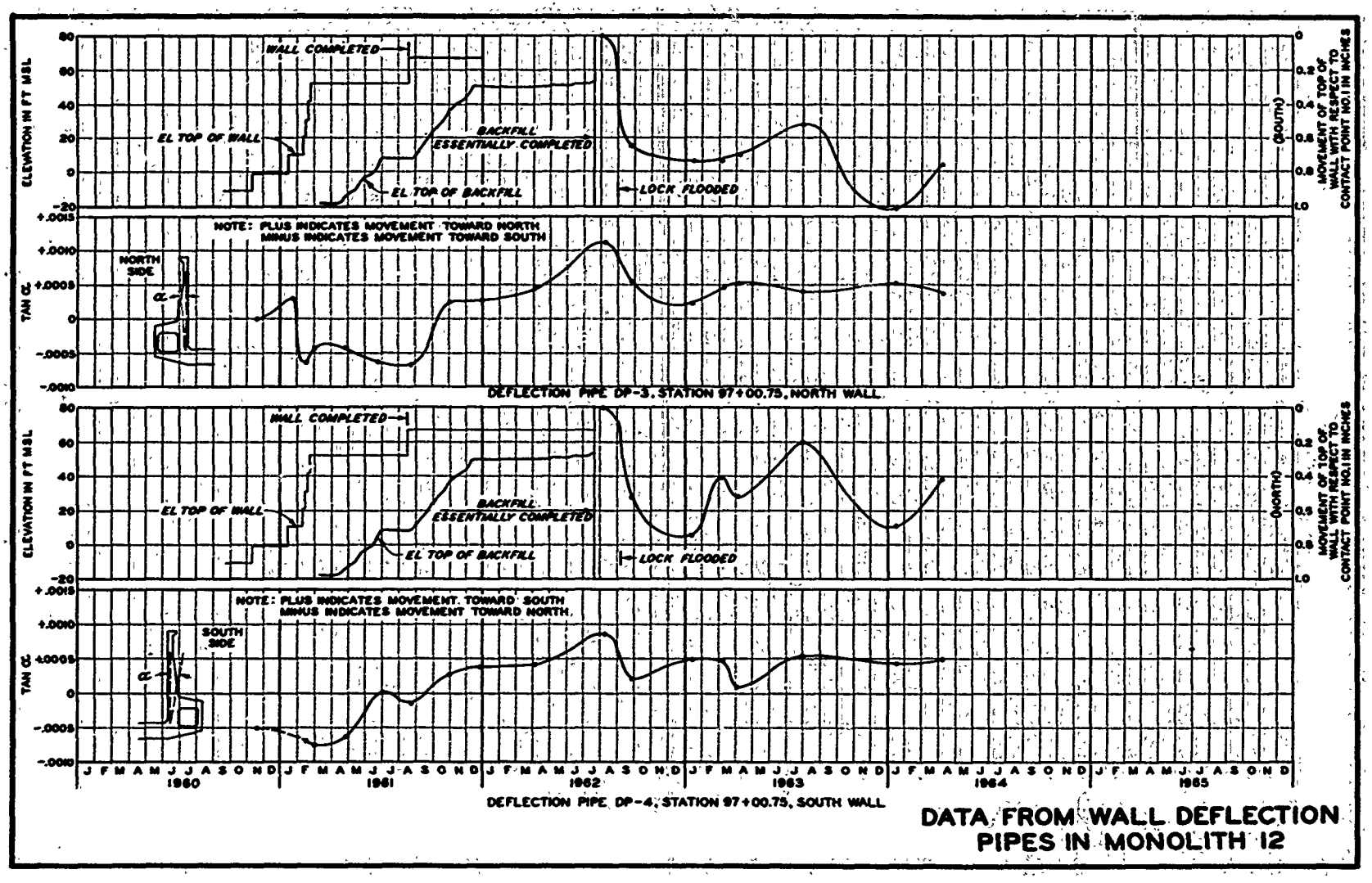

DATA FROM WALL DEFLECTION PIPES IN MONOLITH 12

PLATE 57

PLATE 58

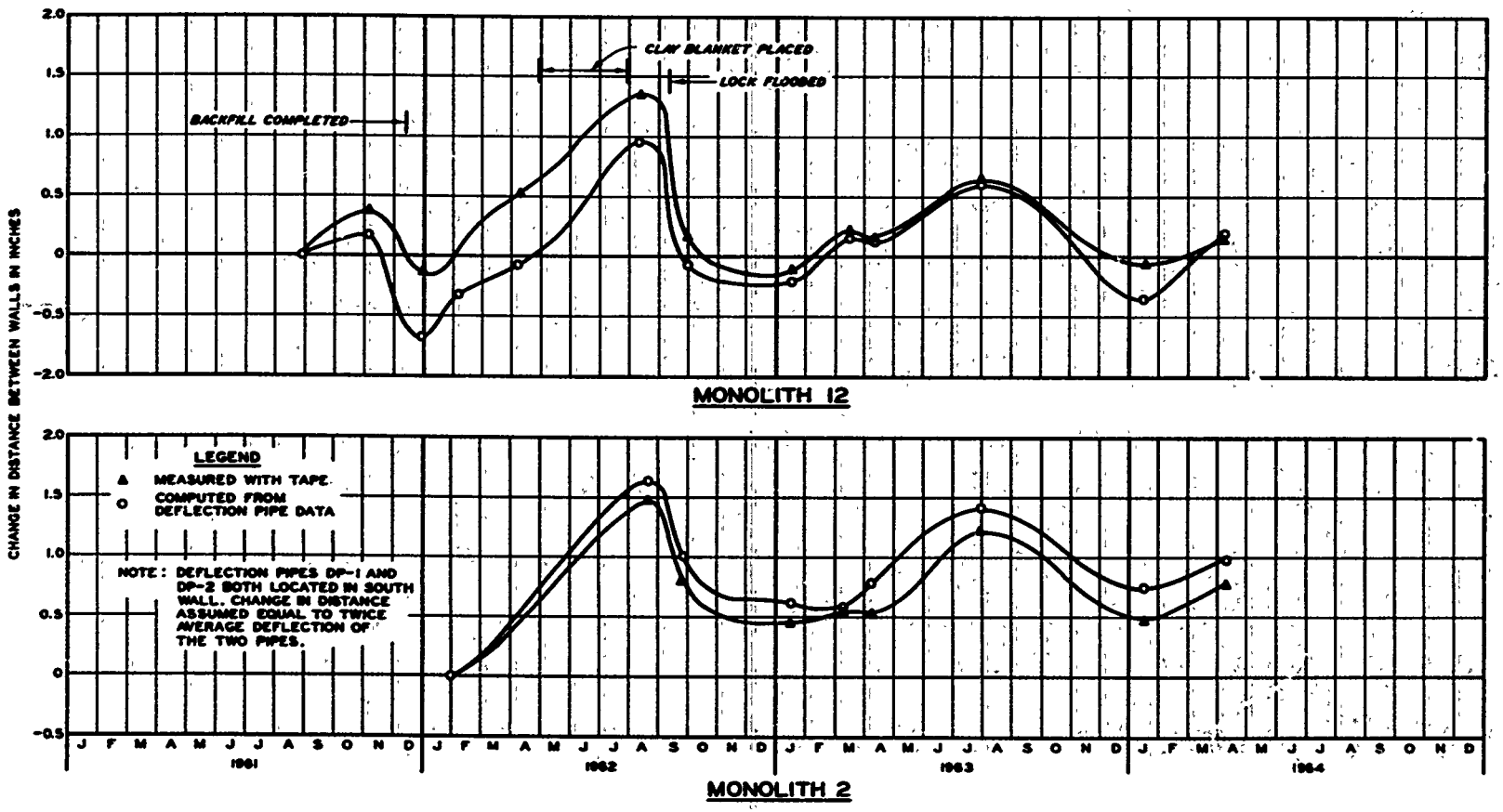

CHANGE IN DISTANCE BETWEEN WALLS VS TIME

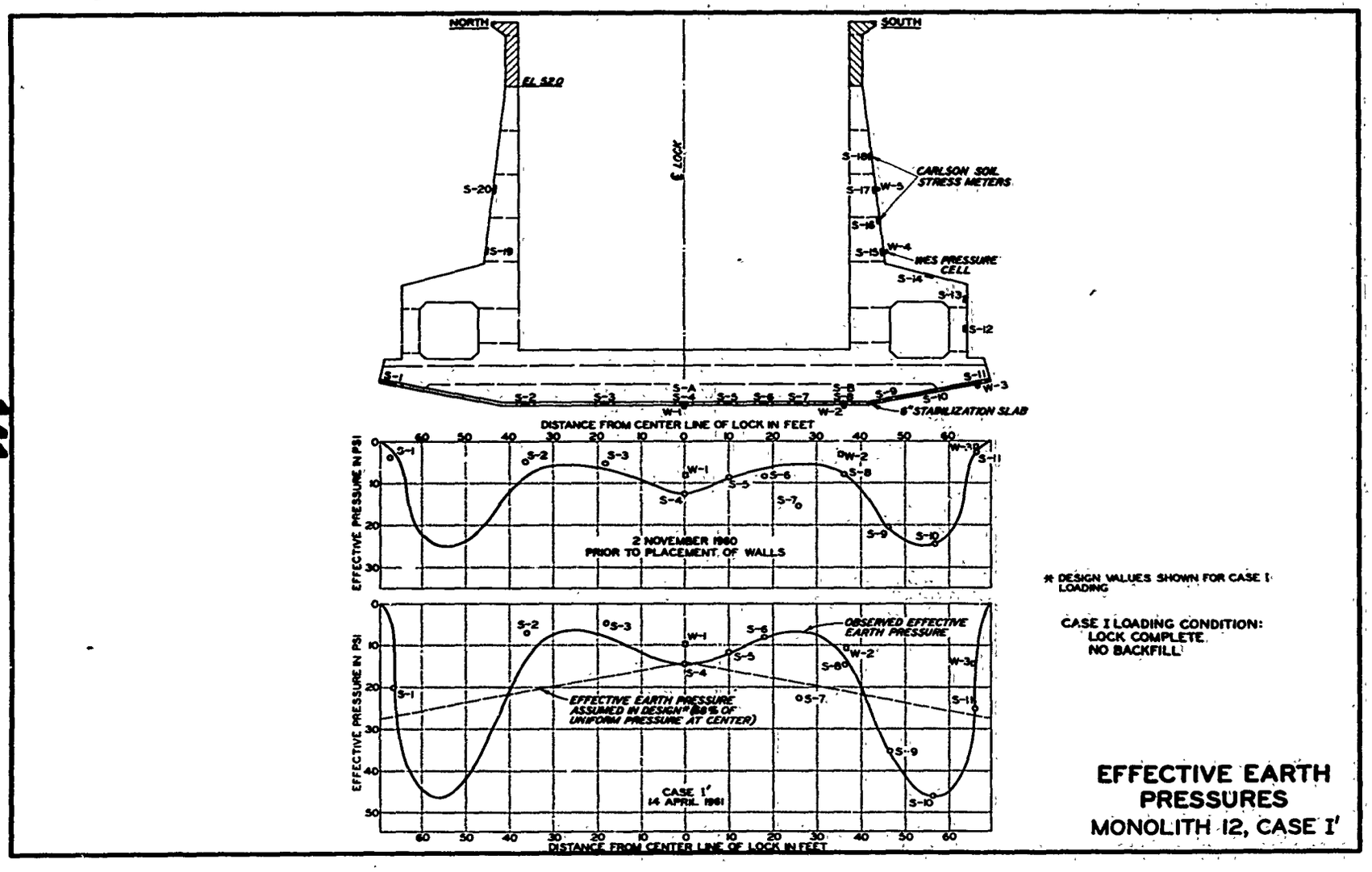

* DESIGN VALUES SHOWN FOR CASE I LOADING

CASE I LOADING CONDITION:
LOCK COMPLETE
NO BACKFILL

EFFECTIVE EARTH PRESSURES
MONOLITH 12, CASE I'

PLATE 59

PLATE 60

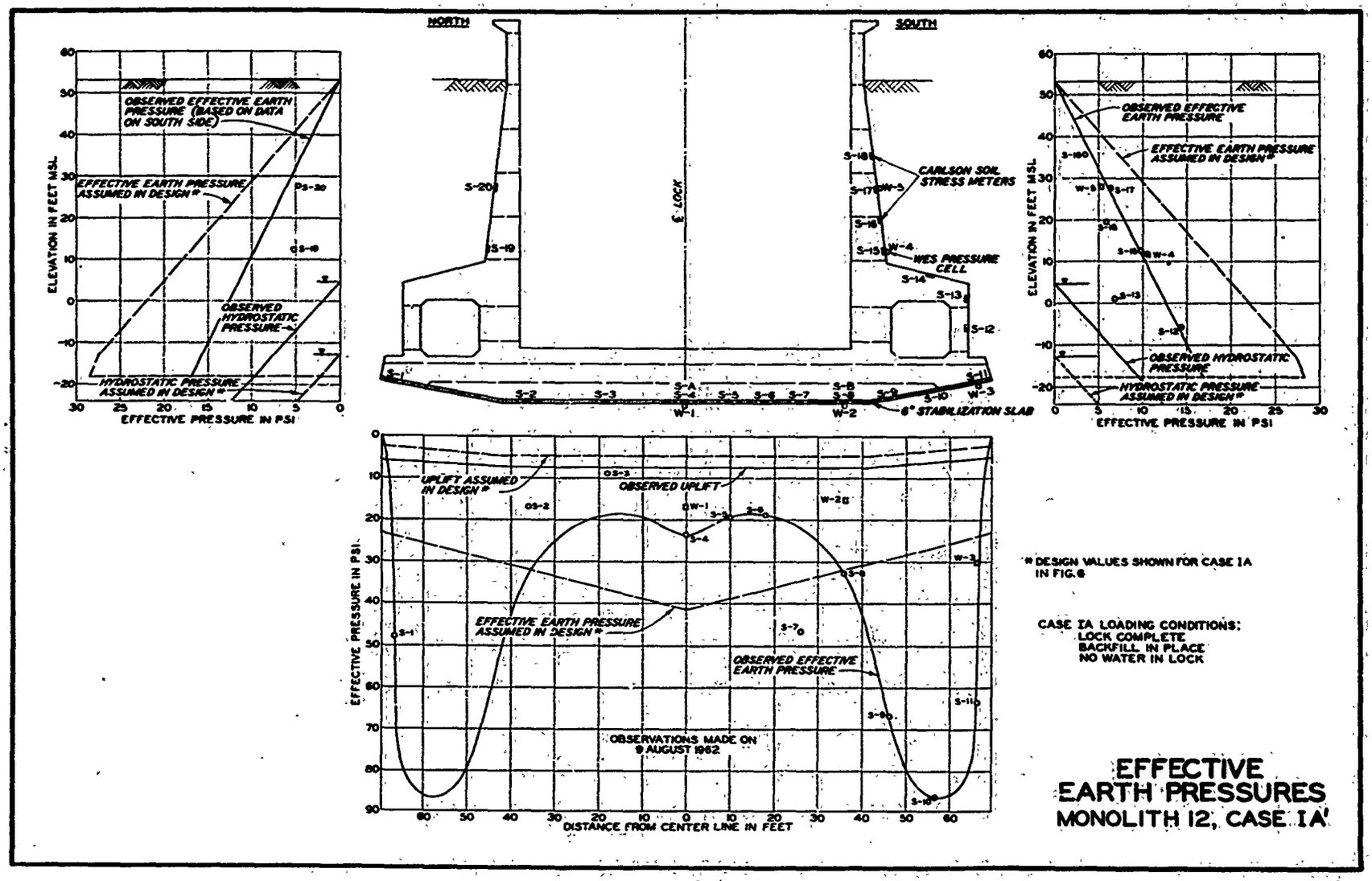

* DESIGN VALUES SHOWN FOR CASE IA IN FIG. 6

CASE IA LOADING CONDITIONS:
LOCK COMPLETE
BACKFILL IN PLACE
NO WATER IN LOCK

EFFECTIVE EARTH PRESSURES MONOLITH 12, CASE IA

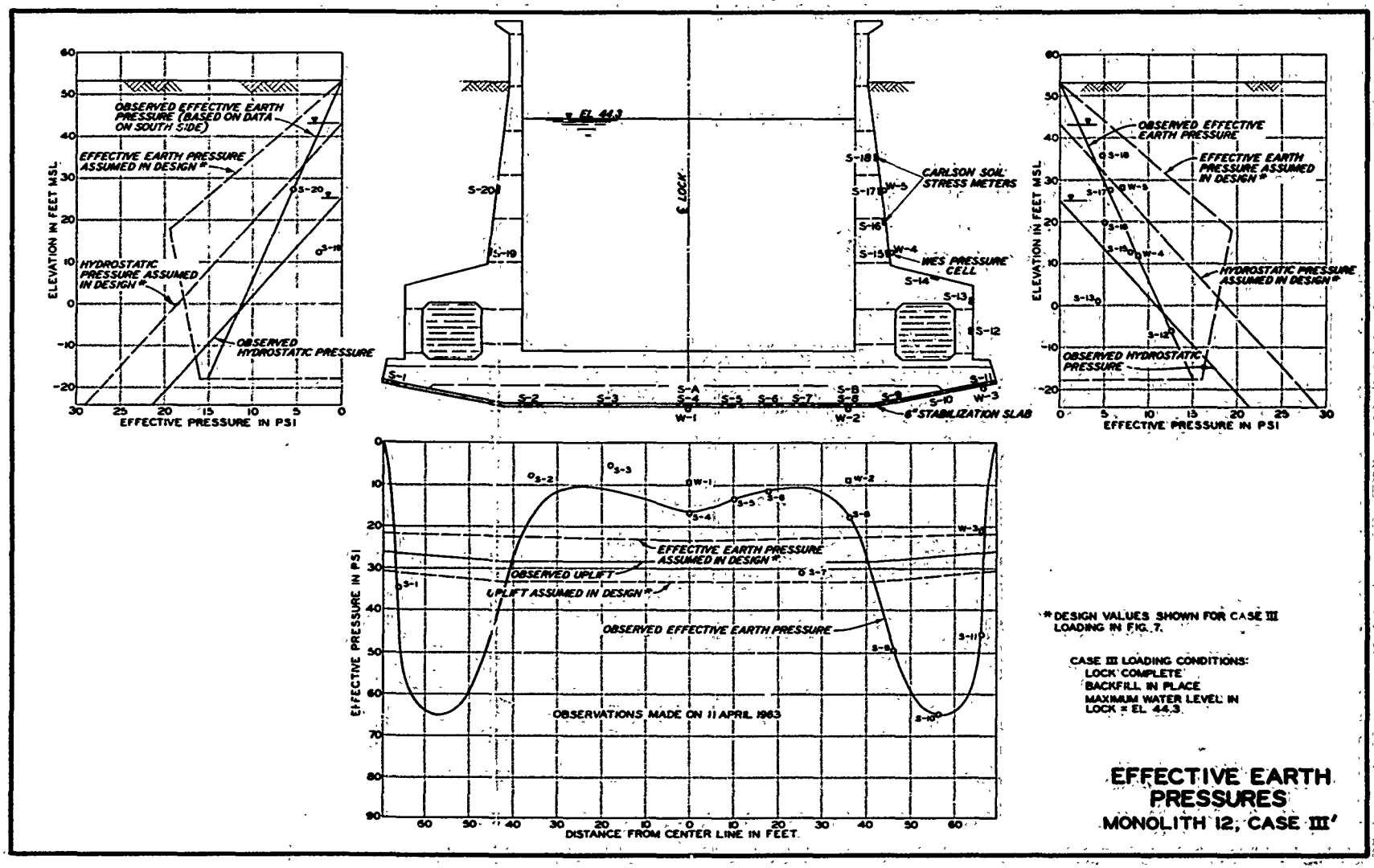

EFFECTIVE EARTH PRESSURES
MONOLITH 12, CASE III'

PLATE 61

PLATE 62

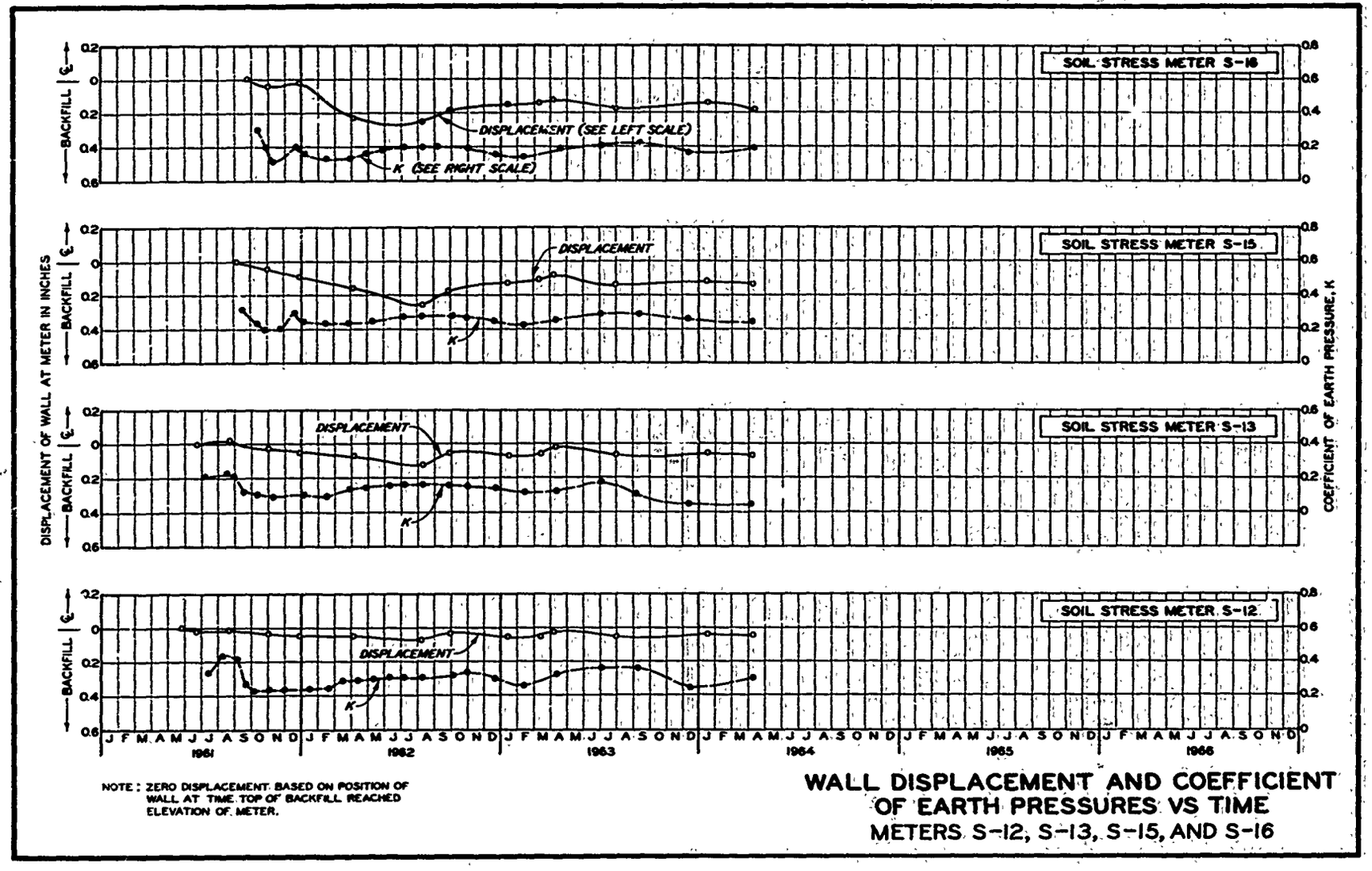

NOTE : ZERO DISPLACEMENT BASED ON POSITION OF WALL AT TIME TOP OF BACKFILL REACHED ELEVATION OF METER.

WALL DISPLACEMENT AND COEFFICIENT OF EARTH PRESSURES VS TIME METERS S-12, S-13, S-15, AND S-16

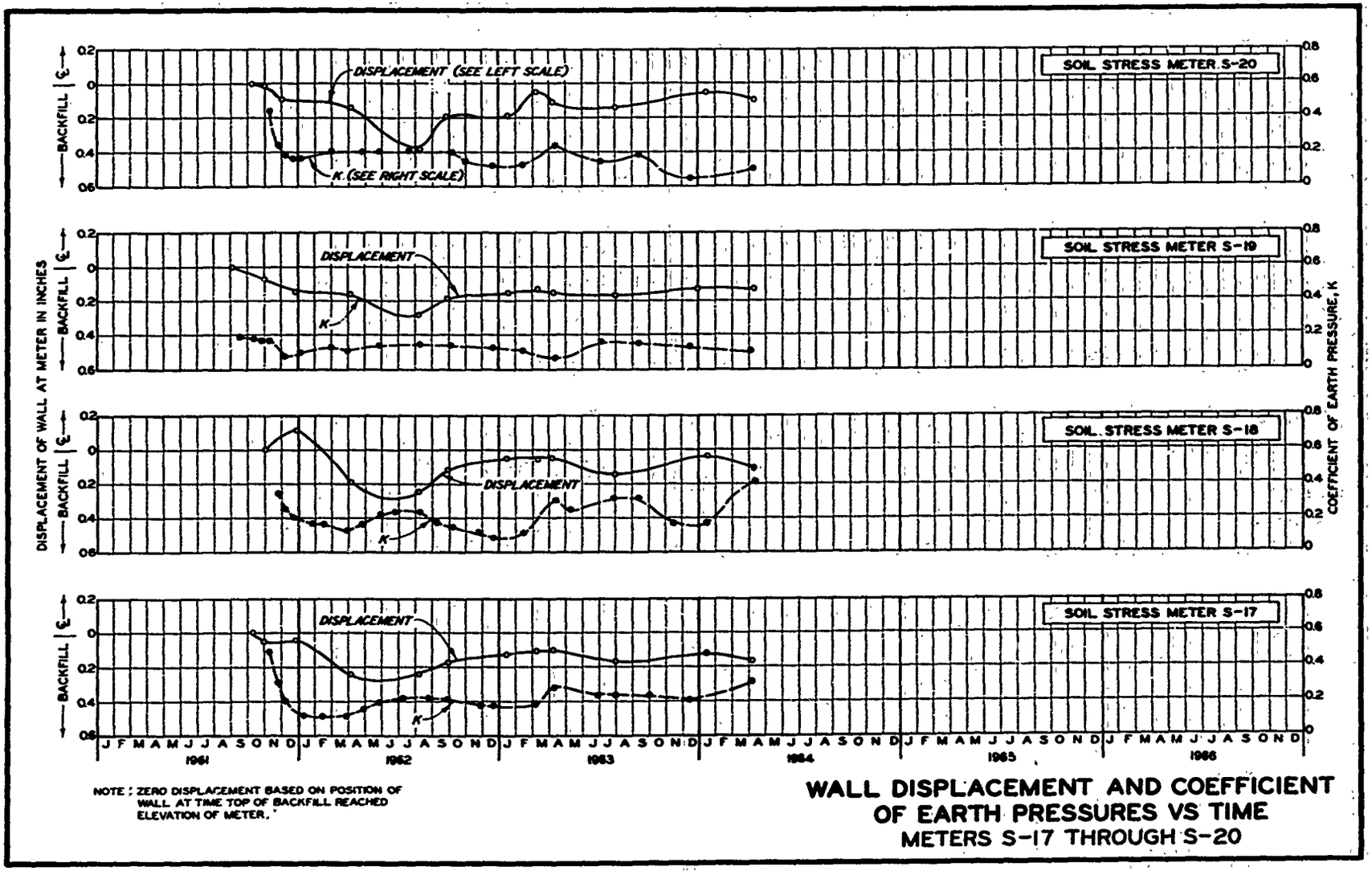

NOTE : ZERO DISPLACEMENT BASED ON POSITION OF WALL AT TIME TOP OF BACKFILL REACHED ELEVATION OF METER.

WALL DISPLACEMENT AND COEFFICIENT OF EARTH PRESSURES VS TIME
METERS S-17 THROUGH S-20

PLATE 63

PLATE 64

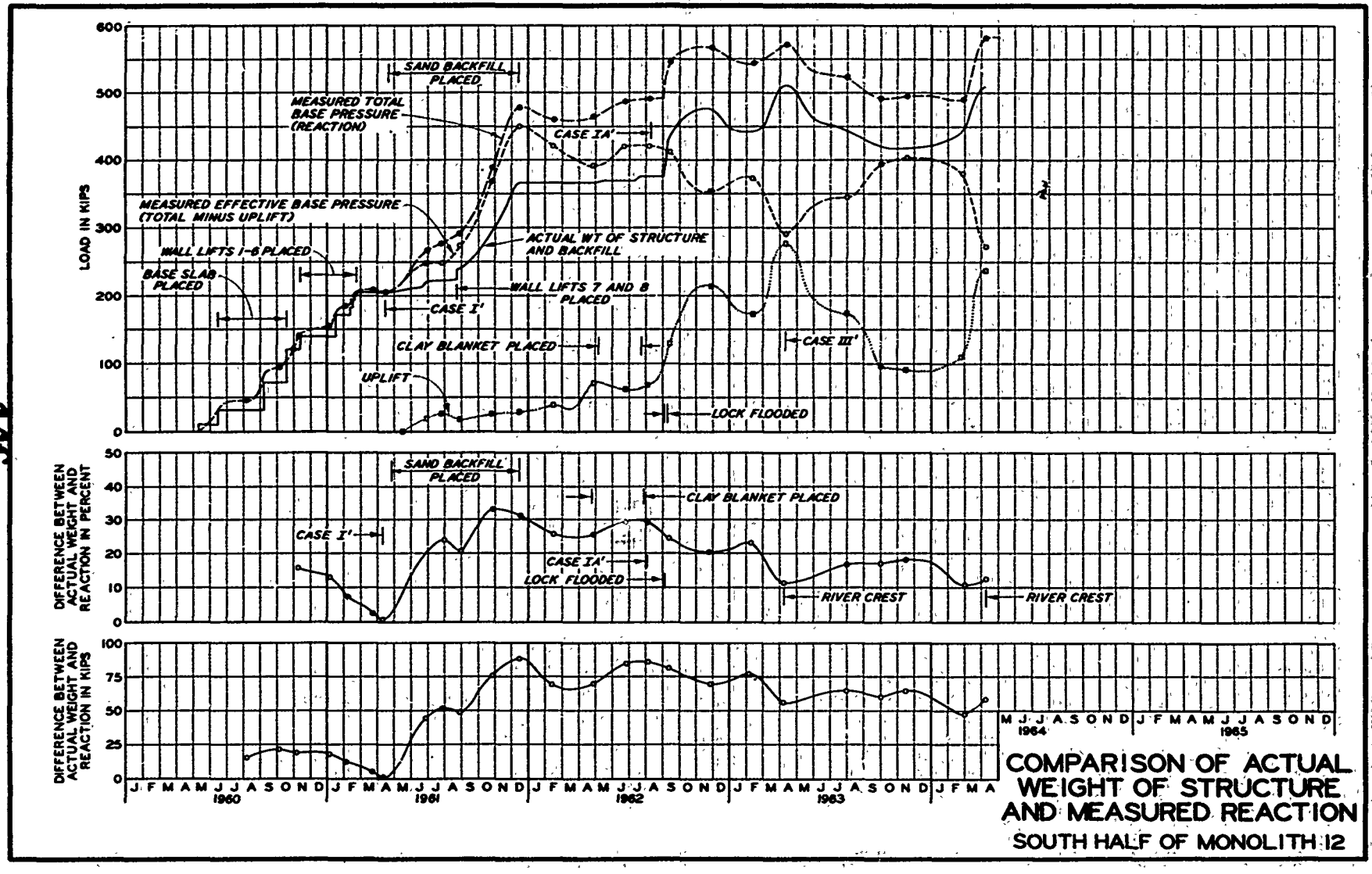

COMPARISON OF ACTUAL WEIGHT OF STRUCTURE AND MEASURED REACTION

SOUTH HALF OF MONOLITH 12

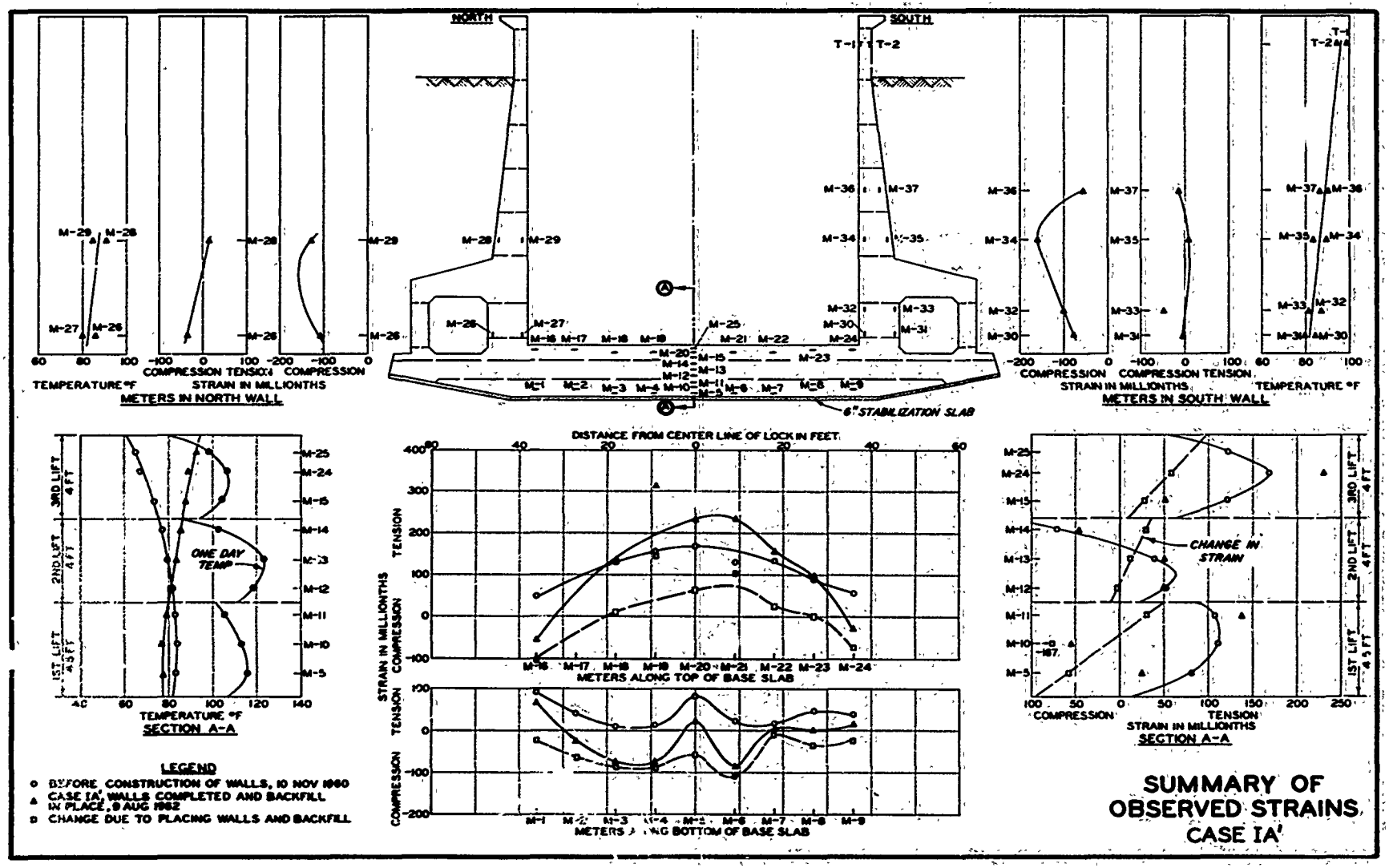
NORTH
SOUTH
T-1
T-2
M-29
M-28
M-27
M-26
M-25
M-24
M-23
M-22
M-21
M-20
M-19
M-18
M-17
M-16
M-15
M-14
M-13
M-12
M-11
M-10
M-9
M-8
M-7
M-6
M-5
M-4
M-3
M-2
M-1
M-37
M-36
M-35
M-34
M-33
M-32
M-31
M-30
6" STABILIZATION SLAB
TEMPERATURE °F
STRAIN IN MILLIONTHS
COMPRESSION TENSION
METERS IN NORTH WALL
METERS IN SOUTH WALL
3RD LIFT 4 FT
2ND LIFT 4 FT
1ST LIFT 4.5 FT
ONE DAY TEMP
SECTION A-A
DISTANCE FROM CENTER LINE OF LOCK IN FEET
TENSION
COMPRESSION
METERS ALONG TOP OF BASE SLAB
METERS ALONG BOTTOM OF BASE SLAB
CHANGE IN STRAIN
-187
LEGEND
BEFORE CONSTRUCTION OF WALLS, 10 NOV 1960
CASE IA', WALLS COMPLETED AND BACKFILL IN PLACE, 9 AUG 1962
CHANGE DUE TO PLACING WALLS AND BACKFILL
SUMMARY OF OBSERVED STRAINS
CASE IA'

PLATE 65

PLATE 66

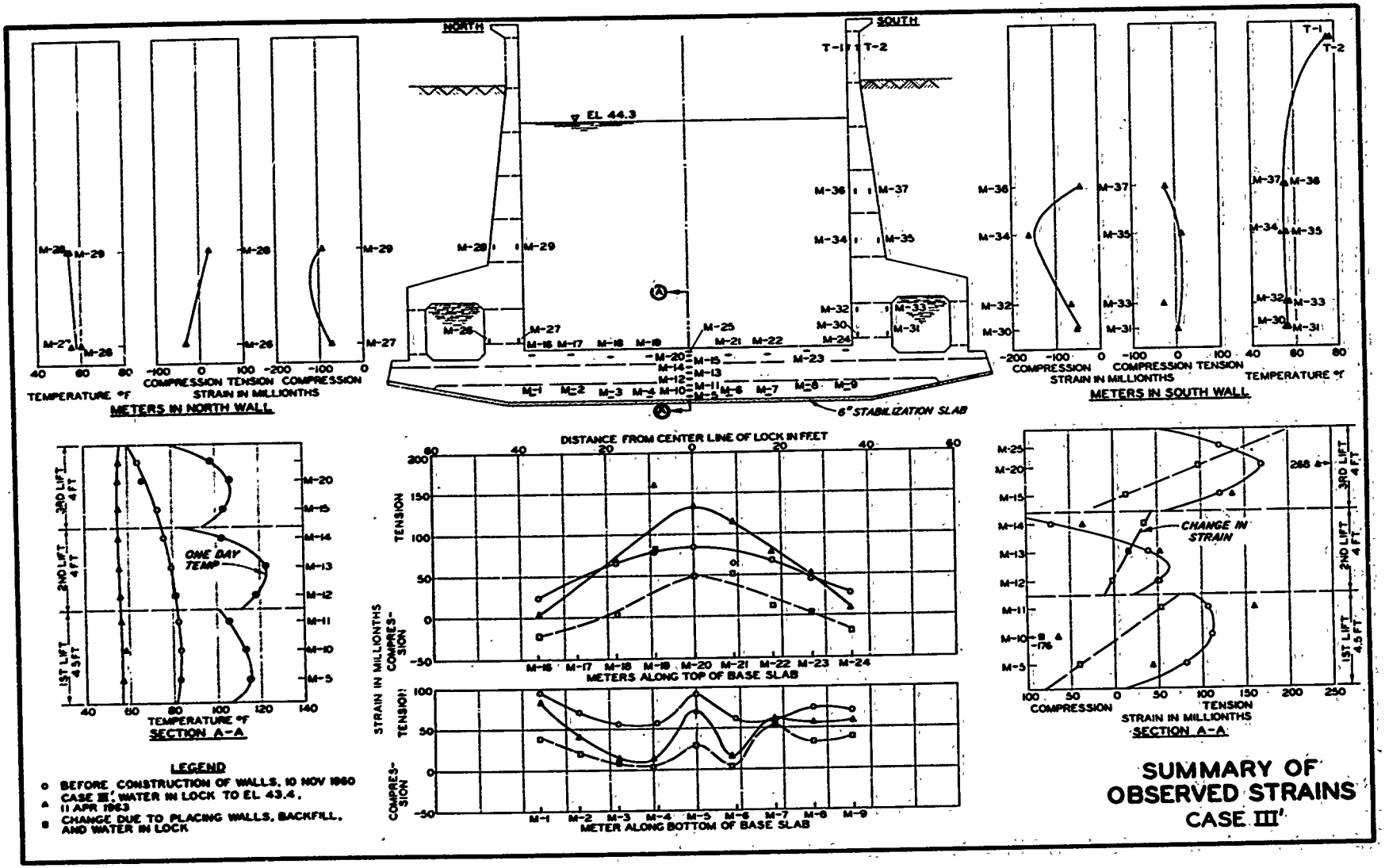
NORTH
SOUTH
EL 44.3
T-1
T-2
M-25
M-26
M-27
M-28
M-29
M-30
M-31
M-32
M-33
M-34
M-35
M-36
M-37
TEMPERATURE °F
COMPRESSION TENSION COMPRESSION
STRAIN IN MILLIONTHS
METERS IN NORTH WALL
COMPRESSION
COMPRESSION TENSION
METERS IN SOUTH WALL
6" STABILIZATION SLAB
3RD LIFT 4 FT
2ND LIFT 4 FT
1ST LIFT 4.5 FT
ONE DAY TEMP
SECTION A-A
DISTANCE FROM CENTER LINE OF LOCK IN FEET
TENSION
COMPRESSION
STRAIN IN MILLIONTHS
METERS ALONG TOP OF BASE SLAB
METER ALONG BOTTOM OF BASE SLAB
CHANGE IN STRAIN
288 Δ
-176
LEGEND
BEFORE CONSTRUCTION OF WALLS, 10 NOV 1960
CASE III', WATER IN LOCK TO EL 43.4, 11 APR 1963
CHANGE DUE TO PLACING WALLS, BACKFILL, AND WATER IN LOCK
SUMMARY OF OBSERVED STRAINS
CASE III'

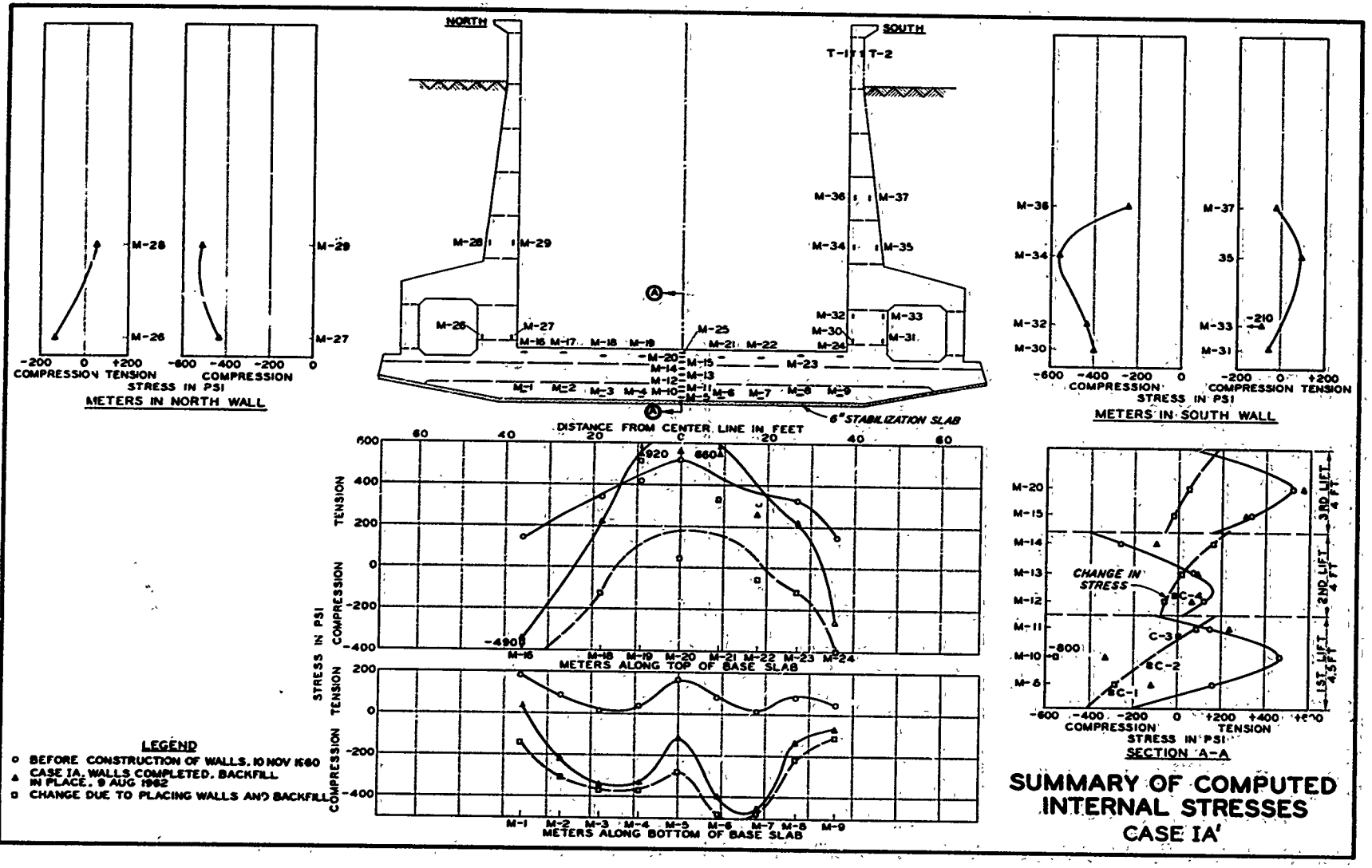

SUMMARY OF COMPUTED INTERNAL STRESSES CASE IA'

PLATE 67

PLATE 68

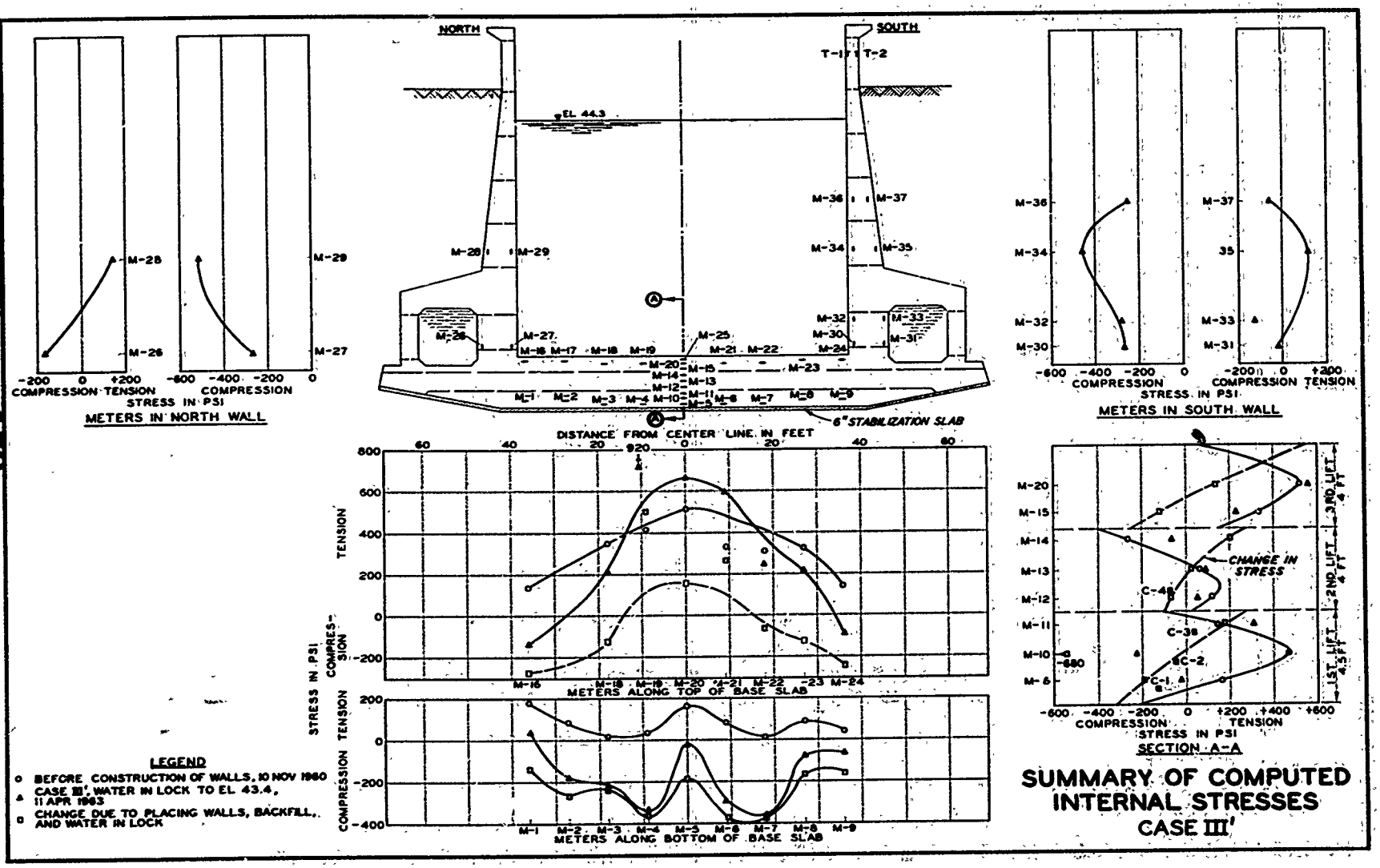

LEGEND

- ○ BEFORE CONSTRUCTION OF WALLS, 10 NOV 1960
- ▲ CASE III', WATER IN LOCK TO EL 43.4, 11 APR 1963
- □ CHANGE DUE TO PLACING WALLS, BACKFILL, AND WATER IN LOCK

SUMMARY OF COMPUTED INTERNAL STRESSES CASE III'

150

APPENDIX A: DESCRIPTION, CALIBRATION, AND INSTALLATION OF ELECTRICAL MEASURING DEVICES AND WALL DEFLECTION PIPES

Electrical Measuring Devices

1. Electrical measuring devices consisted of soil stress meters, strain meters, a pore pressure cell, and resistance thermometers obtained from Dr. R. W. Carlson, Berkeley, Calif.,[10*] and WES earth pressure cells fabricated at WES. Detailed descriptions of the Carlson devices are presented in reference 10. Calibration data for the various types of Carlson measuring devices were furnished by Dr. Carlson. All devices were checked at WES for leakage, and additional calibration tests were performed on a number of the devices as an independent check, the results therefrom being compared with the original data. Complete calibration tests were also performed on the WES pressure cells, and the results are presented herein.

2. Each of the electrical measuring devices had the required length of cable attached. Cable consisted of Spiral-4 communications cable, having four No. 18 stranded conductors, a foil shield, neoprene jacket, and a steel basket-weave braid. This type of cable was used because of its ability to resist rough treatment.

Carlson soil stress meters

3. Carlson soil stress meters, series PE-50, which measure stress to the nearest 0.2 psi within the range of 0 to 50 psi in compression, were used. Photographs of the Carlson soil stress meter are shown in fig. A1.

4. Calibration data furnished by Dr. Carlson for each meter are given in table A1. These data were based on a procedure in which various loads were applied through a rigid plate over the effective area of the meter. However, it was believed that field loading conditions would

---

* Raised numbers refer to similarly numbered items in the Literature Cited at the end of the main text.

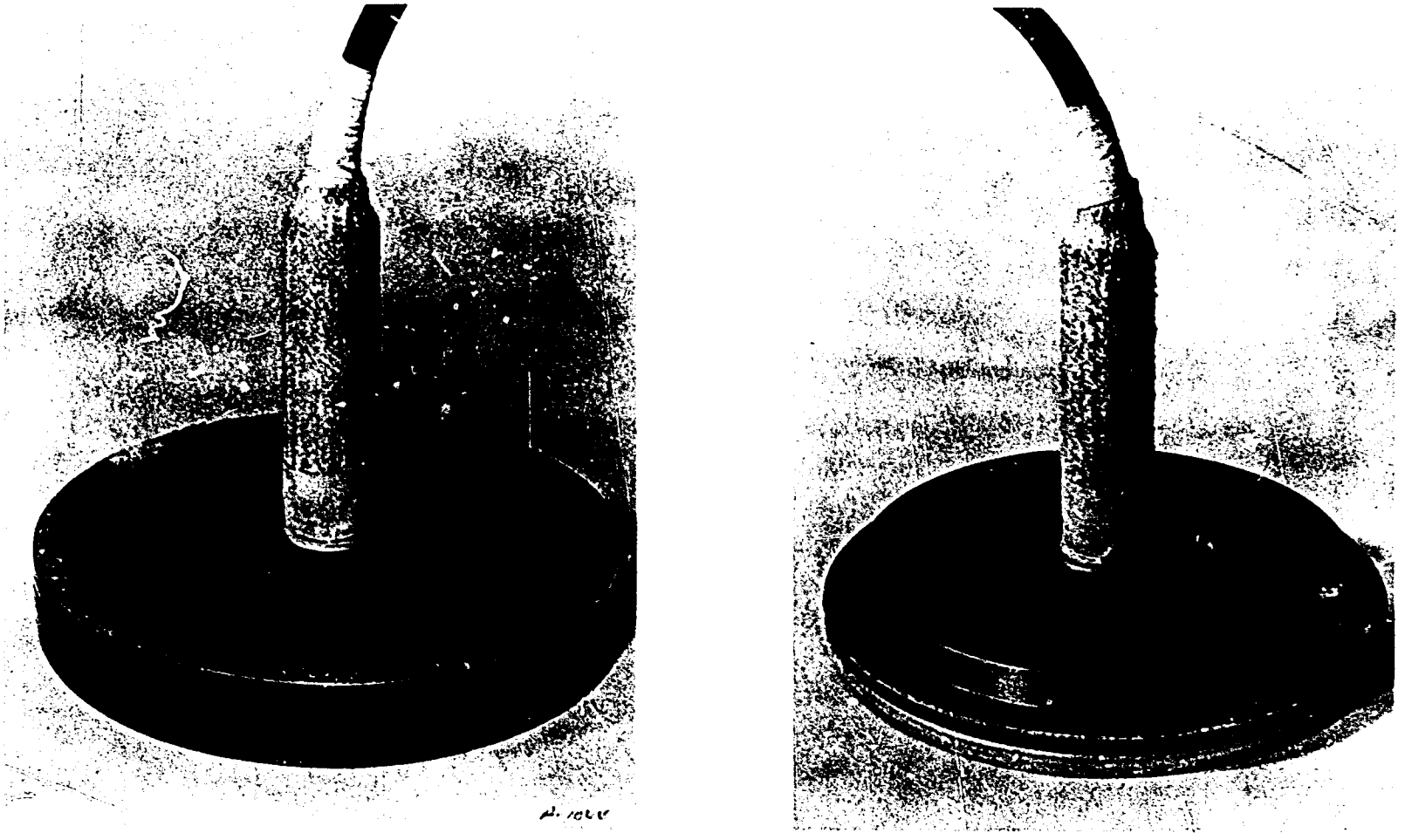

a. As installed

b. Cork and tape removed

Fig. A1. Carlson soil stress meter

be simulated more closely if the calibration loading were applied as a uniform pressure through a flexible diaphragm. Consequently, all soil stress meters were further calibrated at WES by means of diaphragm loading. The soil stress meters were further calibrated at WES by means of hydrostatic loading. The procedures used in the three types of load calibration are shown schematically in fig. A2. The difference between

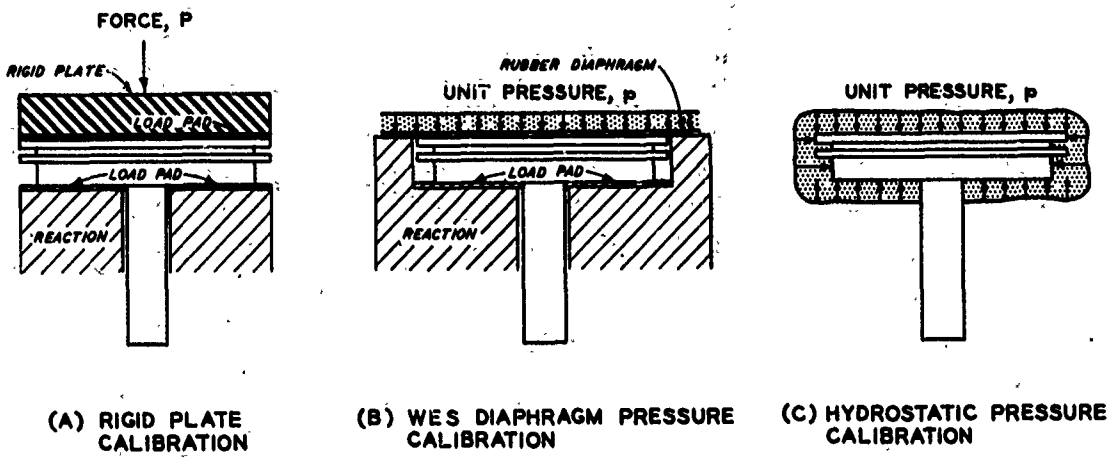

Fig. A2. Methods used in calibrating Carlson soil stress meters

hydrostatic and diaphragm loadings is that in the diaphragm loading the load is distributed uniformly over the entire faceplate, whereas in the hydrostatic loading, the load acting on the face is partially balanced by reaction components existing in the peripheral slot. Direct loading through the diaphragm corresponds to loading in the field under total pressure (intergranular plus hydrostatic pressures). The hydrostatic calibrations were performed to permit computation of intergranular pressures acting on the face of the meter.

5. Leak tests and hydrostatic calibration. When received at WES, the soil stress meters were placed in a pressure chamber for leak tests and calibration under hydrostatic pressure. The resistance ratio was determined at 0- and 40-psi pressure, with the total resistance of the meter observed for each load. The meter was subjected to an air pressure of 40 psi overnight (about 16 to 18 hr), and the resistance ratio and meter resistance were observed again. If the meter did not leak (no change in resistance ratio), it was then calibrated under a hydrostatic

pressure. The meter was loaded in 10-psi increments to a maximum pressure of 40 psi, then unloaded in 10-psi decrements. The resistance ratios were recorded for each pressure. After calibration, the meter and entire length of cable were immersed in water and subjected to a hydrostatic pressure of 40 psi for about 24 hr. The resistance ratio and total resistance of the meter were read before and after the pressure was applied and before and after the pressure was released. The meter insulation and cable insulation were also checked.

6. When received in the WES laboratory, the periphery of each stress meter was covered with tape (see fig. A1). This tape was removed before leak testing and hydrostatic calibration and was afterwards replaced by a 1/16-in.-thick strip of cork held in place by electrician's plastic tape. It was considered that the tape supplied with the meters was not sufficiently rigid to prevent entrance of concrete into the indentation formed by the peripheral groove, and it was also felt that the porosity of the cork would allow entrance of water into the groove and thus provide a true hydrostatic pressure on the loading diaphragm.

7. Load calibration of diaphragm. In the diaphragm pressure calibration method, a uniform pneumatic pressure was applied in a chamber to the face of the stress meter through a single rubber diaphragm. The back of the stress meter was supported by a cork load pad on an accurately machined steel reaction plate forming part of the chamber. The meters were calibrated by applying pressures in the following sequence: (a) during the first cycle of loading, the pressures were increased in 10-psi increments to a maximum load of 40 psi and then decreased in 10-psi decrements to 0; (b) for the next two cycles, the pressures were increased in 10-psi increments to 40 psi, then decreased from 40 to 0 psi. The calibration curves for each meter were plotted using the average value obtained for increasing pressures. Calibration constants were computed based on the average slope of the curve for increasing values.

8. Comparison of calibration constants. Calibration constants furnished by Dr. Carlson are shown in table A1. These calibration

constants were corrected for the resistance of the attached cables using the following equation:

$$C' = C + \frac{YC(0.89)}{R} \qquad \text{(A1)}$$

where

C' = corrected calibration constant, psi/0.01 percent change in resistance ratio

C = original calibration constant, psi/0.01 percent change in resistance ratio

Y = resistance in ohms of a pair of leads = 0.013 × cable length, ft

R = meter resistance in ohms at 0 F

9. The corrected calibration constants varied between 102 and 109 percent of the calibration constants determined by WES. The differences were insignificant, and in subsequent calculations, the WES values were used. The hydrostatic calibration constants determined by WES were greater than the calibration constants furnished by Dr. Carlson or those determined using the WES diaphragm loading calibration method. A conservative estimate was made of the required lengths of cable for each meter. Consequently, when the terminal leads were installed in the instrumentation houses and it became necessary to shorten the cable, the calibration constants were revised to take into account the shortening of the cables.

Carlson strain meters

10. Thirty-eight Carlson strain meters, series SA-10, were obtained initially; one of these served as a replacement in case any of the 37 other meters should be damaged or become inoperative prior to installation. These meters can measure strains between 400 millionths in expansion and 800 millionths in contraction. In addition, the two meters that were used as spares for the Port Allen Lock instrumentation program were used at Old River Lock as no-stress strain meters. A Carlson strain meter is shown in fig. A3. A detailed description of the meter is given in reference 10.

11. After they were received at WES, the strain meters were placed

Fig. A3. Carlson strain meter; complete assembly (top), assembly with fabric cover removed (middle), and assembly with flexible brass cover tube removed (bottom)

in a pressure chamber and checked, both in air and in water, for cable-entry leaks and defective cable as previously described for soil-stress meters. The meters were also checked to ensure that the resistance ratio of the meter at zero strain fell near midrange of the resistance ratios furnished by Dr. Carlson. Of the 38 meters tested, four meters leaked and three developed low insulation resistance during leak tests. Two other meters showed low insulation resistance when checked just prior to installation. All defective meters were returned to Dr. Carlson for repair. The defects of the meters were found to be in the terminals, which were repaired without removing the meter covers; therefore, repairing the meters did not affect the calibration constants.

12. The calibration constants furnished by Dr. Carlson for each of the meters are given in table A2. These calibration constants were corrected for the resistance of the leads as previously described for the stress meters. The calibration constants were revised when it became necessary to shorten the cables.

Carlson concrete stress meters

13. Three concrete stress meters, series PC-800, with a range of 0 to 800 psi in compression were used. One additional meter was subsequently purchased to be used as a spare. A Carlson concrete stress meter is shown in fig. A4. The cork ring around the periphery of the meter is not shown in the photograph. All meters were checked at WES for leakage and low insulation resistance. One meter had a low insulation resistance when received at WES and was returned to Dr. Carlson for repair.

14. Equipment was not available at WES to check the calibration constants in the range of stresses expected, and the calibration

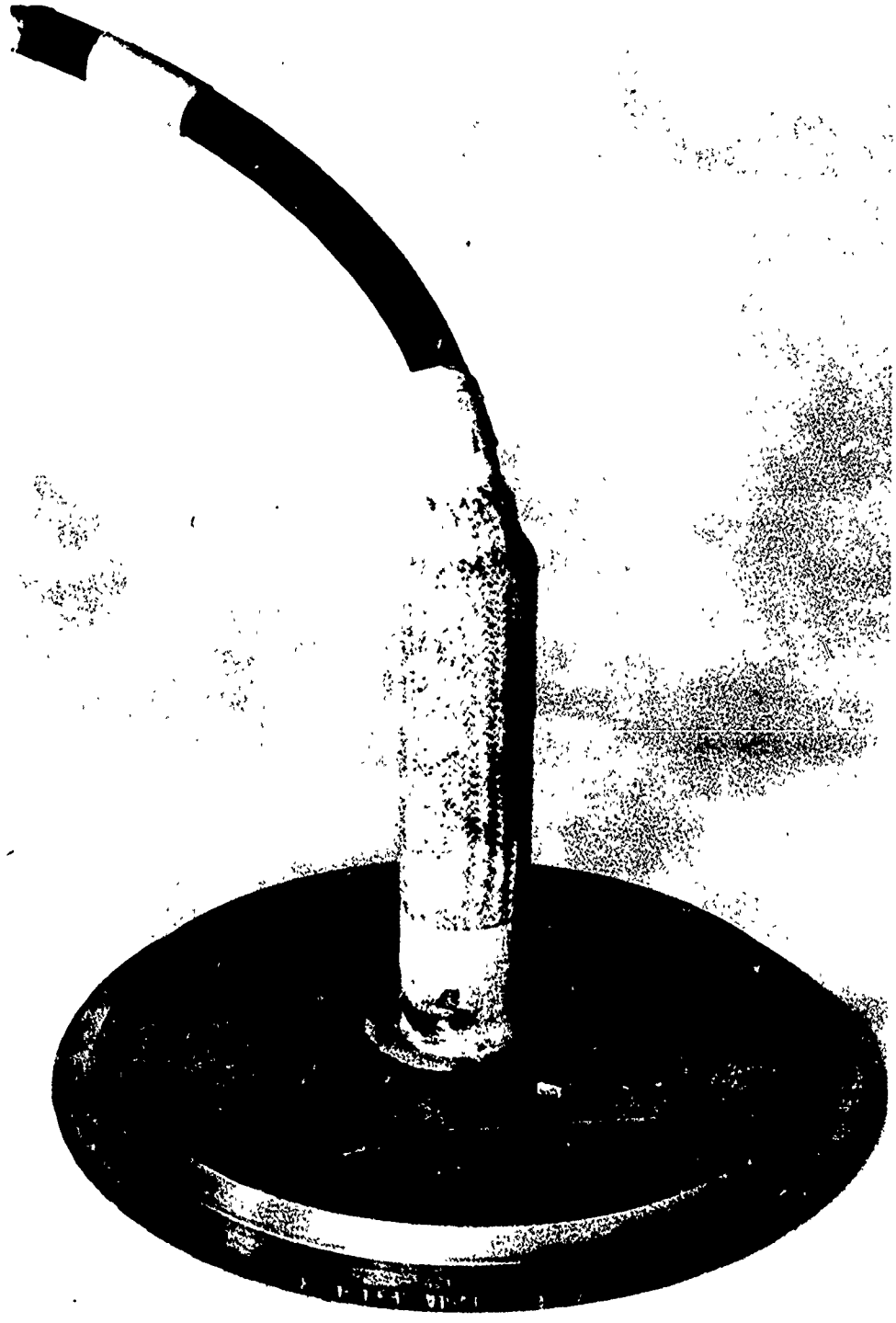

Fig. A4. Carlson concrete stress meter
(peripheral cork ring removed)

constants furnished by Dr. Carlson were accepted for use. The calibration constants furnished by Dr. Carlson are given in table A3 together with constants corrected for the effect of attached cables. The calibration constants were revised when it was necessary to shorten the cables.

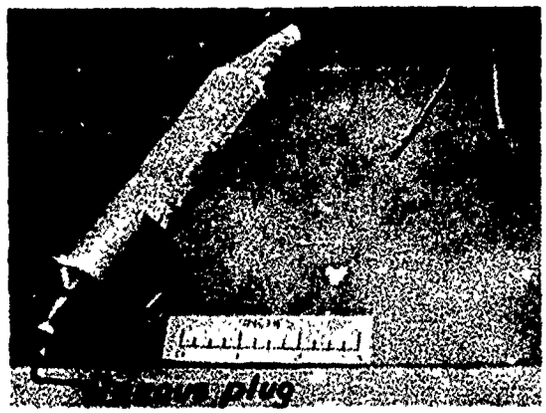

Fig. A5. Carlson pore pressure cell

Carlson pore pressure cell

15. A single Carlson pore pressure cell, series TP-50, was utilized. This device, which is used to measure pore pressure within the concrete, has a range from 0 to 50 psi. The cell (fig. A5) consists of a porous plug, steel diaphragm, and a strain meter unit.

16. After it was received at WES, the cell was checked for leakage and low insulation resistance and was found to be satisfactory. The calibration constant furnished by Dr. Carlson and corrected for resistance of the leads was 0.211 psi/0.01 percent (see table A3). The cell was recalibrated at WES, and a calibration constant of 0.214 psi/0.01 percent was obtained. The calibration constant was based on the average slope of the calibration curve for increasing pressure. Before calibration of the cell, the space between the porous plug and the diaphragm was filled with oil to reduce the time lag. After calibration, the cell was kept in an upright position to prevent the loss of oil. The WES calibration constant of 0.214 psi/0.01 percent was adopted for use.

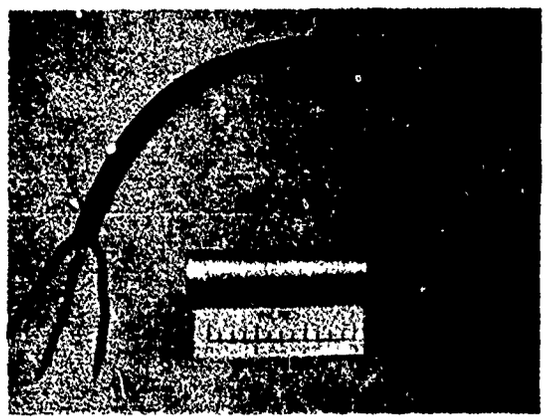

Fig. A6. Carlson resistance thermometer

Carlson resistance thermometers

17. Two resistance thermometers, Carlson type TM-1 (fig. A6), were used. The

resistance thermometer consists of a noninductively wound coil of enameled copper wire inside a brass case. Calibration data furnished by Dr. Carlson are given in table A3. The cable length has no effect on the calibration constant; therefore, it was not necessary to revise the calibration constant when the cables were shortened. The thermometers were checked at WES for leakage and loss of insulation and were found to be satisfactory.

WES earth pressure cells

18. Five WES pressure cells were provided for installation in the base slab and walls of the lock. The WES pressure cell (fig. A7) is a bonded strain-gage-type cell made of stainless steel; it measures stresses within a range of 0 to 50 psi. A detailed description of the device is given in a previously published WES bulletin.[15]

Fig. A7. WES earth pressure cell

19. The WES pressure cells were calibrated by applying pressure through a thin rubber diaphragm to the face of the cell and recording the resulting strain gage readings. As in the case of the soil stress meters, a difference exists between diaphragm and hydrostatic loadings because of hydrostatic pressures in the peripheral slot. Therefore, the cells were also calibrated under a hydrostatic load in the same manner used to calibrate the Carlson soil stress meter. Calibration constants are given in table A3.

Wall Deflection Pipes

20. Four wall deflection pipes were installed at Old River Lock

to measure wall deflections. The wall deflection pipes and deflectometer were designed and constructed at WES. The deflection pipes consist of 5-in.-ID pipe (with protruding contact points inside the pipe) set vertically in the lock wall. The deflectometer consists of a compound vise and dial gages to measure movement of a plumb bob attached to the vise. The deflection pipes and deflectometer used at Old River Lock were similar to those used at Port Allen Lock, which are described in detail in reference 7, except for the following features:

a. The wall deflection pipes are joined by flange connections instead of couplings.

b. The deflectometer for Old River Lock contains a built-in battery-powered indicator.

Details of the deflectometer and deflection pipes used at Old River Lock are given in reference 3.

Installation of Devices

21. Electrical measuring devices and wall deflection pipes were installed essentially as outlined in reference 3. Departures from the described procedures were found to be necessary in some instances, and the revised procedures together with photographs and pertinent features of the installation are presented below. The actual locations of all electrical devices and wall deflection pipes are also described.

Carlson soil stress meters and WES pressure cells beneath base slab

22. The soil stress meters and WES pressure cells beneath the structure were installed in recesses formed in the 6-in.-thick stabilization slab. The stabilization slab consisted of essentially the same concrete as used for the overlying structure, but did not contain reinforcing steel. At positions shown in fig. A8, 4-ft-square recesses were formed in the stabilization slab for installation of the meters. Where a WES pressure cell was to be installed adjacent to a stress meter, a 4- by 6-ft recess was provided in the stabilization slab. Prior to placement of the stabilization slab, the portion of the foundation on

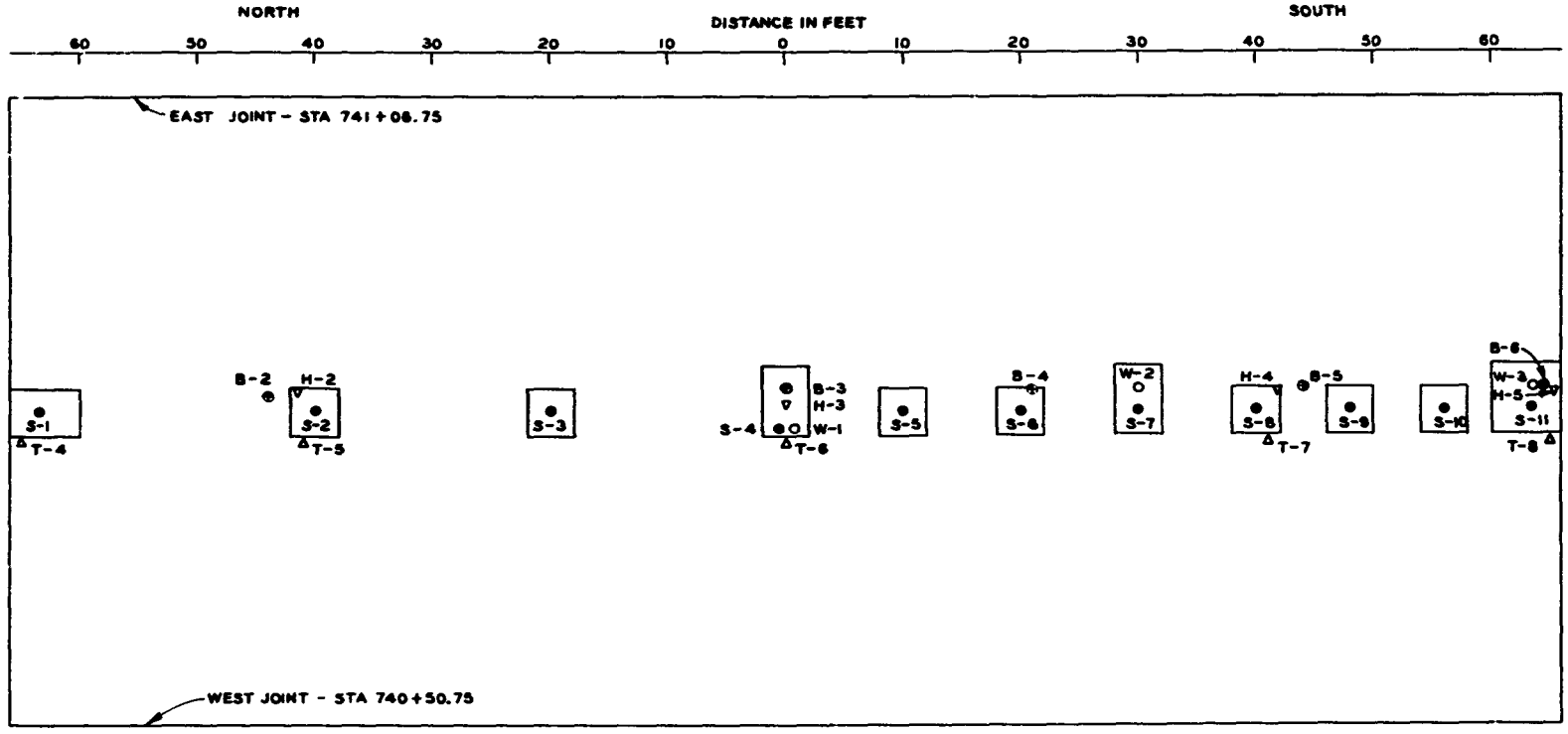

All

LEGEND

- ● CARLSON SOIL STRESS METER
- ○ WES PRESSURE CELL
- ◉ PIEZOMETER
- ▽ HEAVE POINT
- △ TEMPORARY SETTLEMENT POINT

NOTE: THE LOCATIONS OF SEVERAL DEVICES DIFFER FROM THAT SHOWN IN INSTRUCTION REPORT NO. 3. THE RELOCATIONS WERE MADE IN THE FIELD WHEN IT WAS NOTED THAT THEY WOULD HAVE BEEN LOCATED TOO CLOSE TO SOME OF THE PIEZOMETERS AND HEAVE POINTS.

PLAN OF STABILIZATION SLAB

MONOLITH 15

Fig. A8. Locations of soil stress meters and pressure cells

which monolith 12 was to be constructed was excavated carefully to grade except for the recess areas, where about 1 ft of undisturbed foundation soil was left above grade in place. This was done to ensure that an undisturbed foundation surface would be left on a level corresponding to the bottom of the stabilization slab where the meters would be placed.

23. A view of the stabilization slab at monolith 12, showing the recessed areas prior to installation of the instruments, is shown in fig. A9. Just prior to installation of instruments, the sand within the recess was carefully removed by hand. Fig. A10 shows the method employed in leveling the undisturbed foundation surface at the bottom of the recess.

24. All of the meters were seated carefully on the foundation sands. The bedding and natural stratification of the undisturbed foundation sands were clearly visible after the recessed areas were trimmed to grade. A typical recess (for meter S-6) is shown in fig. A11. Organic material interbedded in the sand was found at grade in the recesses for meters S-5 and S-7. The bottoms of these recesses were trimmed by hand, and the meters were relocated where necessary in order that they could be placed only on undisturbed material. The organic deposit in the recess for meter S-7 is shown in fig. A12. As shown in this figure, S-7 was placed on the sand foundation away from the organic deposit. In the case of WES pressure cells, cylindrical holes the same diameter as the cells and 1/4 in. deep were carefully excavated, and the meters were seated in the excavated holes. Some difficulty was encountered in maintaining the vertical sides of the holes during placement. All Carlson soil stress meters were placed directly on the bottom of the recess except for meters S-A and S-B, which were installed below grade to determine the effects of protrusion below the slab on the meter readings. Soil stress meters S-A and S-B were seated in excavated holes 1/4 in. and 3/4 in. below the base of the stabilization slab, respectively. Figs. A13-A17 show the instruments after they were seated on the bottoms of the recesses and before concrete was placed in the recesses. After the meters were placed in the recesses, the recesses were filled with concrete similar to that used for the stabilization slab.

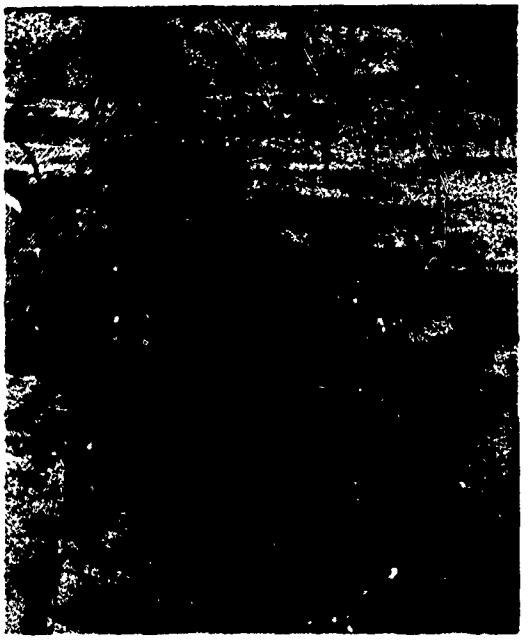

Fig. A9. Top of stabilization slab of monolith 12 prior to hand excavation of foundation sands from recessed areas reserved for installation of instruments

Fig. A10. Final trimming of bottom of recess

Fig. A11. Recess for soil stress meter S-6

Fig. A12. Soil stress meter S-7 in place prior to placement of concrete in recess. Note pocket of organic material exposed in recessed area

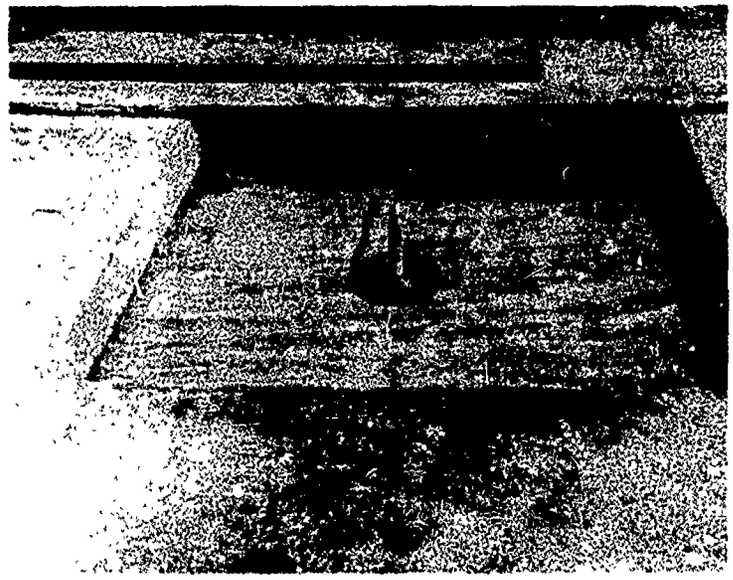

Fig. A13. Soil stress meter S-2 in place prior to placement of concrete in recess

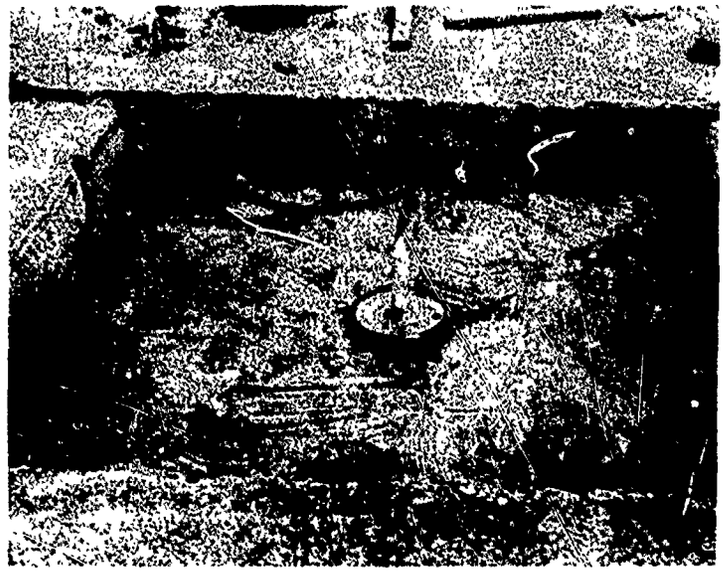

Fig. A14. Soil stress meter S-10 in place prior to placement of concrete in recess

Fig. A15. Soil stress meters S-3 and S-B in place prior to placement of concrete in recess

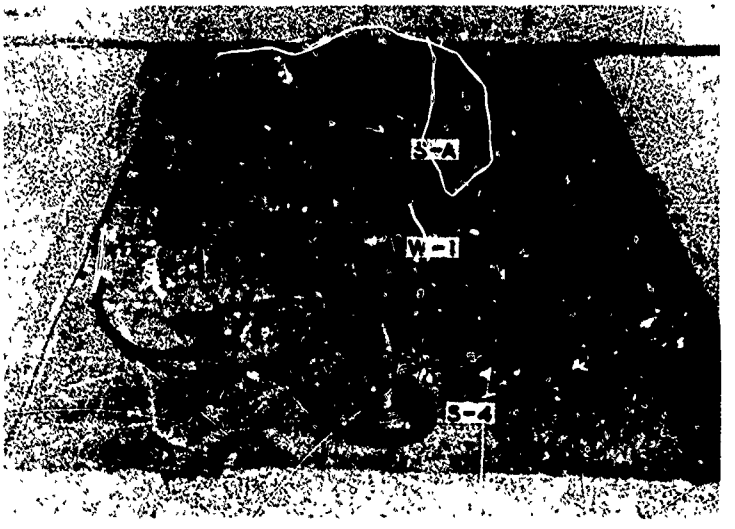

Fig. A16. Soil stress meters S-A and S-4 and WES pressure cell W-1 in place prior to placement of concrete in recess

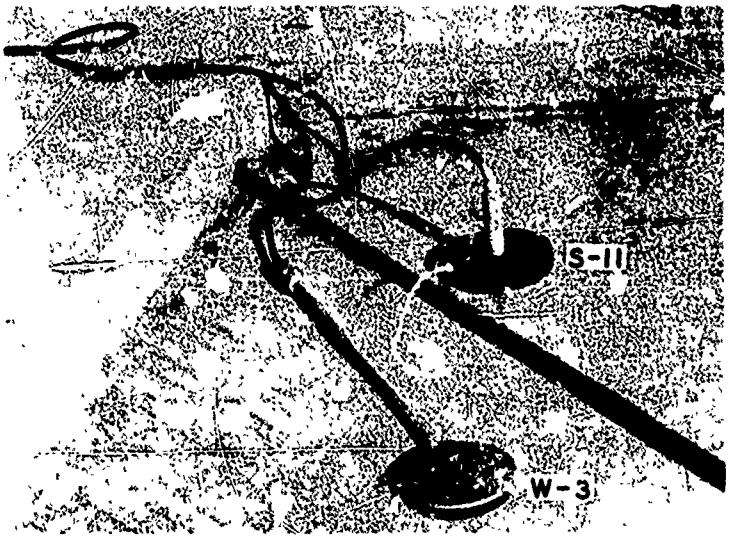

Fig. A17. Soil stress meter S-11 and WES pressure cell W-3 in place prior to placement of concrete in recess

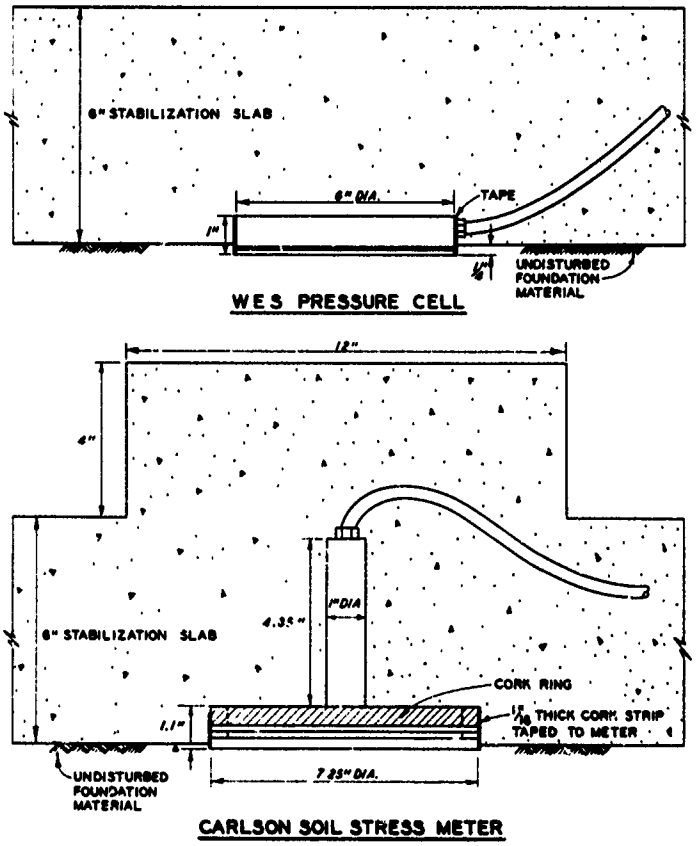

Fig. A18. Details of installation of devices in stabilization slab

The portion of the Carlson stress meter projecting above the top of the slab was encased in a 12- by 12- by 4-in. concrete block. Details of meter installations are shown in fig. A18. Cables from the meters were placed in formed recesses in the stabilization slab and were covered with concrete after all the meters were installed. Each instrument was read just before it was installed and also after the installation was completed. The actual locations of the meters as installed in the stabilization slab are given in table A4.

Carlson soil stress meters and WES pressure cells along the sides of walls

25. The stress meters and pressure cells on the backfill side of the lock walls and culvert were attached to the concrete forms so that after placement of the concrete and removal of the forms the acting faces of the devices were flush with the lock or culvert wall. The stress meters and pressure cells were attached to the forms as shown in fig. A19. The devices were centered between three clips to provide space for the concrete to enter on all sides of the meters. After the concrete had set and before the forms were removed, the bolts holding

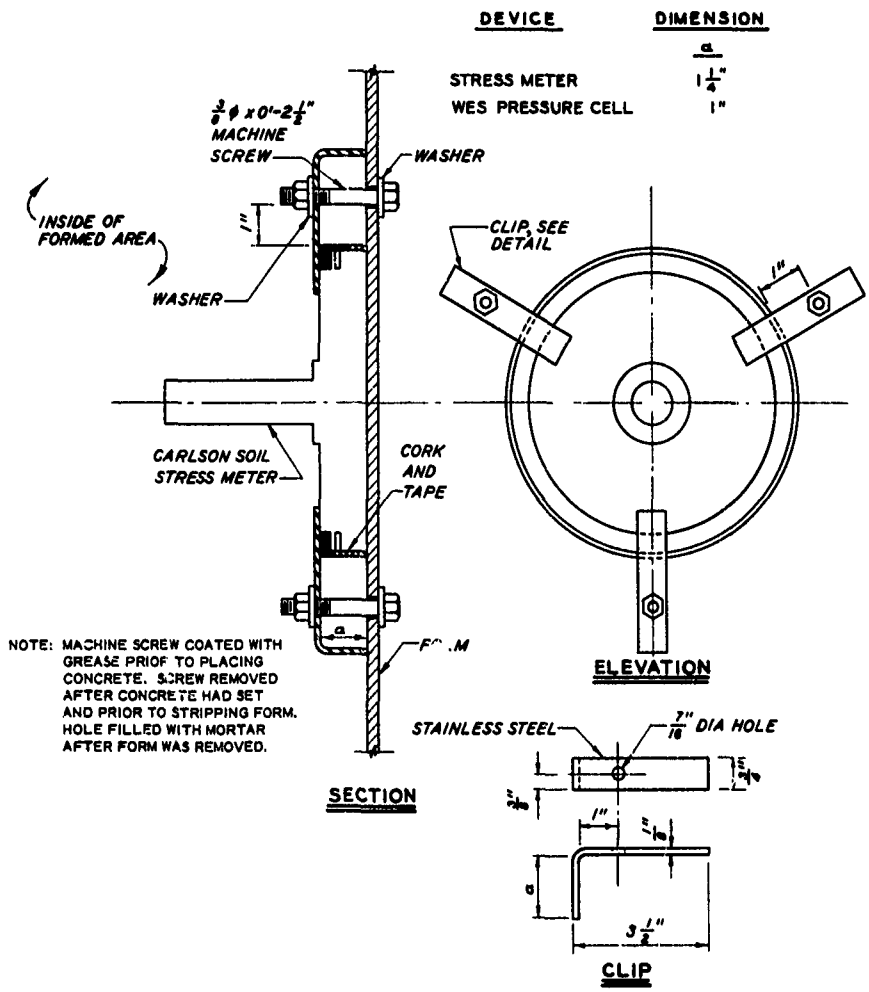

Fig. A19. Attachment of measurement devices to wall forms

the clips to the forms were removed. The holes left by the bolts were backfilled carefully with mortar after removing the forms. Installation data for the stress meters and pressure cells on the walls are given in table A4. A photograph of the installation of one of the devices (S-13) in the lock wall is shown in fig. A20.

26. Soil stress meter S-14 on the top of the culvert was attached to a 2- by 8-in. supporting timber in the same manner used to attach the meters in the walls to the wall forms. During placement of concrete, the timber was extended above the top of the culvert so that the face of the meter was at the same elevation and slope as the top of the culvert. About 3 hr after placement of concrete in the top lift of the culvert,

Fig. A20. Soil stress meter S-13 attached to inside of form prior to placement of concrete

the timber on which the meter was attached was removed, and the concrete in the vicinity of the face of the meter was finished. The bolts holding the clips were removed after the concrete had set, and the holes left by the bolts were filled with mortar. Photographs taken during the installation of stress meter S-14 are shown in fig. A21. A protective cover was placed over the meter until backfill was placed over the device.

27. The sand backfill immediately adjacent to the meters was placed in 4-in.-thick layers, each layer being compacted by hand tamping.

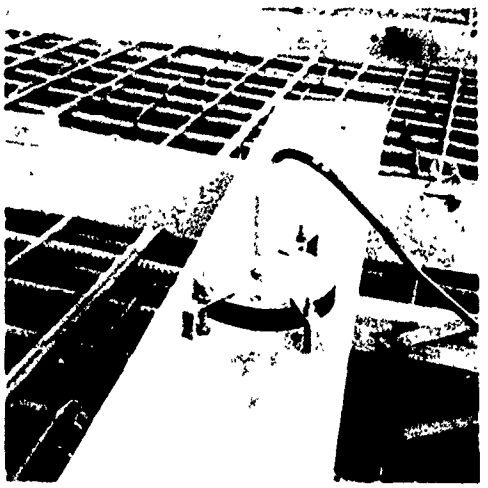

a. Soil stress meter S-14 attached to temporary timber support. Meter and support are in an inverted position

b. Timber support with soil stress meter S-14 attached in position prior to placement of concrete

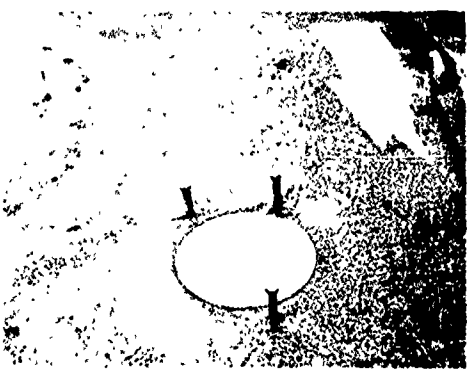

c. Acting face of soil stress meter S-14 after placement of concrete and removal of temporary timber support. Bolts attached to clamps were later removed and holes filled with concrete

Fig. A21. Installation of soil stress meter S-14 on top of south culvert

The remaining sand backfill close to the walls was placed in 8-in.-thick layers and compacted with vibratory compactors.

Installation of concrete
stress meters and pore pressure cell

28. The concrete stress meters and pore pressure cell were installed in the base slab at the center line of the lock with the face of each concrete stress meter vertical and parallel to the center line of the lock and the porous plug of the pore pressure cell facing upward. The locations of the three concrete stress meters and the pore pressure

cell were controlled by using three surveying instruments: two transits and a level. One transit was set up on the lock center line and the other on the station at which the instrument was to be installed. In addition to locating the three meters with surveying instruments, the proper alignment of the face plates also was checked. The concrete stress meters and the pore pressure cell were installed during concrete placement operations in concrete that had set sufficiently to support the instruments but not to such extent as would preclude working the concrete. Particular care was taken to see that the concrete was well vibrated by hand along the cable for pore pressure cell PP-1 for 3 to 4 ft from the cell. The locations of the concrete stress meters and the pore pressure cell are tabulated below:

Meter No.	Installation Location		Date Installed 1960
	Station	Elevation* ft msl	
C-1	97+00	-22.70	15 Jun
C-2	97+00	-21.35	15 Jun
C-3	97+00	-20.00	15 Jun
C-4	97+00	-18.00	8 Sep
FF-1	97+02	-20.50	15 Jun

* Elevation refers to center of face of meter.

Strain meters

29. All strain meters were checked prior to installation to ensure that they were set at approximately the midpoint of the potential strain range. All strain meters in the base slab were supported by brackets constructed of No. 2 bars welded to the reinforcing steel. Reinforcing bars were set vertically in the concrete to support strain meters M-5, -10, -11, -12, -13, -14, and -15. Details of the supports for the strain meters in the walls and in the base slab are shown in figs. A22 and A23, respectively. A dummy cylinder of wood of the same size and shape as the strain meter was used in the position of the meter while the bars were being welded in place. The bars were welded in place after the dummy cylinder was leveled and aligned properly.

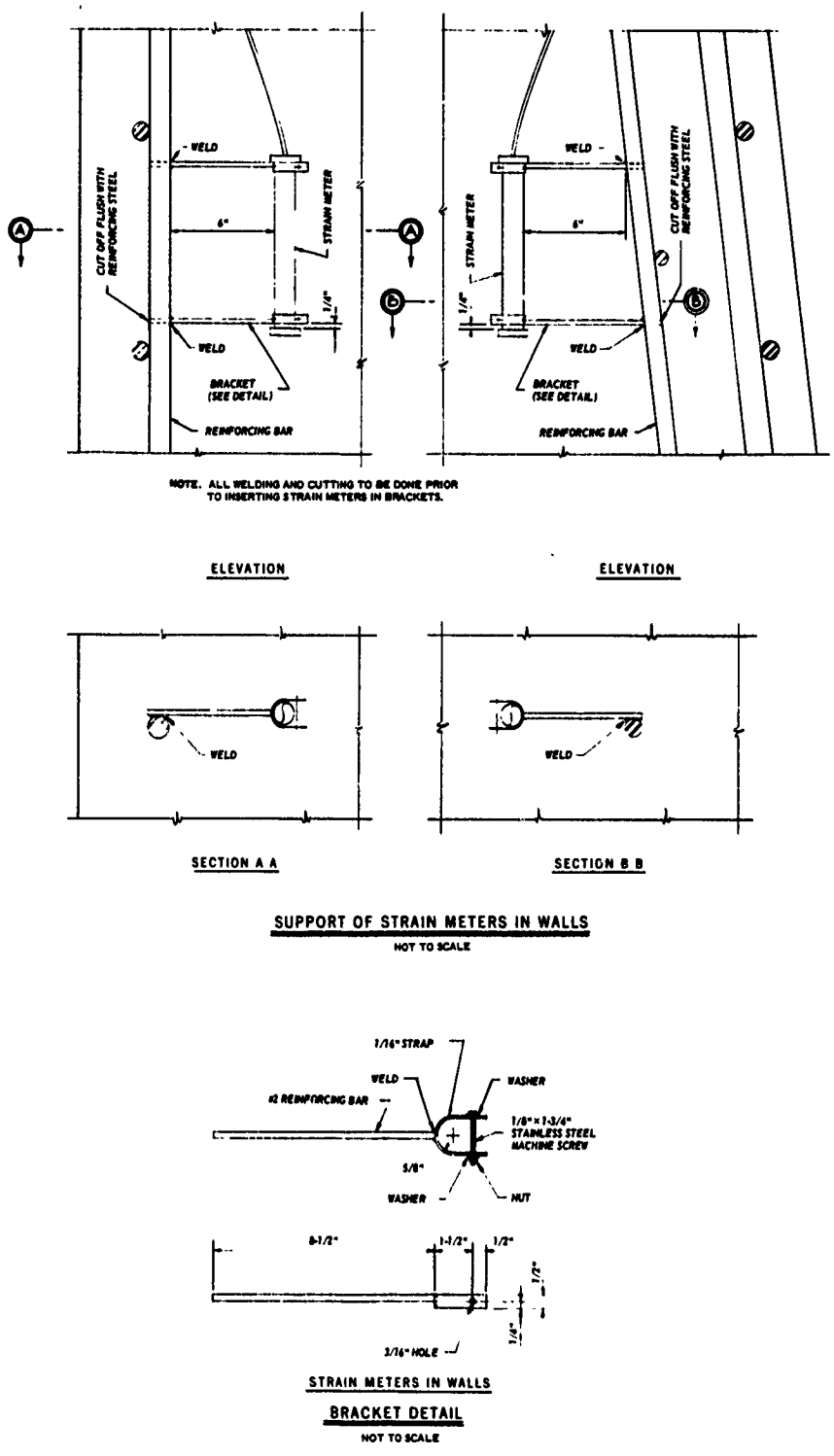

Fig. A22. Support for strain meters in wall

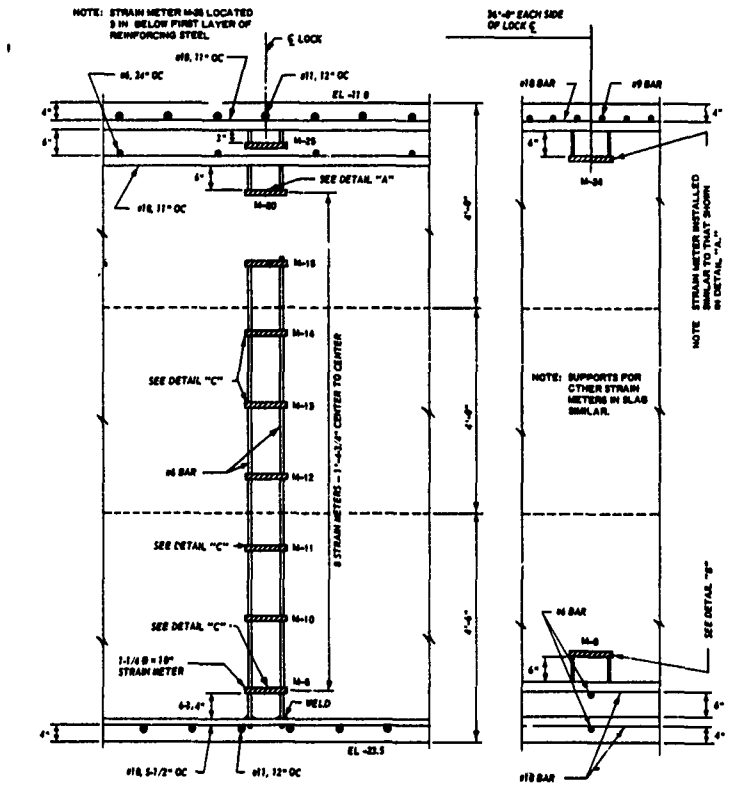

SECTION THROUGH BASE SLAB—MONOLITH NO 12

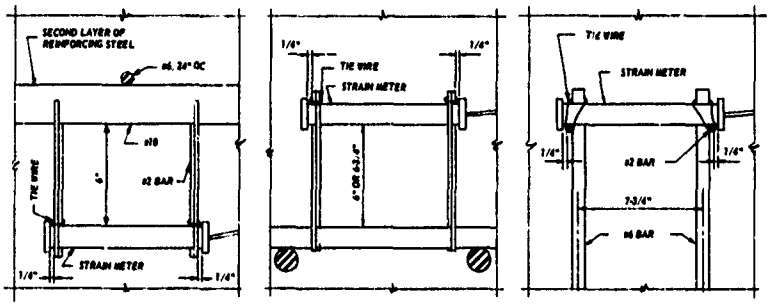

SECTION PERPENDICULAR TO CENTER LINE OF LOCK

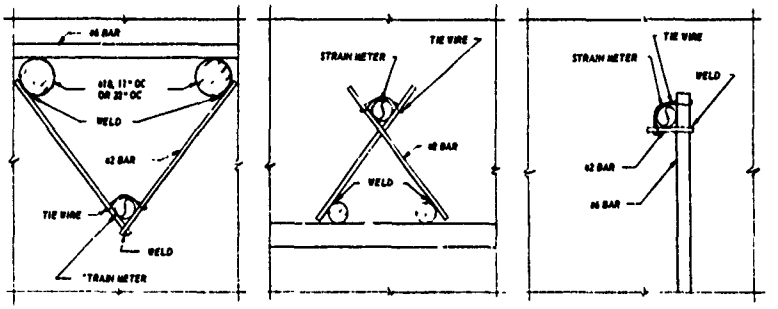

SECTION PARALLEL TO CENTER LINE OF LOCK

DETAIL "A" DETAIL "B" DETAIL "C"

NOT TO SCALE

Fig. A23. Support for strain meters in base slab

Photographs of strain meters attached to the reinforcing steel and in the base slab and walls of the structure prior to placement of concrete are shown in figs. A24-A27. Installation data for the meters are given in table A5.

30. Two "no-stress" strain meters (M-A and M-B) were also installed, one near the top of the base slab and one near the bottom of the base slab (see table A5). The purpose of these meters was to measure strains in the concrete that are independent of stresses. The meters were installed in a 19-in.-high, double-walled copper container having an outside diameter of 10 in. and an inside diameter varying from 9.75 to 8.0 in. Details of the container are shown in fig. A28. It was considered that the container would isolate the strain meters from the deformations due to stresses in the concrete. Photoelastic analyses by Pant and Patil[16] indicated that in order for a meter to be free from stress, the distance from the top of the meter to the top of the isolated zone should be at least one-half the radius of the isolated zone. The "no-stress" meters at Old River Lock were placed 4 in. below the top of the "no-stress" container in order that the meters would not be affected by external stresses. Fig. A29 shows strain meter M-A installed in a "no-stress" container near the bottom of the base slab prior to placement of concrete.

Resistance thermometers

31. The two resistance thermometers were fastened securely in proper position by wires fastened to the reinforcing steel. Installation data for these instruments are as follows:

Meter No.	Station	Elevation of Center of Device, ft msl	Distance from Inside Face of Walls, ft	Date Installed 1961
T-1	97+00	60.50	0.37	16 Aug
T-2	97+00	60.50	2.75	16 Aug

Wall deflection pipes

32. Installation data for the wall deflection pipes are given in table A6. Deflection pipes DP-1 and DP-2, which were to be installed at

Fig. A24. Strain meter M-2 near bottom of base slab prior to placement of concrete

Fig. A25. Strain meter M-15 near top of base slab prior to placement of concrete

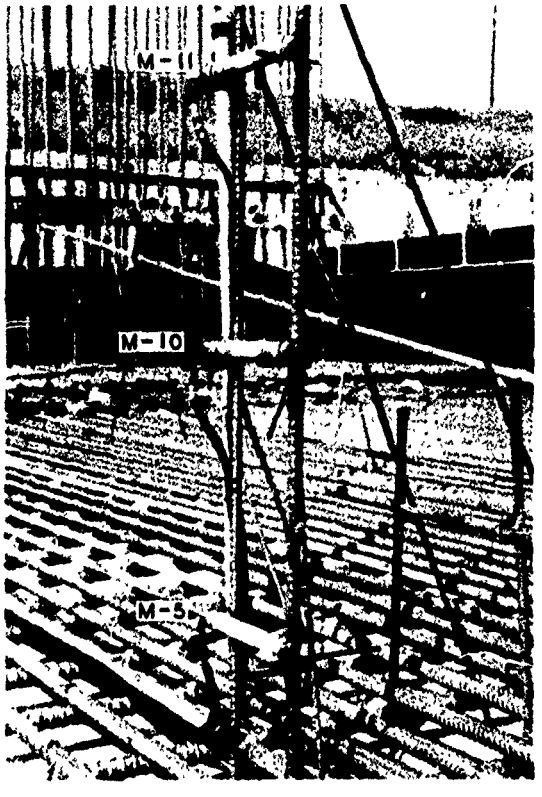

Fig. A26. Strain meters M-5, M-10, and M-11 in base slab prior to placement of concrete

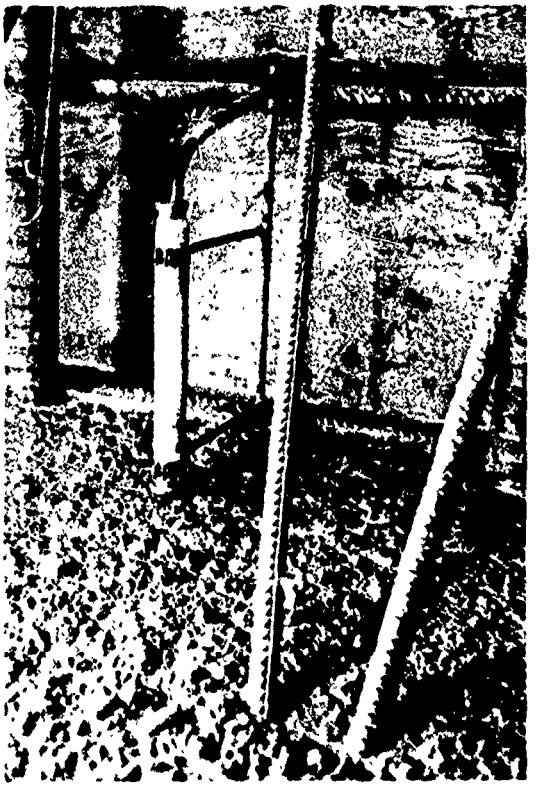

Fig. A27. Strain meter M-33 near inside face of culvert in south wall during concrete placement

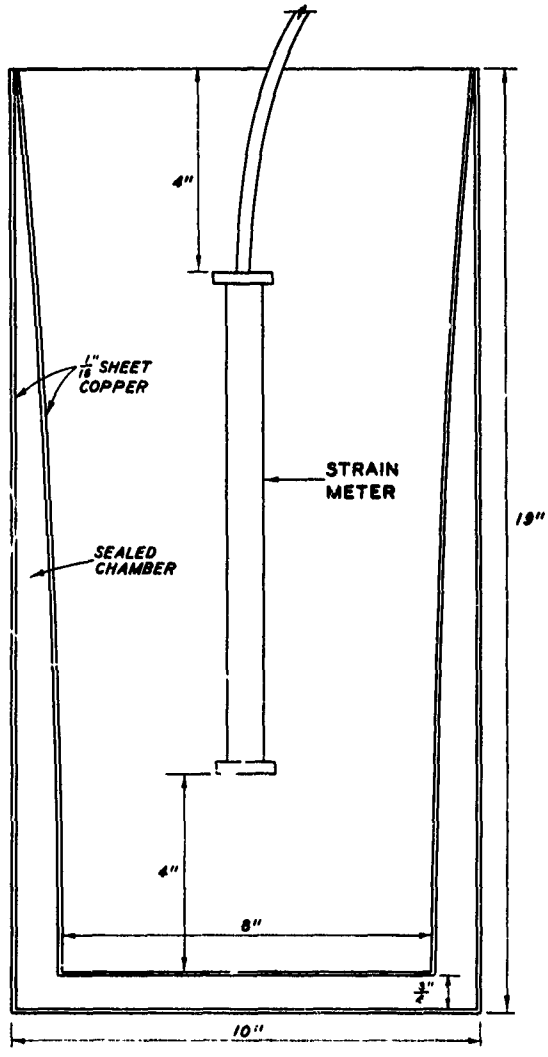

Fig. A28. Details of "no-stress" container

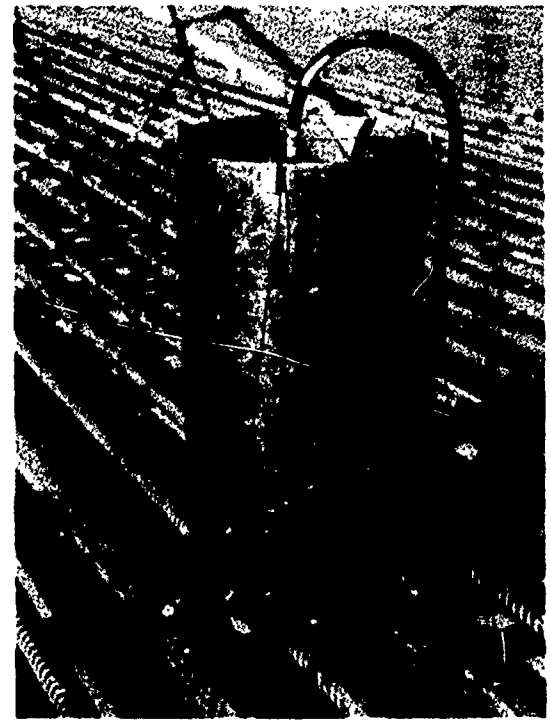

a. Side view

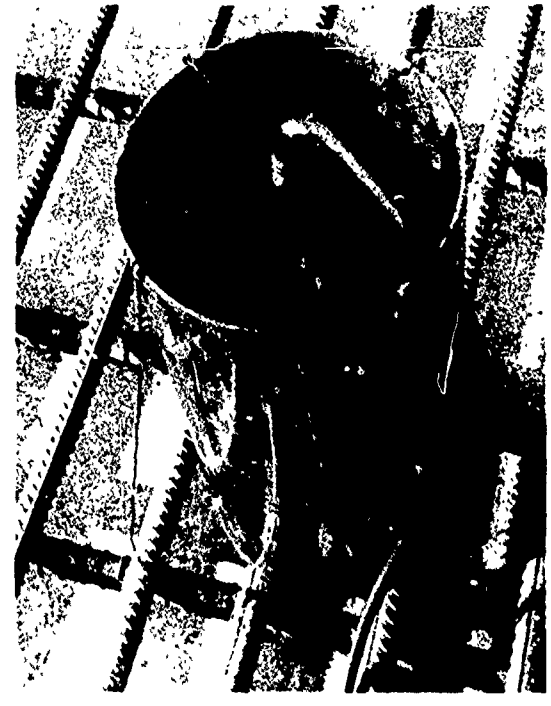

b. Top view

Fig. A29. Strain meter M-A in "no-stress" container near bottom of base slab, prior to placement of concrete

stas 90+33 and 91+23, respectively, were actually installed at stas 90+32.75 and 91+21, respectively, in order to facilitate bracing of the pipes during installation. All pipes were installed with less than 1/2-in. maximum deviation from vertical. Since the wall deflection pipes were designed to measure the changes in vertical alignment of the walls within a range of ± 2 in., the installation of the pipes was considered satisfactory.

Table A1

Calibration Data for Carlson Soil Stress Meters

WES Meter No.	Carlson Meter No.	Cable Length ft	Data Furnished by Carlson: Calibration Constant C psi/0.01%	Calibration Constant C' psi/0.01%	Resistance at 0° F R_I ohms	Resistance Ratio at 0 psi, RR %	ΔRR % per 1° F Temp rise	WES Diaphragm Load Calibration: Calibration Constant C'_W psi/0.01%	RR at 0 psi %	Total Resistance R ohms	Computed Temperature °F	WES Hydrostatic Calibration: Calibration Constant C'_H	Total Resistance R ohms	Computed Temperature °F	RR at 0 psi %
S-1	2	206	0.171	0.177	60.77	103.2	0.0032	0.168	103.14	69.99	77.45	0.191	69.33	71.90	103.13
S-2	11	181	0.170	0.176	60.36	102.6	0.0026	0.164	102.56	69.18	74.09	0.184	69.68	73.29	102.58
S-3	5	196	0.155	0.161	60.56	104.4	0.0035	0.148	104.40	69.06	71.40	0.172	69.20	72.58	104.40
S-4	1	216	0.163	0.170	60.65	103.3	0.0035	0.160	103.24	69.85	77.26	0.180	69.20	71.82	103.23
S-5	3	206	0.153	0.159	60.44	102.8	0.0032	0.146	102.78	68.58	68.38	0.166	69.04	72.24	102.76
S-6	6	196	0.173	0.180	60.46	102.9	0.0030	0.168	102.78	69.03	71.99	0.189	69.72	77.78	102.82
S-7	7	191	0.167	0.178	60.62	102.6	0.0038	0.163	102.66	69.46	74.26	0.185	69.55	75.01	100.66
S-8	12	181	0.154	0.159	60.51	103.2	0.0028	0.148	103.22	69.44	75.01	0.170	69.45	75.10	103.22
S-9	8	186	0.161	0.167	60.41	103.1	0.0030	0.157	102.88	69.41	75.60	0.177	69.41	75.60	102.89
S-10	9	186	0.159	0.165	60.82	102.9	0.0028	0.159	102.73	69.93	76.52	0.178	69.79	75.35	102.73
S-11	4	206	0.165	0.172	60.32	102.2	0.0030	0.157	102.22	68.77	70.98	0.182	68.91	72.16	102.22
S-12	10	186	0.201	0.208	60.48	103.5	0.0026	0.195	103.42	69.66	77.11	0.222	69.29	74.00	103.44
S-13	13	180	0.155	0.160	60.17	104.4	0.0032	0.151	104.31	69.41	77.62	0.168	69.10	75.01	104.31
S-14	14	165	0.180	0.186	60.56	104.2	0.0034	0.175	104.29	69.58	75.77	0.197	69.47	74.34	104.28
S-15	15	150	0.155	0.159	60.26	103.5	0.0036	0.150	103.37	69.47	77.36	0.167	69.18	74.93	103.39
S-16	17	140	0.164	0.168	60.63	102.3	0.0034	0.160	102.26	69.97	78.46	0.182	69.53	74.76	102.25
S-17	18	130	0.144	0.147	60.37	103.5	0.0040	0.141	103.43	68.89	71.57	0.158	68.72	70.14	103.42
S-18	20	120	0.175	0.179	60.42	102.6	0.0024	0.172	102.61	69.33	74.84	0.195	69.45	75.85	102.62
S-19	16	150	0.151	0.155	60.43	103.7	0.0036	0.147	103.67	69.65	77.45	0.163	69.34	74.68	103.66
S-20	19	130	0.169	0.173	60.53	103.1	0.0025	0.16_	103.07	69.31	73.75	0.183	69.57	75.94	103.07
S-A	V-20	215	0.134	0.140	60.68	102.5	0.0036	0.138	103.38	69.53	74.34	0.157	69.21	71.65	103.38
S-B	A-2	175	0.139	0.145	60.54	101.9	0.0040	0.148	101.92	69.27	74.03	0.173	67.81	61.65	101.91

A27

Note: WES diaphragm load calibration performed by applying air pressure to the loading face of the meter by means of a rubber diaphragm.
WES hydrostatic calibration performed by applying a hydrostatic pressure to the meter while submerged underwater.
Calibration constant is the stress in psi required to reduce the resistance ratio by 0.01% (or one least reading on the test set).
C = calibration constant furnished by Carlson. The area used to determine the calibration constant was 42.0 sq in.
C' = calibration constant furnished by Carlson corrected for cable resistance.
C'_W = calibration constant obtained at WES using direct loading (cable resistance included).
C'_H = calibration constant obtained at WES using hydrostatic loading (cable resistance included).
R_I = meter resistance at 0° F. Meter resistance is the total resistance of the meter exclusive of conductor resistance. The meters are provided with 4-conductor cable which permits a direct determination of meter resistance.
R = meter resistance at a given temperature.
The temperature in °F is determined by subtracting R_I from the measured resistance, R, and multiplying by K_I (8.40 for all meters except S-B. K_I for S-B is 8.48).
The resistance ratio is measured directly by the testing set.
RR = approximate resistance ratio at 0 psi; ΔRR = change in resistance ratio in percent due to a temperature change in the meter.

Table A2

Calibration Data for Carlson Strain Meters

WES Meter No.	Carlson Meter No.	Cable Length, ft	Data Furnished by Carlson: Calibration Constant C	Calibration Constant C'	Resistance at 0° F R_I	Degree per ohm K_I	Range of Resistance Ratio, %	Approximate Resistance Ratio When Shipped, %	WES Acceptance Data: RR at 0 psi %	Total Resistance R, ohms	Computed Temp °F
M-1	A	175	3.78	3.92	55.93	8.58	97.3-102.8	101.1	101.15	63.87	68.13
M-2	X-12	190	3.87	4.03	52.42	9.34	97.2-103.5	100.6	100.61	60.39	74.44
M-3	X-8	200	3.84	4.01	52.50	9.32	97.8-104.1	101.2	101.08	60.91	78.38
M-4	X-3	210	3.85	4.03	52.46	9.33	97.0-103.4	100.2	100.29	60.74	77.25
M-5	X-1	215	3.87	4.05	52.50	9.32	97.1-103.5	100.5	100.56	60.80	77.36
M-6	X-4	210	3.87	4.05	52.53	9.32	97.2-103.5	100.9	100.92	60.82	77.26
M-7	X-9	200	3.84	4.01	52.40	9.34	97.2-103.2	101.1	101.41	60.02	71.17
M-8	X-13	190	3.87	4.03	52.43	9.34	97.4-103.7	101.2	101.14	60.40	74.44
M-9	X-17	180	3.85	4.01	52.51	9.32	98.1-104.4	101.6	101.51	60.60	75.40
M-10	X-2	215	3.91	4.10	52.47	9.33	97.2-103.5	100.7	100.73	60.78	77.53
M-11	X-5	210	3.89	4.07	52.53	9.32	96.5-103.7	100.4	100.40	60.84	77.45
M-12	X-6	210	3.87	4.05	52.52	9.32	97.9-104.1	100.7	100.67	60.93	78.38
M-13	X-34	210	3.90	4.08	52.33	9.36	97.0-103.1	100.1	101.21	60.36	75.16
M-14	X-35	210	3.90	4.08	52.46	9.33	96.9-103.2	101.1	101.41	60.03	70.63
M-15	X-36	210	3.90	4.08	52.37	9.35	97.1-103.3	101.1	100.94	60.16	72.84
M-16	X-20	170	3.87	4.05	52.34	9.30	97.3-103.4	100.7	100.74	60.32	74.21
M-17	X-18	180	3.88	4.04	52.37	9.35	97.8-104.1	101.2	100.97	60.42	75.27
M-18	X-14	190	3.87	4.03	52.58	9.31	96.5-102.8	100.3	100.27	60.58	74.48
M-19	X-10	200	3.86	4.03	52.38	9.35	97.4-103.7	100.7	100.63	60.81	78.82
M-20	X-7	205	3.87	4.05	52.34	9.36	97.7-103.9	102.1	102.00	60.74	78.62
M-21	B	175	3.72	3.85	56.12	8.55	97.2-102.7	100.8	100.83	64.20	69.08
M-22	X-15	190	3.89	4.05	52.60	9.31	97.3-103.6	100.9	100.96	60.60	74.48
M-23	X-19	180	3.91	4.07	52.34	9.36	97.6-103.5	101.3	101.14	60.41	75.63
M-24	X-21	170	3.90	4.05	52.76	9.28	97.0-103.1	100.0	99.87	60.49	71.73
M-25	X-37	205	3.90	4.08	52.38	9.35	96.0-102.3	100.1	99.57	60.15	72.65
M-26	X-22	170	3.92	4.07	52.29	9.36	97.8-104.1	101.3	101.83	59.93	71.51
M-27	X-25	160	3.88	4.02	52.73	9.28	97.4-103.5	100.4	100.33	60.44	71.55
M-28	X-28	145	3.83	3.95	52.60	9.31	97.0-103.2	100.3	100.29	60.58	74.29
M-29	X-30	140	3.84	3.96	52.53	9.32	97.3-103.4	100.9	100.95	60.10	70.55
M-30	X-26	160	3.91	4.05	52.67	9.29	97.3-103.4	100.4	100.38	60.38	71.63
M-31	X-23	170	3.86	4.00	52.50	9.32	98.1-104.3	101.2	101.05	60.32	72.88
M-32	X-27	155	3.89	4.02	52.53	9.32	97.3-103.5	100.6	100.62	60.49	74.19
M-33	X-24	165	3.85	3.99	52.57	9.31	97.1-103.4	103.4	99.88	60.43	73.18
M-34	X-31	140	3.86	3.98	52.64	9.30	97.3-103.5	100.6	100.51	60.61	74.12
M-35	X-29	145	3.84	3.96	52.52	9.32	96.8-103.1	100.4	100.36	60.48	74.19
M-36	X-33	120	3.86	3.96	52.53	9.32	97.7-103.9	100.8	100.72	60.01	69.71
M-37	X-32	125	3.84	3.95	52.64	9.30	97.4-103.6	101.0	101.47	60.20	70.31
M-A	H-1	215	3.76	3.94	52.97	9.95	96.7-102.5	99.9	99.93	60.57	75.62
M-B	X-16	200	3.87	4.03	52.44	9.34	97.5-103.7	100.9	101.01	60.25	72.95

Note: Definitions of terms are presented in table A1.

Table A3

Calibration Data for Miscellaneous Electrical Instruments

Device No.	Cable Length ft	Data Furnished by Carlson: Calibration Constant C	Calibration Constant C'	Resistance at 0° F R_I, ohms	Degrees per ohm K_I	Approximate RR at 0 psi, %	Mercury Thickness T, in.	Composition Thickness D, in.	80 T/D	RR Increase per °F Temp Rise	WES Calibration Data: Calibration Constant C'_W	Calibration Constant C'_H
Carlson Concrete Stress Meters												
C-1	210	5.75	5.97	60.57	8.40	103.1	0.011	0.575	1.5	--	--	--
C-2	210	5.45	5.67	60.09	8.40	104.1	0.011	0.575	1.5	--	--	--
C-3	215	5.75	5.98	60.31	8.40	103.3	0.010	0.570	1.4	--	--	--
C-4	215	6.00	6.25	60.49	8.40	102.6	0.008	0.575	1.1	--	--	--
Carlson Pore Pressure Cell												
PP-1	215	0.203	0.211	60.46	8.40	103.20	---	---	---	0.0045	--	0.214
Carlson Resistance Thermometers												
T-1	110	---	---	39.4	10.0	---	---	---	---	--	--	--
T-2	110	---	---	39.4	10.0	---	---	---	---	--	--	--
WES Pressure Cells												
W-1	215	---	---	--	--	---	---	---	---	--	0.0174	0.0213
W-2	180	---	---	--	--	---	---	---	---	--	0.0201	0.0253
W-3	205	---	---	--	--	---	---	---	---	--	0.0191	0.0238
W-4	150	---	---	--	--	---	---	---	---	--	0.0194	0.0227
W-5	140	---	---	--	--	---	---	---	---	--	0.0182	0.0212

Note: T is the thickness of mercury film, in.; D is the thickness of composition diaphragm, in.; and the value 80 T/D is used in the equation for temperature correction.
Definitions of other terms are presented in table A1.

Table A4

Installation Data for Carlson Soil Stress Meters and WES Pressure Cells

Meter No.	Station	Distance from ℄ ft	Elevation ft msl	Location	Date Installed
S-1	97+05	66.5 N	-18.90	Stabilization slab	11 May 60
S-2	97+05	36.2 N	-23.93	Stabilization slab	11 May 60
S-3	97+04	18.1 N	-23.94	Stabilization slab	11 May 60
S-B	97+06	18.1 N	-24.00	Stabilization slab	11 May 60
S-4	97+04	0	-23.94	Stabilization slab	11 May 60
S-A	97+08	0	-23.96	Stabilization slab	11 May 60
W-1	97+06	0.1 S	-23.96	Stabilization slab	11 May 60
S-5	97+05	9.8 S	-23.92	Stabilization slab	10 May 60
S-6	97+05	18.0 S	-23.90	Stabilization slab	10 May 60
S-7	97+05	25.9 S	-23.92	Stabilization slab	10 May 60
S-8	97+05	36.1 S	-23.87	Stabilization slab	10 May 60
W-2	97+07	36.1 S	-23.89	Stabilization slab	10 May 60
S-9	97+05	46.1 S	-23.01	Stabilization slab	10 May 60
S-10	97+05	56.2 S	-21.01	Stabilization slab	10 May 60
S-11	97+05	65.9 S	-19.05	Stabilization slab	10 May 60
W-3	97+07	66.1 S	-19.03	Stabilization slab	10 May 60
S-12	97+05	--	-06.33	South wall	11 Nov 60
S-13	97+05	--	+01.00	South wall	16 Jan 61
S-14	97+05	54.6 S	+06.93	Top of culvert, south wall	16 Jan 61
S-15	97+05	--	+12.57	South wall	11 Feb 61
W-4	97+07	--	+11.95	South wall	11 Feb 61
S-16	97+06	--	+19.53	South wall	11 Feb 61
S-17	97+06	--	+27.32	South wall	14 Feb 61
W-5	97+07	--	+27.02	South wall	14 Feb 61
S-18	97+05	--	+35.45	South wall	18 Feb 61
S-19	97+05	--	+12.65	North wall	11 Feb 61
S-20	97+05	--	+27.32	North wall	14 Feb 61

Note: Locations and elevations refer to center of face of meters. Meters S-12 through S-20 (excluding S-14) and W-4 and W-5 were installed with faces flush with outside face of wall.

Table A5

Installation Data for Strain Meters

WES Meter No.	Station	Distance from Inside Face of Wall, ft	Offset from Center Line of Lock, ft	Elevation ft msl	Lift	Date Installed
			Strain Meters in Base Slab			
M-1	96+97	-	36.0 N	-21.58	First	15 May 1960
M-2	96+97	-	27.0 N	-21.61	First	15 May 1960
M-3	96+97	-	18.0 N	-22.40	First	15 May 1960
M-4	96+97	-	9.0 N	-22.42	First	15 May 1960
M-5	96+97	-	Center line	-22.37	First	15 May 1960
M-6	96+97	-	9.0 S	-22.43	First	15 May 1960
M-7	96+97	-	18.0 S	-22.46	First	15 May 1960
M-8	96+97	-	27.0 S	-21.64	First	15 May 1960
M-9	96+97	-	36.0 S	-21.62	First	15 May 1960
M-10	96+97	-	Center line	-20.97	First	15 May 1960
M-11	96+97	-	Center line	-19.58	First	15 May 1960
M-12	96+97	-	Center line	-18.34	Second	7 Sept 1960
M-13	96+97	-	Center line	-16.95	Second	7 Sept 1960
M-14	96+97	-	Center line	-15.55	Second	7 Sept 1960
M-15	96+97	-	Center line	-14.17	Third	17 Oct 1960
M-16	96+97	-	36.0 N	-12.06	Third	17 Oct 1960
M-17	96+97		27.0 N	-12.04	Third	17 Oct 1960
M-18	96+97	-	18.0 N	-12.75	Third	17 Oct 1960
M-19	96+97	-	9.0 N	-12.76	Third	17 Oct 1960
M-20	96+97	-	Center line	-12.77	Third	17 Oct 1960
M-21	96+97	-	9.0 S	-12.78	Third	17 Oct 1960
M-22	96+97	-	18.0 S	-12.79	Third	17 Oct 1960
M-23	96+97	-	27.0 S	-12.05	Third	17 Oct 1960
M-24	96+97	-	36.0 S	-12.05	Third	17 Oct 1960
M-25	96+97	-	Center line	-11.83	Third	17 Oct 1960
M-A	96+92	-	5.0 S	-21.58	First	15 May 1960
M-B	96+92	-	5.0 S	-13.05	Third	17 Oct 1960
			Strain Meters in Walls			
M-26	96+97	6.5	--	-08.50	First	11 Nov 1960
M-27	96+97	1.5	--	-08.50	First	11 Nov 1960
M-28	96+97	6.0	--	+14.00	Third	11 Feb 1960
M-29	96+97	1.0	--	+14.00	Third	11 Feb 1960
M-30	96+97	1.5	--	-08.50	First	11 Nov 1960
M-31	96+97	6.5	--	-08.50	First	11 Nov 1960
M-32	96+97	1.0	--	-02.50	First	11 Nov 1960
M-33	96+97	6.9	--	-02.50	First	11 Nov 1960
M-34	96+97	1.0	--	+14.00	Third	11 Feb 1961
M-35	96+97	6.0	--	+14.00	Third	11 Feb 1961
M-36	96+97	1.0	--	+26.00	Fourth	14 Feb 1961
M-37	96+97	4.7	--	+26.00	Fourth	14 Feb 1961

Note: Locations and elevations refer to center of face of meters.
Strain meters M-26 through M-29 were installed in north wall.
Strain meters M-30 through M-37 were installed in south wall.

Table A6

Installation Data for Wall Deflection Pipes

Deflection Pipe No.	Contact Point No.	Height Above Contact Point No. 1, ft	Horizontal Distance Between Contact Points,* in. N to S	Horizontal Distance Between Contact Points,* in. E to W	Date Concrete Placed Around Contact Point
DP-1 (monolith 22, south wall, sta 90+32.75)	1	0	4.748	4.749	3 Nov 60
	2	10.00	4.721	4.745	3 Nov 60
	3	16.50	4.749	4.750	4 Jan 61
	4	22.50	4.748	4.746	13 Feb 61
	5	28.50	4.751	4.750	18 Mar 61
	6	34.50	4.748	4.748	18 Mar 61
	7	40.50	4.749	4.749	4 Apr 61
	8	46.50	4.750	4.748	4 Apr 61
	9	58.50	4.750	4.748	24 May 61
	10	69.50	4.748	4.750	2 Sep 61
	11	78.00	4.750	4.750	21 Dec 61
DP-2 (monolith 22, south wall sta 91+21)	1	0	4.743	4.748	3 Nov 60
	2	10.50	4.728	4.746	3 Nov 60
	3	16.50	4.749	4.750	4 Jan 61
	4	22.50	4.749	4.750	13 Feb 61
	5	28.50	4.750	4.750	18 May 61
	6	34.50	4.750	4.751	18 May 61
	7	40.50	4.751	4.753	4 Apr 61
	8	46.50	4.750	4.750	4 Apr 61
	9	58.50	4.750	4.750	24 May 61
	10	70.50	4.750	4.750	2 Sep 61
	11	78.50	4.750	4.750	21 Dec 61
DP-3 (monolith 12, north wall sta 97+00.75)	1	0	4.748	4.745	11 Nov 60
	2	10.00	4.749	4.748	11 Nov 60
	3	21.00	4.749	4.746	14 Jan 61
	4	26.25	4.750	4.750	11 Feb 61
	5	31.50	4.750	4.750	11 Feb 61
	6	36.75	4.750	4.750	14 Feb 61
	7	42.00	4.750	4.750	14 Feb 61
	8	52.50	4.750	4.750	18 Feb 61
	9	63.00	4.750	4.750	23 Feb 61
	10	70.50	4.750	4.750	16 Aug 61
	11	78.00	4.751	4.751	19 Aug 61
DP-4 (monolith 12, south wall sta 97+00.75)	1	0	4.747	4.750	11 Nov 60
	2	10.00	4.745	4.746	11 Nov 60
	3	21.00	4.750	4.750	18 Jan 61
	4	26.25	4.750	4.750	11 Feb 61
	5	31.50	4.750	4.750	11 Feb 61
	6	36.75	4.750	4.750	14 Feb 61
	7	42.00	4.750	4.750	14 Feb 61
	8	52.50	4.750	4.750	18 Feb 61
	9	63.00	4.750	4.750	23 Feb 61
	10	70.50	4.750	4.750	16 Aug 61
	11	78.00	4.750	4.750	19 Aug 61

* Measured with micrometer in WES Machine Shop.

APPENDIX B: RESULTS OF TESTS ON CONCRETE, REINFORCING STEEL, AND SAND BACKFILL

Purpose of Tests

1. Laboratory tests were performed to determine pertinent engineering properties of the concrete and reinforcing steel used in monolith 12. The data obtained from these tests were used to interpret data obtained from the instruments embedded in the concrete base slab and walls of the lock. The data were also used to check certain assumptions made in the design of the lock. Laboratory tests were conducted to determine the coefficient of thermal expansion, volume change in water, autogenous growth, Poisson's ratio, modulus of elasticity, creep, compressive and tensile strength of concrete, and modulus of elasticity and tensile strength of reinforcing steel. Additional laboratory tests were performed on cylinders of concrete obtained in the field during construction of monolith 12 to permit a qualitative comparison of the concrete actually used in the structure with that used in the laboratory testing program. In-place density determinations were made of the sand backfill used behind the lock walls, and representative samples were tested in the laboratory to determine the relative density and shear strength of the backfill material.

Laboratory Tests on Concrete

Mixture proportions

2. Concrete specimens were fabricated in the laboratory from materials that were to be used in monolith 12, and the mixture proportions used were those selected for that monolith. The mixture proportions were as follows:

Maximum size of aggregate, in.	1-1/2
Sand/total aggregate ratio by weight, %	35
Fineness modulus	2.38
Cement factor, bags per cu yd	4.5

Water-cement ratio, by weight	0.51
Water-cement ratio, gal/bag	5.7
Air content, %	4.1
Slump, in.	2-1/4
Bleeding, %	1.1
Portland cement, type (No. 25 C-9)	II
Air-entraining admixture (air-in, double strength) ml/bag	29

Coefficient of thermal expansion

3. Six 3-1/2- by 4-1/2- by 16-in. prisms were fabricated for tests to determine the linear coefficient of thermal expansion. The tests were conducted at the age of 90 days at a temperature range of 40 to 140 F, using Method CRD-C 39.* Each specimen was subjected to five cycles of heating and cooling. Test results are as follows:

Linear Coefficient of Thermal Expansion
millionths per deg F

Specimen No.						
M-4	M-5	M-6	M-10	M-11	M-12	Avg
6.71	6.58	6.47	6.43	6.44	6.40	6.51

The average value of 6.5×10^{-6} per deg F is the value normally expected for concrete of this type, i.e., concrete containing chert coarse aggregate and siliceous sand fine aggregate. Based on the above test results, a value of coefficient of thermal expansion of 6.5×10^{-6} per deg F was selected to correct data from strain meters.

4. As a check, the coefficient of thermal expansion was also determined on two autogenous length change specimens (6- by 16-in. cylinders) with embedded Carlson concrete strain meters, which were tested in conjunction with creep tests. An average of 6.7×10^{-6} per deg F was obtained, which is in good agreement with the value obtained from Method CRD-C 39.

* All CRD-C test methods mentioned herein are presented in reference 17.

Volume change

5. Six 3-1/2- by 4-1/2- by 16-in. prisms were fabricated for volume (length) change tests. The specimens were measured at the ages of 3, 7, 28, and 90 days and approximately 1 year. Test Method CRD-C 25 and applicable portions of Method CRD-C 56 were used. Volume changes of the specimens are listed below:

Specimen No.	Volume Change, percent (based on linear measurement)				
	3 days	7 days	28 days	90 days	357 days
M-1	-0.0150	-0.0087	-0.0450	+0.0063	-0.0042
M-2	+0.0021	-0.0063	-0.0213	0.0000	-0.0063
M-3	-0.0150	-0.0108	-0.0492	+0.0021	-0.0087
M-7	-0.0087	-0.0087	-0.0213	-0.0021	-0.0129
M-8	-0.0237	-0.0042	-0.0408	-0.0150	-0.0042
M-9	-0.0237	-0.0150	-0.0279	-0.0087	-0.0042

A plot of volume change versus time is shown in fig. B1. Test results were somewhat erratic and showed no definite trend either to increase or decrease with time.

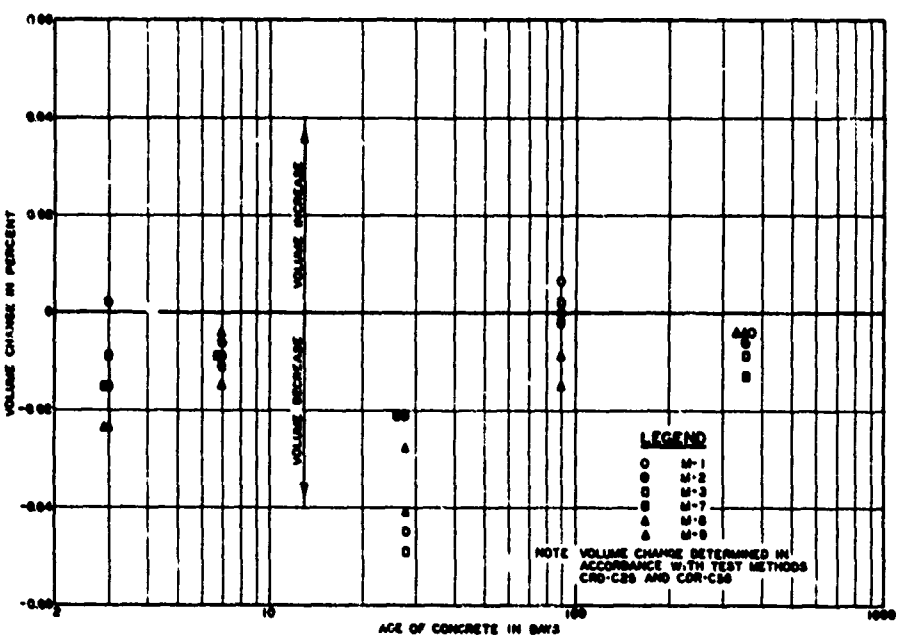

Fig. B1. Volume change of concrete versus time

Poisson's ratio

6. Poisson's ratios of the six prism specimens were determined at the ages of 1, 3, 7, 28, and 90 days and approximately 1 year (at the same time that the lengths of the specimens were measured). Poisson's ratio was calculated from Young's dynamic modulus of elasticity and the dynamic modulus of rigidity of the specimens, since the value of Poisson's ratio is believed to be independent of the method used. The dynamic (sonic) method, as described in CRD-C 18, was used to determine values of modulus of elasticity and modulus of rigidity. Test results are shown in table B1.

7. Values of Poisson's ratio shown in table B1 fell within the range of values that are usually obtained for this type of test. Poisson's ratio of concrete is generally considered to be independent of time. Average values obtained in the tests ranged from 0.15 for concrete tested at 90 days to 0.21 for specimens tested at 1 day. The variation in test results may be due to experimental error. A value of Poisson's ratio of 0.18 was selected for use in the analysis of data from the electrical measuring devices.

Modulus of elasticity and compressive strength

8. Twelve 6- by 12-in. concrete cylinders were fabricated for tests to determine the static modulus of elasticity and compressive strength. Two specimens were tested at the ages of 1, 3, 7, 28, and 90 days and approximately 1 year. The modulus of elasticity was determined from the stress-strain curves using the secant method at a strain of 300 μin./in. Values of modulus of elasticity and compressive strength obtained in the tests are shown in table B1.

9. Values of compressive strength are plotted versus time in fig. B2; values of modulus of elasticity are plotted versus time in fig. B3. Values of compressive strength varied from 1050 psi at 1 day to 6040 psi at approximately 1 year. As can be seen in figs. B2 and B3, both the compressive strength and modulus of elasticity of specimens tested at 28 days were somewhat low. The reason for this is not known. Also shown for comparison in figs. B2 and B3 are the values obtained

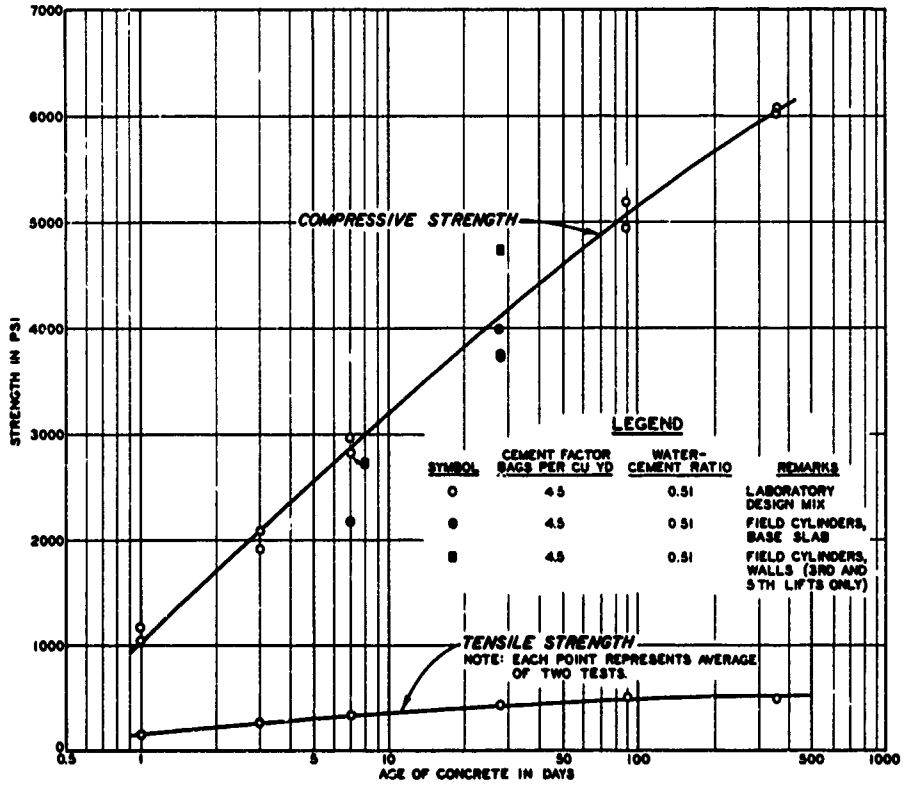

Fig. B2. Strength of concrete versus time

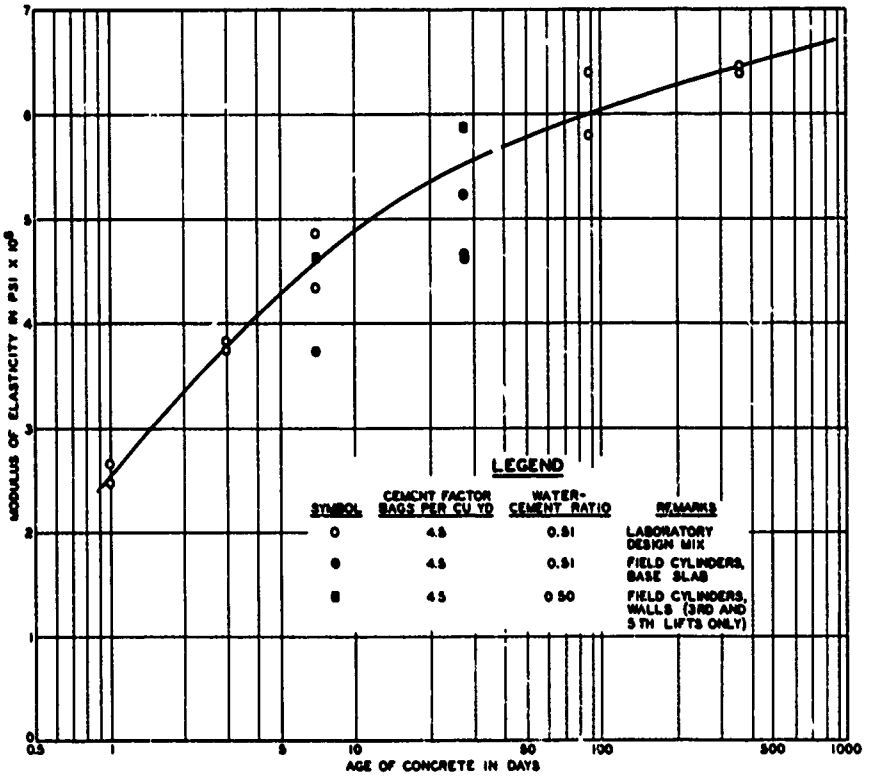

Fig. B3. Modulus of elasticity of concrete versus time

from tests on the field cylinders. These values will be discussed later in this appendix.

Tensile strength

10. Tensile splitting tests were performed on twelve 6- by 12-in. concrete cylinders using Method CRD-C 77. The tensile strength of two cylinders was determined at ages of 1, 3, 7, 28, and 90 days and 1 year. Results of the tests are shown in table B1 and are plotted versus time in fig. B2. Results show that the tensile strength also increased with time, varying from about 160 psi at one day to about 600 psi at one year.

Creep tests

11. Creep tests were performed using Method CRD-C 54 on 16 concrete cylinders 6 in. in diameter by 16 in. long with embedded Carlson concrete strain meters. Based on experience gained at Port Allen Lock, it was decided that creep tests on Old River Lock concrete would be performed on saturated specimens to simulate field conditions more closely. Creep tests were also performed on a few sealed specimens to provide a comparison with Port Allen Lock data. Creep tests were performed on duplicate saturated specimens at ages of 1, 3, 7, 28, and 90 days and 1 year. Tests were performed on sealed specimens at the ages of 3 and 28 days. In general, tests were conducted by applying loads of 200 psi to the specimens and measuring the unit length change at various intervals of time by means of the embedded strain meters. Results were reported in terms of unit length change per psi as a function of time. After a test was completed, a curve of best-fit was determined for the test results, the curve being in the form of the equation

$$\varepsilon = 1/E + F(K)\ln(t + 1) \qquad \text{(B1)}$$

where

ε = unit length change per psi

$1/E$ = elastic deformation in μin./in.

$F(K)$ = creep constant

t = time after loading in days

12. Autogenous length change measurements were made on two specimens similar to the creep specimens (6- by 16-in. concrete cylinders). One specimen was saturated, and the other was sealed. Measurements of autogenous length change were made on the same days that creep measurements were made so that creep data could be corrected for autogenous length change. Length change measurements on the saturated specimen were used to correct creep data from saturated specimens, and length change measurements from the sealed specimen were used to correct creep data from sealed specimens.

13. Values of 1/E and F(K) obtained from each creep test are shown in table B2. Arrangements were made for the University of California to conduct similar creep tests (sealed) on concrete containing the same materials as those used at Old River Lock. The results of this independent series of tests are given in table B2. Values obtained from similar tests on concrete (sealed) for Port Allen Lock are also given for comparison. All of these test results are plotted versus time in fig. B4. As can be seen in fig. B4, test results for sealed specimens

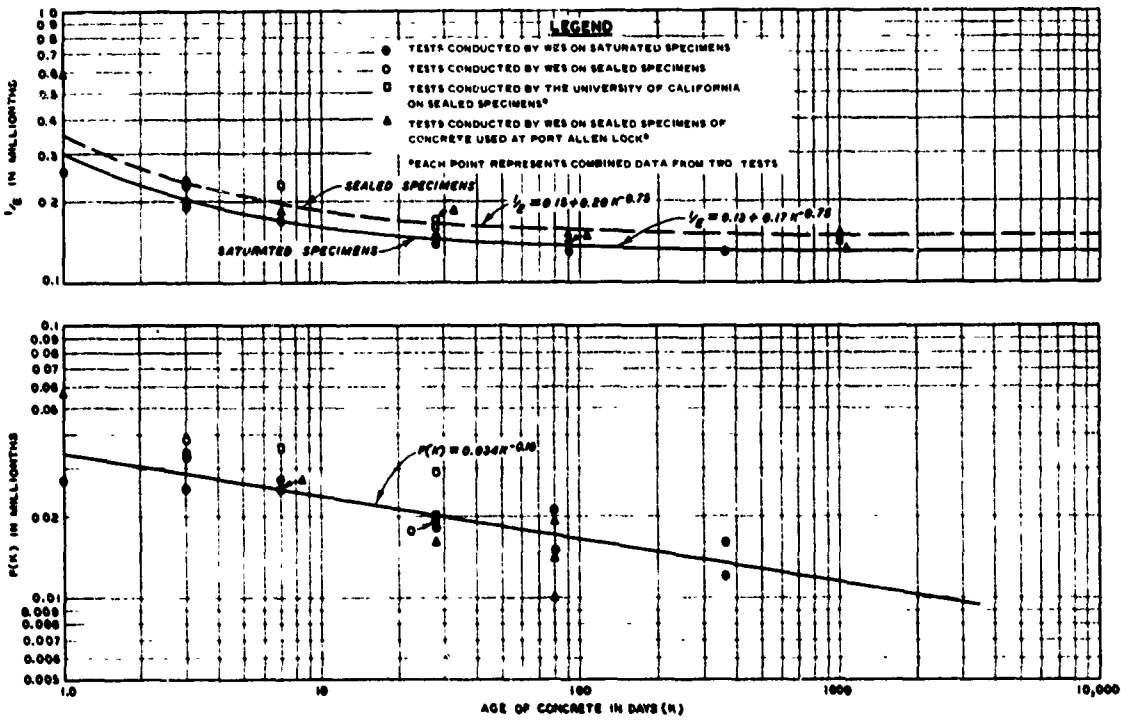

Fig. B4. Laboratory creep data on concrete cylinders

of Old River Lock concrete are in good agreement with test results on Port Allen Lock concrete and also agree with results of tests conducted by the University of California. Values of $1/E$ for saturated specimens were slightly lower than those for sealed specimens. Values of $F(K)$ were somewhat erratic, and one curve of best-fit was drawn for all data. The equations for the curves shown in fig. B4 are as follows:

$$1/E = 0.13 + 0.17K^{-0.75} \text{ (for saturated specimens)} \qquad \text{(B2a)}$$

$$1/E = 0.15 + 0.20K^{0.75} \text{ (for sealed specimens)} \qquad \text{(B2b)}$$

$$F(K) = 0.034K^{-0.16} \text{ (for all specimens)} \qquad \text{(B3)}$$

The equations above were used to compute stress in the concrete from strain meter readings at Old River Lock.

Tests on Reinforcing Steel

14. A limited number of laboratory tests were performed to develop tensile stress-strain data and to determine the modulus of elasticity of the reinforcing steel used in monolith 12 of Old River Lock. Six representative samples (two No. 9 bars, two No. 10 bars, and two No. 18 bars) were tested. As both Laclede steel and Sheffield steel were used in monolith 12, one complete set of specimens of Laclede steel was tested and two specimens of Sheffield steel (No. 10 bars) were tested for comparative purposes.

15. The steel was machined to conform with ASTM Designation: E-8[18] and tested in accordance with ASTM Methods A-15 and E-8. Values of tensile strength, yield point, and elongation obtained in the tests are given in table B3. Values obtained in the modulus of elasticity tests are given in table B4. Results of the modulus of elasticity tests were fairly consistent, with the exception of those for bar No. 18-L-1. The average secant and chord moduli for bar 18-L-1 were 25.3×10^6 and

27.1 × 10^6 psi, respectively. The average secant moduli for other specimens ranged from 28.1 to 29.1 × 10^6 psi. The average chord moduli ranged from 28.2 to 28.8 × 10^6 psi. In analyzing data from electrical measurement devices in the structure, a value of 28.6 × 10^6 psi was selected for the modulus of elasticity of reinforcing steel.

Tests of Concrete Cylinders

Concrete Design

16. Concrete for the base slab and walls of Old River Lock was designed for a 28-day compressive strength (f'_c) of 3000 psi. Materials used in the concrete for monolith 12 were as follows:

a. Type II portland cement purchased from the Ideal Cement Company, Baton Rouge, La.

b. Fine aggregate purchased from the Central Sand and Gravel Company and obtained from Paradise Pit, Grand Parish, La.

c. Coarse aggregate (1-1/2-in. maximum size), a chert gravel purchased from Big Rock Pit, Grand Parish, La.

d. Coarse aggregate (3/4-in. maximum size), a chert gravel purchased from Gifford Hill and Company, Turkey Creek, La.

e. An air-entraining admixture, Air-in, purchased from the Hunt Process Company, Ridgeland, Miss.

The maximum size of coarse aggregate used in monolith 12 was 1-1/2 in. The specified gradation of aggregate was as follows:

Fine Aggregate		Coarse Aggregate		
			% Passing by Weight	
Sieve Size	% Passing by Weight	Sieve Size	No. 4 to 3/4 in.	3/4 in. to 1-1/2 in.
No. 4	100	2 in.		100
No. 8	80-90	1-1/2 in.	100	90-100
No. 16	55-80	1 in.	90-100	20-45
No. 30	30-60	3/4 in.	90-100	0-10
No. 50	12-30	3/8 in.	30-55	0-5
No. 100	3-10	No. 4	0-5	—

The basic design for concrete in monolith 12 is described in paragraph 2.

Slight adjustments were made to the water-cement ratio in the field, as shown in table B5. The design mixture for concrete in monolith 12 differed from that used in the remainder of the lock in that a cement factor of 4.0 bags per cu yd was used for all base slab construction outside of monolith 12. It was decided to use a uniform cement factor of 4.5 bags per cu yd throughout monolith 12 to facilitate interpretation of the data from instruments in this monolith.

Sample preparation

17. Two sets of concrete cylinders were obtained from each lift of concrete in the base slab of monolith 12 and from every other lift of the walls, except the fifth wall lift, from which only one set of cylinders was obtained. Each set of cylinders consisted of six 6- by 12-in. standard test cylinders. Information pertinent to the concrete in each set of cylinders was recorded at the structure site. This information, summarized in table B5, included air content, slump, cement factor, and water-cement ratio.

18. During placement of the seventh wall lift of concrete, it was noted that the concrete was setting up prematurely in the concrete buckets while being transported from the batch plant to the jobsite. In order to remove the concrete from the buckets, additional water had to be placed in the concrete; consequently, the true water-cement ratio of the concrete in the seventh wall lift is not known. Because of this difficulty, concrete cylinders were also obtained from concrete placed in the eighth wall lift.

Laboratory tests

19. Compressive strength and modulus of elasticity. Compressive strength and modulus of elasticity were determined for each concrete cylinder. The locations of cylinders are given in table B5. In each set of six cylinders, three were tested at the age of 7 days and the other three at 28 days.

20. Results of the compressive strength and modulus of elasticity determinations are given in table B5. Results of the 7-day compressive strength tests for the entire monolith ranged from 1980 to 2980 psi, with an average of 2420 psi and a standard deviation of 327 psi.

Results of the 28-day compressive strength tests ranged from 3610 to 4980 psi, with an average of 4170 psi and a standard deviation of 382 psi.

21. As shown in table B5, the compressive strength and modulus of elasticity of concrete in the base slab are somewhat lower than those in the walls. The reason for this difference is not known. The difference may be due to the variation in strength-producing characteristics of different shipments of cement or the variation in temperature at which the concrete was made. Concrete made in cool weather, if cured properly, generally will show higher strength than concrete made in hot weather. The 28-day compressive strengths for both the walls and base slab were well above the 28-day compressive strength (f'_c = 3000 psi) assumed for design.

22. The purpose of obtaining concrete field cylinders was to permit a comparison of the concrete in which the electrical measurement devices were installed with the concrete used in the laboratory testing program previously described. A comparison of average values of modulus of elasticity and compressive strength of concrete field cylinders and concrete used in the laboratory program is given below:

	Compressive Strength, psi		Modulus of Elasticity 10^6 psi	
	7 days	28 days	7 days	28 days
Concrete in base slab	2180	4000	3.73	5.22
Concrete in walls (3d ard 5th lifts)	2810	4720	4.62	5.88
Laboratory specimens	2890	3740	4.60	4.62

Only data for cylinders from the third and fifth wall lifts are shown for the concrete in the lock walls for the following reasons: (a) electrical measurement devices were installed only in wall lifts one through five, and (b) cylinders from the first wall lift are not considered to be representative of concrete placed in that lift, as the water-cement ratio (0.54) of the batch from which the cylinders were taken was somewhat greater than the average water-cement ratio (0.50) of all concrete

placed in the lift. A comparison of values of modulus of elasticity and compressive strength of field cylinders and laboratory cylinders is also shown in figs. B1 and B2. As shown in figs. B1 and B2, values from field cylinders from the structure as a whole are in reasonably close agreement with those determined from laboratory cylinders. On the basis of the tests described above, it is concluded that the concrete used in the structure was essentially the same as the concrete used for the program of laboratory tests to establish specific properties of concrete; therefore, these properties can be applied with confidence to the in-place concrete.

23. Density. The densities of all concrete cylinders were determined to establish a proper value to use in the analytical studies. Density determinations were made prior to conducting other tests. The densities were computed from the bulk specific gravity determined in accordance with Method CRD-C 23. The densities determined are shown in table B5 and indicate an average value of 145.5 lb/cu ft. In the analytical studies, a value of 146 lb/cu ft was selected for the concrete throughout monolith 12. Adjustments in density were made where necessary to account for the presence of steel in the concrete.

Tests on Backfill Material

Description of sand backfill

24. A wedge-shaped section of sand backfill was placed behind the lock walls to provide free drainage behind the walls and to provide lateral support for the walls during period when high water is in the lock. A 5-ft-thick layer of clay was placed on the bottom of the excavation between the outside edge of the lock walls and the upper impervious foundation strata to prevent unrestricted seepage from entering the backfill from the foundation sand. A 3-ft-thick layer of clay was placed on the top of the backfill to prevent surface waters from entering the sand backfill. Initially it was planned for the remainder of the backfill to consist of random materials (silty sand, sandy silt, silt, and lean clay) obtained from the stockpile of excavated materials.

However, in accordance with an agreement between the contractor and the contracting officer, sand dredged from a sandbar in Old River was used in the random-fill area.

25. Specifications for materials for the sand wedge behind the walls required that the sand be clean and free draining, contain not more than 10 percent of materials passing the No. 100 sieve, and have a permeability greater than 100×10^{-4} cm per sec. Material for the clay blankets was specified to consist of approved clays having a liquid limit of not less than 40.

Backfill placement and compaction

26. Backfill placement. Sand backfill placed below about el +8 was brought in by hauling equipment from spoil banks of material from the structure excavation. Backfill placed above el +8 was dredged directly into the excavation area from a sandbar in Old River. Before the dredged sand was placed, a small dike of sand, 3 to 5 ft high, was constructed along the entire length of the lock and about halfway between the lock wall and the excavation slope. The space between the dike and the excavation slope was filled with dredged material, the effluent being carried along the length of the dike into sumps near the downstream end of the lock. After sufficient sand had been placed, the dredge discharge pipes were removed and the sand was spread between the dike and lock wall. This procedure was repeated with the dredge pipe at successively higher elevations.

27. Material for the clay blanket was obtained from a stockpile of material from structure excavation. The clay was brought in by hauling equipment and compacted as described in paragraph 29.

28. Compaction. Sand backfill obtained from the stockpile was placed in 8-in.-thick layers, saturated by flooding, and then compacted by either two passes of a tractor, usually a D8 with blade, or at least two passes of a vibrating roller (a Tampo Model VC 80 pulled by a rubber-tired tractor). Sand backfill dredged from the sandbar was spread in 8-in.-thick layers and compacted with the vibrating roller only. Backfill within 2 ft of the walls was placed in 8-in.-thick layers and compacted with a power tamper, usually a Chicago pneumatic backfill tamper.

Backfill adjacent to soil stress meters in the walls was placed in 4-in.-thick layers and compacted by hand.

29. Materials for the clay blanket were placed in 8-in.-thick layers and compacted with at least six passes of a tamping roller pulled by a D8 tractor. Material placed within 2 ft of the wall was placed in 4-in.-thick layers and compacted with power tampers.

30. Evaluation of vibrating roller. Specifications required that the sand backfill be compacted in 8-in.-thick lifts by two passes of a tractor. However, at the beginning of backfilling operations, the contractor expressed a desire to use a vibrating roller pulled by a rubber-tired tractor in order to avoid severe wear of the tractor treads resulting from compacting the sand. The contractor was allowed to do so under the conditions that (a) the vibrating roller produced the desired compaction, and (b) the roller would not have any adverse effect on the electrical instruments embedded in the walls of the lock. To determine if the vibrating roller produced the required compaction, about 12 control density tests were made on each side of the lock for comparing the density of backfill compacted with the tractor with the density of backfill compacted with the vibrating roller. The samples were taken with a standard 3-in. drive cylinder. Results of the tests indicated average densities of 102 lb/cu ft for sands compacted with the tractor and 106 lb/cu ft for sands compacted with the vibrating roller. Based on the test results, it was considered that the vibrating roller was more than adequate in achieving the desired compaction.

31. To determine whether the vibrating roller had any adverse effect on the electrical instruments embedded in the walls of the lock, two series of tests were performed. One series was performed with the backfill about 1.5 ft above meter S-12 and one series with the backfill about 3 ft above the meter. The vibrating roller was operated at various frequencies and at various distances from the wall, and the dynamic pressures exerted on the wall were measured with meter S-12. Results of the tests are shown in fig. B5. With the roller operating at a distance of 3 ft from the wall, the maximum observed dynamic pressure acting on the wall was about 3 psi. The dynamic pressure decreased rapidly when

the distance from the roller to the wall was increased. The vibrating roller was operated at frequencies of 1000 to 1700 vibrations per min during the test; the roller was normally operated at a frequency of 1000 vibrations per min. On the basis of the test results, it was decided that the vibrating roller would not have any adverse effect on the operation of meters in the walls of the lock, provided the roller was not operated within 3 ft of the meters. During subsequent operations, the vibrating roller was not used within 3 ft of the wall.

Samples obtained

32. During construction, in-place density determinations were made of tne sand wedge behind the walls of monoliths 2, 12, and 24. Locations from which these record samples were taken are shown in fig. B6. Before a sample was taken, a hole about 1 to 1-1/2 ft deep was dug. A sample was taken from the

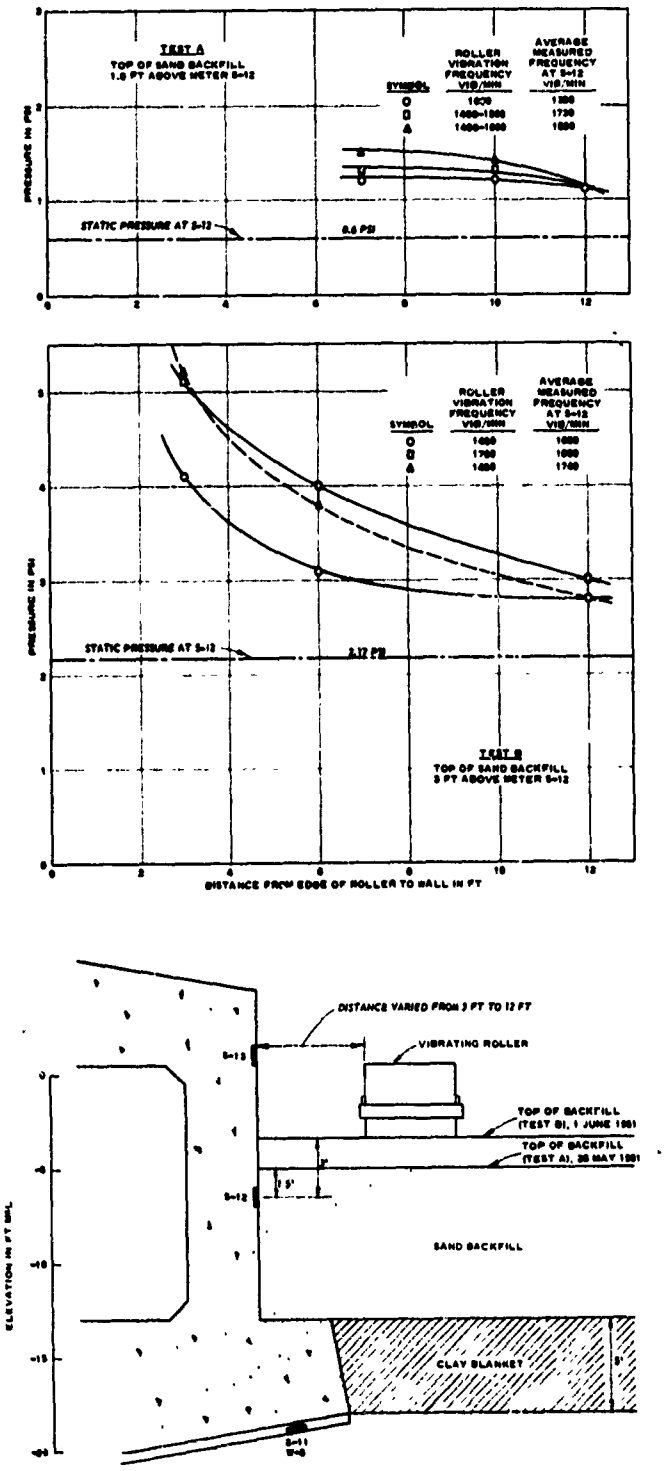

Fig. B5. Dynamic pressure produced by vibrating roller

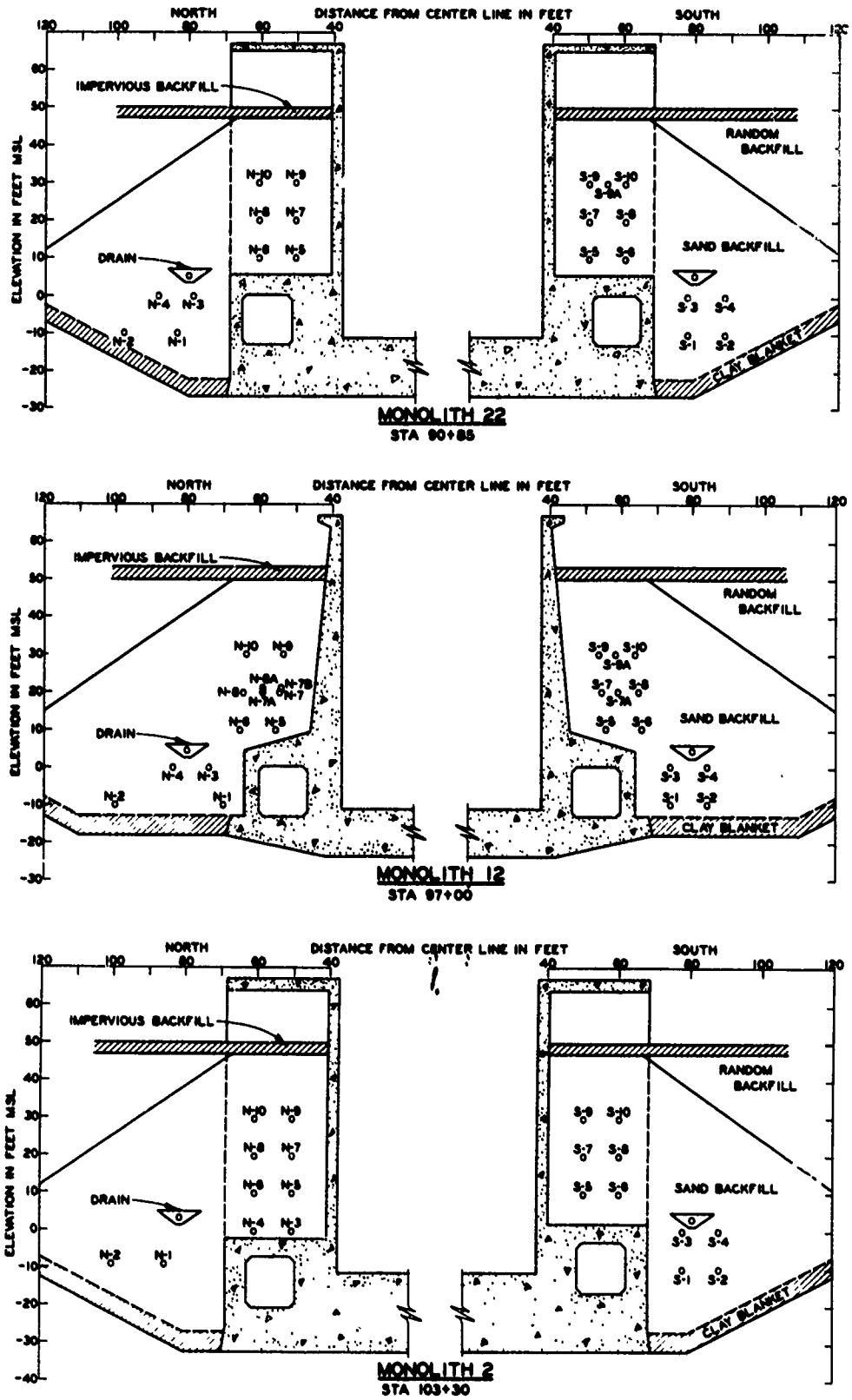

Fig. B6. Locations of record samples

bottom of the hole with a standard 3-in. drive cylinder. The density and water content of the sample were determined in the field laboratory, and the results are shown in table B6. Representative material adjacent to the density sample was taken for grain-size analysis by WES.

33. Additional control density tests were also conducted to determine the amount of compaction achieved by the vibrating roller, as discussed in paragraph 30, and to compare the values of density obtained with a drive cylinder with the values of density obtained with a Volumeasure, as discussed subsequently. In addition to the samples mentioned above, representative samples of the sand backfill were obtained for various tests conducted by WES and the New Orleans District (NOD) soils laboratories.

Laboratory tests

34. Grain-size curves. Grain-size analyses of all record samples were performed in the WES soils laboratory, and the results are shown in fig. B7. The grain-size curves indicated that the materials obtained from the sandbar were essentially the same as those obtained from the stockpile of materials from structure excavation. As can be seen in fig. B7, all grain-size curves fell within a narrow range, indicating a

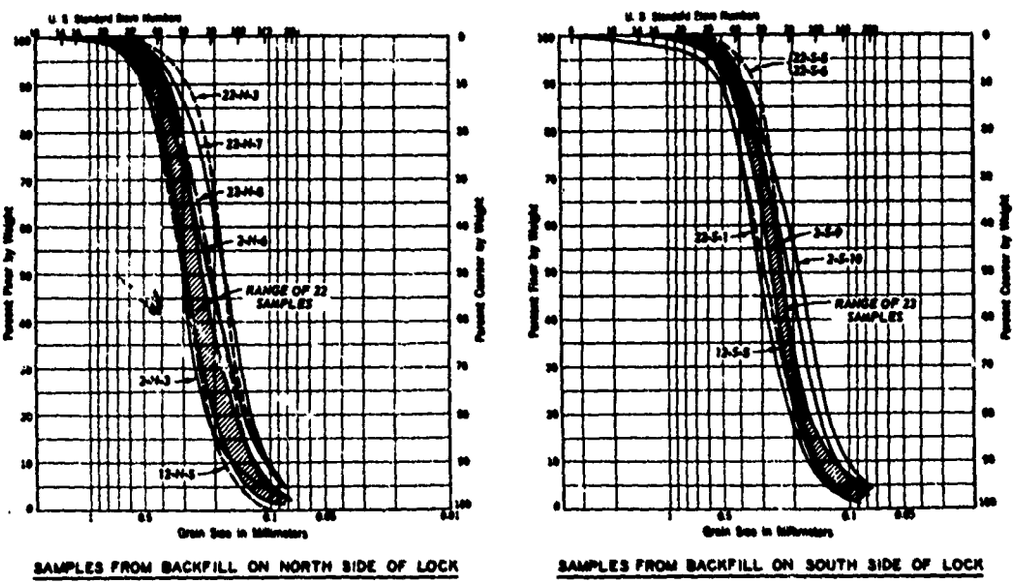

Fig. B7. Grain-size curves of density samples

relatively homogeneous backfill. Values of D_{10} size varied from 0.10 to 0.18 mm, with an average value of 0.14 mm. Values of D_{50} size varied from 0.18 to 0.30 mm, with an average value of 0.25 mm.

35. Density determinations. Density determinations on record samples of sand backfill were made by the field laboratory, and results are shown in table B6. Density values versus elevation are plotted in fig. B8. The densities varied from 94 to 110 lb/cu ft, with an average of 103 lb/cu ft.

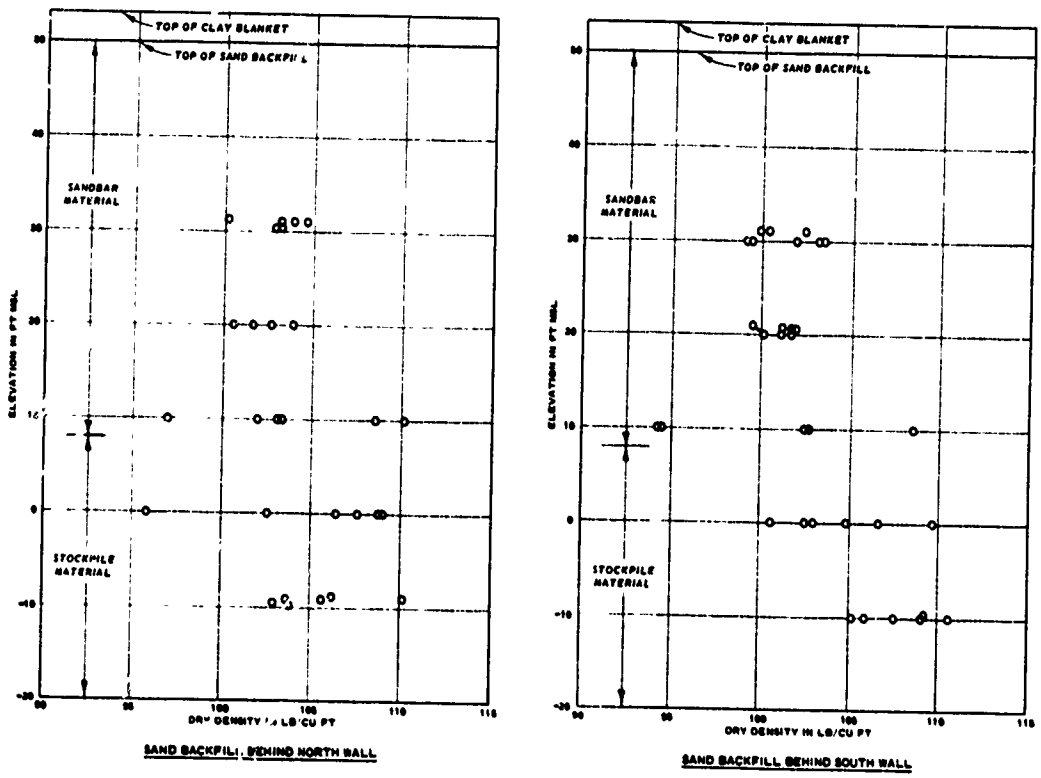

Fig. B8. Density versus elevation

36. During the course of construction, some of the record samples indicated densities somewhat less than the recommended minimum value of 103 lb/cu ft (paragraph 37), although the sand appeared to be well compacted. For that reason, an investigation was made to determine the accuracy of the densities determined with the drive cylinder by comparing these values with values of densities determined with a Soil Test Volumeasure (water balloon). Six initial tests were made using each of the methods. The average densities as determined using the Volumeasure and

the drive cylinder were 105.3 and 100.5 lb/cu ft, respectively. During the investigation, the following observations were made. In the Volumeasure method of density determinations, the hole left in the sand appeared to be quite stable, with no signs of creep or fluffing. However, when the drive cylinder was driven in the soil, considerable disturbance was evident, i.e. the sand around the cylinder tended to crack and displace. On the basis of these observations, it was determined that the density values obtained with the Volumeasure were more realistic than values obtained with the drive cylinder. As most of the backfill was in place at the time the investigation was made, it was decided that the remainder of the record samples would be taken with the drive cylinder and that periodic checks would be made with the Volumeasure to provide a correlation that could be applied to the previous density determinations. Subsequently, 17 additional comparative tests were made. Results of all comparative tests are given in table B7 and plotted in fig. B9. Results of these tests showed an average difference in density of 5.4 lb/cu ft, with densities obtained with the Volumeasure being higher than those obtained with the drive cylinder. Consequently, the average values of the densities determined with the drive cylinder (shown in table B6) were corrected by a value of 5.4 lb/cu ft. The corrected densities were used in subsequent calculations. It should be noted, however, that the densities shown in fig. B8 are uncorrected values.

37. Compaction tests and maximum and minimum density determinations. At the beginning of backfilling operations, a standard Proctor compaction test was conducted and maximum and minimum density determinations were made on representative samples of backfill obtained from the stockpile of excavated materials. The compaction test indicated a maximum density of 105 lb/cu ft at an optimum water content of 14 percent. The maximum and minimum densities of the materials were 111.8 and 81.8 lb/cu ft, respectively. It was initially decided that backfill should be placed at a relative density of 60 percent, which was equivalent to a density of 103 lb/cu ft. A dry density of 103 lb/cu ft was used as the minumum for compaction control. Subsequently, a question arose as to whether the density of the sand was affected by difference

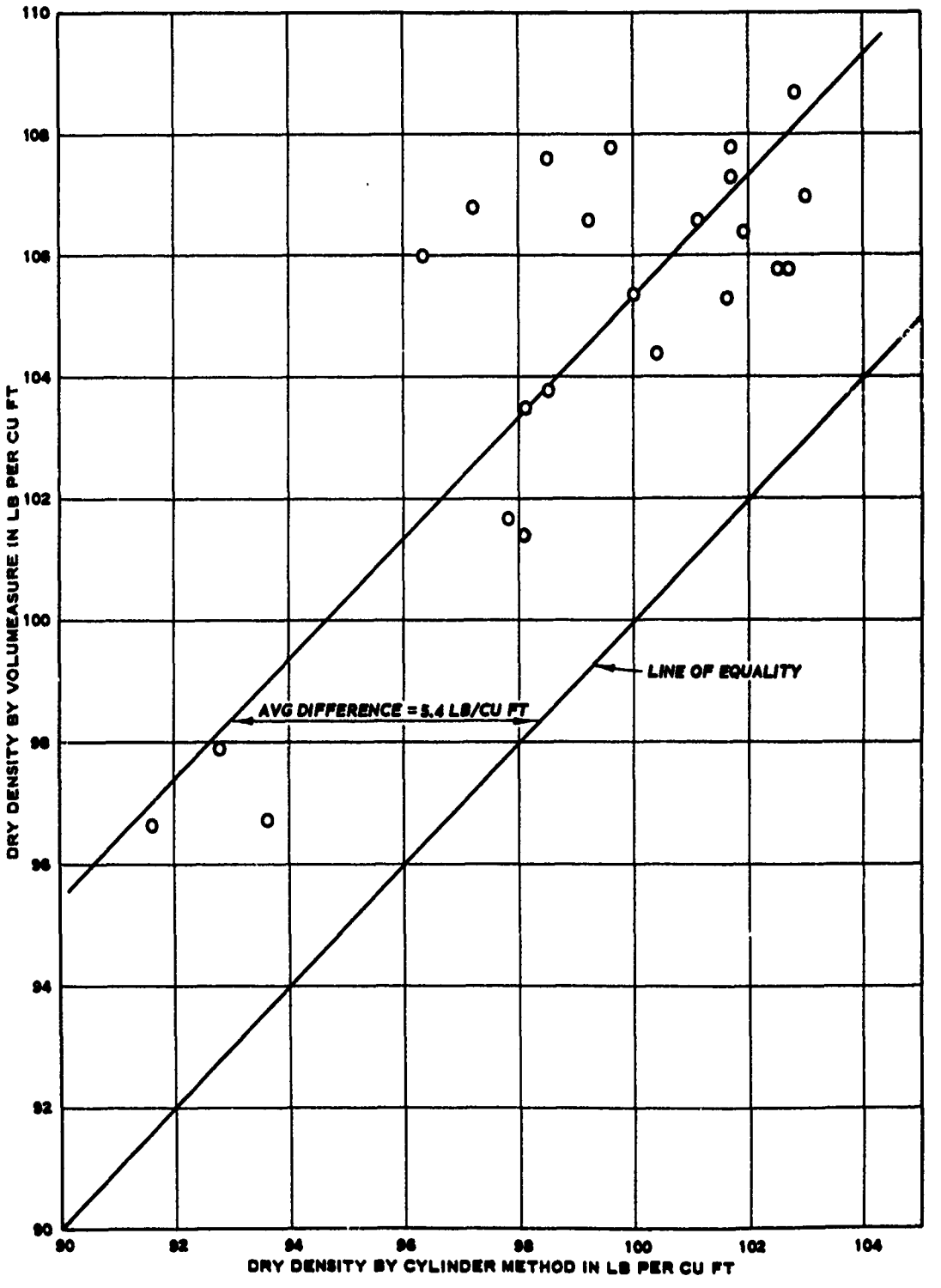

Fig. B9. Comparison of densities obtained using drive cylinder and Volumeasure methods

in gradation. Four samples representing different gradations of the backfill were taken by NOD, and compaction and gradation curves were determined for each of the samples. Results of the compaction tests are shown in table B8; compaction and grain-size curves are shown in fig B10.

38. During the second stage of backfilling operations, when sand was dredged directly into the excavation from a sandbar, two samples of the backfill material were sent to WES for compaction tests and maximum and minimum density determinations. One of the samples represented the coarser sands in the backfill, and the other represented the finer sands.

39. Results of all laboratory compaction tests and maximum and minimum density determinations are given in table B8. Compaction and gradation curves are shown in fig. B10. From the results of these tests, it was concluded that materials dredged from the sandbar were essentially the same as backfill materials obtained from the stockpile.

40. In order to determine the relative density and percent compaction of the record samples, a correlation was made of D_{50} sizes and the minimum densities, maximum densities, and maximum standard Proctor densities of samples tested in the laboratories, as shown in fig. B11. As indicated in fig. B11, the standard Proctor maximum density was considered to be equivalent to a relative density of about 62 percent. The values of the relative density and percent compaction of all record samples, as estimated from fig. B11, are shown in table B6. As previously mentioned, it was considered that in-place densities determined with the drive cylinder were probably lower than the true values. The average values of density for the record samples were corrected as discussed in paragraph 36, and the corrected values of density and corresponding percent compaction and relative density are shown in table B6.

41. Permeability tests. Permeability tests were performed by NOD on two samples of backfill obtained from the sandbar; one sample represented the coarser sand in the backfill, and the other sample represented the fine sand. The coefficient of permeability of the samples of coarser sand (D_{50} = 0.27) was 213 × 10^{-4} cm per sec; the coefficient of permeability of the samples of finer sand (D_{50} = 0.20) was 130 × 10^{-4} cm per sec. Both of the values are greater than the specified minimum

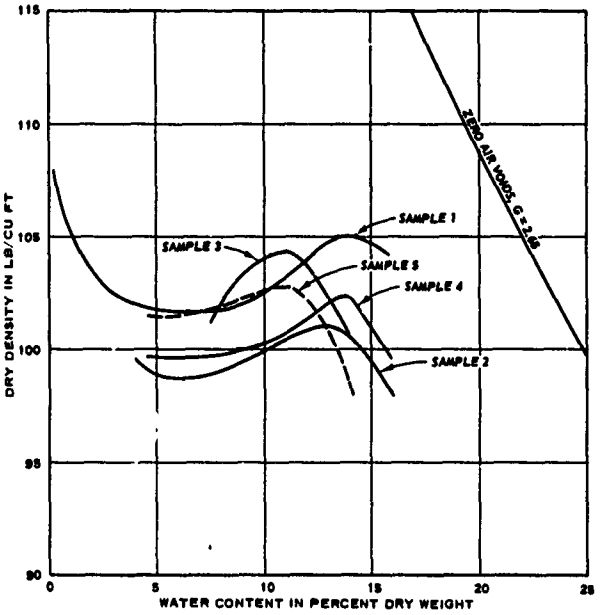

COMPACTION DATA

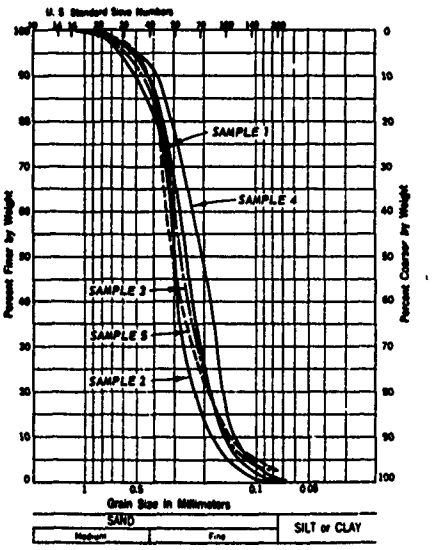

GRAIN SIZE CURVES

STOCKPILE MATERIAL

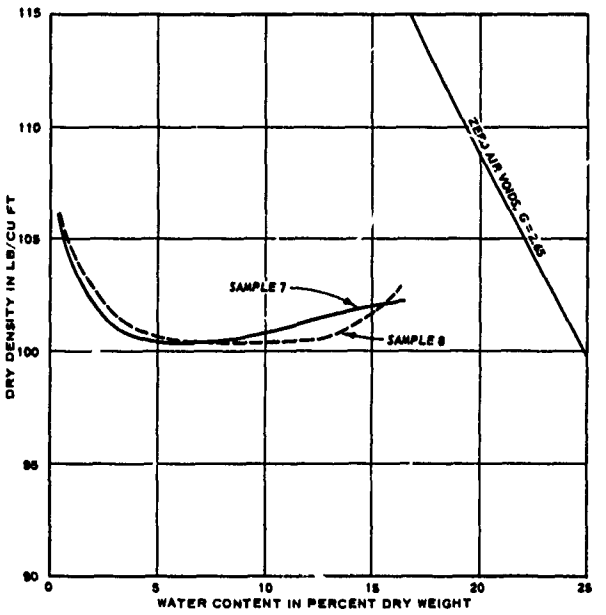

COMPACTION DATA

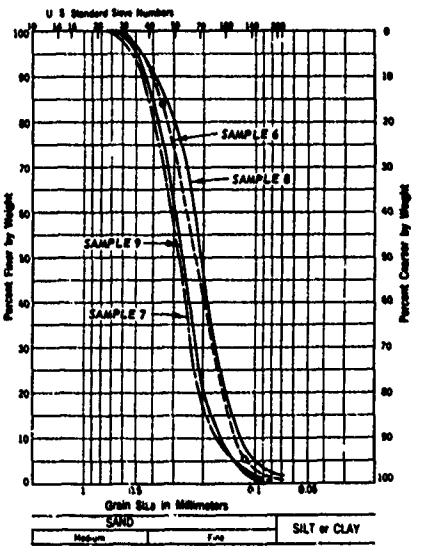

GRAIN SIZE CURVES

SANDBAR MATERIAL

Fig. B10. Laboratory compaction data

coefficient of permeability, i.e., 100×10^{-4} cm per sec.

42. Shear strength tests. Consolidated-drained triaxial compression tests were performed by WES on a sack sample that was representative of backfill material obtained from the sandbar. Since gradation curves indicated that the sand from the sandbar was essentially the same as that from the stockpile of excavated material, it was considered that the results of the shear strength tests would be representative of the shear strength of all sand backfill materials.

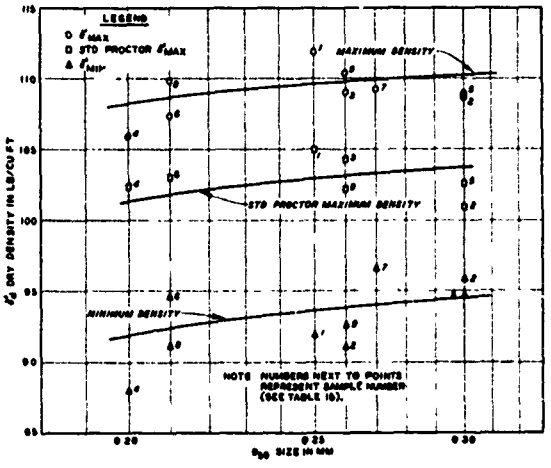

Fig. B11. Correlation of D_{50} size and density

43. Specimens for the shear strength tests were prepared at dry densities of 97, 103, and 108 lb/cu ft. The specimens, which were 2.8 in. in diameter, were saturated under a low confining pressure by allowing the water to enter under a low head and were then tested under a drained condition. Stress-strain curves and Mohr's envelopes for each test are shown in fig. B12. The shear strengths ranged from $\phi = 36$ deg for a dry density of 97.0 lb/cu ft to $\phi = 40$ deg for a dry density of 107.6 lb/cu ft.

Shear strength of sand backfill

44. Shear strength (angle of internal friction) versus relative density is plotted in fig. B13. The shear strengths for all record samples were estimated from this plot, and the results are shown in table B6. The estimated shear strengths varied from $\phi = 35.3$ deg to $\phi = 43.7$ deg, with an average of $\phi = 38.5$ deg. The values of strength were estimated from the densities determined from drive samples. The average values of densities were corrected as previously discussed and are shown in table B6. The average value of shear strength corresponding to the corrected values of density was 41.8 deg. In computations

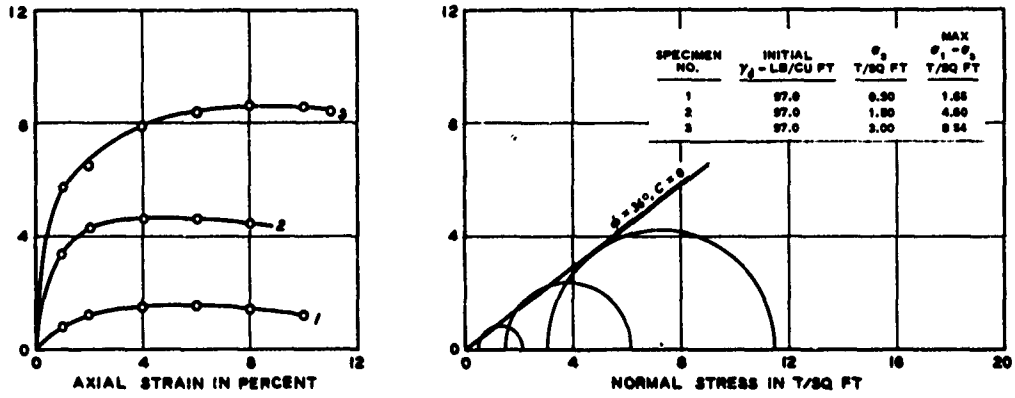

SHEAR STRENGTH AT RELATIVE DENSITY = 27.6 PERCENT (97.0 LB/CU FT)

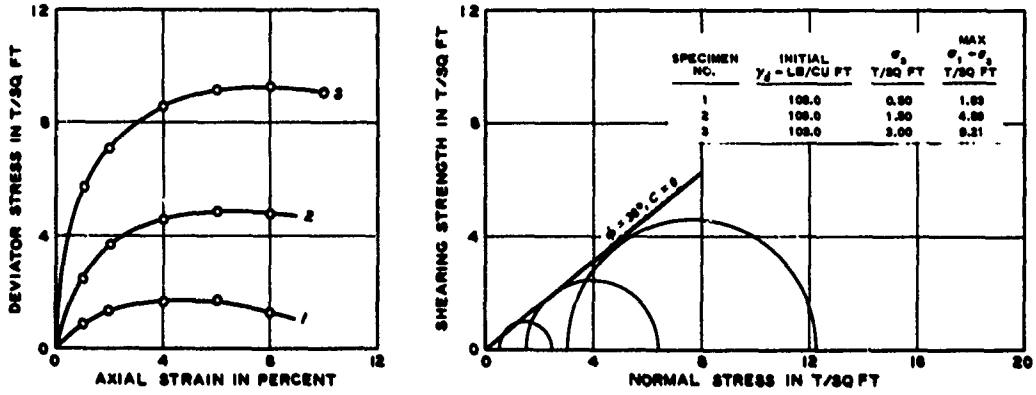

SHEAR STRENGTH AT RELATIVE DENSITY = 62.7 PERCENT (103.0 LB/CU FT)

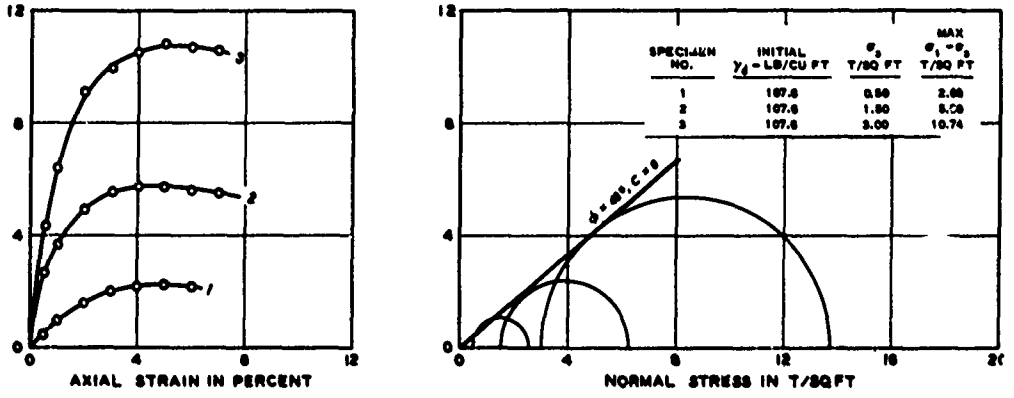

SHEAR STRENGTH AT RELATIVE DENSITY = 87.0 PERCENT (107.6 LB/CU FT)

NOTE. ALL TESTS PERFORMED ON SATURATED SPECIMENS UNDER DRAINED CONDIT ONS.

SPECIMENS WERE 2.8 IN. N DIAM BY 6.6 IN. HIGH.

Fig. B12. Shear strength data

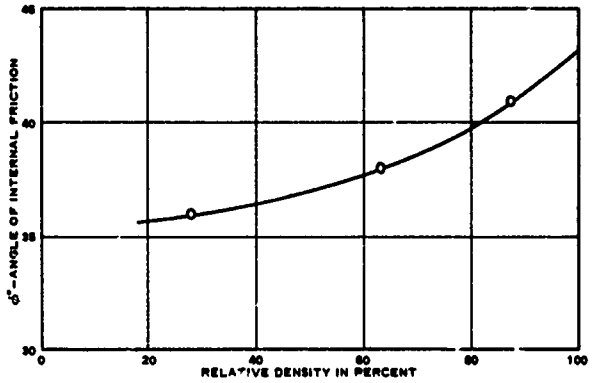

TEST	AVG γ_d	RELATIVE DENSITY	$\phi°$
1	97.0	27.8	36°
2	103.0	62.7	38°
3	107.6	87.0	40°

Fig. B13. Shear strength versus relative density

involved in analysis of data from the instrumentation program, a shear strength of $\phi = 40.0$ deg was selected for sand backfill behind the walls.

Table B1

Results of Laboratory Strength Tests on Concrete

Specimen No.	Results of Dynamic Tests, 10^6 psi																	
	1-day Age			3-day Age			7-day Age			28-day Age			90-day Age			1-yr Age		
	E	G	μ	E	G	μ	E	G	μ	E	G	μ	E	G	μ	E	G	μ
M-1	4.51	1.89	0.20	5.33	2.29	0.16	5.94	2.56	0.16	6.48	2.77	0.17	6.73	2.94	0.14	7.00	2.90	0.21
M-2	4.58	1.83	0.25	5.37	2.31	0.16	6.02	2.52	0.19	6.58	2.84	0.16	6.79	2.90	0.17	7.04	2.85	0.24
M-3	4.60	1.80	0.28	5.37	2.31	0.16	5.98	2.51	0.19	6.55	2.80	0.17	6.92	3.04	0.14	7.11	2.98	0.19
M-7	4.11	1.78	0.15	4.93	2.14	0.15	5.57	2.34	0.19	6.16	2.57	0.20	6.39	2.79	0.15	6.70	2.91	0.15
M-8	4.11	1.75	0.17	4.95	2.11	0.17	5.58	2.37	0.18	6.16	2.64	0.17	6.60	2.80	0.18	6.76	2.82	0.20
M-9	4.36	1.82	0.20	5.21	2.26	0.15	5.83	2.47	0.18	6.43	2.62	0.23	6.77	2.97	0.14	6.99	2.92	0.20
Avg	4.38	1.81	0.21	5.19	2.24	0.16	5.82	2.46	0.18	6.39	2.71	0.18	6.70	2.91	0.15	6.93	2.90	0.20

Age	Results of Static Compression and Tension Tests				
	Compression Tests			Tension Tests	
	Specimen No.	Modulus of Elasticity 10^6 psi	Compressive Strength, psi	Specimen No.	Tensile Strength, psi
1 day	828	2.66	1190	834	170
	840	2.48	1050	846	150
3 days	829	3.83	2070	835	280
	841	3.73	1910	847	270
7 days	830	4.86	2980	836	360
	842	4.33	2810	848	330
28 days	831	4.62	3730	837	430
	843	4.66	3740	849	410
90 days	832	6.39	5180	838	475
	844	5.80	4950	850	505
1 year	833	6.39	6040	839	620
	845	6.43	6020	851	560

Note: For dynamic tests, E denotes dynamic modulus of elasticity in 10^6 psi; G denotes dynamic modulus of rigidity in 10^6 psi; and μ denotes dynamic Poisson's ratio.

Table B2

Results of Laboratory Creep Tests

Age of Concrete at Time of Loading days	Load psi	1/E in millionths			F(K) in millionths		
		Old River Concrete		Port Allen Concrete	Old River Concrete		Port Allen Concrete
		WES*	University of Calif.**	WES**	WES*	University of Calif.**	WES**
			Sealed Specimens				
1	200	--	--	0.60	--	--	0.057
3	200	0.23	--	--	0.038	--	--
		0.24	--	--	0.034	--	--
7	200	--	0.23	0.18	--	0.036	0.025
28	200	0.17	0.16	0.17	0.029	0.020	0.016
		0.17	--	--	0.019	--	--
90	200	--	--	0.14	--	--	0.010
90	400	--	--	0.14	--	--	0.019
90	600	--	--	0.15	--	--	0.014
			Saturated Specimens				
1	200	0.26	--	--	0.027	--	--
		0.26	--	--	0.027	--	--
3	200	0.19	--	--	0.025	--	--
		0.20	--	--	0.025	--	--
7	200	0.17	--	--	0.025	--	--
		0.17	--	--	0.027	--	--
28	200	0.14	--	--	0.019	--	--
		0.15	--	--	0.018	--	--
90	200	0.13	--	--	0.015	--	--
		0.14	--	--	0.021	--	--
360	200	0.13	--	--	0.016	--	--
		0.13	--	--	0.012	--	--

* Functions were computed independently for each of two specimens.
** Functions were computed using combined data on duplicate specimens.

Table B3

Results of Strength Tests of Reinforcing Bars

Bar No.*	Turned Diameter in.	Area sq in.	Yield Point psi	Ultimate Load psi	Rate of Load psi/min	Gaged Section** Length in.	Gaged Section** Elongation in.	Gaged Section** Elongation %	Full Section† Length in.	Full Section† Elongation in.	Full Section† Elongation %
9-L-1	1.000	0.7854	56,000	109,500	13,000	4.0	0.75	18.8	8.0	1.18	14.8
9-L-2	1.000	0.7854	56,000	109,500	32,000	4.0	0.78	19.5	8.0	1.18	14.8
10-L-1	1.125	0.9940	46,300	83,500	25,000	4.5	1.28	28.4	8.0	1.78	22.2
10-L-2	1.110	0.9677	48,000	85,300	25,000	4.5	1.30	28.9	8.0	1.85	23.1
10-S-1	1.110	0.9677	45,500	77,500	25,000	4.5	1.45	32.2	8.0	2.00	25.0
10-S-2	1.125	0.9940	46,300	74,900	25,000	4.5	1.37	30.4	8.0	2.00	25.0
18-L-1	1.989	3.1070	41,200	82,400	32,000	8.0	1.80	22.5	8.0	1.80	22.5
18-L-2	1.989	3.1070	43,900	77,700	32,000	8.0	0.65	8.1††	8.0	0.65	8.1††

* First number refers to bar size; letter refers to source (L for Laclede, S for Sheffield).

** As specified in ASTM Designation: E 8-57T, a length of four diameters.

† Elongation measured over full turned section of 8 in.

†† Bar 18-L-2 did not fracture but pulled out of chuck.

Table B4

Modulus of Elasticity Determinations for Reinforcing Bars

Total Load, lb	Stress psi	Modulus* Secant	Modulus* Chord	Total Load, lb	Stress psi	Modulus* Secant	Modulus* Chord
	Bar No. 9-L-1				Bar No. 9-L-2		
5,000	6,365	28.7	28.7	5,000	6,365	28.3	28.3
10,000	12,730	28.7	28.7	10,000	12,730	29.4	30.6
15,000	19,100	29.1	30.0	15,000	19,100	29.2	28.9
20,000	25,465	29.3	29.7	20,000	25,465	29.2	28.9
25,000	31,830	29.3	29.5	25,000	31,830	29.3	30.0
30,000	38,195	29.1	28.3	30,000	38,195	29.2	28.3
35,000	44,560	28.8	26.7	35,000	44,560	28.8	26.7
40,000	50,930	28.4	26.0	40,000	50,930	28.2	25.0
	Avg	28.9	28.4		Avg	29.0	28.3
	Bar No. 10-L-1				Bar No. 10-L-2		
5,000	5,030	26.2	26.2	5,000	5,165	28.4	28.4
10,000	10,060	27.8	29.6	10,000	10,335	28.9	29.5
15,000	15,090	28.3	29.2	15,000	15,500	28.8	28.4
20,000	20,120	28.6	29.6	20,000	20,670	28.8	29.0
25,000	25,150	28.7	29.2	25,000	25,835	29.1	30.4
30,000	30,180	28.7	28.7	30,000	31,000	29.0	28.4
35,000	35,210	28.3	26.2	35,000	36,170	28.7	27.2
40,000	40,240	28.2	27.2	40,000	41,340	28.7	28.7
45,000	45,270	28.1	27.6				
	Avg	28.1	28.2		Avg	28.8	28.8
	Bar No. 10-S-1				Bar No. 10-S-2		
5,000	5,165	28.7	28.7	5,000	5,030	29.2	29.2
10,000	10,335	30.4	32.3	10,000	10,060	29.4	29.6
15,000	15,500	30.1	29.5	15,000	15,090	29.6	29.9
20,000	20,670	29.5	27.9	20,000	20,120	29.1	27.6
25,000	25,835	28.6	25.6	25,000	25,150	29.2	29.9
30,000	31,000	28.9	30.4	30,000	30,180	29.4	30.5
35,000	36,170	28.4	25.8	35,000	35,210	29.0	26.8
40,000	41,340	28.5	28.7	40,000	40,240	28.4	24.9
45,000	46,505			45,000	45,270	28.6	29.6
	Avg	29.1	28.6		Avg	29.1	28.7
	Bar No. 18-L-1				Bar No. 18-L-2		
20,000	6,435	25.5	25.5	20,000	6,435	28.6	28.6
40,000	12,875	24.1	22.8	40,000	12,875	28.9	29.3
60,000	19,310	24.3	24.6	60,000	19,310	28.8	28.6
80,000	25,745	25.1	28.2	80,000	25,745	28.1	26.3
100,000	32,180	26.1	30.9	100,000	32,180	28.3	29.0
120,000	38,620	26.8	30.7				
	Avg	25.3	27.1		Avg	28.5	28.4

* Modulus of elasticity in 10^6 psi.

Table B9

Summary of Compressive Strength Tests on Concrete Placed in Monolith 12

Lift and Wall Location	Date Placed	Cement Factor, bags/yd³	Water-Cement Ratio	Air Content %	Slump in.	7-day Strength: Cylinder No.	7-day: Density lb/cu ft	7-day: Elastic Modulus psi x 10⁻⁶	7-day: Compressive Strength psi	28-day Strength: Cylinder No.	28-day: Density lb/cu ft	28-day: Elastic Modulus psi x 10⁻⁶	28-day: Compressive Strength psi
Base Slab													
1st lift	16 Jun 60	4.5	0.52	5.2	1-3/4	5 (A)	146.6	3.81	2350	5 (G)	146.6	5.43	4240
						5 (B)	146.0	3.67	2310	5 (H)	146.0	4.71	4160
						5 (C)	146.6	3.81	2440	5 (I)	146.6	5.25	3980
						5 (D)	146.0	3.81	2470	5 (J)	146.6	5.45	4100
						5 (E)	146.6	3.67	2080	5 (K)	146.6	4.90	4050
						5 (F)	146.6	3.47	2230	5 (L)	146.6	5.11	4130
					Avg		146.4	3.71	2310		146.5	5.14	4140
2d lift	8 Sep 60	4.5	0.51	5.3	2	6 (A)	144.8	3.69	2120	6 (G)	145.4	4.96	3860
						6 (B)	145.4	3.77	2200	6 (H)	144.7	5.48	3860
						6 (C)	144.8	3.52	2050	6 (I)	144.7	5.04	3610
						6 (D)	145.4	3.49	2020	6 (J)	146.0	5.52	4040
						6 (E)	145.4	3.50	2100	6 (K)	145.4	5.19	3840
						6 (F)	145.4	3.46	2180	6 (L)	145.4	5.56	3780
					Avg		145.2	3.57	2070		145.3	5.29	3830
3d lift	18 Oct 60	4.5	0.50	5.4	2-1/4	8 (A)	145.4	3.96	2150	8 (G)	144.7	5.16	4210
						8 (B)	144.8	4.00	2140	8 (H)	144.7	5.22	3810
						8 (C)	144.8	3.90	2200	8 (I)	145.4	5.36	4180
						8 (D)	144.8	4.05	2200	8 (J)	144.7	4.99	3770
						8 (E)	145.4	3.84	2050	8 (K)	145.4	5.28	4130
						8 (F)	144.8	3.98	2200	8 (L)	145.4	5.36	4040
					Avg		145.0	3.92	2160		145.0	5.23	4020
					Avg for base slab		145.5	3.73	2180		145.6	5.22	4000
Walls													
1st lift, south wall	11 Nov 60	4.4	0.54	5.9	2-3/4	9 (A)	144.1	3.59	2130	9 (G)	143.5	5.16	4370
						9 (B)	143.5	3.67	2200	9 (H)	144.1	5.14	4000
						9 (C)	144.1	3.65	2060	9 (I)	144.8	5.69	4340
						9 (D)	144.1	3.43	1980	9 (J)	144.8	5.35	4070
						9 (E)	144.1	3.75	2020	9 (K)	144.1	5.08	4090
						9 (F)	144.8	3.47	1980	9 (L)	144.1	5.34	4180
					Avg		144.1	3.63	2060		144.2	5.28	4170
3d lift, north and south walls	10 Feb 61	4.5	0.50	5.2	1-3/4	10 (A)	146.6	4.42	2670	10 (G)	146.6	5.70	4980
						10 (B)	146.6	4.50	2750	10 (H)	146.6	5.76	4910
						10 (C)	146.6	4.60	2840	10 (I)	147.3	6.12	5340
						10 (D)	147.3	4.72	2810	10 (J)	147.3	6.13	4830
						10 (E)	147.9	4.78	2910	10 (K)	147.3	5.97	4960
						10 (F)	147.3	4.42	2730	10 (L)	147.3	5.87	4860
					Avg		147.0	4.57	2780		147.1	5.92	4980
5th lift, north and south walls	27 Feb 61	4.5	0.50	5.3	2	24 (A)*	146.0	4.86	2800	24 (G)	146.0	5.82	4520
						24 (B)*	146.0	4.51	2890	24 (H)	146.0	5.89	4400
						24 (C)*	146.0	4.64	2830	24 (I)	146.6	5.79	4470
					Avg		146.0	4.67	2840		146.2	5.83	4460
7th lift, north and south walls	16 Aug 61	4.5	--	5.2	2-1/4	12 (A)	145.4	4.17	2400	12 (G)	145.4	5.14	3950
						12 (B)	146.0	4.22	2400	12 (H)	144.8	5.32	3820
						12 (C)	146.0	4.07	2460	12 (I)	145.4	5.26	3980
						12 (D)	144.8	4.07	2360	12 (J)	144.8	5.30	3870
						12 (E)	145.4	4.19	2360	12 (K)	145.4	5.18	3770
						12 (F)	146.0	4.13	2320	12 (L)	145.4	5.42	4020
					Avg		145.6	4.14	2380		145.2	5.27	3910
8th lift, north and south walls	19 Aug 61	4.5	0.50	5.4	2-1/4	13 (A)*	144.1	4.46	2790	13 (G)	144.8	5.10	4110
						13 (B)*	145.4	4.27	2960	13 (H)	144.8	5.27	4120
						13 (C)*	144.1	4.41	2960	13 (I)	144.8	5.19	3980
						13 (D)*	144.8	4.41	2760	13 (J)	144.1	5.37	3730
						13 (E)*	144.8	4.64	2860	13 (K)	144.8	4.90	4040
						13 (F)*	144.8	4.29	2810	13 (L)	144.8	4.89	3640
					Avg		144.7	4.13	2860		144.7	5.12	3940
					Avg for walls		145.5	4.23	2580		145.5	5.48	4290
					Avg for lifts 3 and 5		146.5	4.62	2810		146.6	5.88	4720

* 4-day tests.

Table B6

Results of Tests on Sand Backfill Samples

Sample No.	Station	Distance from Wall, ft	Elevation ft msl	D_{10} Size mm	D_{50} Size mm	In Place γ_d lb/cu ft	In Place Water Content %	Percent Compaction	Relative Density %	Estimated Shear Strength ϕ, deg
Monolith 2, North Side of Lock										
N-1	103+00	17	-9.2	0.14	0.26	105.7	--	102	77	39.5
N-2	103+00	32	-9.2	--	--	103.7	--	--	--	--
N-3	103+30	10	0.0	0.16	0.30	102.6	--	99	55	37.3
N-4	103+30	20	0.0	0.12	0.23	106.3	--	104	83	40.3
N-5	103+30	10	10.0	0.12	0.22	96.8	19.4	95	28	36.0
N-6	103+30	20	10.0	0.11	0.21	103.1	18.2	101	70	38.5
N-7	103+30	10	20.0	0.14	0.25	100.5	--	98	47	36.8
N-8	103+30	20	20.0	0.11	0.24	103.8	--	101	68	38.5
N-9	103+30	10	30.0	0.14	0.26	103.8	19.2	100	66	38.3
N-10	103+30	20	30.0	0.14	0.24	100.2	16.7	98	46	36.8
			Average			102.6		100	59	38.0
			Corrected Average*			108.0		105	89	41.2
Monolith 2, South Side of Lock										
S-1	103+00	10	-10.0	0.16	0.27	109.2	--	106	96	42.5
S-2	103+00	20	-10.0	0.12	0.24	109.1	--	106	98	42.8
S-3	103+30	10	0.0	0.18	0.27	104.8	--	101	71	38.7
S-4	103+30	20	0.0	0.15	0.27	102.5	--	99	57	37.5
S-5	103+30	10	10.0	0.16	0.27	94.4	12.4	91	3	35.3
S-6	103+30	20	10.0	0.16	0.27	94.5	10.1	91	4	35.3
S-7	103+30	10	20.0	[illegible]7	0.27	101.6	18.5	98	51	37.2
S-8	103+30	20	20.0	[illegible].8	0.25	101.0	16.9	98	51	37.2
S-9	103+30	10	30.0	[illegible].12	0.21	101.9	9.8	100	62	38.9
S-10	103+30	20	30.0	0.10	0.18	99.4	20.0	99	57	37.5
			Average			101.8		99	55	38.3
			Corrected Average*			107.2		104	86	41.0
Monolith 12, North Side of Lock										
N-1	97+06	6	-9.8	0.15	0.26	103.8	--	100	66	38.3
N-2	97+05	36	-9.5	--	--	102.9	--	--	--	--
N-3	97+00	10	0.0	0.12	0.22	102.6	21.3	100	64	38.1
N-4	97+00	20	0.0	0.13	0.25	109.0	14.2	109	96	42.5
N-5	97+00	10	10.0	0.18	0.30	103.2	24.3	100	59	37.7
N-6	97+00	20	10.0	0.17	0.28	108.5	4.6	105	91	41.6
N-7	97+00	10	20.3	0.14	0.27	99.2	5.6	96	36	36.3
N-7A	97+00	15	20.3	--	--	100.8	6.3	--	--	--
N-7B	96+80	10	20.5	--	--	103.1	5.0	--	--	--
N-8	97+00	20	20.3	0.12	0.23	97.4	5.0	95	30	36.0
N-8A	96+80	15	20.5	--	--	102.6	7.7	--	--	--
N-8B	96+80	20	20.5	--	--	104.5	5.7	--	--	--
N-9	97+17	10	31.1	0.15	0.25	103.2	17.6	100	63	38.0
N-10	97+17	20	31.1	0.14	0.26	104.6	20.4	101	71	38.7
			Average			103.2		100	64	38.6
			Corrected Average*			108.6		105	93	42.3

(Continued)

Note: In-place density determinations were made with 3-in. drive sampler. Percent compaction based on standard Proctor maximum density estimated from curve shown in fig. B11.

* Average values of density were corrected to correspond to values of density determined with Volumeasure.

Table B6 (Concluded)

Sample No.	Station	Distance from Wall, ft	Elevation ft msl	D_{10} Size mm	D_{50} Size mm	In Place γ_d lb/cu ft	In Place Water Content %	Percent Compaction	Relative Density %	Estimated Shear Strength ϕ, deg
Monolith 12, South Side of Lock										
S-1	97+05	10	-10.0	0.12	0.22	105.9	--	103	83	40.3
S-2	97+05	20	-10.0	0.16	0.26	110.6	--	107	104	43.7
S-3	97+00	10	0.0	0.14	0.25	106.6	18.8	103	83	40.3
S-4	97+00	20	0.0	0.13	0.24	109.7	16.0	107	101	43.5
S-5	97+00	10	10.0	0.16	0.29	108.5	19.6	105	91	41.7
S-6	97+00	20	10.0	0.15	0.26	105.9	18.3	102	78	39.5
S-7	97+15	10	20.5	0.15	0.27	101.8	7.7	98	52	37.2
S-7A	97+15	15	20.5	--	--	101.6	5.3	--	--	--
S-8	97+15	20	20.5	0.16	0.28	101.1	5.0	98	47	36.8
S-9	97+15	10	30.0	0.14	0.25	103.5	16.2	100	65	38.2
S-9A	97+15	15	30.0	--	--	103.2	16.5	--	--	--
S-10	97+15	20	30.0	0.13	0.25	99.2	17.1	96	39	36.4
			Average			104.8		102	74	39.8
			Corrected Average*			110.2		107	102	43.7
Monolith 22, North Side of Lock										
N-1	90+67	15	-8.4	0.16	0.29	106.2	--	102	77	39.5
N-2	90+67	30	-8.4	0.17	0.28	110.1	--	106	100	43.2
N-3	90+85	10	0.0	0.10	0.18	103.8	18.5	104	82	40.1
N-4	90+85	20	0.0	0.12	0.24	95.9	20.4	94	18	35.6
N-5	90+85	10	10.0	0.13	0.24	101.9	18.7	99	57	37.5
N-6	90+85	20	10.0	0.16	0.28	110.1	16.6	106	100	43.2
N-7	90+85	10	20.0	0.11	0.18	102.7	15.3	103	70	37.3
N-8	90+85	20	20.0	0.12	0.21	101.6	9.9	100	61	37.8
N-9	90+85	10	30.4	0.15	0.24	103.2	16.0	100	64	38.1
N-10	90+85	20	30.4	0.14	0.24	102.8	15.7	100	63	38.0
			Average			103.8		101	70	39.0
			Corrected Average*			109.2		106	94	42.2
Monolith 22, South Side of Lock										
S-1	90+77	10	-10.0	0.16	0.30	105.2	--	101	71	38.7
S-2	90+65	20	-10.0	--	--	107.5	--	--	--	--
S-3	90+85	10	0.0	0.16	0.27	100.6	17.3	97	45	36.7
S-4	90+85	20	0.0	0.16	0.26	102.9	14.1	100	60	37.7
S-5	90+85	10	10.0	0.15	0.24	102.6	--	100	61	37.8
S-6	90+85	20	10.0	0.15	0.23	102.4	--	100	62	37.9
S-7	90+85	10	21.0	0.12	0.26	100.1	19.1	97	43	36.7
S-8	90+85	20	21.0	0.12	0.26	100.1	18.0	97	43	36.7
S-9	90+85	10	31.0	0.13	0.23	99.9	17.4	97	46	36.8
S-9A	90+85	15	31.0	--	--	100.3	17.0	--	--	--
S-10	90+85	20	31.0	0.14	0.24	102.4	18.0	100	60	37.7
			Average			102.2		99	55	37.4
			Corrected Average*			107.4		104	87	41.0

* Average values of density were corrected to correspond to values of density determined with Volumeasure.

Table B7

Density Determinations Made with Drive Cylinder and Volumeasure

Date	Station	Distance from Center Line ft	Elevation ft msl	Density, lb/cu ft		
				Volumeasure	Drive Cylinder	Difference
13 Nov 61	91+60	70 N	+37.0	105.8	102.7	3.1
13 Nov 61	91+65	70 N	+37.0	106.6	101.1	5.5
14 Nov 61	92+20	54 S	+39.5	105.4	100.0	5.4
14 Nov 61	92+80	52 S	+39.5	108.7	102.8	5.9
14 Nov 61	93+40	44 S	+39.5	103.8	98.5	5.3
14 Nov 61	94+00	44 S	+39.5	101.4	98.1	3.3
27 Nov 61	95+80	55 S	+42.0	105.8	102.5	3.3
27 Nov 61	98+20	100 S	+41.6	107.8	101.7	6.1
19 Dec 61	97+60	64 S	+47.0	107.8	99.6	8.2
19 Dec 61	97+60	75 S	+47.0	106.4	101.9	4.5
19 Dec 61	98+11	65 S	+47.0	106.6	99.2	7.4
21 Dec 61	97+30	51 N	+50.0	103.5	98.1	5.4
21 Dec 61	97+90	50 N	+50.0	104.4	100.4	4.0
21 Dec 61	97+60	76 N	+50.0	101.7	97.8	3.9
22 Dec 61	101+50	50 N	+50.0	107.0	103.0	4.0
22 Dec 61	101+50	60 N	+50.0	105.3	101.6	3.7
22 Dec 61	101+50	70 N	+50.0	107.3	101.7	5.6
29 Dec 61	92+02	56 S	+47.0	96.6	91.6	5.0
29 Dec 61	93+10	70 S	+48.0	106.8	97.2	9.6
29 Dec 61	93+10	89 S	+48.0	107.6	98.5	9.1
3 Jan 62	90+85	70 N	+43.0	106.0	96.3	9.7
3 Jan 62	90+85	58 N	+44.0	96.7	93.6	3.1
3 Jan 62	91+05	60 N	+44.0	97.9	92.8	5.1
			Average	104.6	99.2	5.4

Table B8

Compaction and Density Test Data

Sample No.	Backfill Source	Tested by and Date of Report	D_{50} Size mm	Maximum γ_d lb/cu ft	Minimum γ_d lb/cu ft	Standard Proctor Compaction Data	
						Maximum γ_d lb/cu ft	D_R, % at Maximum γ_d
1*	Stockpile	WES (16 Jun 61)	0.25	111.8	91.8	105.0	70
2	Stockpile	NOD (17 Aug 61)	0.30	108.7	95.8	101.0	44
3	Stockpile	NOD (17 Aug 61)	0.26	109.1	91.1	104.3	77
4	Stockpile	NOD (17 Aug 61)	0.20	106.0	85.5	102.4	85
5	Stockpile	NOD (17 Aug 61)	0.30	108.9	94.6	102.6	59
6	Sandbar	NOD (7 Sep 61)	0.21	107.3	94.7	--	--
7	Sandbar	NOD (7 Sep 61)	0.27	109.2	96.6	--	--
8	Sandbar	WES	0.21	109.8	91.2	103.2	68
9	Sandbar	WES	0.26	110.3	92.7	102.2	58

* Original control sample.